CONTROLLED SYNTHESIS OF STIMULI-RESPONSIVE NETWORK ALGINATE

by

Ariel Wan-Ju Chan

A thesis submitted to the Department of Chemical Engineering
In conformity with the requirements for
the degree of Doctoral of Philosophy

Queen's University
Kingston, Ontario, Canada
July 2009

Abstract

Stimuli-responsive hydrogels swell or contract in response to external pH, ionic strength or temperature, and are of considerable interest as pharmaceutical controlled release devices. Alginate, a linear polysaccharide consisting of mannuronic and guluronic acids, was used as starting material in semisynthesis of pH-responsive hydrogel. Linear alginate was chemically modified with di-aldehyde via acid-catalyzed acetalization, forming a tetrafunctional acetal-linked semisynthetic network alginate polymer (SNAP) with carboxylate moieties preserved as stimuli-responsive sensors. The kinetics of acetalization were found to undergo zero and second-order reaction with respect to di-aldehyde and alginate respectively. With the determined rate constant of 19.06 $\mu L \cdot mole^{-1} \cdot s^{-1}$ at $40^{o}C$ and activation energy of 78.58 $kJ \cdot mol^{-1}$, a proposed predictive reaction model may be used *a priori* to select reaction conditions providing specific polymer properties. Gel swelling and average pore size were then able to be kinetically or thermodynamically controlled between 80-1000 fold and 30 nm-1 μm respectively. As a proof of concept, SNAP hydrogel was fine-tuned with specific swelling and pore sizes for absorptive encapsulation and controlled release of a wide spectrum of molecular sizes of proteins ranging between 1.3 to 546 kDa. SNAP hydrogels/granules demonstrated limited swelling in the simulated gastric environment, protecting proteins from enzymatic and acid degradation, while swelling in alkaline media, releasing active therapeutics in a simulated intestinal lumen (pH ~ 7.8), so is under the consideration as an oral delivery vehicle for protein therapeutics.

A constitutive polyelectrolyte gel model based on non-Gaussian polymer elasticity, Flory-Huggins liquid lattice theory, and non-ideal Donnan-membrane equilibria was derived, to describe SNAP gel swelling in dilute and ionic solutions. The derived model accurately describes the SNAP hydrogel swelling in acid and alkaline solutions of wide range of ionic strength. The pore sizes of SNAP hydrogel were estimated by the derived model and were comparable to those determined experimentally by thermoporometry and protein diffusion. The derived model can characterize hydrogel structure such as molecular weight between crosslinks, or can be used as predictive model for swelling and pore size if gel structural information is known, and can potentially be applied to other point-link network polyelectrolytes such as hyaluronic acid gel.

Co-Authorship

The thesis has been prepared in manuscript format. The material presented represents the PhD thesis work of Ariel Chan. Professor Ronald J. Neufeld from the Department of Chemical Engineering is the thesis research supervisor and is named as co-author on the publications. Professor Ralph A. Whitney from the Department of Chemistry is named as co-author on chapters 3 and 4, for providing valuable guidance in the development of the reaction mechanism for acid-catalyzed acetalization, and also guidance in the NMR characterization of the chemically modified alginate polymer.

Acknowledgements

I am deeply indebted to my supervisor Dr. Ronald Neufeld whose guidance, stimulating suggestions and encouragements helped me throughout my research. I would especially like to express my sincere appreciation for his patience, and devotion in time and effort in assisting me through the thesis writing process, for which he has made this research an enjoyable learning process and my graduate study a memorable experience.

I would like to offer my profound thanks to Dr. Ralph Whitney from the Department of Chemistry for offering his technical expertise during the initial stage of the thesis research in the development of chemically modified alginate.

Special thanks are given to Dr. Brian Amsden for his valuable suggestions in the area of solute diffusion modeling, and help from his lab group members: Abby Sakudo, Steve Sharpka, and Darryl Knight.

I would like to express my sincere gratitude to Mr. Charles Cooney and Drs. Francoise Sauriol, Mike Cunningham, and Huge Horton for their assistance in polymer characterization, kindness in equipment usage, and warm encouragements.

I would like to thank my lab colleagues, Natinee Suvanasinga, Burak Erdinc, Frank Gu and Kristen Bowey for their invaluable help, advice and friendship.

Finally, I would like to give my special thanks to my parents for their unconditional love, support and encouragements.

Table of Contents

List of Figures

List of Tables

List of Symbols

a_i	Activity of a solute substance *i*
b	Average linear charge spacing of the polyelectrolyte
$\beta^{(1)}, \beta^{(2)}, \beta^{(3)}$	First, second and third viral coefficients
c_+, c_-	Concentrations of the mobile cations and anions inside the gel
c_+^*, c_-^*	Concentrations of the cations and anions in the external electrolyte solution
c_s	Concentrations of the mobile electrolyte solution inside the gel
c_s^*	Concentrations of the external electrolyte solution
c^o	Standard value of the molar concentration (1 mol L^{-1})
$c_\pm$	Mean ionic molarity
c_2	Molar concentration of the polymer repeated units
C_n	Characteristic ratio
D_{gel}	Protein diffusion coefficient in the gel matrix
D_{water}	Protein diffusion coefficient in water
η	Viscosity
$[\eta]$	Intrinsic viscosity of polymer in defined solution condition
$[\eta]_\theta$	Intrinsic viscosity of a polymer at theta condition
f_ζ	Fraction of non-condensed counterions (Manning-Fraction)
f	Functionality of a structural unit
F_G	Fraction of guluronic acid residue in alginate
F_M	Fraction of mannuronic acid
F_{GG}	Fraction of guluronic acid block
F_{MM}	Fraction of mannuronic acid block
ΔG_{el}	Change of Gibbs free energy due to polymer elastic reaction
ΔG_{mix}	Change of Gibbs free energy due to mixing
ΔH_{mix}	Heat of mixing
$\Delta H_f(T)$	Temperature-dependent heat of fusion
i	Degree of ionization
I	Ionic strength of the electrolyte solution
k_B	Boltzmann's constant
k_θ	Unperturbed parameter
K_a	Acid dissociation constant
l	Carbon-carbon bond length of monomer unit
m_p	Dry polymer mass
M_o	Primary molecular weight of the polymer
M_c	Molecular weight between two consecutive crosslink points
M_r	Molecular weight of the monomer unit
M_w	Molecular weight by weight of polymer

N_A	Avogadro number
PDI	Polydispersity index
$\rho(T)$	Density of the probe fluid used in Thermoporometery
dQ/dt	Heat flow recorded by differential scanning calorimeter (DSC)
r_H	Hydrodynamic radius of the solute
R	Gas constant
R_p	Average pore radius determined by thermoporometry technique (nm)
ΔS_{mix}	Entropy of mixing
T	Absolute temperature
$d(\Delta T)/dt$	Scanning rate of the DSC experiment
μ	Chemical potential
μ_1	Chemical potential of the solvent molecule inside the gel
μ_1^0	Chemical potential of the solvent molecule in the pure liquid
μ_1^*	Chemical potential in the external solution comprising mobile electrolytes
μ_+^0, μ_-^0	Standard state chemical potentials of cationic and anionic species
$(\Delta\mu_1)_i$	Chemical potential difference due to mixing with the ionic constituents
$(\Delta\mu_1)_{mix}$	Chemical potential difference due to polymer mixing with solvent
$(\Delta\mu_1)_{el}$	Chemical potential difference due to elastic refractive reaction
$(\Delta\mu_1^*)_{ion} - (\Delta\mu_1)_{ion}$	Chemical potential difference due to uneven distribution of mobile ions in the external electrolyte and gel matrix
v_1	Volume fractions of solvent
v_2	Volume fractions of solute
v_e	Effective number of chains
v_2, $v_{2,s}$	Volume fraction of polymer in the swollen gel
$v_{2,r}$	Volume fraction of polymer in the relaxed gel (formed right after the crosslinking prior to swelling)
$\bar{\upsilon}$	Specific volume of the polymer
v_+ , v_-	Stoichiometric formula of the electrolyte
V_1	Molar volume of the suspended solvent
V_s	Swollen state of the gel volume
V_r	Relaxed, non-deformed network gel volume
V_p	Dry polymer volume
x	Degree of polymerization or chain length
χ_1	Flory-Huggins interaction parameter
X_b	Concentration of the counterion-polymer-fixed ion pairs
X_f	Concentration of osmotically active counterions in the swollen gel
γ	Activity coefficient
$\gamma_\pm^*$	Mean ionic activity coefficient of the external electrolyte solution
$\gamma_\pm$	Mean ionic activity coefficients of ions inside the gel matrix

γ_-	Ionic activity coefficient of co-ions (anions) inside the gel
γ_+	Ionic activity coefficient of counterion (cations) inside the gel
z^+ z^-	Valence of cations and anions
Z	Valence charge of the ionic species
ξ	Mesh pore size
ζ	Linear polyelectrolyte charge density
Φ	Flory viscosity constant
ϕ	Fraction of osmotically active counterions in the swollen gel
π	osmotic pressure

Chapter 1

General Introduction

Stimuli-responsive biomaterials swell, contract or undergo phase or conformational transitions with environmental stimuli, such as pH, temperature, ionic strength, or presence of specific ions. So-called “smart polymers” have potential applications in targeted drug delivery, cosmetic formulations, cell/protein encapsulation, tissue engineering, and as bioactuators. Stimuli-responsive polysaccharides like alginate are of considerable interest in the fields of biotechnology and biomedical engineering due to biodegradability, biocompatibility, natural abundance, and unique chemical structures and physico-chemical/biological properties.

Alginate, a linear polysaccharide consisting of mannuronic (M) and guluronic acid (G) residues, is considered as a stimuli-responsive polymer which undergoes sol-gel transition in the presence of di-valent or multi-valent cations such as Ca^{++} and changes polymer hydrophilicity in response to external pH environment. Physically crosslinked alginate gel is widely used for encapsulation purposes and has been studied for many years in an effort to relate composition of the polymer to its gel properties such as pore size, swelling and mechanical stability. However, since natural materials have fixed structures, the ability to modify polymer properties is limited as are the applications. Therefore, there is considerable interest in this natural material and in the ability to chemically modify and thus alter its properties.

To enable the control of properties generally not possible with physical alginate gel and to increase the spectrum of the gel properties such as pore size, swelling and mechanical stability for many biological applications, native alginate may be used as starting material/building blocks in semisynthesis of new classes of biopolymers. The overall objective of this PhD research was to develop a new biomaterial from a known natural polymer, hopefully with new properties, and to consider possible applications as protein and drug retentive/controlled release device. Therefore, I proposed that native, linear alginate be chemically modify with bi-functional aldehyde crosslinker, forming semi-synthetic network hydrogel, to enable the control of properties generally not possible with the native polymer. The physical properties such as pH-responsive swelling, pore size and solute diffusivity can be tailored for various biological applications such as oral delivery of a wide range of molecular sizes of active biomolecules including insulin. The following literature review outlines the fundamental properties of alginate polymer and network hydrogel including rheological, gelling and swelling properties, theoretical modeling of gel swelling, and the most recent developments on chemical modification of alginate and the potential use of network alginate gel in biomedical applications. In the results and discussion section, the development of semi-synthetic network alginate polymer is described, along with the characterization of reaction mechanism and kinetics of the chemical modification process. The structural information, mechanical stability, gel pore size, and stimuli-responsive swelling properties of the developed network polymer were studied and the potential use as an oral delivery vehicle for a wide range in molecular sizes of protein therapeutics including insulin was demonstrated.

Part of the research scope was to derive a polyelectrolyte gel model which can be used to readily estimate molecular weight between two consecutive crosslinks (ie. crosslinking density) from the determined swollen gel volume in salt-free or un-univalent, uni-bivalent, bi-univalent or bi-bivalent ionic concentration media. Such information can be used to estimate the gel pore size which is critical for biomaterial design, especially in controlling the solute transport properties of the hydrogel. The pore sizes of the semi-synthetic alginate hydrogel were estimated by the derived gel model and were compared to those determined by thermoporometry and protein diffusion. With the developed understanding of alginate semisynthesis reaction, the derived gel model may be used *a priori* to select reaction conditions for obtaining desired crosslinking density, providing specific polymer properties.

Semi-synthetic network alginate gel showed pronounced swelling in alkaline while remaining in compact state in acid medium. Mechanical stability was demonstrated after repeated dehydration and rehydration in various ionic media. The chemically modified alginate may have application as oral delivery vehicle for bioactive drugs, as superabsorbent for environmental clean-up application or as bioscaffold for tissue engineered implants. Recommendations on future research direction are addressed in the last section of the thesis to enhance the utility of SNAP hydrogel in many bioengineering or tissue regeneration applications.

Chapter 2

Literature review

2.1 Hydrogels as "smart" biomaterials

Hydrogels are hydrophilic, three-dimensional network polymers which can absorb ten to several hundred times the dry polymer weight without dissolving in compatible solvents. Because of high water content and structural and mechanical similarities to macromolecular-based components in natural tissues, hydrogels have been utilized extensively in many biotechnological, medical and pharmaceutical applications, such as for biosensors, drug delivery devices, cell encapsulation matrices, and tissue scaffolds for transplantation[1-6].

Many synthetic and naturally derived polymers have been reported to form physical hydrogels through polymer entanglement or electrostatic interaction such as dipole-dipole interaction, hydrogel bonding or van der Waals forces. These polymers can also form chemical hydrogels by connecting water-soluble polymers with chemical crosslinkers in permanent tie-junction points. In contrast to physical gels, chemical gels are mechanically stable, and the rate of biodegradation and the many physical and mechanical properties of the polymer network are generally controllable. Although the polymeric network provides a structural framework that holds the liquid in place, water molecules are free to migrate resulting in gel swelling or contraction. Similarly, other small molecular weight solutes may diffuse into or out from the gel network.

A class of hydrogel which changes its shape, surface characteristics, solubility, or undergoes formation of an intricate molecular self-assembly or phase or conformational transition with external stimuli, such as pH, temperature, ionic strength, solvent composition, presence of salt ions, light, or electric field, is considered to be a "smart" hydrogel (also referred to as stimuli-responsive hydrogel)[5, 7, 8]. Smart hydrogels have been proposed for biomedical applications, such as in the delivery of therapeutic agents, tissue engineering, flow control, sensors/diagnostic devices and actuators. As examples, poly(N-isopropylacrylamide) hydrogel undergoes sol-gel transition or volume transition in response to the change of external temperature, and poly(methacrylic acid) gels [9, 10] and poly(vinyl alcohol)/poly(acrylic acid) interpenetrating network hydrogel[11] undergoes pH-sensitive volume transition from a collapsed to a highly swollen state.

2.2 Polysaccharide based pH-responsive hydrogels

Natural-based polyelectrolyte, especially polysaccharides, have received increasing attention in biomedical and pharmaceutical fields due to biodegradability, biocompatibility, natural abundance, unique chemical structures and physico-chemical/biological properties, and the ability to form hydrogels. Generally, the pH-responsive hydrogel consists of ionizable acidic or basic pendant groups such as carboxylic acid, sulfonic acid or amines. When the pH of the external environment is above the pK_a value of the acidic pendants, the polymer becomes polyanionic, while below the pK_b of the basic pendants, the polymer is polycationic. Examples of anionic

polysaccharides are alginate and carrageenans from algal origin, and examples of cationic polysaccharides are chitin and its derivative chitosan from marine invertebrates such as shrimp and crab shells.

The on-set of pH-responsive swelling is controlled by the ionization of the pendant groups which change water activity of the gel network near the pK_a or pK_b. The ionic pendants increase the hydrophilicity of the polymer and generate an electrostatic repulsion between the polymer chains, leading to the swelling of the polymer network. As an example, alginate hydrogel consists of carboxylic acid moieties ($pK_a \approx 3.6$). In pH 1 solution, the hydrogel remains in compact state due to limited water solubility of carboxylic acid, whereas the hydrogel swells in pH 7 solution as a result of deprotonated carboxylate anions, increasing hydrophilicity of the polymer chains. Polysaccharide based pH-responsive hydrogels are of particular interest in the development of transmucosal pharmaceutical formulations for the delivery of therapeutic proteins. The concept of using pH as a trigger to release a drug at the intestinal absorptive site is based on varying pH down the GI tract. Gastric-irritating or pH and protease labile protein therapeutics can be protected by the collapsed/compact gel matrix in gastric environment (pH~1.2) while being released in the intestinal lumens (pH~7.8) through matrix swelling or erosion. In addition, encapsulation within mucoadhesive polymers was found to improve bioavailability since contact between the drug and mucosal surface was enhanced, increasing the residence time at the site of drug absorption and reducing drug metabolism by luminal secreted proteases[12]. For tissue engineering application, pH-responsive hydrogels which contain carboxylate anions on the hydrophilic surface may mimic the

characteristics of the cell surface in vertebrates, minimizing immunogenic effects, thus improving biocompatibility [13].

2.3 Alginate based stimuli-responsive biomaterials

Alginates are by far the most extensively characterized of the marine polysaccharides[15]. Alginates are used widely in food processing for their gelling, thickening and stabilizing properties, and in biomedical applications such as in esophageal reflux treatment, as wound dressing, dental impression, cell/protein encapsulation, and as tissue scaffold [15-19]. Alginates are one of the favoured formulation excipients in the pharmaceutical industry for its mucoadhesive property[12, 19, 20]. In addition, alginates are widely applied in bioseparation process since they can act as smart macroaffinity ligands for pectinase α-amylase, phospholipase D, and lipases[21-24].

2.3.1 Alginate chemistry and polymer properties

Alginate is a linear high-molecular mass polysaccharide extracted from various species of kelp and is one of the most abundant marine polysaccharides. Among the brown algal species, the most widely used are *Laminaria hyperborea*, *Macrocystis pyrifera*, and *Ascophyllum nodosum* due to their abundance [25]. Alginate, a linear polyhexuronic acid glycoside, consists of (1→4)-O-glycosidic links of β-D-

mannuronopyranosyl (M) and α-L-guluronopyranosyl (G) in varying sequential arrangements and proportions. The M and G sugar residues are C5 epimers which only differ by their chair conformations. As illustrated in Figure 2-1, D-mannuronic acid residues are joined together by $^4C_1$ diequatorial glycosidic linkages while L-guluronic acid residues are linked by $^1C_4$ diaxial bonds. The relative amount of the two uronic acid monomers and the sequential arrangements vary accordingly to the source of brown algae and the extraction site. As examples, M/G of alginate from *Laminaria hyperborean* (stem) is about 0.45 whereas that from *Macrocystis pyrifera* (leaf) is about 1.50 [26]. Most commercial alginates are extracted from brown seaweed, however alginates can also be synthesized by some bacterial species such as *Azotobacter* and *Pseudomonas*[15]. Bacterial alginates are additionally O-acetylated on the 2 and/or 3 positions of the D-mannuronic acid residues, and exhibit a greater water binding ability [27, 28].

Nuclear magnetic resonance (NMR) and statistical modelling have shown that M and G residues occur in block-wise conformations, namely as homopolymeric M and G blocks (i.e. MM and GG), and heteropolymeric sequentially alternating blocks (i.e. MG or GM) within the alginate polymer [29, 30]. From a combination of viscosity measurements, statistical-mechanical calculations, and C13-NMR data, the stiffness of alginate chain blocks was shown to increase in the order of MG<MM<GG[25]. Thus alginate polymer with high content of guluronate and long G-blocks generally showed a more extended, less flexible chain conformation than long M-block alginates. In general, the relative dimensions for the neutral unperturbed alginate chain at theta condition, a

measure of chain stiffness, was higher than that of carboxyl methyl cellulose, dextran and amylase, but lower than double stranded DNA[31].

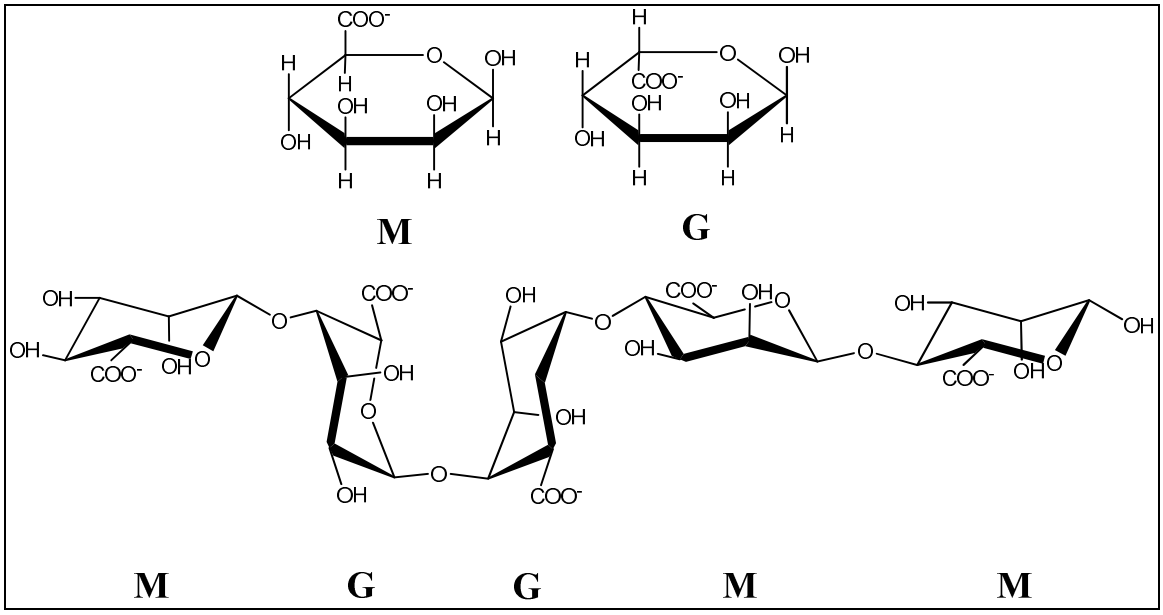

Figure 2-1.The chemical structure of alginate; the top figure illustrates the two monomers: mannuronic acid (M) and guluronic acid (G) residues in their Haworth conformation whereas the bottom figure shows a sample block structure of alginate.

2.3.2 Alginate solubility and rheological properties

Alginates are soluble in aqueous solution at pH ranging from 5-10. Alginate solution concentrations of less than 0.5% w/v flow like Newtonian solution, whereas solutions of 0.5-2.5% w/v behave as pseudo-plastic fluids over a wide range of shear rates (10-10,000 sec^{-1})[32]. As alginate concentration increases to a point where the solution passes through stages of a viscous liquid to a thick paste, any further addition of alginate to the suspension medium may not be properly dispersed and hydrated. Alginate solution

viscosity depends on polymer molecular weight, composition and sequence of M and G residues, and decreases with increasing temperature [31].

The quantity of alginate which can be dissolved in water is limited by the physical nature of the solution. In high ionic strength of inorganic salt solution such as potassium chloride, alginate can experience salting-out effect of non-gelling cations, resulting in precipitation[33]. In addition, alginate solubility decreases in suspension medium containing sugars, starches or proteins which changes water activity necessary for its hydration. The presence of polyvalent cations inhibits the hydration of alginates and larger quantities can induce precipitation or gel formation[33]. In addition, alginates are insoluble in organic solvents. However, alginate solution (fully hydrated in water) can tolerate about 10-20% addition of water-miscible solvents such as alcohols and ketones without precipitation[34].

2.3.3 Gel forming properties of alginate

2.3.3.1 Stability of alginates as function of pH

Alginates contain one carboxylic acid moiety per uronic acid monomer. The acid dissociation constants (pK_a) of alginate polymers differ only slightly from those of the monomeric residues which were determined to be 3.38 and 3.65 for mannuronic and guluronic acid, respectively, determined from potentiometric titration [35]. The pK_a of alginate is ionic strength dependent and affected by the monomeric block compositions. For instance, the pK_a of alginate (fraction of guluronic acid content, $F_G = 0.42$) decreased from 3.92 to 3.42 when 0.1 M NaCl was added to the solution.

Alginates are susceptible to both acid and alkaline degradation [36-38], via cleavage of the glycosidic linkages. Compared to other sugars, glycosidic linkages involving uronic acids such as M and G, are more strongly resistant toward hydrolysis in very strong acid, conditions normally used to fully hydrolyse polysaccharides to monosaccharides. At very low pH (pH < 1), the homopolymeric blocks of alginates have tendency to crystallize due to inductive effects, protecting the polymer from acid hydrolysis[35]. However, the rate of acid degradation near the pK_a (pH range 1-4) is much higher than for neutral polysaccharides. In this range, the protonated carboxylate acid of M and G contributes to the hydroysis by intramolecular catalysis in addition to the free H+ ions, making alginate less stable than neutral polysaccharides such as methylcellulose. The rate of degradation is approximately 3 times higher for MM blocks compared to GG blocks, but is almost independent of pH within this pH range [37]. Optimum stability is at pH 7-8. Under alkaline condition (pH 8-12), the polymer is degraded by β-alkoxy-elimination and the rate increases linearly with time as a pseudo zero order reaction and increases in proportion to OH-concentration[38].

2.3.3.2 Formation of alginic acid gel

Alginates are hydrophilic, however the polymers are nearly insoluble in solution near pH 3 or less. Within this pH range, proton-dissociation and chain flexibility do not prevent chain aggregation [39, 40]. Since the presence of carboxylate ions due to proton-dissociation is the most effective contribution to the solubility of alginate polymer, the

conversion of polyuronate salt solution to the acid form can nevertheless lead to molecular aggregates or gel formation.

Addition of acid to an alginate solution may result in the formation of alginic acid gel when the pH of the microenvironment is below the pK_a values of the two uronic acid residues [25, 41-43]. The properties of alginic acid gel are affected by the chemical composition and molecular weight of the alginate polymer chains[44]. An equilibrium study of acid gel during re-solvation showed that the GG and MM blocks were important in acid gel formation and the gel strength increased in the order of MG<MM<GG. For instance, alginate with a high content of GG blocks demonstrated a considerably higher mechanical strength compared to MG rich alginate, possibly due to homopolymeric blocks favouring the formation of crystalline regions through hydrogen bonds [41]. However, by increasing the degree of disorder in the alginate chain, such as in alginate derived from *Ascopyllum nodosum* which consists mainly of MG blocks, these crystalline regions are not as easily formed and alginate remains soluble even at pH values near pH 1.4 [45]. Since the formation of acid gel is carried out in a very acidic environment, such a drug delivery system may not be suitable for encapsulating pH-labile therapeutic proteins.

2.3.3.3 Ion binding and physical properties of ionotropic alginate gels

Alginates have limited solubility in solution containing gelling ions such as Ca^{2+}, Ba^{2+}, and Zn^{2+}. However, pre-dissolved alginates in aqueous solution at physiological pH are polyanionic and can undergo sol-gel transition in the presence of divalent or multi-

valent cations, most commonly with Ca^{2+} or form interpenetrating polymer complex with polycations such as chitosan. Due to spatial arrangement of the ring and hydroxyl oxygen atoms of the monomers as shown in Figure 2-2, poly-guluronate (GG block) can form a stronger type of cooperative bonding with calcium ions (or other multi-valent cations), resulting in ionotropic gelation [25, 46]. Based upon the steric arrangements of the junction zones, this characteristic property has been described as an 'egg-box' model or zipper mechanism [46] (Figure 2-2).

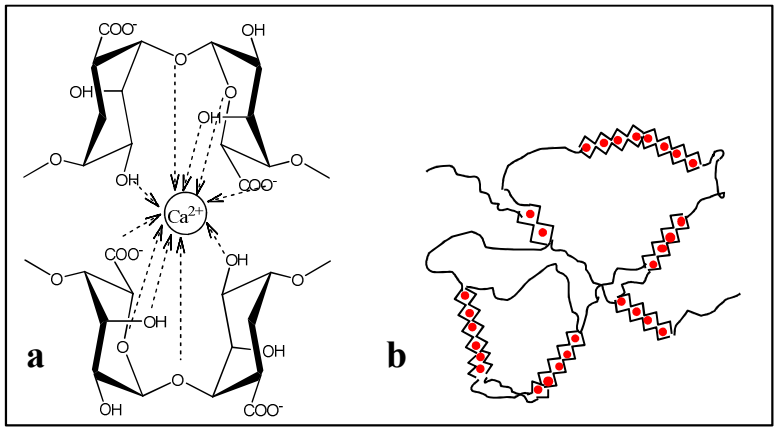

Figure 2-2. Schematic illustration of the molecular structure of alginate hydrogel. (a) Polyguluronate ionically interacting with calcium ions (circle) (b) "egg-box" model where GG blocks are represented by the zigzag ("egg-box") portions, and the MM and MG blocks are represented by the smooth parts of the polymer chains.

Haug and Smisdrod showed that the characteristic ion-binding properties were exclusive to polyguluronate with the affinity for alkaline earth metal ions increasing in the order of $Mg^{2+} << Ca^{2+} < Sr^{2+} < Ba^{2+}$, while polymannuronate and polyalternating blocks (MG or GM blocks) were almost without selectivity [47]. In addition, the amount of the ions which must be bound to the alginate is essential for the formation of alginate gels. For instance, below 3 mM Ca^{2+}, alginate remains soluble, yet formed stable gel at

calcium ion concentrations above the critical value[44]. The critical concentration was ion-specific, but independent of alginate concentration, and increased according to metal ion of the following order [48]:

$$Ba < Pb < Cu < Sr < Cd < Ca < Zn < Ni < Co < Mn = Fe < Mg$$

However, due to toxicity concerns when utilizing the gel in biomedical or tissue engineering applications, Ca^{2+} is the most commonly used gelling ion for alginates.

The consequent gelling capacity and physical properties of alginate gels such as permeability, pore size and mechanical strength, depend not only on the type and concentration of cations introduced, but also depend strongly on the molecular size and concentration of alginate polymer, and chemical composition and sequential arrangements of uronic acid blocks within the polysaccharide chain[25,44,49,50]. For instance, guluronate rich alginates tend to form stronger but brittle gels whereas mannuronic rich alginates form softer, yet more flexible gels [25]. According to Draget, the highest mechanical strength, lowest shrinkage, and best stability of alginate gels were found when the fraction of guluronate distribution was about 70% and guluronic acid residue length (polyguluronate) or GG block length was greater than 15 [25]. In addition, the gel strength increases as the molecular size of alginate polymer increases, yet the gel strength is independent of the molecular weight when the size of the polymer is greater than 80 kDa[25]. A linear relation between the gel compression strength and the alginate concentration was noted by Smidsrod in which an increase in calcium-alginate concentration resulted in increased gel stiffness[51].

Since physical gels such as calcium alginate are stabilized through cooperative binding with divalent cations, the gel can gradually loose its mechanical stability in biological fluids, due to an outwards flux of crosslinked calcium ions into the surrounding medium. In addition, calcium alginate readily destabilized and reversed back to sol state in the presence of EDTA or monovalent cations such as Na^+ or complex anions such as phosphate, citrate, and lactate, which have high affinity for calcium ions.

2.3.3.4 Diffusion and pore properties of calcium alginate

The average pore size or mesh size of an encapsulation matrix is an important factor to be considered for selection of an effective encapsulation matrix or controlled release device. The permeability of solutes such as proteins within alginate gels is largely related to the size and charge of proteins, and the matrix porosity, which is dependent on alginate chemical composition, and the gelling agent/multi-valent cation concentration [25, 44, 52]. The pore size distribution of alginate matrix was reported to be in the range between 5 and 200 nm as observed in electron micrographs [53]. Decho used atomic force microscopy to exam 2% alginate gel formed in seawater (30 ppt salinity mainly composed of 14.73 g/L NaCl, 1.32 g/L $CaCl_2$, 4.66 g/L $MgCl_2$, 4.66 g/L of $MgSO_4$) and observed that the diameter of solvent cavities (pore size) ranged between 22 and 58 nm (Figure 2-3) [54]. Variations between pore sizes observed could likely be due to different microscopic techniques or gel preparation methods. Studies on transport characteristics of alginate through measuring the diffusion coefficients of various molecular size solutes

into the gel provided estimates of the gel pore sizes ranging between 15-20 nm for 1.5-3.0% calcium alginate [55-57].

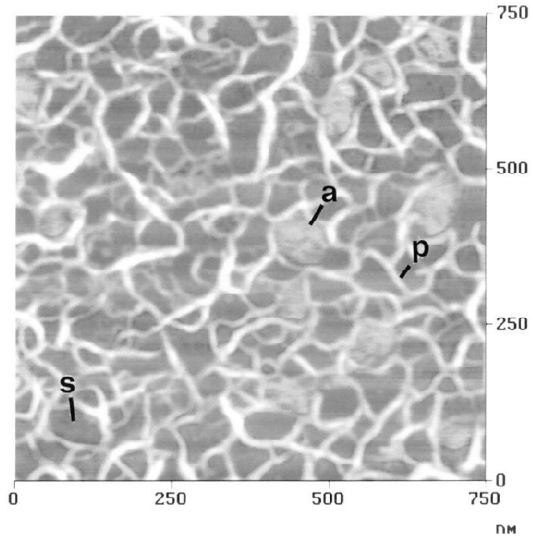

Figure 2-3. AFM topography of an alginate gel (2%) in seawater (30 ppt salinity) where **s** is solvent cavity, **p** is alginate polymer and **a** is artifact. Duplicated image from *Carbohydrate Research*, 1999. **315**(3-4): p. 330-333.

Many attempts to control/modify the porous structure and the release characteristics of alginate gel have been described, mainly through selection or blending of alginate materials [58] that can provide differences in molecular weight or distribution of one or both of the two monomers making up the polymer. Other approaches have included enzymatic synthesis of alginate with specific monomeric composition and molecular weight[59], or by applying cationic polymer coatings[60]. However, alginate is too porous for encapsulation of small molecular weight solutes. According to Tanaka *et al.*, proteins with molecular weight less than 20 kDa were able to diffuse freely into and out of alginate gel beads [61]. In contrast, for tissue engineering applications, alginate gel pores must be large enough to allow the passage of large nutrient molecules. The largest

biomolecule reported which was able to diffuse through alginate was immunoglobulin G (IgG, 155 kDa) into weakly crosslinked calcium alginate gel made from 1.5% alginate with 1% $CaCl_2$ for 1 min [56]. For 2% alginate, larger solutes such as bovine serum abumin (BSA, 67 kDa) cannot penetrate into or be released from 2% alginate matrix [62].

2.3.3.5 Formation of calcium alginate microspheres

The most common technique for preparation of calcium alginate microspheres is to extrude alginate solution dropwise into a calcium chloride gelation solution. This method is known as the extrusion/external gelation or dialysis/diffusion method as the alginate solution is gelled by diffusion of gelling ions (typically calcium) from an external source. Alternatively, an alginate solution can be gelled by internal release of the calcium, i.e., *in situ* gelling [63, 64]. The emulsification/internal gelation method can produce very small diameter (nano to micro to millimetre size range) and large quantities of gel beads. By this method, an insoluble calcium salt is mixed with alginate sol prior to gelation. The alginate sol is then dispersed in oil resulting in water-in-oil (W/O) emulsion, and the on-set of gelation triggered by the reduction of pH from 7.0 to 6.5. Calcium ions are liberated from insoluble calcium carbonate salt inducing gelation [64-66]. The bead size can be controlled from nanometers to millimeters in diameter through the adjustment of the emulsification conditions[64]. Homogeneous alginate gels are usually formed using this technique compared to external gelation [67] in which calcium, alginate and protein are non-uniformly distributed, forming heterogeneous gels [68].

2.3.3.6 Protein encapsulation by absorptive encapsulation protocol

Typically, protein encapsulation within calcium-alginate gel involves dropwise extrusion of alginate sol containing protein biomolecules into a calcium ion rich solution, forming instantaneous, ionotropic alginate microspheres. This encapsulation procedure involves the introduction of active biomolecules (encapsulant) to the alginate sol, *a priori*, prior to gelation. Due to the hydrophilic nature of most proteins and porous characteristics of alginate gels, poor protein retention within the gel matrix is normally encountered following the on-set of gelation, and in aqueous environment. Mass encapsulation yield of small proteins/peptides having molecular weight less than 20 kDa is often less than 0.1% [61, 69].

Alternative protein encapsulation approaches can be achieved by absorptive encapsulation whereby preformed alginate beads are loaded in bioactive concentrates [52]. In this procedure, active biomolecules are encapsulated *a postori*, thus following gelation. The absorptive encapsulation approach utilizes the porous nature of the alginate gel, and decouples the loading of bioactives from the bead production environment, offering the ability to customize gel bead properties without damaging the labile or sensitive biologicals. Subtilisin was previously loaded into calcium alginate with the resultant dry beads consisting of over 50% active subtilisin by mass and near zero loss in enzymatic activity, levels that are considerably higher than that achieved by most encapsulation technologies[52].

Absorptive encapsulation is cost-effective since "blank" gel beads may be formulated in large batches, decoupling this process from the subsequent loading of individual actives in smaller, customized batches. In addition, fines or oversized blanks can be rejected or recycled prior to loading, minimizing the loss of more valuable active ingredients. Gels in particular are permeable to molecules with a wide range of molecular weights including enzymes and therapeutic proteins, so the encapsulation technique can be applied to wide range of active biologicals. However, since flexibility in alginate polymer selection is limited, as is control of the final pore properties of the hydrogel, only small molecular sizes of biomolecules can diffuse freely into calcium alginate. Li et al attempted to formulate large pore sized calcium alginate gel by controlling the gelation time in calcium solution, follow by swelling the hydrogel in NaCl solution prior to protein loading. This enabled BSA to freely diffuse into the swollen, loosely crosslinked calcium alginate (less than 1% w/v)[56]. This is the largest biomolecule ever reported to diffuse into calcium alginate gel. In addition, due to the physical nature of the ionotropic gel, calcium alginate disintegrates in an uncontrollable fashion and may lead to complete dissolution during protein loading in phosphate buffered saline (PBS) or medium containing citrate, phosphates, or high concentration of sodium ion. Therefore, chemical modification of alginate, forming semi-synthetic biopolymer, may enable control of properties generally not possible with the native polymer such as improved mechanical properties, control of biodegradability, biocompatibility, swelling, diffusion/release characteristics and pore sizes. The focus of this thesis is therefore to develop chemically modified alginate gels with controlled pore properties for encapsulation of a wide range of molecular sizes of biomolecules, particularly for drug delivery application.

2.4 Chemical modification of alginate

Alginates may be utilized as starting materials/building blocks in semisynthesis of new classes of biopolymers, chemically tailored to match, improve, and offer unique physical, chemical, and in some cases biological functionality for a desired end use. Propylene glycol alginate (PGA) as an example is a chemically modified, semi-synthetic alginate polymer produced by reaction with propylene oxide. The carboxylic acid group is substituted with hydroxyester, and the polymer gelling capacity decreased with increased substitution. Complete substitution can lead to absence of gelling ability of polymer in ionic or acidic solutions [17]. PGA is the only commercially available alginate derivative, which is used as an emulsifier, stabilizer, and thickener in acidic food applications such as salad dressing, yogurt and ice cream.

Alginate can alter its hydrophilic nature through chemical attachment of cyclodextrins or copolymerization with hydrophobic polymers. For instance, to utilize alginate for encapsulation and sustained release of hydrophobic drugs, cyclodextrins (CD) can be covalently linked to alginate polymer, resulting in new class of biopolymers[70]. CD-derivatives of alginate conjugates exhibited size specificity of cyclodextrin and transport properties of alginate polymer matrix [70]. To control polymer degradation, which ultimately controls the rate of drug release, or to improve cell adhesive properties in the tissue scaffold, Bouhadir *et al.* [71] isolated polyguluronate from alginates and covalently crosslinked it with adipic dihydrazide and cell adhesion peptides. For specific adhesion to

protein substrates, alginate was chemically modified with both poly(acrylic acid) and poly(N,N-dimethylaminoethyl acrylate) through radical grafting of acrylic monomers[72].

To improve biocompatibility of tissue implants, the hydrogel scaffolds are generally designed to reduce protein adsorption, minimizing the cascade of the undesirable biological responses such as thrombus formation, capsulation, and inflammation. Laurienzo *et al*. modified alginate with poly(ethylene glycol) (PEG) which is known for its reduction in non-specific protein adsorption, low toxicity and immunogenic properties to form graft copolymer [73, 74]. Alginate-g-PEG still retains the gelation characteristics of alginate and showed improved cell viability in the scaffold [73]. Another strategy to improve biocompatibility of alginates is by inserting medium-long chain (C_4-C_{16}) alkylic amines to linear alginate (hydrophobization)[17]. Alkylated alginate derivatives demonstrate amphiphilic properties in aqueous medium and have been reported to promote cell grow and attachment.

2.4.1 Synthesis of chemical alginate gels

Alginate chemical gel can be formed by reaction with reactive functional molecules such as epoxy[75-77], cyanimide[78], carbodiimides and ethylenediamine[71, 79-82], and glutaraldehyde[83-86], resulting in three-dimensional network hydrogel. The first covalent crosslinked alginate was introduced by Burns *et al.* to improve the mechanical strength of the alginate for chromatographic bioseparation[87]. Alginate was chemically crosslinked with organic titanates at the hydroxyl functional sites. Alginate chemical hydrogel can

also be prepared by reaction with cyanogen bromide and 1,6-diaminohexane, and used for contaminant removal (Cu^{2+}, Mn^{2+})[78]. Biodegradable alginate gel was prepared by crosslinking reaction between carbodiimide and ethylenediamine with polyguluronates[80, 81]. Glutaraldehyde was used to crosslink alginate for encapsulation of liquid pesticide for soil pest control, for cadmium and heavy metals removal, and for pervaporation separation of water-acetic acid mixtures[83-86].

Alginate is cooperatively bound with di- or trivalent cations and exhibits high degree of crosslinking in the physical gel system, resulting in comparatively short, and inflexible elastic chains with limited swelling capacity. In contrast, the long, inflexible junction zones are substituted by small, discrete crosslinks distributed throughout alginate chemical gel. This leads to chemical gel with dramatically different swelling behavior. Skjak-Braek *et al.* demonstrated the superswelling characteristics of epichlorohydrin crosslinked alginate which can absorb water up to a hundred times its dry state volume[75,88]. The superabsorbent/superswelling property of covalent crosslinked alginate has found applications in environmental clean up and personal hygiene products.

2.4.1.1 Physical properties of glutaraldehyde and its use in biomedical applications

Glutaraldehyde (pentanedial) consists of two reactive aldehyde functional groups (Figure 2-4, structure 1) and is an effective crosslinker in generating chemically, biologically and thermally stable crosslinks with amines and hydroxyls. Glutaraldehyde has been used for the preparation of bioprostheses such as heart valves, vascular grafts,

elastic cartilages, and artificial skin, and for the fixation of cells, immobilization of enzymes and crosslinking of proteins and polysaccharides in controlled drug delivery applications[89, 90]. In addition, the cytotoxicity of glutaraldehyde was found to be much lower compared to other types of aldehyde and chemical crosslinkers and can be reduced after complete removal or inactivation of the excess unreacted aldehydes[89,91,92]. Since glutaraldehyde is highly soluble in both organic and aqueous phases, the unreacted reagent can be readily removed by adequate rinsing of the biomaterial with normal saline or quenching with high concentration of L-glutamic acid, glycine, or methanol[89, 93]. Post-fixation treatment of glutaraldehyde crosslinked bioprostheses using amino acid solutions has been reported to increase biocompatibility and endothelial cell attachment[94].

Although there have been controversial findings on the cytotoxicity of glutaraldehyde-fixed bioprostheses in animal models, most researchers reported that the adverse effects of glutaraldehyde were mainly due to residual glutaraldehyde remaining in the materials/device. According to the US Occupational Safety and Health Administration, the permissible exposure limit for glutaraldehyde is 0.8 mg/m^3 (0.2 ppm)[95]. This ceiling concentration was based on the irritant effects to the eyes, nose, and throat that have been associated with short-term exposure. In addition, preliminary results of a developmental toxicity study in which rabbits were administered glutaraldehyde for 13 consecutive days indicated that the high dose of greater than 15 mg/kg was severely toxic while doses lower than the critical limit were non-toxic[96]. According to pharmacokinetic study, glutaraldehyde was metabolized through urinary excretion and the probable metabolic pathway involves a series of oxidation, decarboxylation, and

hydration reactions[97]. The initial step is probably oxidation of glutaraldehyde to glutaric semialdehyde, followed by oxidation to glutaric acid, which can undergo further metabolism to acetate or be converted to CO_2.

Aqueous solutions of monomeric glutaraldehyde have ultraviolet absorption spectra at 280 nm. In the presence of oxygen and at elevated temperature, monomeric glutaraldehyde can undergo oxidative degradation, resulting in glutaric acid (**3**) and aldol-polymerization/condensation, forming poly-cyclic (**4**) and α,β-unsaturated poly-glutaraldehyde (**5**) as shown in Figure 2-4[98,99]. The cyclic or linear polymeric glutaraldehyde possesses different reactivity as compared to the monomeric form [100]. The glutaraldehyde derivatives of structures 5-7 absorb at 235 nm and these impurities can be removed by various means such as activated carbon or distillation.

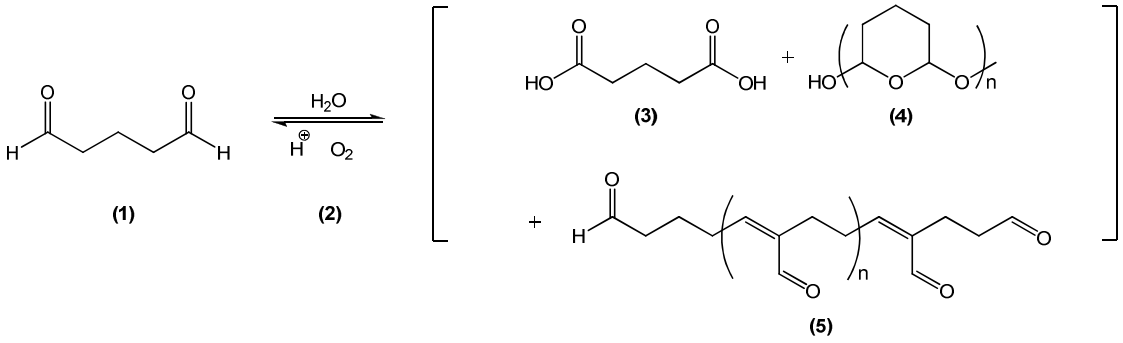

Figure 2-4. Chemical structures of glutaraldehyde and its derivates.

2.4.1.2 Glutaraldehyde crosslinked alginate gel

Aldehydes are known to react with alcohols in the presence of an acid catalyst to yield acetals, $R_2C(OR')_2$ (Figure 2-5) [101]. Alginate chemical gel prepared by reaction with

aldehyde could preserve carboxylic acid moieties as stimuli-responsive sensors on the polymer backbone.

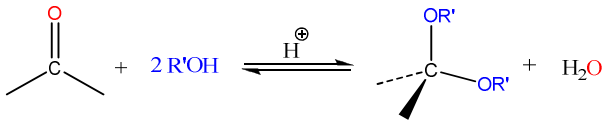

Figure 2-5. Acid-catalyzed acetal formation by reaction of an aldehyde with an alcohol.

Soluble alginate polymers can be interconnected by glutaraldehyde, forming network polymer gel in the presence of acid catalyst [83-86]. From X-ray diffractometry and swelling analysis, the extent of crosslinking increases with increase in the exposure time to the chemical crosslinkers, and increase in glutaraldehyde concentration[83-86]. However, these studies only characterized the effect of the exposure time to glutaraldehyde of less than 30 min and the highest concentration of glutaraldehyde attempted was less than 25 mM [83-86]. The focus of these previous studies was mainly to improve gel mechanical properties for ion-exchange or encapsulation purposes, and no attempts to characterize the reaction mechanism or kinetics have been reported. Therefore, as part of the research scope, the detailed reaction mechanism and kinetics will be developed along with a predictive reaction model which may be used *a priori* to select reaction conditions such as duration, temperature, and reactant concentrations for ultimate control of crosslink density, providing specific polymer properties.

2.5 Swelling of network polyelectrolyte gels

The well-known fundamental concept of rubber elasticity has been described in the early work of Flory and Rehner [102, 103]. At equilibrium, the swelling potential due to polymer mixing $(\Delta\mu_1)_{mix}$, analogous to dissolving ordinary polymer in a good solvent (volume exclusion effect), is equal to the opposite elastic retractive potential $(\Delta\mu_1)_{el}$ consequential to the expansion of the network structure. The equilibrium relation can be described by equation 1,

$$-\left[\ln(1-v_2)+v_2+\chi_1 v_2^2\right] = (V_1/\bar{\upsilon}M_c)(1-2M_c/M_0)(v_2^{1/3}-v_2/2) \qquad \text{-Eq. 1}$$

where v_2 is the volume fraction of the polymer in the equilibrium swollen gel, χ_1 is the Flory-Huggins interaction parameter which represents the difference in energy of a solvent molecule surrounded by polymer molecules compared with that of the pure solvent environment, V_1 is the molar volume of solvent, M_o and $\bar{\upsilon}$ are the primary molecular weight and specific density of the polymer, and M_c is the molecular weight between two crosslink points. The right-hand term of equation 1 represents the chemical potential owing to mixing of polymer and solvent, and the right-hand term corresponds to elastic potential of the network.

If the polymeric network consists of charged moieties, swelling becomes more complex in which the swelling pressure may be greatly enhanced as a result of the localization of charge moieties, setting up an electrostatic repulsion between charged

polymers. Since polymers are covalently crosslinked, mobility of the charged moieties is constrained within the gel network and cannot diffuse into the outer solution. Counterions dissociated from the polymer chains are confined inside the gel due to electroneutrality effect. Consequently, the total mobile ion concentration inside the gel will exceed that in the external solution, leading to an osmotic pressure difference which tends to drive solvent into the gel from the less concentrated external solution (closely resembles Donnan membrane equilibria) to reestablish the state of equilibrium [103-106]. At equilibrium, chemical potential differences of solvents inside the gel network must be equal to that of outside electrolytes. Symbolically,

$$(\Delta\mu_1^*)_{ion} - (\Delta\mu_1)_{ion} = (\Delta\mu_1)_{mix} + (\Delta\mu_1)_{el} \qquad \text{-Eq.2}$$

where $(\Delta\mu_1^*)_{ion} - (\Delta\mu_1)_{ion}$ represents the chemical potential difference due to uneven distribution of mobile ions in the external electrolyte (where the asterisk denotes external solution environment), and inside gel compartments. This term is also known as Donnan membrane potential.

2.5.1 Donnan membrane potential, $(\Delta\mu_1^*)_{ion} - (\Delta\mu_1)_{ion}$

Many mathematical models have been derived in attempts to approximate Donnan membrane potential for polyelectrolyte network gels [107-109]. Most swelling models were based on the pioneering work of Flory [104]. The electrical imbalance caused by mobile ions

diffusing from the external solution into the gel in an effort to establish individual ion equilibrium between the two phases, induces an osmotic pressure difference which expands the network by absorbing solvent from the less concentrated external solution. Flory derived a swelling model for polycationic gel with the incorporation of Donnan-Type equilibria and assumed ideal solution conditions [104, 110]. With reconsideration of the electroneutrality effect, Flory's gel model can be modified to accommodate polyanionic gel swelling as is the case for alginate gel. If the external swelling medium is significantly greater than the gel volume at equilibrium and the electrolyte completely dissociates into $C_{v_+}^{z^+} A_{v_-}^{z^-}$, then the external ionic concentration can be assumed to be vc_s^*, where v_+ and v_- represent the stoichiometric formula of the electrolyte and $v_+ z^+ = v_- z^-$ and $v = v_+ + v_-$ (asterisk denotes external solution environment).

In the case of equilibrium for networked polyanionic polymer, the gel will have acquired a concentration of c_s of mobile electrolyte from the external phase plus the cations, z^+, dissociated from the polymer. The concentrations of the mobile cations, c_+, and anions, c_-, in the gel, including those contributed by dissociation from the polymer, also known as gegen ions belonging to the polymer and occurring in the gel, ic_2, are:

$$c^+ = v_+ c_s + ic_2/v_+ z^+ \text{ and } c_- = v_- c_s \qquad \text{-Eq. 3}$$

where i is the degree of ionization of anionic polymer and c_2 is the molar concentration of the monomer unit which can be calculated from:

$$c_2 = \frac{V_p}{\bar{\upsilon} M_r} \frac{1}{V_s} = \frac{v_{2,s}}{\bar{\upsilon} M_r} \qquad \text{-Eq. 4}$$

Together with Van't Hoff's equation, $\Pi = \sum_i^n c_i RT$, and the thermodynamic relationship, $\pi = -(\mu_1 - \mu_1^0)/V_1$, the chemical potential difference of the solvent due to uneven mobile ion distribution can be estimated by equation 5.

$$(\Delta\mu_1^*)_{ion} - (\Delta\mu_1)_{ion} \cong -V_1 RT\left[ic_2 / v_+ z^+ + v(c_s^* - c_s)\right] \qquad \text{-Eq. 5}$$

Assuming the activity of a solute can be approximated to equal its concentration at low ionic concentration, equation 5 can be shown as:

$$[(c_s + ic_2 / v_+ z^+)/c_s^*]^{v_+} = (c_s^* / c_s)^{v_-} \qquad \text{-Eq. 6}$$

Since there is no explicit general solution in evaluating the quantity of $c_s^* - c_s$, Flory resorted to the consideration of special cases. For the case of comparable or larger external electrolyte concentration compared with the gegen ions belonging to the polymer, $c_s^* > \frac{ic_2}{z^+ v_+}$:

$$(\Delta\mu_1^*)_i - (\Delta\mu_1)_i = V_1 RT(i^2 c_2^2 / 4I^*)\left\{1 + (z^+ - z^-)ic_2 / 3I^* + [2(z^+)^2 - 5z^- z^+ + 2(z^-)^2](ic_2)^2 / 16(I^*)^2 + \ldots\right\} \qquad \text{-Eq. 7}$$

where I is the ionic strength of the electrolyte solution. A relationship equivalent to equation 7 was obtained by Vermaas and Hermans[111] which only include the first two

terms in the expansion series. In the case of binary electrolyte for which $z^+ = z^- = z$, and $v_+ = v_- = 1$ and $v = 2$, the second term in the series vanishes but not the third in equation 7.

$$(\Delta\mu_1^*)_i - (\Delta\mu_1)_i = V_1 RT\,(i^2 c_2^2 / 4I^*)[1 - z^2 (ic_2)^2 / 16(I^*)^2 + ...] \qquad \text{-Eq. 8}$$

Combining equation 2 and 8 with the expression of elastic and mixing potentials from equation 1, the equilibrium swelling of electrolyte gels can be described by equation 8b.

$$\begin{aligned} &V_1 RT(i^2 c_2^2 / 4I^*)[1 - z^2 (ic_2)^2 / 16(I^*)^2 + ...] = \\ &(V_1 / \bar{\upsilon} M_c)(1 - 2M_c / M_0)(v_2^{1/3} - v_2 / 2) + \left[\ln(1 - v_2) + v_2 + \chi_1 v_2^2\right] \end{aligned} \qquad \text{-Eq. 8b}$$

In the limit of a large ratio of the ionic strength compared with the gegen ion concentration in the gel, ic_2, the ionic terms in equation 8 vanish and the swelling relationship reverts to that similar for the uncharged network in equation 1. In this case, the uneven distribution of mobile ion concentration is greatly suppressed by the large excess of simple electrolyte. In the opposite case in which the external electrolyte concentration is extremely small compared with the fixed ionic concentration inside the gel, $c_s^* << \frac{ic_2}{z^+ v_+}$, then the appropriate series expansion according to Flory [104] is:

$$(\Delta\mu_1^*)_i - (\Delta\mu_1)_i = V_1 RT\,(ic_2 / z) - 2c_s^*[1 - zc_s^* / ic_2 + (zc_s^* / ic_2)^3 - 2(zc_s^* / ic_2)^5 + ...] \qquad \text{-Eq. 9}$$

The equilibrium relation can be rewritten as:

$$\begin{aligned} &V_1 RT(ic_2 / z) - 2c_s^*[1 - zc_s^* / ic_2 + (zc_s^* / ic_2)^3 - 2(zc_s^* / ic_2)^5 + ...] = \\ &(V_1 / \bar{\upsilon} M_c)(1 - 2M_c / M_0)(v_2^{1/3} - v_2 / 2) + \left[\ln(1 - v_2) + v_2 + \chi_1 v_2^2\right] \end{aligned} \qquad \text{-Eq. 9b}$$

The gel swelling depends on the crosslink density (commonly known as molecular weight between crosslink points), and solution ionic strength and pH of the electrolyte solution. According to Moe, the swelling induced by the imbalance in electric potential has been shown to far exceed the mixing potential, which contribute to approximately 90% of the overall swelling pressure in an epoxy-crosslinked alginate gel [75]. Using equation 8b or 9b, the equilibrium swelling volume of electrolyte gels can be estimated from the known crosslink density and suspending electrolyte environments. The swelling models can also be used vice versa to predict the crosslink density of the gel network from the measured equilibrium swelling volume of the gel.

2.5.2 Ion-pairing phenomena of polyelectrolyte

The concept of counter ion condensation was described by Manning [112]. When the polyelectrolyte is strongly charged, the electrostatic potential on the chain is large and some of the dissociated counterions remain bound to the chain. This phenomenon is known as ion-pairing or counterion condensation. The effective charge is lower than the nominal charge of the monomers, thus counterion condensation can be effective even at infinite dilution and reduces the electrostatic interactions between monomers. The Manning theory describes the counterion distribution by a step function. For an infinitely dilution solution, the fraction of non-condensed counterions f_ζ can be estimated by equation 10[113].

$$\varsigma < Z^{-1}, \quad f_{\varsigma} = (Z\varsigma)^{-1}$$
$$\varsigma > Z^{-1}, \quad f_{\varsigma} = 1 \qquad \text{-Eq. 10}$$

where Z is the counterion valence and ζ is a dimensionless measure of linear polyelectrolyte charge density as defined by equation 11.

$$\varsigma = \frac{e^2}{\varepsilon k_B T b} \qquad \text{-Eq. 11}$$

where e is the protonic charge, ε the bulk dielectric constant of solvent, k_B is Boltzmann's constant, T is the temperature in Kelvin, and b is the average linear charge spacing of the polyelectrolyte (ie. between two uronic acids) taken along the contour length of the polymeric chain. f_{ξ} is also known as the Manning-Fraction which is predicted not to depend on ionic strength or concentration of free counterions and remains a constant at very high dilutions[113].

Manning demonstrated that DNA, a linear polyelectrolyte had a maximum charge density such that when this maximum was exceeded, the counterions would "condense" onto the polymer chains, reducing the anticipated osmotic activities. The charges on the polyelectrolyte were separated by about 0.7 nm in water at 25^{o}C, corresponding to a linear charge density of 1.4 unit charges per nm as the limiting (maximum) charge. NMR experiments showed that a charge fraction of DNA between 0.15 and 0.35 was measured and remained fairly constant in NaCl solution in the range of 0.006-0.6 M. Although condensed counterion resides in the vicinity of a polyelectrolyte due to high electrostatic

interaction, it may exchange rapidly with a free counterion of higher affinity in the suspended solution.

2.5.3 Electrochemistry and ionic activity of electrolytes

The exchange of ions and solvent between chemically networked polyelectrolyte gels and the surrounding electrolyte closely resembles Donnan membrane equilibria in which charged moities are fixed on the polymer and cannot diffusion into the outer solution while small electrolytes such as NaCl, KCl and solvent are free to diffuse in and out to establish the ionic equilibria. At the state of equilibrium, the electrostatic potential on both sides of the compartment (gel and external suspending solution) must be equal. Therefore, the activity of diffusible/mobile ion concentrations must be the same on both sides. The basis of the electrochemistry of the electrolyte is presented in the following sections.

2.5.4 Chemical potential of the electrolyte

2.5.4.1 Activity of the electrolyte solution

The activity of a solute substance *i* can be defined by equation 12.

$$a_i = \frac{\gamma_i c_i}{c^o} \qquad \text{-Eq. 12}$$

where c^o is the standard value of the molar concentration (1 mol L^{-1}), and in dilute solution environment, $\lim_{c_i \to 0} \gamma_i = 1$, the activity coefficient is approaching unity and activity

can be approximate with concentration of the solution. For ionic solution containing strong electrolyte, $A_{v_+}B_{v_-}$, of concentration c_s, the activity of the electrolytes can be expressed as:

$$a_{A_{v+}B_{v-}} = \left(\gamma_{\pm} c_{\pm}\right)^{v_{\pm}} = \gamma_{\pm}^{v_{\pm}} c_s^{v_{\pm}} \left(v_+^{v_+} v_-^{v_-}\right) \qquad \text{-Eq. 13}$$
$$v_{\pm} = v_+ + v_-$$

As examples, the activities of uni-univalent (1:1), bi-univalent (2:1), bi-bivalent (2:2) and tri-univalent (3:1) electrolytes expressed using equation 13 are:

$$\begin{aligned} a_{1:1} &= c_s^2 \gamma_{\pm}^2 \\ a_{2:1} &= 4 c_s^3 \gamma_{\pm}^3 \\ a_{2:2} &= c_s^2 \gamma_{\pm}^2 \\ a_{3:1} &= 27 c_s^4 \gamma_{\pm}^4 \end{aligned} \qquad \text{-Eq. 14}$$

Due to electroneutrality, equation 15 has to hold true at all times:

$$c_s = \frac{c_+}{v_+} = \frac{c_-}{v_-} \qquad \text{-Eq. 15}$$

The chemical potentials, μ, of the cation and anion are given by:

$$\begin{aligned} \mu &= v_+ \mu_+ + v_- \mu_- \\ \mu_+ &= \mu_+^0 + RT \ln \gamma_+ c_+ \\ \mu_- &= \mu_-^0 + RT \ln \gamma_- c_- \end{aligned} \qquad \text{-Eq. 14}$$

where μ_+^0, μ_-^0 are the standard state chemical potentials and γ_-, γ_+ are the activity coefficients of the cation and anion. The chemical potential for the electrolyte can be recast as,

$$\mu = \left(v_+ \mu_+^0 + v_- \mu_-^0\right) + RT \ln \gamma_+^{v_+} \gamma_-^{v_-} c_+^{v_+} c_-^{v_-} \qquad \text{-Eq. 15}$$

Mean ionic molarity, $c_{\pm}$ and mean ionic activity coefficient, $\gamma_{\pm}$ are defined as

$$c_{\pm} = c_s \left(v_+^{v_+} v_-^{v_-} \right)^{1/v_{\pm}}$$
$$\gamma_{\pm} = \left(\gamma_+^{v_+} \gamma_-^{v_-} \right)^{1/v_{\pm}} \qquad \text{-Eq. 16}$$

Combining equations 12-16, chemical potential of the electrolyte can be described by equation 17.

$$\mu = \mu^0 + v_{\pm} RT \ln \gamma_{\pm} c_{\pm} \qquad \text{-Eq. 17}$$

2.5.4.2 Mean electrolyte activity

The activity coefficient deviates away from unity as the dilute solution environment no longer holds true. Pitzer-Mayorga derived an equation to estimate activity coefficients of simple electrolyte which is based on Debye-Huckel radial distribution function and the osmotic pressure equation of statistical mechanics [114]. Mean electrolyte coefficient can be approximated using equation 18.

$$\ln \gamma_{\pm} = |z_+ z_-| f + m \left(\frac{2 v_+ v_-}{v} \right) B + m^2 \left(\frac{2 (v_+ v_-)^{3/2}}{v} \right) C \qquad \text{-Eq. 18}$$

$$f = -A \left[\frac{I^{1/2}}{1 + bI^{1/2}} + \frac{2}{b} \ln(1 + bI^{1/2}) \right]$$

$$B = 2\beta^{(1)} + \frac{2\beta^{(2)}}{\alpha^2 I} \left[1 - e^{\alpha I^{1/2}} (1 + \alpha I^{1/2} - (1/2)\alpha^2 I \right]$$

$$C = (3/2)\beta^{(3)}$$

where v_+ and v_- are the valences of cation and anion in the electrolyte, and z_+ and z_- are the respective charges and $v = v_+ + v_-$, m is the solvent concentration in molality, I is the ionic strength, A is the Debye-Huckel coefficient for the osmotic function which has the value of 0.392 for water at 25°C, b and are constants which have values of 1.2 and 2.0, respectively for most of the electrolytes, and $\beta^{(1)}$, $\beta^{(2)}$, $\beta^{(3)}$, are the first, second and third viral coefficients. The viral coefficients of some common electrolytes are shown in Table 2-1. Plots of activity coefficients of various electrolytes as function of solution ionic strength are presented in Figure 2-6 in which increased ionic strength of the solution, subsequently deviated the activity coefficients away from unity.

Table 2-1. The viral coefficients of common inorganic salts[115]

Electrolyte	$\beta^{(1)}$	$\beta^{(2)}$	$\beta^{(3)}$
LiCl	0.1494	0.3074	0.00359
NaCl	0.0765	0.2664	0.00127
NaBr	0.0973	0.2791	0.00116
NaH_2PO_4	-0.0533	0.0396	0.00795
KCl	0.04835	0.2122	-0.00084
Na_2SO_4	0.0196	1.113	0.02584
K_2HPO_4	0.02475	1.2742	0.08515
MgCl2	0.4698	2.242	0.00979
MgBr2	0.5769	2.337	0.0589
CaCl2	0.4212	2.152	-0.00064
BaCl2	0.3504	1.995	-0.03654

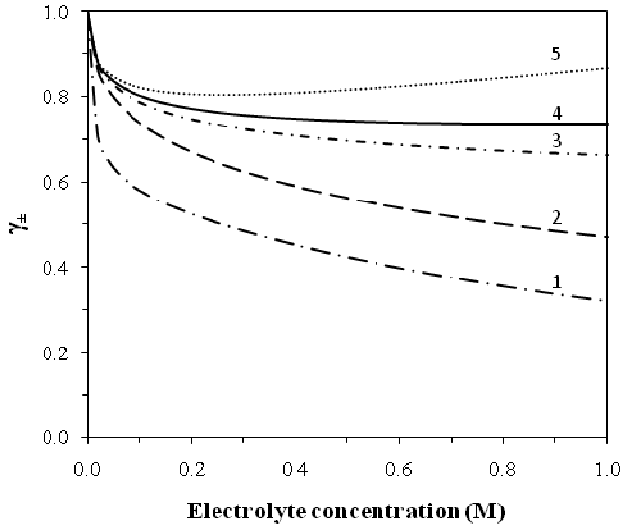

Figure 2-6. Mean activity coefficients of Na_2HPO_4 (1), NaH_2PO_4 (2), KCl (3), NaCl (4), $NaCH_3COO$ (5) calculated using Pitzer-Mayorga equation.

2.6 Scope of research and objectives

Alginates have been studied for many years in an effort to relate chemical composition of the polymer to its physical properties, however flexibility in polymer selection is limited, as is control of the final properties of the polymer constructs. The scope of this PhD research has been to chemically modify alginate to enable the control of properties generally not possible with the native polymer. Properties of interest include pH-responsive swell/contraction for controlled release devices in the GI tract, and controlled permeability and pore size. The overall objective is to formulate tuneable alginate based pH-sensitive biomaterial for encapsulation of a wide range of molecular sizes of therapeutic proteins via the absorptive encapsulation method. As a potential oral drug delivery vehicle, a responsive swelling-controlled system should contract under

acidic condition, thus retain and protect the bioactive within the tight alginate matrix, while swelling at alkaline pH, releasing active encapsulant.

The specific objectives of this research are:

1. Kinetic and thermodynamic controlled synthesis of acetal-linked alginate based hydrogel, involving:

    i. establishing a formulation protocol for glutaraldehyde crosslinked alginate gel beads/granules;
    ii. proposing a reaction mechanism;
    iii. and studying the acetalization reaction kinetics for alginate with glutaraldehyde.

2. Characterization of the developed alginate based hydrogel by:

    i. conducting a structural analysis of glutaraldehyde crosslinked alginate gel by nuclear magnetic resonance;
    ii. studying the effect of reaction parameters on crosslink density which include a) concentrations of glutaraldehyde and acid catalyst, b) reaction time and temperature, and c) the effect of solvent composition in the reaction media;
    iii. characterizing the alginate network structure based on the quantitative analysis of molecular weight between crosslinks and the corresponding mesh size. The matrix porosity will also be determined experimentally by

diffusion of model solutes such as bovine serum albumin. The surface topography and morphology of alginate gel beads and granules will be studied;

iv. characterizing pH-swelling behaviour of covalent crosslinked alginate granules and studying the effect of degree of crosslinking, alginate G content, and alginate concentration on the equilibrium swelling ratio.

3. Diffusion characterization of chemically modified alginate gel beads/granules by:

   i. characterizing diffusion of model biomolecules of wide range molecular weight, including vitamin B12, insulin, BSA, lysozyme, subitlisin, and urease into and out from chemical alginate gels. Alginate beads with a theoretical pore size greater than that of the model proteins are produced and the corresponding encapsulation efficiencies will be evaluated;

   ii. Demonstration of the potential use of chemically crosslinked alginate gel as an oral drug delivery vehicle for therapeutic proteins. The encapsulation efficiency of insulin and its release kinetics, and the bioactivity of the released insulin in a simulated gastrointestinal pH environment will be determined.

4. Derivation of a generalized swelling model for chemically modified alginate which can readily estimate molecular weight between two consecutive crosslinks, crosslink density, or pore sizes from the determined swollen gel volume in both salt-free and high ionic concentration environments, involving:

i. rheological study of alginate polymers in various ionic and pH solutions;

ii. estimation of pore sizes of the cross-linked hydrogel by the derived swelling model and comparison to those determined by thermoporometry and protein diffusion.

2.7 References

1. Bajpai, A. K.; Shukla, S. K.; Bhanu, S.; Kankane, S., Responsive polymers in controlled drug delivery. *Progress in Polymer Science* **2008,** 33, (11), 1088-1118.

2. Cartmell, S., Controlled Release Scaffolds for Bone Tissue Engineering. *Journal of Pharmaceutical Sciences* **2009,** 98, (2), 430-441.

3. Quaglia, F., Bioinspired tissue engineering: The great promise of protein delivery technologies. *International Journal of Pharmaceutics* **2008,** 364, (2), 281-297.

4. Mano, J. F., Stimuli-responsive polymeric systems for biomedical applications. *Advanced Engineering Materials* **2008,** 10, (6), 515-527.

5. Yoshida, R., Design of functional polymer gels and their application to biomimetic materials. *Current Organic Chemistry* **2005,** 9, (16), 1617-1641.

6. Roy, I.; Gupta, M. N., Smart polymeric materials: Emerging biochemical applications. *Chemistry & Biology* **2003,** 10, (12), 1161-1171.

7. Galaev, I. Y., Smart Polymers in Biotechnology and Medicine. *Uspekhi Khimii* **1995,** 64, (5), 505-524.

8. Chaterji, S.; Kwon, I. K.; Park, K., Smart polymeric gels: Redefining the limits of biomedical devices. *Progress in Polymer Science* **2007,** 32, (8-9), 1083-1122.

9. Katchalsky, A.; Eisenberg, H., Molecular Weight of Polyacrylic and Polymethacrylic Acid. *Journal of Polymer Science* **1951,** 6, (2), 145-154.

10. Katchalsky, A., Rapid Swelling and Deswelling of Reversible Gels of Polymeric Acids by Ionization. *Experientia* **1949,** 5, (8), 319-320.

11. Gudeman, L. F.; Peppas, N. A., Ph-Sensitive Membranes from Poly(Vinyl Alcohol) Poly(Acrylic Acid) Interpenetrating Networks. *Journal of Membrane Science* **1995,** 107, (3), 239-248.

12. Bernkop-Schnurch, A.; Kast, C. E.; Richter, M. F., Improvement in the mucoadhesive properties of alginate by the covalent attachment of cysteine. *Journal of Controlled Release* **2001,** 71, (3), 277-285.

13. Smetana, K., Cell Biology of Hydrogels. *Biomaterials* **1993,** 14, (14), 1046-1050.

14. Khalil, M.; Shariat-Panahi, A.; Tootle, R.; Ryder, T.; McCloskey, P.; Roberts, E.; Hodgson, H.; Selden, C., Human hepatocyte cell lines proliferating as cohesive spheroid colonies in alginate markedly upregulate both synthetic and detoxificatory liver function. *Journal of Hepatology* **2001,** 34, (1), 68-77.

15. Garcia-Cruz, C. H.; Foggetti, U.; da Silva, A. N., Bacterial Alginate: Technological Aspects, Characteristics and Production. *Quimica Nova* **2008,** 31, (7), 1800-1806.

16. Qin, Y. M., Alginate fibres: an overview of the production processes and applications in wound management. *Polymer International* **2008,** 57, (2), 171-180.

17. d'Ayala, G. G.; Malinconico, M.; Laurienzo, P., Marine derived polysaccharides for biomedical applications: Chemical modification approaches. *Molecules* **2008,** 13, (9), 2069-2106.

18. Boateng, J. S.; Matthews, K. H.; Stevens, H. N. E.; Eccleston, G. M., Wound healing dressings and drug delivery systems: A review. *Journal of Pharmaceutical Sciences* **2008,** 97, (8), 2892-2923.

19. Elzatahry, A. A.; Eldin, M. S. M.; Soliman, E. A.; Hassan, E. A., Evaluation of Alginate-Chitosan Bioadhesive Beads as a Drug Delivery System for the Controlled Release of Theophylline. *Journal of Applied Polymer Science* **2009,** 111, (5), 2452-2459.

20. Tafaghodi, M.; Tabasi, S. A. S.; Jaafari, M. R., Formulation, characterization and release studies of alginate microspheres encapsulated with tetanus toxoid. *Journal of Biomaterials Science-Polymer Edition* **2006,** 17, (8), 909-924.

21. Smidsrod, O.; Skjakbraek, G., Alginate as Immobilization Matrix for Cells. *Trends in Biotechnology* **1990,** 8, (3), 71-78.

22. Sharma, A.; Sharma, S.; Gupta, M. N., Purification of wheat germ amylase by precipitation. *Protein Expression and Purification* **2000,** 18, (1), 111-114.

23. Sharma, S.; Gupta, M. N., Alginate as a macroaffinity ligand and an additive for enhanced activity and thermostability of lipases. *Biotechnology and Applied Biochemistry* **2001,** 33, 161-165.

24. Mondal, K.; Sharma, A.; Lata; Gupta, M. N., Macroaffinity ligand-facilitated three-phase partitioning (MLFTPP) of alpha-amylases using a modified alginate. *Biotechnology Progress* **2003,** 19, (2), 493-494.

25. Draget, K. I.; SkjakBraek, G.; Smidsrod, O., Alginate based new materials. *International Journal of Biological Macromolecules* **1997,** 21, (1-2), 47-55.

26. Haug, A.; Larsen, B., Quantitative Determination of Uronic Acid Composition of Alginates. *Acta Chemica Scandinavica* **1962,** 16, (8), 1908-1918.

27. Skjakbraek, G.; Zanetti, F.; Paoletti, S., Effect of Acetylation on Some Solution and Gelling Properties of Alginates. *Carbohydrate Research* **1989,** 185, (1), 131-138.

28. Skjakbraek, G.; Paoletti, S.; Gianferrara, T., Selective Acetylation of Mannuronic Acid Residues in Calcium Alginate Gels. *Carbohydrate Research* **1989,** 185, (1), 119-129.

29. Smidsrod, O.; Whitting.Sg, Monte Carlo Investigation of Chemical Inhomogeneity in Copolymers. *Macromolecules* **1969,** 2, (1), 42-44.

30. Larsen, B.; Smidsrod, O.; Haug, A.; Painter, T., Determination by a kinetic method of the nearest-neighbour frequencies in a fragment of alginic acid. *Acta Chem Scand* **1969,** 23, (7), 2375-88.

31. Smidsrod, O., Solution Properties of Alginate. *Carbohydrate Research* **1970,** 13, (3), 359-372.

32. Rioux, L. E.; Turgeon, S. L.; Beaulieu, M., Rheological characterisation of polysaccharides extracted from brown seaweeds. *Journal of the Science of Food and Agriculture* **2007,** 87, (9), 1630-1638.

33. Yuryev, V. P.; Grinberg, N. V.; Braudo, E. E.; Tolstoguzov, V. B., Study of the Boundary-Conditions for the Gel Formation of Alginates of Polyvalent Metals. *Starke* **1979,** 31, (4), 121-124.

34. McHugh, D. J., Production, Properties and Uses of Alginates. In *Production and Utilization of Products from Commercial Seaweeds*, Fish.Tech.Pap., F., Ed. 1987; Vol. 288.

35. Haug, A.; Larsen, B.; Smidsrod, O., A Study of Constitution of Alginic Acid by Partial Acid Hydrolysis. *Acta Chemica Scandinavica* **1966,** 20, (1), 183-190.

36. Larsen, B.; Smidsrod, O.; Painter, T.; Haug, A., Calculation of Nearest-Neighbour Frequencies in Fragments of Alginate from Yields of Free Monomers after Partial Hydrolysis. *Acta Chemica Scandinavica* **1970,** 24, (2), 726-728.

37. Haug, A.; Smidsrod, O.; Larsen, B., Degradation of Alginates at Different Ph Values. *Acta Chemica Scandinavica* **1963,** 17, (5), 1466-1468.

38. Holme, H. K.; Davidsen, L.; Kristiansen, A.; Smidsrod, O., Kinetics and mechanisms of depolymerization of alginate and chitosan in aqueous solution. *Carbohydrate Polymers* **2008,** 73, (4), 656-664.

39. Cesaro, A.; Delben, F.; Paoletti, S., Thermodynamics of the Proton Dissociation of Natural Polyuronic Acids. *International Journal of Biological Macromolecules* **1990,** 12, (3), 170-176.

40. Rey-Castro, C.; Herrero, R.; de Vicente, M. E. S., Gibbs-Donnan and specific-ion interaction theory descriptions of the effect of ionic strength on proton dissociation of alginic acid. *Journal of Electroanalytical Chemistry* **2004,** 564, (1-2), 223-230.

41. Draget, K. I.; Braek, G. S.; Smidsrod, O., Alginic Acid Gels - the Effect of Alginate Chemical-Composition and Molecular-Weight. *Carbohydrate Polymers* **1994,** 25, (1), 31-38.

42. Draget, K. I.; SkjakBraek, G.; Christensen, B. E.; Gaserod, O.; Smidsrod, O., Swelling and partial solubilization of alginic acid gel beads in acidic buffer. *Carbohydrate Polymers* **1996,** 29, (3), 209-215.

43. Smidsrod, O.; Haug, A., Dependence Upon Uronic Acid Composition of Some Ion-Exchange Properties of Alginates. *Acta Chemica Scandinavica* **1968,** 22, (6), 1989-&.

44. Draget, K. I.; Skjak-Braek, G.; Stokke, B. T., Similarities and differences between alginic acid gels and ionically crosslinked alginate gels. *Food Hydrocolloids* **2006,** 20, (2-3), 170-175.

45. Haug, A.; Larsen, B., Solubility of Alginate at Low Ph. *Acta Chemica Scandinavica* **1963,** 17, (6), 1653-1662.

46. Braccini, I.; Perez, S., Molecular basis of Ca2+-induced gelation in alginates and pectins: The egg-box model revisited. *Biomacromolecules* **2001,** 2, (4), 1089-1096.

47. Haug, A.; Smidsrod, O., Selectivity of Some Anionic Polymers for Divalent Metal Ions. *Acta Chemica Scandinavica* **1970,** 24, (3), 843-854.

48. Morch, Y. A.; Donati, I.; Strand, B. L.; Skjak-Braek, G., Effect of Ca2+, Ba2+, and Sr2+ on alginate microbeads. *Biomacromolecules* **2006,** 7, (5), 1471-1480.

49. Pasut, E.; Toffanin, R.; Voinovich, D.; Pedersini, C.; Murano, E.; Grassi, M., Mechanical and diffusive properties of homogeneous alginate gels in form of particles and cylinders. *Journal of Biomedical Materials Research Part A* **2008,** 87A, (3), 808-818.

50. Augst, A. D.; Kong, H. J.; Mooney, D. J., Alginate hydrogels as biomaterials. *Macromolecular Bioscience* **2006,** 6, (8), 623-633.

51. Smidsrod, O., Properties of Poly(1,4-Hexuronates) in Gel State .2. Comparison of Gels of Different Chemical Composition. *Acta Chemica Scandinavica* **1972,** 26, (1), 79-88.

52. Chan, A. W. J.; Becker, T.; Neufeld, R. J., Subtilisin absorptive encapsulation and granulation. *Process Biochemistry* **2005,** 40, (5), 1903-1910.

53. Smidsrod, O., Molecular-Basis for Some Physical-Properties of Alginates in Gel State. *Faraday Discussions* **1975,** 1974, (57), 263-275.

54. Decho, A. W., Imaging an alginate polymer gel matrix using atomic force microscopy. *Carbohydrate Research* **1999,** 315, (3-4), 330-333.

55. Klein, J.; Stock, J.; Vorlop, K. D., Pore-Size and Properties of Spherical Ca-Alginate Biocatalysts. *European Journal of Applied Microbiology and Biotechnology* **1983,** 18, (2), 86-91.

56. Li, R. H.; Altreuter, D. H.; Gentile, F. T., Transport characterization of hydrogel matrices for cell encapsulation. *Biotechnology and Bioengineering* **1996,** 50, (4), 365-373.

57. Jorgensen, T. E.; Sletmoen, M.; Draget, K. I.; Stokke, B. T., Influence of oligoguluronates on alginate gelation, kinetics, and polymer organization. *Biomacromolecules* **2007,** 8, (8), 2388-2397.

58. Boontheekul, T.; Kong, H. J.; Mooney, D. J., Controlling alginate gel degradation utilizing partial oxidation and bimodal molecular weight distribution. *Biomaterials* **2005,** 26, (15), 2455-2465.

59. Morch, Y. A.; Donati, I.; Strand, B. L.; Skjak-Braek, G., Molecular engineering as an approach to design new functional properties of alginate. *Biomacromolecules* **2007,** 8, (9), 2809-2814.

60. Thu, B.; Bruheim, P.; Espevik, T.; Smidsrod, O.; SoonShiong, P.; SkjakBraek, G., Alginate polycation microcapsules .1. Interaction between alginate and polycation. *Biomaterials* **1996,** 17, (10), 1031-1040.

61. Tanaka, H.; Matsumura, M.; Veliky, I. A., Diffusion Characteristics of Substrates in Ca-Alginate Gel Beads. *Biotechnology and Bioengineering* **1984,** 26, (1), 53-58.

62. Cheetham, P. S. J.; Blunt, K. W.; Bucke, C., Physical Studies on Cell Immobilization Using Calcium Alginate Gels. *Biotechnology and Bioengineering* **1979,** 21, (12), 2155-2168.

63. Chan, A. W. J.; Mazeaud, I.; Becker, T.; Neufeld, R. J., Granulation of subtilisin by internal gelation of alginate microspheres for application in detergent formulation. *Enzyme and Microbial Technology* **2006,** 38, (1-2), 265-272.

64. Poncelet, D.; Lencki, R.; Beaulieu, C.; Halle, J. P.; Neufeld, R. J.; Fournier, A., Production of Alginate Beads by Emulsification Internal Gelation .1. Methodology. *Applied Microbiology and Biotechnology* **1992,** 38, (1), 39-45.

65. Poncelet, D., Production of alginate beads by emulsification/internal gelation. *Bioartificial Organs Iii: Tissue Sourcing, Immunoisolation, and Clinical Trials* **2001,** 944, 74-82.

66. Poncelet, D.; Desmet, B. P.; Beaulieu, C.; Huguet, M. L.; Fournier, A.; Neufeld, R. J., Production of Alginate Beads by Emulsification Internal Gelation .2. Physicochemistry. *Applied Microbiology and Biotechnology* **1995,** 43, (4), 644-650.

67. Draget, K. I.; Ostgaard, K.; Smidsrod, O., Homogeneous Alginate Gels - a Technical Approach. *Carbohydrate Polymers* **1990,** 14, (2), 159-178.

68. Quong, D.; Neufeld, R. J.; Skjak-Braek, G.; Poncelet, D., External versus internal source of calcium during the gelation of alginate beads for DNA encapsulation. *Biotechnology and Bioengineering* **1998,** 57, (4), 438-446.

69. Gehrke, S. H.; Uhden, L. H.; McBride, J. F., Enhanced loading and activity retention of bioactive proteins in hydrogel delivery systems. *Journal of Controlled Release* **1998,** 55, (1), 21-33.

70. Pluemsab, W.; Sakairi, N.; Furuike, T., Synthesis and inclusion property of alpha-cyclodextrin-linked alginate. *Polymer* **2005,** 46, (23), 9778-9783.

71. Bouhadir, K. H.; Kruger, G. M.; Lee, K. Y.; Mooney, D. J., Sustained and controlled release of daunomycin from cross-linked poly(aldehyde guluronate) hydrogels. *Journal of Pharmaceutical Sciences* **2000,** 89, (7), 910-919.

72. Laurienzo, P.; Malinconico, M.; Mattia, G.; Russo, R.; La Rotonda, M. I.; Quaglia, F.; Capitani, D.; Mannina, L., Novel alginate-acrylic polymers as a platform for drug delivery. *Journal of Biomedical Materials Research Part A* **2006,** 78A, (3), 523-531.

73. Laurienzo, P.; Malinconico, M.; Motta, A.; Vicinanza, A., Synthesis and characterization of a novel alginate-poly (ethylene glycol) graft copolymer. *Carbohydrate Polymers* **2005,** 62, (3), 274-282.

74. Fukai, R.; Dakwa, P. H. R.; Chen, W., Strategies toward biocompatible artificial implants: Grafting of functionalized poly(ethylene glycol)s to poly(ethylene terephthalate) surfaces. *Journal of Polymer Science Part a-Polymer Chemistry* **2004,** 42, (21), 5389-5400.

75. Moe, S. T.; Skjakbraek, G.; Elgsaeter, A.; Smidsrod, O., Swelling of Covalently Cross-Linked Alginate Gels - Influence of Ionic Solutes and Nonpolar-Solvents. *Macromolecules* **1993,** 26, (14), 3589-3597.

76. Fundueanu, G.; Nastruzzi, C.; Carpov, A.; Desbrieres, J.; Rinaudo, M., Physico-chemical characterization of Ca-alginate microparticles produced with different methods. *Biomaterials* **1999,** 20, (15), 1427-1435.

77. Sharma, S.; Roy, I.; Gupta, M. N., Separation of phospholipase D from peanut on a fluidized bed of crosslinked alginate beads. *Biochemical Engineering Journal* **2001,** 8, (3), 235-239.

78. Gotoh, T.; Matsushima, K.; Kikuchi, K. I., Adsorption of Cu and Mn on covalently cross-linked alginate gel beads. *Chemosphere* **2004,** 55, (1), 57-64.

79. Tanihara, M.; Suzuki, Y.; Yamamoto, E.; Noguchi, A.; Mizushima, Y., Sustained release of basic fibroblast growth factor and angiogenesis in a novel covalently crosslinked gel of heparin and alginate. *Journal of Biomedical Materials Research* **2001,** 56, (2), 216-221.

80. Lee, K. Y.; Alsberg, E.; Mooney, D. J., Degradable and injectable poly(aldehyde guluronate) hydrogels for bone tissue engineering. *Journal of Biomedical Materials Research* **2001,** 56, (2), 228-233.

81. Bouhadir, K. H.; Hausman, D. S.; Mooney, D. J., Synthesis of cross-linked poly(aldehyde guluronate) hydrogels. *Polymer* **1999,** 40, (12), 3575-3584.

82. Xu, J. B.; Bartley, J. P.; Johnson, R. A., Preparation and characterization of alginate hydrogel membranes crosslinked using a water-soluble carbodiimide. *Journal of Applied Polymer Science* **2003,** 90, (3), 747-753.

83. Kulkarni, A. R.; Soppimath, K. S.; Aminabhavi, T. M.; Dave, A. M., Polymeric sodium alginate interpenetrating network beads for the controlled release of chlorpyrifos. *Journal of Applied Polymer Science* **2002,** 85, (5), 911-918.

84. Kulkarni, A. R.; Soppimath, K. S.; Aminabhavi, T. M.; Dave, A. M.; Mehta, M. H., Glutaraldehyde crosslinked sodium alginate beads containing liquid pesticide for soil application. *Journal of Controlled Release* **2000,** 63, (1-2), 97-105.

85. Park, J. K.; Jin, Y. B.; Chang, H. N., Reusable biosorbents in capsules from Zoogloea ramigera cells for cadmium removal. *Biotechnology and Bioengineering* **1999,** 63, (1), 116-121.

86. Yeom, C. K.; Lee, K. H., Characterization of sodium alginate membrane crosslinked with glutaraldehyde in pervaporation separation. *Journal of Applied Polymer Science* **1998,** 67, (2), 209-219.

87. Burns, M. A.; Kvesitadze, G. I.; Graves, D. J., Dried Calcium Alginate Magnetite Spheres - a New Support for Chromatographic Separations and Enzyme Immobilization. *Biotechnology and Bioengineering* **1985,** 27, (2), 137-145.

88. Skjak-Braek, G.; Moe, S. T. Alginate gels. 5144016, 1992.

89. Jayakrishnan, A.; Jameela, S. R., Glutaraldehyde as a fixative in bioprostheses and drug delivery matrices. *Biomaterials* **1996,** 17, (5), 471-484.

90. Korn, A. H.; Feairhel.Sh; Filachio.Em, Glutaraldehyde - Nature of Reagent. *Journal of Molecular Biology* **1972,** 65, (3), 525-529.

91. Edwards, F. C.; Di, Y.; Dye, J. F., In vitro assessment of the cytotoxicity and inflammatory potential of glutaraldehyde as a crosslinking agent for protein scaffolds. *Tissue Engineering* **2007,** 13, (7), 1711-1712.

92. Sung, H. W.; Huang, R. N.; Huang, L. L. H.; Tsai, C. C., In vitro evaluation of cytotoxicity of a naturally occurring cross-linking reagent for biological tissue fixation. *Journal of Biomaterials Science-Polymer Edition* **1999,** 10, (1), 63-78.

93. Gendler, E.; Gendler, S.; Nimni, M. E., Toxic Reactions Evoked by Glutaraldehyde-Fixed Pericardium and Cardiac-Valve Tissue Bioprosthesis. *Journal of Biomedical Materials Research* **1984,** 18, (7), 727-736.

94. Grimm, M.; Grabenwoger, M.; Eybl, E.; Moritz, A.; Bock, P.; Muller, M. M.; Wolner, E., Improved Biocompatibility of Bioprosthetic Heart-Valves by L-Glutamic Acid Treatment. *Journal of Cardiac Surgery* **1992,** 7, (1), 58-70.

95. Kari, F. W., NTP Technical Report on Toxicity Studies of Glutaraldehyde. In NIH Publication 93-3348: Research Triangle Park, 1993.

96. BASF, C. *Substantial Risk Report on Glutaraldehyde*; Public Files 89-900000423 and 88-900000179; 1990; pp EPA number 83HQ-0990-1008.

97. Beauchamp, R. O.; Stclair, M. B. G.; Fennell, T. R.; Clarke, D. O.; Morgan, K. T.; Kari, F. W., A Critical-Review of the Toxicology of Glutaraldehyde. *Critical Reviews in Toxicology* **1992,** 22, (3-4), 143-174.

98. Margel, S.; Rembaum, A., Synthesis and Characterization of Poly(Glutaraldehyde) - Potential Reagent for Protein Immobilization and Cell-Separation. *Macromolecules* **1980,** 13, (1), 19-24.

99. Migneault, I.; Dartiguenave, C.; Bertrand, M. J.; Waldron, K. C., Glutaraldehyde: behavior in aqueous solution, reaction with proteins, and application to enzyme crosslinking. *Biotechniques* **2004,** 37, (5), 790-802.

100. Purss, H. K.; Qiao, G. G.; Solomon, D. H., Effect of "'glutaraldehyde" functionality on network formation in poly(vinyl alcohol) membranes. *Journal of Applied Polymer Science* **2005,** 96, (3), 780-792.

101. McMurry, J., *Organic chemistry*. Fourth edition ed.; Brooks/Cole Publishing Company: Pacific Grove, 1996.

102. Flory, P. J.; John Rehner, J., Statistical Mechanics of Cross-Linked Polymer Networks I. Rubberlike Elasticity. *The Journal of Chemical Physics* **1943,** 11, (11), 512-520.

103. Flory, P. J.; John Rehner, J., Statistical Mechanics of Cross-Linked Polymer Networks II. Swelling. *The Journal of Chemical Physics* **1943,** 11, (11), 521-526.

104. Flory, P. J., *Principles of polymer chemistry*. Ithaca, New York, 1953.

105. Huggins, M. L., Some Properties of Solutions of Long-chain Compounds. *J. Phys. Chem.* **1942,** 46, (1), 151-158.

106. Flory, P. J., *Statistical mechanics of chain molecules*. Repr. ed. with corrections ed.; Oxford University Press: New York, 1989.

107. Brannonpeppas, L.; Peppas, N. A., Equilibrium Swelling Behavior of Ph-Sensitive Hydrogels. *Chemical Engineering Science* **1991,** 46, (3), 715-722.

108. Brannonpeppas, L.; Peppas, N. A., Equilibrium Swelling Behavior of Dilute Ionic Hydrogels in Electrolytic Solutions. *Journal of Controlled Release* **1991,** 16, (3), 319-330.

109. Mafe, S.; Ramirez, P.; Tanioka, A.; Pellicer, J., Model for counterion-membrane-fixed ion pairing and donnan equilibrium in charged membranes. *Journal of Physical Chemistry B* **1997,** 101, (10), 1851-1856.

110. Flory, P. J., Statistical Mechanics of Swelling of Network Structures. *Journal of Chemical Physics* **1950,** 18, (1), 108-111.

111. Vermaas, D.; Hermans, J. J., The Swelling of Cellulose Xanthate Gels in Dilute Salt Solutions. *Recueil Des Travaux Chimiques Des Pays-Bas-Journal of the Royal Netherlands Chemical Society* **1948,** 67, (12), 983-997.

112. Manning, G. S., Counterion condensation on charged spheres, cylinders, and planes. *Journal of Physical Chemistry B* **2007,** 111, (29), 8554-8559.

113. Manning, G. S., Limiting Laws and Counterion Condensation in Polyelectrolyte Solutions .I. Colligative Properties. *Journal of Chemical Physics* **1969,** 51, (3), 924-933.

114. Pitzer, K. S.; Mayorga, G., Thermodynamics of Electrolytes .2. Activity and Osmotic Coefficients for Strong Electrolytes with One or Both Ions Univalent. *Journal of Physical Chemistry* **1973,** 77, (19), 2300-2308.

115. Pitzer, K. S., Thermodynamics of Electrolytes .1. Theoretical Basis and General Equations. *Journal of Physical Chemistry* **1973,** 77, (2), 268-277.

Chapter 3

Kinetic controlled synthesis of pH-responsive network alginate

Ariel W. Chan, Ralph A. Whitney and Ronald J. Neufeld

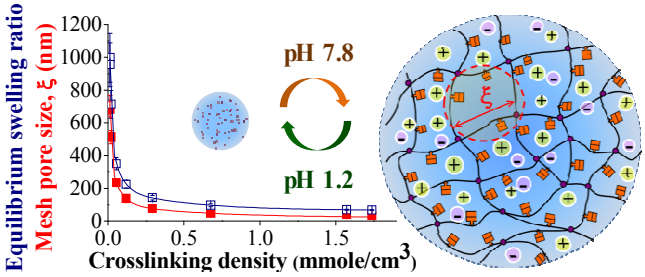

Keywords: alginate, polyelectrolyte, hydrogel, kinetics, equilibrium swelling, pore size

Manuscript published in *Biomacromolecules*. 2008. 9(9): 2536-2545.

Abstract

Alginates are of considerable interest in the fields of biotechnology and biomedical engineering. To enable the control of properties generally not possible with the native polymer, we have chemically modified alginate with di-aldehyde via acid-catalyzed acetalization. The kinetics of acetalization measured through equilibrium swelling of the networked polymer were found to undergo zero and second-order reaction with respect to alginate and di-aldehyde, respectively. With the determined rate constants of 19.06 $\mu L \cdot mole^{-1} \cdot s^{-1}$ at 40^{o}C and activation energy of 78.58 $kJ \cdot mol^{-1}$, a proposed predictive reaction model may be used *a priori* to select reaction conditions providing specific polymer properties. Gel swelling and average pore size were then able to be controlled between 80-1000 fold and 35-840 nm respectively, by predictive estimation of reagent concentration and formulation conditions. This semi-synthetic but natural polymer is stimuli-responsive, and exhibits high water absorbency which may potentially be used as drug delivery vehicle for protein therapeutics.

3.1 Introduction

Natural polymers like alginate are of considerable interest in the fields of biotechnology and biomedical engineering and as pharmaceutical controlled release devices[1, 2]. The benefits in the use of natural polymers are considerable due to the biodegradable and biocompatible nature. Alginate, one of the most abundant polysaccharides, is extracted from brown algae, and consists of (1→4)-O-glycosidic links of β-D-mannuronic (M) and α-L-guluronic acid (G) residues in varying sequential arrangements and proportions. Alginate can form an ionotropic physical gel by cooperative binding with multi-valent cations, such as calcium. Since the sol-gel transition is rapid yet gentle, calcium alginate has been used in wound dressing, dental impression, cell/protein encapsulation, and as tissue scaffold[3].

Alginate gel is porous and its gelling properties depend on the types and concentration of gelling cations, polymer size and relative amount of the two uronic acid monomers and the sequential arrangements which vary broadly accordingly to the extraction site, sources of brown algae, and harvest seasons and geographical locations. Alginate has been studied for many years in an effort to relate composition of the polymer to its physical properties[4-7]. However, the ability to control or modify the porous structure and the release characteristics of the gel matrix is often limited to selection or blending of materials from various natural sources that can provide differences in molecular weight or distribution of one or both of the two monomers making up the polymer. Alternative approaches have included enzymatic synthesis of alginate with specific monomeric

composition and molecular weight[6], or by applying cationic polymer coatings[8]. In addition, ionotropic alginate gels such as Ca^{++}-alginate, are stabilized through electrostatic interaction, have limited water absorbency or swelling ability and exhibit mechanical instability in the presence of chelators such as phosphates, citrates, or EDTA due to ion exchange. Thus, flexibility in polymer selection is limited, as is control of the final properties of the polymer constructs.

In contrast to natural materials which have limited flexibility to modify properties, chemical modification of the native polymer, forming semi-synthetic polymeric structures may enable a more direct control in tailoring the gel properties toward specific applications. Chemically networked polymers (chemical hydrogels) are formed by interlinking soluble polymers with small reactive compounds, substituting the inflexible junction zones in ionic physical gel with discrete distributed crosslinks, leading to a flexible elastic network of infinite molecular weight. In addition, modification with biodegradable linkages or functional molecules, may be used to tailor the intrinsic physiochemical properties for applications in which sustainable degradation and controlled release, or superswelling/superabsorbing properties are required [9-11]. Hexuronic acid monomer units in alginate have reactive carboxylic acid and hydroxyls available for crosslinking. Chemical gels can be produced by reacting the hydroxyl functional groups with a di-aldehyde such as glutaraldehyde (1,5-pentanedial) via acid-catalyzed acetalization[3, 12-15], with an epoxide such as epichlorohydrin via base-catalyzed ring-opening polymerization[11], or by an amine reaction targeting the carboxylic acid functional site, forming imide or amide bond linkages[16, 17]. To preserve the carboxylate

moieties for greater pH-sensitive response, the hydroxyl functional groups are the preferable reaction site. Aldehydes react with alcohols in the presence of an acid catalyst to yield 1,1-geminal diethers which are known as acetals, $R_2C(OR')_2$. Glutaraldehyde is an effective crosslinker in generating chemically, biologically and thermally stable crosslinks with hydroxyl groups, and its cytotoxicity was found to be much lower compared to other types of aldehyde and chemical crosslinkers[18,19]. In addition, glutaraldehyde is highly soluble in both organic and aqueous phases, thus the unreacted reagent can be removed by rinsing with normal saline or quenching with high concentration of L-glutamic acid, glycine, or methanol[18,20]. Since the formation of chemical hydrogels is not instantaneous or rapid, as is the case with the formation of alginate physical gel, the time-dependent gelation kinetics allow a more predictable control for designing desirable gel properties.

Although the study of gel formation kinetics is common for synthetic polymers, very limited kinetic information is available for the synthesis of chemical gels from natural polysaccharides. Our interest has been to chemically modify alginate to enable the control of properties generally not possible with the native polymer and to develop a predictive model which may be used *a priori* to select reaction conditions providing specific polymer properties. In the present study, the most probable reaction mechanism was proposed and the chemical kinetics of acetalization reaction between hydroxyls in hexuronic acid residues and glutaraldehyde was studied by equilibrium swelling. The kinetic and thermodynamic parameters of gel formation were determined and the effect of monomeric composition and molecular weight of alginate on the reaction kinetics was

characterized. This new class of semi-synthetic but natural polymer, using controlled reagents and formulation conditions to provide desired gel properties may find applications in regenerative medicine as tissue scaffold, in pharmaceutical science as drug delivery vehicle for protein therapeutics, and in environmental clean up as superabsorbent and ion-exchange biomaterials.

3.2 Materials and Methods

Ultrapure sodium alginates were purchased from FMC Biopolymer (Drammen, Norway) and the corresponding technical data provided by the supplier is summarized in Table 3-1. Alginate of sample (A) was degraded at pH 4, 30^{o}C and time course samples lyophilized to give alginates of different molecular weights, samples A-1 and A-2. Intrinsic viscosities of alginate solutions (<0.2% in 0.1 M NaCl) were obtained at 25^{o}C using an Ubbelohde type glass viscometer (No. 0B, Cannon Instrument Company) from isoionic dilution experiments[21]. The Huggins ($\eta_{reduced}$/c vs c) and Kraemer plots ($\ln(\eta/\eta_o)$/c vs. c) were constructed and the best fitted lines were extrapolated to zero concentration[21].

Table 3-1. Chemical compositions and molecular weights of alginate samples

Alginate Sample	Product name/ Batch no.	F_G[a]	F_{GG}[b]	M_w (kDa)	PDI[c]	$[\eta]_{0.1\ M\ NaCl}$ (dL/g)
A	Protanal SF 120 577469	0.72	0.60	325	3.2	8.63 (A)*
B	Pronova UP MVG FP-110-03	0.69	0.58	240	1.8	7.89 (B)
C	Pronova UP MVM FP-202-02	0.43	0.23	215	1.6	7.48 (C)
D	Pronova UP LVG FP-011-06	0.66	0.54	164	2.0	4.95 (D)
E	Pronova UP LVM FP-105-02	0.44	0.23	133	1.7	4.70 (E)

*Polymer A-1 and A-2 were obtained from acid hydrolysis of the original polymer (A) with the corresponding intrinsic viscosity of 4.45 and 2.22 dL/g, respectively.

a. F_G is the fraction of guluronic acid residue in alginate and the corresponding fraction of mannuronic acid is $F_M = 1\text{-}F_G$

b. F_{GG} is the fraction of guluronic acid block copolymer (GG) in the alginate sample and the corresponding fraction of mannuronic acid block (MM) is $F_{MM} = 1+F_{GG}\text{-}2F_G$

c. PDI is the polydispersity index determined by gel permeation chromatography

3.2.1 Synthesis of chemically networked polyhexuronic acid gel

Sodium alginate solution of 4 g/dL were extruded dropwise via an automatic liquid dispenser (EFD, Model 1000XL, East Providence, USA) into 0.05 M HCl, resulting in 2.9 ± 0.1 mm alginic (polyhexuronic) acid gel beads. Beads were incubated in the supernatant solutions for 4 h prior to use. Glutaraldehyde (1,5-pentanedial) in water of 25% w/w was purchased from Sigma-Aldrich (Oakville, Canada). The absorbance ratio measured for polymeric to monomeric form of pentanedial was no greater than A_{235}/A_{280} = 0.3. Covalently networked polyhexuronic acid gel was obtained by suspending preformed acid gel beads (from extruding a 4 g/dL Protanal SF 120 alginate in acid capture solution) in crosslinking reaction medium containing 1.58 M glutaraldehyde and

0.38 M HCl at 40^{o}C, unless otherwise specified. The mass ratio of beads to reaction medium was 0.30 and accounting for the water content inside gel beads, the initial reactant concentrations were 0.38 M hydroxyls (or 0.19 M hexuronic acid residue) and 3.16 M aldehyde which was about 10 fold greater than that of hydroxyls from polyhexuronic acid.

3.2.2 Study of the reaction kinetics by equilibrium swelling

Kinetics of network formation was determined by equilibrium gel swelling. Beads sampled from the reaction medium were washed with 4^{o}C, 40% ethanol, and then submerged in the swelling medium containing 0.1 M NaCl at pH 7.8 for 72 hours. To provide an infinite sink, the solution was constantly replaced with fresh medium. The critical gelation point was monitored by suspending 3 reacted beads in 30 mL of swelling medium for 24 h and the supernatant was used to determine non-crosslinked polymer sol fraction by phenol-sulphuric acid total carbohydrate assay[22]. At the critical gelation point, a stable, maximum attainable gel volume was obtained, and the sol carbohydrate content was less than 5% of the total initial soluble polymer which was considered to be within experimental error of the assay. The equilibrium swelling volume of the gel beads, V_s, was calculated from the bead diameter in aqueous solution determined under Leica stereomicroscope (D3, Germany) with the assumption of a perfect sphere. The corresponding equilibrium swelling ratio was calculated with respect to the initial compact volume of polymer according to Equation 1:

$$Equilibrium \quad swelling \quad ratio = \frac{V_s}{\bar{\upsilon} m_p} = v_{2,s}^{-1} \qquad \textbf{(Eq. 1)}$$

where $\bar{\upsilon}$ and m_p are the specific density and the mass of the polymer. The bead volume measured microscopically was compared with volume displacement in paraffin oil. Since the difference between the two volume measurements was less than 5% for beads formed at the critical gelation point and less than 8% for beads prior to the swelling test, subsequent bead volumes were measured microscopically. Sample mean and standard deviation were calculated based on 3 beads for each experiment. All data reported were the pooled mean and standard deviation of three repeated experiments.

3.2.3 Determination of Flory-Huggins interaction parameter, χ

The Flory-Huggins interaction parameter was experimentally measured to be 0.24 using Flory viscosity theory and Stockmayer-Fixman relationship[23] in 0.1 M NaCl pH 7 solution as described in Smidsrod[24]. In brief, molecular weights and intrinsic viscosities of ten alginate samples ranged from 85 to 490 kDa and 2.2-9.2 dL/g, were determined from static light scattering (Nanosizer ZS, Malvern) and Ubbelohde type glass viscometer (No. 0B, Cannon Instrument Company). A linear plot of $M^{1/2}$ versus $[\eta]M^{-1/2}$ was constructed and the slope obtained from the best fitted line ($y=0.018x+0.895$, $R^2=0.98$) was used to calculated the Flory-Huggin's Interaction parameter, χ, using equations 2.

$$\frac{[\eta]}{M_0^{\frac{1}{2}}} = k_\theta + 0.51\Phi B M_0^{\frac{1}{2}} \quad \text{and} \quad B = \frac{2\bar{\upsilon}^2\left(\frac{1}{2} - \chi\right)}{N_A V_1} \qquad \textbf{(Eq. 2)}$$

where k_θ is the unperturbed parameter (mLg^{-1}), $\bar{\upsilon}$ is the specific density of alginate (0.8 cm^3g^{-1}), V_1 is molar volume of the solvent (cm^3g^{-1}), N_A is Avogadro number, M_0 is the primary molecular weight of alginate and Φ is the Flory viscosity constant (which is 1.21 $x10^{21}$ mol^{-1} in 0.1 M NaCl solution approximateed using data from Smidsrod [24])

3.2.4 Determination of the intrinsic viscosity at theta condition, [η] and characteristic ratio C_n

The intrinsic viscosity at theta condition was determined following procedures described in Amsden and Turner[25]. In brief, the intrinsic viscosity of SF120 alginate dissolved in various NaCl concentrations ranging from 0.005 to 2 M was measured and a plot of $I^{-1/2}$ versus intrinsic viscosity (dL/g) at I was constructed. The intrinsic viscosity at theta condition for polyelectrolyte, in which the polymer coil expansion due to intramolecular electrostatic repulsion is eliminated, was obtained by extrapolating to an infinite ionic strength which is equal to 6.9 dL/g and the corresponding characteristic ratio determined from equation 3 is 27.3,

$$C_n = \left(\frac{[\eta]_\theta}{\Phi}\right)^{2/3} \frac{M_r}{M_0^{1/3} l^2} \qquad \textbf{(Eq. 3)}$$

where l is carbon-carbon bond length of monomer unit (ie. uronic acid residue has bond length of 5.15 Å)[24] and M_r is monomer molecular weight (198 g/mol).

3.2.5 Pore size measurement by differential scanning calorimeter

Thermoporometry technique was used to approximate the average pore size of alginate hydrogels[26] based on the principle of liquid-solid transformation (ie. triple point temperature). Through measuring the shift in equilibrium temperature (ΔT) of the liquid-solid transformation, we can approximate the average pore radius (R_p in nanometers) of the hydrogel using equation 4 derived by Iza et al[27].

$$R_p = -273.15\left(\frac{0.25}{\Delta T} + 0.0023\right) \qquad \textbf{(Eq. 4)}$$

where ΔT=T-273.15 and T is the triple point depression temperature in Kelvin. The shift in freezing and melting temperature of water was determined by differential scanning calorimeter (DSC Q100, TA Instruments) equipped with a liquid nitrogen-cooling accessory. Samples weighing 10-20 mg were placed in a sealable aluminum pan and one drop of the solvent was added to prevent premature drying prior to the measurement. The samples were first equilibrated at -30^{o}C, held for 10 min, followed by heating up to 15^{o}C at a rate of 2.0^{o}C/min and held for 10 min, and then cooled down from 15^{o}C to -30^{o}C at a rate of 2.0^{o}C/min.

3.3 Results and Discussion

3.3.1 Reaction mechanism and kinetics of acetal formation

A proposed reaction mechanism between glutaraldehyde (1,5-pentanedial) and alginate (polyhexuronic acid) is shown in Figure 3-1. Alcohols as weak nucleophiles have limited reactivity toward an aldehyde under neutral conditions. However, under acidic conditions, the carbonyl oxygen is protonated, strongly polarizing the carbonyl group. The oxygen lone-pair electrons from alcohol can readily attack the activated carbonyl group, resulting in rapid addition of an alcohol to the aldehyde. There are two hydroxyls in each of the uronic acid residues. In the presence of HCl, the nucleophilic addition of hydroxyls from polyhexuronic acid (**1**) to aldehyde (**2**) initially yields an oxonium ion (**3**). Deprotonation of the alcoholic oxonium produces a neutral hemiacetal tetrahedral intermediate (**4**). Further protonation of the hemiacetal hydroxyl by hydrochloric acid converts it into a good leaving group. The loss of water from the hemiacetal results in an intermediate carbocation (**5).** The second equivalent alcohol undergoes nucleophilic addition to the polarized carbonyl group of the carbocation (**5**), generating protonated acetal. Loss of a proton yields neutral acetal product (**6**). Since the second hydroxyl group is in near proximity and due to the excluded volume effect of macromolecules in dilute solution[28], it is more thermodynamically favourable to add the hydroxyl from the same hexuronic acid monomer to the carbocation (**5**) than any other hydroxyls from the nearby polymer chain. To generate predominantly intermolecular crosslinking, the chemical crosslinker should be tetrafunctional as is the case with 1,5-pentanedial which is

capable of reacting with four hydroxyl groups, forming two acetal linkages between two hexuronic acid monomers from adjacent polymer chains (**7**).

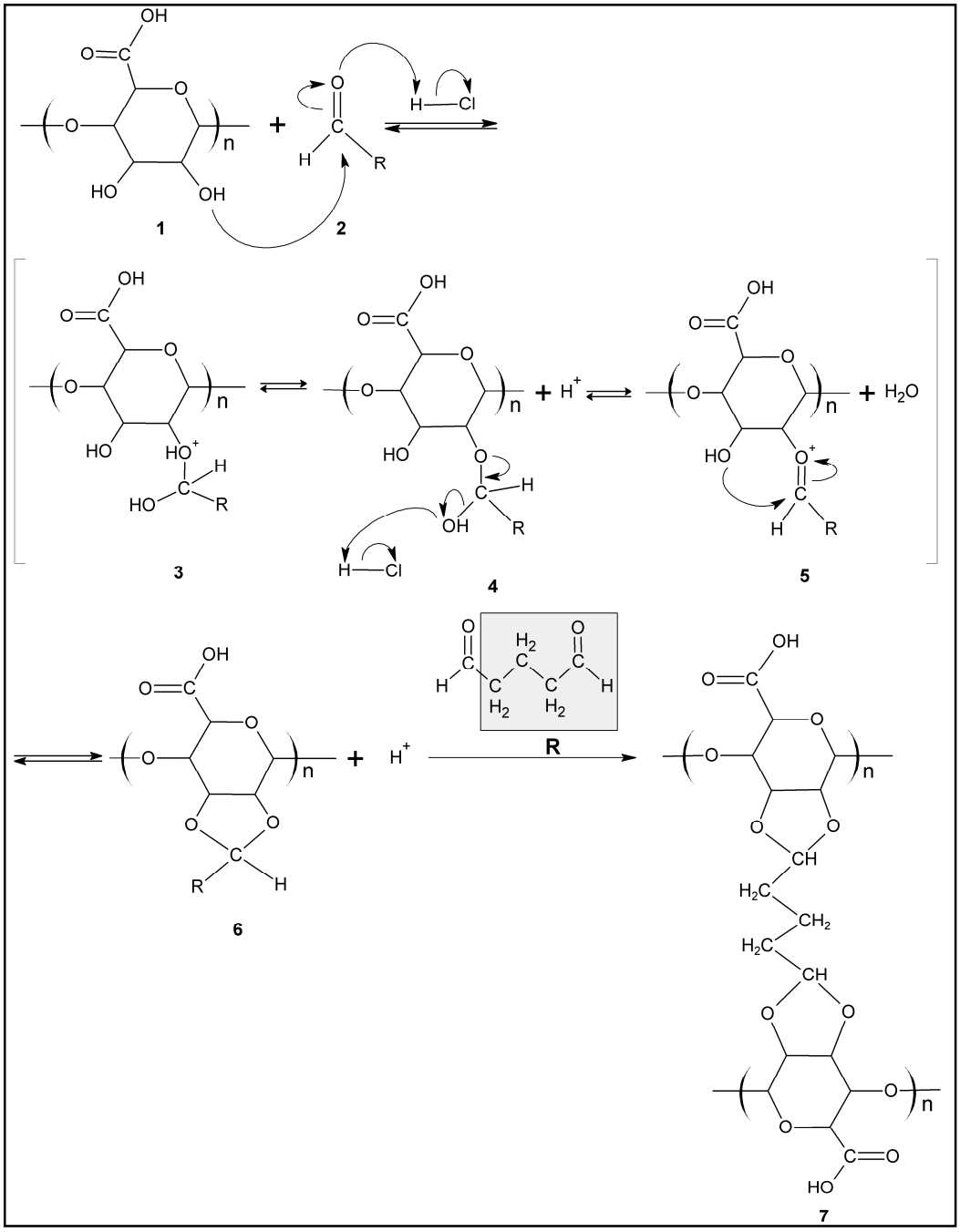

Figure 3-1. Proposed mechanism of acid-catalyzed acetal formation by reaction of a di-aldehyde with polyhexuronic acid.

Acetalization kinetics based on the mechanism described in Figure 3-1 can be described by equation 5:

$$\frac{\delta[R_2C(OR')_2]}{\delta t} = k[R-OH]^a[R-CHO]^b \qquad \textbf{(Eq. 5)}$$

where k is the rate constant and a and b are the reaction orders with respect to polyhexuronic acid and pentanedial concentrations.

3.3.2 Derivation of swelling equation for tetra-functional networked alginate

The gel swelling of a charged polymer (polyelectrolyte) is a phenomenon induced by chemical potential differences (Δμ) of solvents inside and outside of the gel network. According to Flory and his contemporaries[29-31], the swelling of Donnan-type equilibria in polyelectrolyte gels can be separate into three terms (Equation 6) which represent the chemical potential changes due to the volume exclusion effect (also known as mixing effect), $(\Delta\mu_1)_{mix}$, due to uneven distribution of mobile ions in the external electrolyte, $(\Delta\mu_1)_{ion}$, and the elastic free energy consequential to the expansion of the network structure, $(\Delta\mu_1)_{el}$.

$$(\Delta\mu_1) = (\Delta\mu_1)_{ion} + (\Delta\mu_1)_{mix} + (\Delta\mu_1)_{el} = 0 \qquad \textbf{(Eq. 6)}$$

To estimate the quantity of mixing potential under constant pressure, Flory and Huggins derived an expression based on van Laar equation and assumed liquid lattice model with each cell able to accommodate either a solvent or a polymer segment

molecule[29,30]. For network polymer in which the final molecular weight after crosslinking approaches infinity, it is permissible to approximate the chemical potential of the solvent with:

$$(\Delta\mu_1)_{mix} = RT[\ln(1 - v_{2,s}) + v_{2,s} + \chi_1 v_{2,s}^2] \qquad \textbf{(Eq. 7)}$$

where R is the gas constant; T is the temperature of the mixing polymer system; $v_{2,s}$ is the volume fraction of the polymer in the equilibrium swollen gel; and χ_1 is the Flory-Huggins interaction parameter which represents the difference in energy of a solvent molecule surrounded by polymer molecules compared with that of the pure solvent environment.

The conformational energy of the elastic network can be evaluated from the commonly used conceptual template derived by Flory and Rehner (Equation 8) which assumes unaltered polymer configuration before and after the vulcanization (ie. proceeds in the absent of diluent or swelling agent) and all of the chains follow Gaussian distribution [32]. The Gibbs free energy change on elastic reaction in molar quantity can be written as:

$$\Delta G_{el} = \left(\frac{kTv_e}{2}\right)\left(3\alpha_s^2 - 3 - \frac{4}{f}\ln\alpha_s^3\right) \quad \text{and} \quad v_e = \frac{V_p}{\bar{\upsilon} M_c}\left[1 - \left(\frac{M_c}{M_0}\frac{f}{(f-2)}\right)\right] \qquad \textbf{(Eq. 8)}$$

where v_e is the effective number of chains in the real network, k is Boltzmann's constant, M_o and $\bar{\upsilon}$ are the primary molecular weight and specific density of the polymer, M_c is the molecular weight between two crosslinking points, V_1 is the molar volume of solvent, V_r

is the volume of the network polymer after crosslinking and before deformation or swelling process, *f* is the functionality of a structural unit which defines as *f* number of sub-chains extending from one crosslink point (according to Figure 3-1, *f*=4 for networked alginate), and $\alpha_s = (V_s / V_r)^{1/3}$ which is the linear deformation factor of a network structure assuming isotropic swelling. For natural rubber, it is reasonable to assume unaltered polymer configuration before and after the vulcanization which proceeds in the absent of diluent or swelling agent. However, this is not normally the case for hydrogels since the solvated polymer chains which have absorbed substantial quantity of solvent (diluent), exhibit greater mobility prior to crosslinking and the distance between polymer chains decrease after crosslinking. To account for this deviation from natural rubber, we modified the original Flory's expression with the redefined expression of linear deformation factor for hydrogel from Bray and Merrill[33] (Equation 9).

$$\alpha_s^3 = \frac{V_s}{V_r} = \frac{V_P + n_1 V_1 / N}{V_r} \qquad \textbf{(Eq. 9)}$$

Subsisting equation 9 back to 8, the chemical potential due to the elastic reaction can be calculated by taking the first derivative of ΔG_{el} with respect to number of solvent molecules and multiplying by Avogadro's number, *N*:

$$(\Delta\mu_1)_{el} = N\left(\frac{\partial \Delta G_{el}}{\partial \alpha}\right)_{T,P}\left(\frac{\partial \alpha}{\partial n_1}\right)_{T,P} = RT\,\frac{V_1}{\bar{\upsilon} M_c}\, v_{2,r}\left[1-\left(\frac{M_c}{M_0}\frac{f}{(f-2)}\right)\right]\left[\left(\frac{v_{2,s}}{v_{2,r}}\right)^{1/3} - \frac{2}{f}\frac{v_{2,s}}{v_{2,r}}\right]$$

$$\text{where } v_{2,s} = \frac{m_p \bar{\upsilon}}{V_s} \qquad \text{and} \qquad v_{2,r} = \frac{m_p \bar{\upsilon}}{V_r} \qquad \textbf{(Eq. 10)}$$

We also included a non-Gaussian effect correction term from Kovac[34] and Barrhowell and Peppas[35] and the modified function has the form in Equation 11,

$$\Delta(\mu_1)_{el} = RT\frac{V_1}{\bar{\upsilon}M_c}v_{2,r}\left[1-\left(\frac{M_c}{M_0}\frac{f}{(f-2)}\right)\right]\left[\left(\frac{v_{2,s}}{v_{2,r}}\right)^{1/3}-\frac{2}{f}\frac{v_{2,s}}{v_{2,r}}\right]\left[1+\frac{v_{2,s}^{1/3}}{fM_c/2M_r}\right]^2\left[1-\frac{v_{2,s}^{2/3}}{fM_c/2M_r}\right]^{-3}$$

(Eq. 11)

According to Flory, due to concentration gradient and electroneutrality, mobile ions diffuse from the external solution into the gel to establish individual ion equilibrium between the gel and external solution compartments (Equation 12). In the case of equilibrium with an infinite external solution containing uni-univalent electrolyte (ie. NaCl) that dissociates completely to give a solution concentration c_s^*, and assuming an ideal solution environment in which the activities of the solvent are equal to concentrations in dilute solutions ($a = \gamma c$ and $\gamma=1$), the chemical potential of the solvent in the swollen gel due to the uneven distribution of mobile ions and ionic constituents from polymer can be approximated by equation 15:

$$c_+ = c_- + ic_2 \qquad c_+^* = c_-^* = c^* \qquad c_+c_- = c_s^{*2} \qquad \textbf{(Eq. 12)}$$

where subscript "+" and "-" denote positive and negative ions respectively, the asterisk indicates external solution compartment, and i and c_2 are the degree of ionization of polyhexuronic acid polymer and the molar concentration of the monomer unit which can be estimated using Henderson-Hasselbalch in equation 13 and 14, respectively,

$$pH = pK_a + \log\frac{[RCOO^-]}{[RCOOH]} \text{ and } i = \frac{[RCOO^-]}{[RCOOH]+[RCOO^-]} = \frac{10^{-pK_a}}{10^{-pH}+10^{-pK_a}} \qquad \textbf{(Eq. 13)}$$

$$c_2 = \frac{V_p}{\upsilon M_0}\frac{1}{V_s} = \frac{v_{2,s}}{\upsilon M_0} \qquad \textbf{(Eq. 14)}$$

$$(\Delta\mu_1)_{ion} = V_1RT\left[c_+ + c_- - (c_+^* - c_-^*)\right] = V_1RT(i^2c_2^2/4I^*)\left[1+(ic_2)^2/16(I^*)^2\right] \qquad \textbf{(Eq. 15)}$$

where I is the ionic strength of the external electrolyte and K_a is the acid dissociation constant which is 2.51 x 10^{-4} M for alginate or $pKa \approx 3.54$. Gel swelling in electrolyte solution (ie. $\gamma \neq 1$) generally deviates from that of the ideal one. In addition, due to counter-ion condensation effect (also known as ion-pairing effect), 60% of the free charged carboxylate group in alginate were regarded as bound in ion-pairs to the polymer according to Katchalsky *et al*.[36]. Therefore, to closely approximate the mobile ion concentration, c_- and c_+, inside the hydrogel, we modified the ideal Donnan-Type equilibrium expression derived by Flory for polyelectrolyte to address these considerations. As a further condition of equilibrium, the activity of the electrolyte inside and outside the swollen polyhexuronic acid gel must be equal. This condition may allow us to restate equation 12 to:

$$a_+a_- = a_+^*a_-^* \qquad \text{and} \qquad (c_- + ic_2)c_- = \frac{\gamma_+^*\gamma_-^*}{\gamma_+\gamma_-}c^{*2} \qquad \textbf{(Eq. 16)}$$

where a is the activity ($a=\gamma c$) and γ is the activity coefficient . For strong electrolyte, it is reasonable to assume $\gamma_+^* = \gamma_-^* = \gamma_\pm^*$. In this study, 0.1 M NaCl has a mean ionic activity

coefficient of $\gamma_{\pm}^{*}$ = 0.8 estimated using Pitzer-Mayorga equation[37]. Since co-ions (c_-) should be in regions far away from the fixed charge moieties and do not participate in the ion-pairing phenomenon, its ionic activity coefficient should be similar to that of external anions, $\gamma_- \approx \gamma_-^* = \gamma_{\pm}^*$. Due to the ion-pairing phenomenon in which positive counterions condensed onto the free charged carboxylate, the decreased effective charge concentration can lead to lowering of the corresponding ionic activity coefficient which can be estimated from the empirical relationship[38]:

$$\frac{\gamma_+\gamma_-}{\gamma_+^*\gamma_-^*} \approx \frac{\gamma_+}{\gamma_{\pm}^*} = \frac{1}{1+K_a\phi i c_2} \qquad \textbf{(Eq. 17)}$$

where ϕ is the fraction of the free charged, non-condensed ion groups on the polymer which is equal to 0.4 for alginate in 0.1 M NaCl. Combining equation 12-14 and 16-17, the co-ion concentration in the gel can be estimated using equation 18 and the chemical potential induced by the ionic substituent and mobile electrolytes can be evaluated using equation 19 :

$$c_- = \left[\left(\frac{\gamma_{\pm}^*}{\gamma_+\gamma_-}\right)c^{*2} + \left(\frac{\phi i c_2}{2}\right)^2\right]^{1/2} - \frac{i c_2}{2}$$

$$c_- = \left[\left(\frac{\gamma_{\pm}^*}{\gamma_+\gamma_-}\right)c^{*2} + \frac{\phi^2}{4}\left(\frac{v_{2,s}}{\bar{\upsilon}M_r}\right)^2\left(\frac{10^{-pK_a}}{10^{-pH}+10^{-pK_a}}\right)^2\right]^{1/2} - \frac{\phi}{2}\left(\frac{v_{2,s}}{\bar{\upsilon}M_r}\right)\left(\frac{10^{-pK_a}}{10^{-pH}+10^{-pK_a}}\right) \qquad \textbf{(Eq. 18)}$$

$$(\Delta\mu_1)_{ion} = V_1 RT\left[c_+ + c_- - (c_+^* - c_-^*)\right]$$
$$= V_1 RT\left\{\left[4\left(\frac{\gamma_\pm^*}{\gamma_+\gamma_-}\right)c^{*2} + \phi^2\left(\frac{v_{2,s}}{\bar{\upsilon}M_r}\right)^2\left(\frac{10^{-pK_a}}{10^{-pH}+10^{-pK_a}}\right)^2\right]^{1/2} - 2c^*\right\} \qquad \textbf{(Eq. 19)}$$

Substituting equations 9, 11, and 19 into 6, a modified swelling expression describing the swelling of alginate network can be recast as:

$$V_1\left\{\left[4\left(\frac{\gamma_\pm^*}{\gamma_+\gamma_-}\right)c^{*2} + \phi^2\left(\frac{v_{2,s}}{\bar{\upsilon}M_r}\right)^2\left(\frac{10^{-pK_a}}{10^{-pH}+10^{-pK_a}}\right)^2\right]^{1/2} - 2c^*\right\} = \left[\ln(1-v_2) + v_2 + \chi_1 v_2^2\right] +$$
$$\frac{V_1}{\bar{\upsilon}M_c}v_{2,r}\left[1-\left(\frac{M_c}{M_0}\frac{f}{(f-2)}\right)\right]\left[\left(\frac{v_{2,s}}{v_{2,r}}\right)^{1/3} - \frac{2}{f}\frac{v_{2,s}}{v_{2,r}}\right]\left[1+\frac{v_{2,s}^{1/3}}{fM_c/2M_r}\right]^2\left[1-\frac{v_{2,s}^{2/3}}{fM_c/2M_r}\right]^{-3}$$

(Eq. 20)

With the known equilibrium swelling gel volume, the extent of crosslinking characterized by molecular weight between crosslinks, M_c, can be estimated from equating equations 20. The crosslinking density, ρ_c, defined as moles of elastically effective chains per unit volume of network can be calculated from equation 21.

$$\rho_c = \frac{1}{\bar{\upsilon}M_c} \qquad \textbf{(Eq. 21)}$$

The mesh pore size, ξ, can be estimated from equation 22:

$$\xi = v_{2,s}^{-1/3}\left[C_n\left(\frac{2\overline{M_c}}{M_r}\right)\right]^{1/2} l \qquad \textbf{(Eq. 22)}$$

where C_n is the characteristic ratio which can be estimated from the intrinsic viscosity of the polymer at theta condition, $[\eta]_\theta$, l is carbon-carbon bond length of monomer unit and Φ is the Flory viscosity constant.

3.3.3 Characterization of the network structure of alginate gel via equilibrium swelling

Chemically networked polyhexuronic acid was synthesized by extruding 4 g/dL Protanal SF120 alginate into acid solution, forming acid gel followed by suspending in reaction medium containing reactive di-aldehyde. The extent of crosslinking was studied via equilibrium swelling together with the derived equilibrium swelling model (Equation 20). A time course profile of the reaction is presented in Figure 3-2 in which the time scale is replaced by the controlled variable, crosslinking density, using the obtained equilibrium swelling data and plotted against the average mesh pore size.

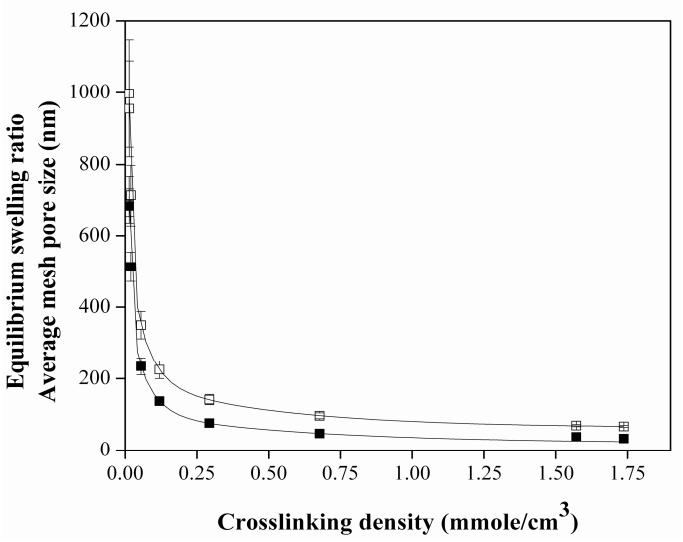

Figure 3-2. Equilibrium swelling ratio (□) and the average mesh pore size (■) of the swollen gel network corresponding to calculated crosslinking density from equation 21-22.

At the lowest cross-linking density necessary to achieve a stable swollen network, defined as the gel point, the swollen gel approached 1000 times the volume of the compact dry polymer network, representing a substantial amount of absorbed water. The molecular weight between consecutive crosslink points, M_c, was calculated to be 71,319 g/mol, which represents 4 to 5 crosslinks in the primary polymer chain. The calculated crosslinking density was 0.014 mmole/cm^3, equivalent to 0.38 mM of acetal bonds formed in the hydrogel of initial concentration 4 g/dL. The mean pore size at the gel point was calculated to be 720 nm. With increased extent of reaction, equilibrium swelling of the gel decreased, reaching a stable minimum swelling ratio of less than 100. The crosslinking density at this point is 1.75 mmole/cm^3, equivalent to 36.26 mM acetals. At this maximum crosslinking density, the molecular weight between crosslinks was down to

1050 g/mole, approximately 5 monomeric units between crosslink points and the network pore size was less than 35 nm. The time required to convert available hydroxyls can range from 1 to over 10 h depending on the concentrations of the aldehyde, catalyst, or temperature as will be subsequently shown.

We also characterized the porous structure of alginate gel via thermoporometry. As the chemical reaction proceeded, beads were removed from the reactor and subjected to equilibrium swelling. The freezing points of the solvent in the swollen beads were determined using differential scanning calorimeter (DSC) which was used to calculate the median mesh pore size of the ultrastructure of the porous system using Equation 4. A series of thermographs from chemical gel beads obtained shortly after reaching the critical gel point to maximum achievable crosslinking density are shown in Figure 3-3. The median pore sizes determined using DSC as tabulated in the inset to Figure 3-3 are seen to be comparable to pore sizes measured by the equilibrium swelling experiment, validating the adequacy of the derived swelling model. In addition, atomic force microscopy and scanning electron microscopy were both employed to provide direct measurement of the porous structure, with images showing a porous structure of 500-800 nm for gel beads obtained shortly after the critical gelation time and 25-200 nm for densely crosslinked hydrogel (images available from author). Therefore, through carefully controlling the kinetics, the extent of crosslinking can be manipulated, allowing modification of the gel network to provide desired physical and mechanical properties.

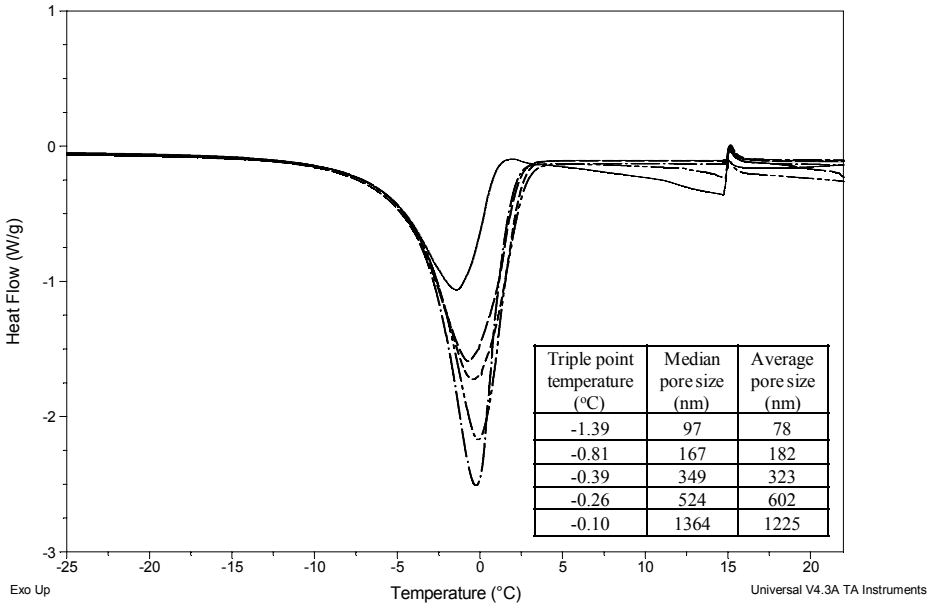

Triple point temperature (°C)	Median pore size (nm)	Average pore size (nm)
-1.39	97	78
-0.81	167	182
-0.39	349	323
-0.26	524	602
-0.10	1364	1225

[1.] Median pore sizes estimated from triple point temperatures by DSC.
[2.] Average pore sizes estimated from equilibrium swelling data.

Figure 3-3. Thermographs of networked alginates obtained at various reaction durations. Sequence of curves corresponds to order in table.

3.3.4 Influence of polyhexuronic acid concentration on the reaction kinetics

Polyhexuronic acid gel at initial concentrations of 2 and 4 g/dL, was reacted in excess di-aldehyde, forming cross-linked gel. The equilibrium swelling ratio and computed acetal concentration which is the product of inversed molecular weight between crosslinks and the concentration of polyhexuronic acid in the gel are plotted in Figure 3-4, as they vary with time of reaction. The gel point was reached within 30 min for both gel concentrations, at which point an equilibrium swelling ratio of 1000 was attained. With additional time of cross-linking, the swelling ratio decreased to a stable level of just under 100, corresponding to a crosslinked saturation of the hydroxyls. Very

similar curve profiles are seen for both concentrations of polyhexuronic acid. The acetal concentration is seen to increase linearly with a similar slope for both polyhexuronic concentrations. Since the reactive hydroxyls were the limiting reactants, the acetal concentrations reached a maximum of 16.7 and 36.3 mM for hydrogel with initial polymer concentration of 2 and 4 g/dL after 6.8 and 13.1 h, respectively.

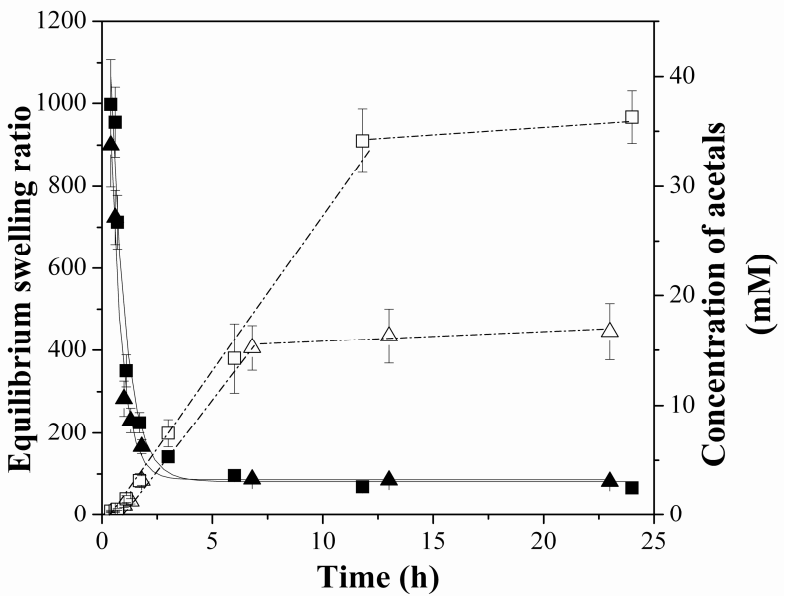

Figure 3-4. Kinetics of the acetalization reaction with 2 (▲,△) and 4% (■,□) polyhexuronic acid gel characterized by the equilibrium swelling ratio (closed symbols, left hand ordinate) and the corresponding crosslinking density (open symbols, right hand ordinate).

The reaction order with respect to hydroxyl concentration was determined by the isolation method in which the aldehyde concentration was provided at least 80 fold higher than hydroxyl concentration. A pseudo-first order reaction follows the differential rate law as shown in equation 23:

$$\frac{\delta[R_2C(OR')_2]}{\delta t} = k'[R-OH]^a \qquad \textbf{(Eq. 23)}$$

where k' is the pseudo-first order rate constant, and $[R_2C(OR')_2]$ and [R-OH] are the concentrations of the acetal bonds and hydroxyls respectively, at time t. Since the kinetic plot of acetal concentration is linear, a zero-order rate behavior may be expected from equation 23, where *a=0*.

$$[R_2C(OR')_2] = [R_2C(OR')_2]_0 + k't \qquad \textbf{(Eq. 24)}$$

Thus it appears that the reaction is zero-order with respect to the overall acetalization reaction. The pseudo-first order rate constants, k', determined from the slope for 2 and 4% polyhexuronic acid gels were 2.58 and 2.84 μmol L^{-1} h^{-1}, indicating similar reaction mechanism for both gel concentrations. The gel point was reached about 15 min earlier for hydrogel prepared with 2 g/dL of polyhexuronic acid, compared to the one with 4 g/dL.

3.3.5 Influence of alginate monomeric composition and molecular weight on the reaction kinetics

Five different samples of alginates (polyhexuronates) ranging in molecular weight from 133 to 325 kg/mole, of which three were composed of close to 70% G-residues while the remaining two were composed of around 40% G-residues, were used to prepare 4 g/dL acid gel beads. One sample (sample A) was hydrolyzed to produce lower molecular weight polymer (samples A-1, A-2) to study the effect of molecular weight on the reaction kinetics with minimum influence from the variation of chemical composition. The reaction was carried out in pentanedial to total hydroxyl concentration of 10:1.

The effect of polymer molecular weight and monomeric composition in polyhexuronic acid on the reaction kinetics was studied and the crosslinking kinetic profiles are plotted in Figure 3-5. The kinetic profiles of polyhexuronic acid gel of similar molecular weights (curves B and C, and curves D, E and A-1 of Figure 3-5) were very similar, indicating no apparent effect of composition and sequential arrangement of the two hexuronic acid monomers on the acetalization reaction. As compared to physical gels in which gel properties depend primarily on the G-monomers due to the spatial arrangement of the ring and hydroxyl oxygen atoms, the formation of crosslinked gel exhibits no apparent dependence on the fraction of G- or M-acid residues. Thus the two monomers appear to be equally reactive towards the aldehyde, forming acetal linkage.

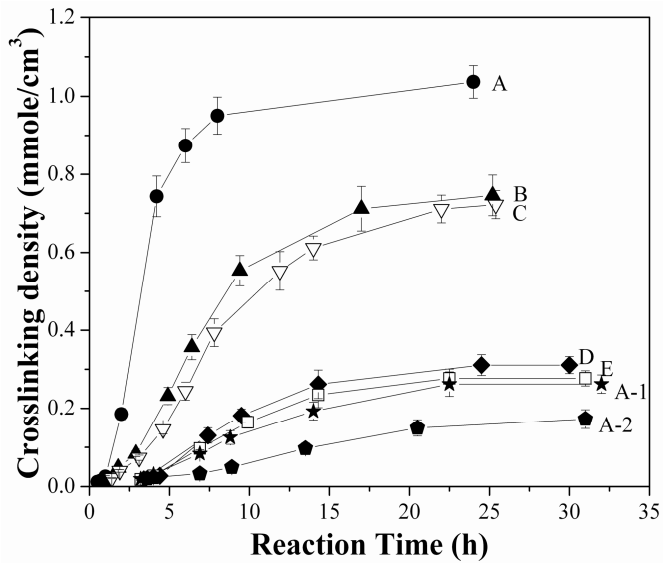

Figure 3-5. Influence of monomeric compositions, and primary molecular weight of polyhexuronic acid on crosslinking kinetics. The molecular weights of the samples studied were characterized by the intrinsic viscosity with the descending order: 8.63 (A,●), 7.89 (B, ▲), 7.48 (C,▽), 4.95 (D,◆), 4.70 (E, □), 4.45 (A-1, ★), and 2.22 dL/g (A-2, ⬟). Samples A,B, D, A-1 and A-2 consisted of high G-content (closed symbols) whereas samples C and E (open symbols) were medium G-content polyhexuronic acid.

By comparing the slopes of the linear region of the curves, the rate of reaction increased with an increase in the molecular weight of polyhexuronic acid. In addition, samples A, A-1 and A-2 from the same polyhexuronic acid sample but hydrolyzed to produce different molecular weight, demonstrated similar curve profiles to other polyhexuronic acid gels of similar molecular weight, but with different monomeric compositions. Faster reaction kinetics with greater molecular weight may be attributed to a lower mobility of higher molecular weight polymer, increasing the probability of collision with chemical crosslinkers. As the first crosslink is formed in the gel of higher molecular weight polymer, polymer mobility and flexibility is further restricted, increasing the likelihood of the available hydroxyl colliding with the reactive aldehyde, forming the next acetal linkage. Therefore, it appears that reaction kinetics are molecular weight dependent with very limited effect from the stereochemistry of the two hexuronic acid monomers.

3.3.6 Influence of di-aldehyde concentration on the reaction kinetics

Polyhexuronic acid gels were reacted with pentanedial at concentrations ranging from 0.44 to 1.65 M, equivalent from 0.88 to 3.30 M of reactive aldehyde. The reaction order with respect to pentanedial concentration was studied by method of initial rates which involved measuring the instantaneous rate of reaction before significant changes to the reactant concentrations. From the equilibrium swelling data in Figure 3-4 at the gel point, the amount of acetal bonds required to form a stable network in 4 g/dL

polyhexuronic acid gel was about 0.4 mM, and the extent of hydroxyls reacted was approximately 1.5 mM, or 0.25% of the initial hydroxyl concentration. Since the amount of reactant (hydroxyls and aldehydes) consumed was insignificant compared to the initial concentrations, the reaction time required for the formation of stable gel network at this gel point was used to study the instantaneous rate information described by equation 25.

$$\frac{\Delta[R_2C(OR')_2]}{t} = k''[R-CHO]_0^b \qquad \textbf{(Eq. 25)}$$

where $k'' = k[R\text{-}OH]_0$ is the pseudo-first order rate constant, $\Delta[R_2C(OR')_2]$ is the critical acetal concentration and t is the critical time at the gel point, and $[R\text{-}CHO]_0$ is the initial pentanedial concentration.

A kinetic plot of inversed critical gelation time (ie. time required to achieve a stable network structure), which is directly proportional to the initial rate, plotted against the square initial pentanedial concentration results in a linear plot as seen in Figure 3-6, indicating a second-order rate behavior with $b = 2$. Therefore, doubling the pentanedial concentration increased the rate of reaction by a factor of four. A slope change at around 0.65 M, corresponding to about 0.8 M of the initial pentanedial concentration was observed. Since the reaction between polyhexuronic acid (hydrogel) and aqueous aldehyde was heterogeneous, reactive aldehyde must diffuse from the continuous external phase into the gel phase. At initial pentanedial concentration lower than 0.9 M (or 0.8 M^2 in the plot), the reaction is more diffusional controlled, whereas at higher pentanedial

concentration, the aldehyde concentration difference between the external solution and the gel phase is sufficiently large to ensure that the reaction is kinetically controlled.

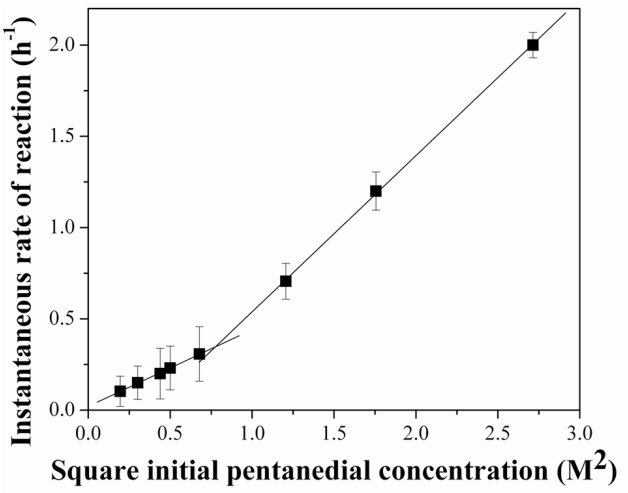

Figure 3-6. Second-order reaction kinetics with respect to pentanedial concentration in the formation of acetal linkage. The effective pentanedial concentration was calculated based on the total amount of water present during the reaction which accounts for the diluent present in the hydrogel.

3.3.7 Influence of acid catalyst concentration on the reaction kinetics

The reaction order with respect to acid catalyst concentration may be determined by the initial rate method as was the case with Figure 3-7. From the initial rate data, the increase in reaction rate was directly proportional to acid catalyst concentration with first order reaction kinetics as observed in Figure 3-7. Under the acidic conditions, the carbonyl oxygen is protonated, strongly polarizing the carbonyl group for rapid addition of weak nucleophilic alcohols. Therefore, increased HCl concentration subsequently increased the reactivity of the carbonyl group towards hydroxyls in polyhexuronic acid.

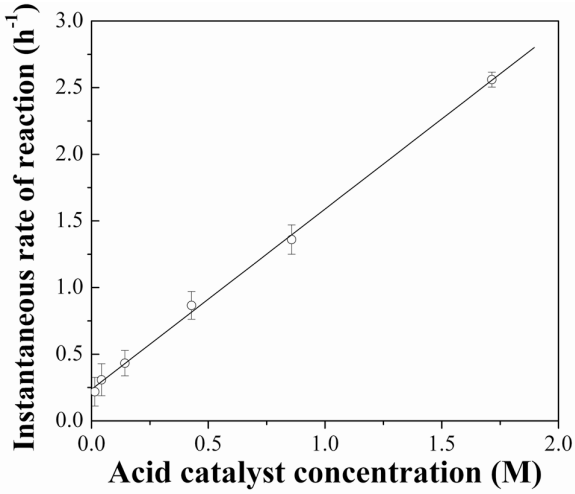

Figure 3-7. First-order reaction kinetics with respect to acid catalyst concentration in the formation of acetal linkage.

Temperature effect on the acetalization kinetics and the thermodynamic parameters

The formation of chemically networked polyhexuronic acid at various reaction temperatures was studied by equilibrium swelling and the kinetic profiles are presented in Figure 3-8. The rate constants at various temperatures were calculated from equation 5 using the pre-determined reaction orders (*a=0* and *b=2*) and the known acetal, polyhexuronic acid and pentanedial concentrations at the critical gel point, and are plotted as an Arrhenius plot in the inset of the same figure.

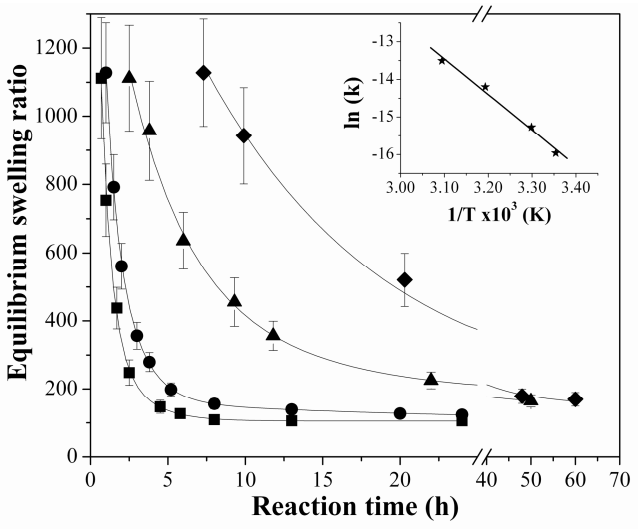

Figure 3-8. Kinetics of acetal bond formation at 22 (◆), 30 (▲), 40 (●) and 50°C (■). Inset: Arrhenius relationship between natural logarithm of rate constant and reciprocal reaction temperature.

The rate of network formation was observed to decrease with decreased reaction temperature. Since pentanedial undergoes parallel oxidative degradation forming non-reactive glutaric acid, as the crosslinking reaction proceeds, the acetalization reaction carried out at room temperature did not reach the expected maximum crosslinking density, which would result in a minimum equilibrium ratio of around 100. In addition, the reaction carried out at 4°C did not form a stable network even after 72 h of reaction time (data not shown). The critical time required to form a stable network at the gel point was observed to increase exponentially as the reaction temperature decreased. The rate constants at 22, 30, 40 and 50°C were 3.27, 6.54, 19.06, and 38.12 x 10^{-6} $Lmole^{-1}s^{-1}$, respectively using the known acetal, di-aldehyde and hydroxyls concentrations which were 0.39, 2.18 and 0.18 M at the critical gel point. The rate constants in the range of 22

to 50°C with 0.42 M of acid catalyst were observed to follow Arrhenius kinetics. The activation energy and the frequency factor of the acetalization reaction determined from the slope and y-intercept of the Arrhenius plot are 78.58 kJ/mol (or 18.78 kcal/mol) and 7.6 x 10^6, respectively. Because of the high activation energy, a Bronsted-acid catalyzed acetalization reaction may not take place at low temperature as was the case at 4°C. Since the estimated critical time to achieve the gel point based on the Arrhenius equation was about 33 h, with the parallel oxidation side reaction, it is difficult to achieve sufficient crosslinks at 4°C. The activation energy associated with the acetalization reaction of polyhexuronic acid and pentanedial is comparable to that of the reaction of polyvinyl alcohol with formaldehyde which is 17.4 kcal/mol[39] and to the reaction of acetaldehyde and methanol which is 72.35 kJ/mol[40]. The closeness of these values indicates similar reaction mechanisms in the formation of acetal bonds.

In summary, networked polyhexuronic acid gel was synthesized by acid-catalyzed acetalization. Permanent acetal linkages interconnect individual soluble alginate polymers, giving the resulting gel network enormous water absorbing/swelling ability while maintaining polymer structural stability in ionic solution. In contrast, physical gels such as Ca^{2+}- or Al^{3+}-alginate are stabilized through cooperative binding with divalent or trivalent cations. Chemical gels are not stabilized/destabilized by the presence/removal of these gelling ions, nor are they affected by high concentrations of monovalent cations or chelating ions such as phosphate, citrate and EDTA, which can destabilize alginate physical gels.

The extent of acetals distributed throughout the gel network controls the magnitude of gel swelling. We studied the kinetics of acetalization reaction via equilibrium swelling and found that the reaction is a second-order with respect to pentanedial concentration, a doubling effect on the rate of acetal formation, and zero-order with respect to polyhexuronic acid concentration. According to the proposed reaction mechanism, the connectivity of each crosslink point of 4 (f=4) was assumed and used in the derived equilibrium swelling equation to calculate network structural properties such as molecular weight between crosslinks, crosslinking density, and mesh pore size. Given the developed rate equation, $\frac{\Delta[R_2C(OR')_2]}{t} = k[R-CHO]^2$ where k is 19.06 x 10^{-6} L·mol^{-1}·sec^{-1} at 40^{o}C and 0.38 M acid solution, the reaction time required achieving the desired acetal product concentration at known aldehyde concentration and controlled reaction temperature can be estimated. The aldehyde concentration can be predicted using the assumed stoichiometric ratio of 1:2 aldehydes to hydroxyls, and the rate constant at the controlled temperature can be calculated from the Arrhenius kinetics with activation energy and frequency factor of 78.58 kJ/mol and 7.6 x 10^6, respectively. Through controlling the reaction time to achieve the desire concentration of acetal crosslink throughout the gel network, the extent of swelling in aqueous solution which relates to the resultant mesh pore size can therefore be manipulated and the release and diffusion properties can ultimately be modified.

Since the networked polyhexuronic acid consisted of ionizable carboxylate pendants, of which the degree of ionization depended on the solution pH and ionic

strength, it is stimuli-responsive and has potential application in oral delivery of protein therapeutics. In acid environment such as the stomach (pH 1.2), polyhexuronic acid gel contracts due to limited solubility of non-ionized acid moieties and protects therapeutic peptides from enzymatic and acid degradation while swelling in the alkaline environment of the intestinal tract (pH 7.8), as a result of increased hydrophilicity of ionized carboxylate moieties, releasing the active therapeutic. In addition, similar reactivity between the two hexuronic acid epimers may reduce the effect of batch variations between alginate sample chemistries, which is not the case in the formation of ionotropic gels (ie. calcium alginate). This insensitivity to alginate chemistry may allow some alginate types which do not form stable ionotropic gels (ie. low G-content alginate) to be used in many biomedical applications, extending the spectrum of the gelling properties of alginates.

3.4 Conclusion

Networked alginate hydrogel exhibiting pH-sensitive swelling was synthesized by Bronsted-acid catalyzed acetalization between hydroxyls in hexuronic acid residues and glutaraldehyde. The rate of acetalization was influenced by alginate molecular weight, aldehyde and acid catalyst concentrations. In addition, similar reactivity between the two hexuronic acid epimers may allow some alginate types which do not form stable ionotropic gels to be used in the formation of chemically network hydrogel, extending the spectrum of the gelling properties of alginates. From the developed rate equation of the

synthesized hydrogel, the desired acetal concentration which controls the resultant swelling and mesh pore size can be calculated and controlled with pre-selected reagents and formulation conditions. We studied the chemical kinetics of the acetalization reaction, enabling the ability to control properties which have as yet not been controlled to this extent for this particular polymer. The viscoelastic and rheological properties of this new class of polymer will be characterized in an upcoming publication. This controlled, semi-synthetic but natural polymer may potentially be used in oral drug delivery of peptide therapeutics, regenerative medicine as tissue scaffold, and environmental clean-up applications as biosorbent.

3.5 Acknowledgements

The authors thank the Natural Sciences and Engineering Research Council of Canada for financial support.

3.6 References

1. Wilson, J. I.; Chaikof, E. L., Challenges and emerging technologies in the immunoisolation of cells and tissues. *Advanced Drug Delivery Reviews* **2008,** 60, (2), 124-145.

2. Degim, I. T.; Celebi, N., Controlled delivery of peptides and proteins. *Current Pharmaceutical Design* **2007,** 13, (1), 99-117.

3. Augst, A. D.; Kong, H. J.; Mooney, D. J., Alginate hydrogels as biomaterials. *Macromolecular Bioscience* **2006,** 6, (8), 623-633.

4. Russo, R.; Malinconico, M.; Santagata, G., Effect of cross-linking with calcium ions on the physical properties of alginate films. *Biomacromolecules* **2007,** 8, (10), 3193-3197.

5. Draget, K. I.; Skjak-Braek, G.; Stokke, B. T., Similarities and differences between alginic acid gels and ionically crosslinked alginate gels. *Food Hydrocolloids* **2006,** 20, (2-3), 170-175.

6. Morch, Y. A.; Donati, I.; Strand, B. L.; Skjak-Braek, G., Molecular engineering as an approach to design new functional properties of alginate. *Biomacromolecules* **2007,** 8, (9), 2809-2814.

7. de Kerchove, A. J.; Elimelech, M., Formation of polysaccharide gel layers in the presence of Ca2+ and K+ ions: Measurements and mechanisms. *Biomacromolecules* **2007,** 8, (1), 113-121.

8. Thu, B.; Bruheim, P.; Espevik, T.; Smidsrod, O.; SoonShiong, P.; SkjakBraek, G., Alginate polycation microcapsules .1. Interaction between alginate and polycation. *Biomaterials* **1996,** 17, (10), 1031-1040.

9. Hennink, W. E.; van Nostrum, C. F., Novel crosslinking methods to design hydrogels. *Advanced Drug Delivery Reviews* **2002,** 54, (1), 13-36.

10. Bouhadir, K. H.; Hausman, D. S.; Mooney, D. J., Synthesis of cross-linked poly(aldehyde guluronate) hydrogels. *Polymer* **1999,** 40, (12), 3575-3584.

11. Moe, S. T.; Skjakbraek, G.; Elgsaeter, A.; Smidsrod, O., Swelling of Covalently Cross-Linked Alginate Gels - Influence of Ionic Solutes and Nonpolar-Solvents. *Macromolecules* **1993,** 26, (14), 3589-3597.

12. Chan, L. W.; Heng, P. W. S., Effects of aldehydes and methods of cross-linking on properties of calcium alginate microspheres prepared by emulsification. *Biomaterials* **2002,** 23, (5), 1319-1326.

13. Kim, Y. J.; Yoon, K. J.; Ko, S. W., Preparation and properties of alginate superabsorbent filament fibers crosslinked with glutaraldehyde. *Journal of Applied Polymer Science* **2000,** 78, (10), 1797-1804.

14. Kulkarni, A. R.; Soppimath, K. S.; Aminabhavi, T. M.; Dave, A. M.; Mehta, M. H., Glutaraldehyde crosslinked sodium alginate beads containing liquid pesticide for soil application. *Journal of Controlled Release* **2000,** 63, (1-2), 97-105.

15. Yeom, C. K.; Lee, K. H., Characterization of sodium alginate membrane crosslinked with glutaraldehyde in pervaporation separation. *Journal of Applied Polymer Science* **1998,** 67, (2), 209-219.

16. Leone, G.; Torricelli, P.; Chiumiento, A.; Facchini, A.; Barbucci, R., Amidic alginate hydrogel for nucleus pulposus replacement. *Journal of Biomedical Materials Research Part A* **2008,** 84A, (2), 391-401.

17. Xu, J. B.; Bartley, J. P.; Johnson, R. A., Preparation and characterization of alginate hydrogel membranes crosslinked using a water-soluble carbodiimide. *Journal of Applied Polymer Science* **2003,** 90, (3), 747-753.

18. Jayakrishnan, A.; Jameela, S. R., Glutaraldehyde as a fixative in bioprostheses and drug delivery matrices. *Biomaterials* **1996,** 17, (5), 471-484.

19. Migneault, I.; Dartiguenave, C.; Bertrand, M. J.; Waldron, K. C., Glutaraldehyde: behavior in aqueous solution, reaction with proteins, and application to enzyme crosslinking. *Biotechniques* **2004,** 37, (5), 790-802.

20. Gendler, E.; Gendler, S.; Nimni, M. E., Toxic Reactions Evoked by Glutaraldehyde-Fixed Pericardium and Cardiac-Valve Tissue Bioprosthesis. *Journal of Biomedical Materials Research* **1984,** 18, (7), 727-736.

21. Yamanaka, J.; Yamada, S.; Ise, N.; Yamaguchi, T., Revisit to the Intrinsic Viscosity-Molecular Weight Relationship of Ionic Polymers .7. Examination of the Pals-Hermans Dilution Method with Reference to the Viscosity Behavior of Dilute Aqueous Dispersion of Ionic Polymer Latex. *Journal of Polymer Science Part B-Polymer Physics* **1995,** 33, (10), 1523-1526.

22. Masuko, T.; Minami, A.; Iwasaki, N.; Majima, T.; Nishimura, S. I.; Lee, Y. C., Carbohydrate analysis by a phenol-sulfuric acid method in microplate format. *Analytical Biochemistry* **2005,** 339, (1), 69-72.

23. Kashyap, A. K.; Kalpagam, V., Dilute-Solution Properties of Methyl Methacrylate-Acrylonitrile Random Co-Polymers .2. Stockmayer Fixman Relations. *Makromolekulare Chemie-Macromolecular Chemistry and Physics* **1981,** 182, (4), 1147-1152.

24. Smidsrod, O., Solution Properties of Alginate. *Carbohydrate Research* **1970,** 13, (3), 359-372.

25. Amsden, B.; Turner, N., Diffusion characteristics of calcium alginate gels. *Biotechnology and Bioengineering* **1999,** 65, (5), 605-610.

26. Boontheekul, T.; Kong, H. J.; Mooney, D. J., Controlling alginate gel degradation utilizing partial oxidation and bimodal molecular weight distribution. *Biomaterials* **2005,** 26, (15), 2455-2465.

27. Iza, M.; Woerly, S.; Danumah, C.; Kaliaguine, S.; Bousmina, M., Determination of pore size distribution for mesoporous materials and polymeric gels by means of DSC measurements: thermoporometry. *Polymer* **2000,** 41, (15), 5885-5893.

28. Flory, P. J., *Statistical mechanics of chain molecules*. Repr. ed. with corrections ed.; Oxford University Press: New York, 1989.

29. Flory, P. J., *Principles of polymer chemistry*. Ithaca, New York, 1953.

30. Huggins, M. L., Some Properties of Solutions of Long-chain Compounds. *J. Phys. Chem.* **1942,** 46, (1), 151-158.

31. Flory, P. J.; John Rehner, J., Statistical Mechanics of Cross-Linked Polymer Networks II. Swelling. *The Journal of Chemical Physics* **1943,** 11, (11), 521-526.

32. Flory, P. J.; John Rehner, J., Statistical Mechanics of Cross-Linked Polymer Networks I. Rubberlike Elasticity. *The Journal of Chemical Physics* **1943,** 11, (11), 512-520.

33. Bray, J. C.; Merrill, E. W., Polyvinyl-Alcohol) Hydrogels - Formation by Electron-Beam Irradiation of Aqueous-Solutions and Subsequent Crystallization. *Journal of Applied Polymer Science* **1973,** 17, (12), 3779-3794.

34. Kovac, J., Modified Gaussian Model for Rubber Elasticity. *Macromolecules* **1978,** 11, (2), 362-365.

35. Barrhowell, B. D.; Peppas, N. A., Importance of Junction Functionality in Highly Crosslinked Polymers. *Polymer Bulletin* **1985,** 13, (2), 91-96.

36. Katchalsky, A.; Upadhyay, J.; Wassermann, A.; Cooper, R. E., Counter-Ion Fixation in Alginates. *Journal of the Chemical Society* **1961**, (Dec), 5198-5204.

37. Pitzer, K. S.; Mayorga, G., Thermodynamics of Electrolytes .2. Activity and Osmotic Coefficients for Strong Electrolytes with One or Both Ions Univalent. *Journal of Physical Chemistry* **1973,** 77, (19), 2300-2308.

38. Mafe, S.; Ramirez, P.; Tanioka, A.; Pellicer, J., Model for counterion-membrane-fixed ion pairing and donnan equilibrium in charged membranes. *Journal of Physical Chemistry B* **1997,** 101, (10), 1851-1856.

39. Kormanovskaya, G. N.; Vlodavets, I. N., Kinetics of acetalization of poly(vinyl alcohol) with aliphatic aldehydes in aqueous solutions. *Russian Chemical Bulletin* **1965,** 14, (4), 718-720.

40. Gandi, G. K.; Silva, V. M. T. M.; Rodrigues, A. E., Process development for dimethylacetal synthesis: Thermodynamics and reaction kinetics. *Industrial & Engineering Chemistry Research* **2005,** 44, (19), 7287-7297.

Chapter 4

Semisynthesis of controlled stimuli-responsive alginate hydrogel

Ariel W. Chan, Ralph A. Whitney and Ronald J. Neufeld

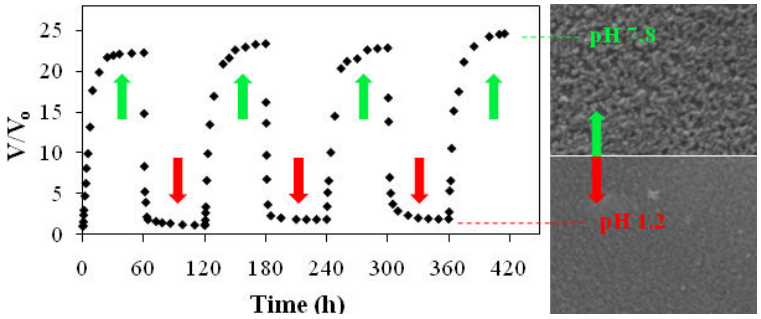

Keywords: alginate, pH-responsive hydrogel, thermodynamically controlled synthesis, pore size, equilibrium swelling

Manuscript published in *Biomacromolecules*. 2009. 10(3):609-616.

Abstract

Benefits in the use of natural polymers include biodegradability, biocompatibility, natural abundance, and unique physico-chemical/biological properties. Native alginate was used to semi-synthesize a new class of biomaterial in which the physical properties such as swelling and pore size can be chemically tailored for desired end use. Semi-synthetic network alginate polymer (SNAP) was prepared by reaction with glutaraldehyde, forming an acetal-linked network polymer gel with carboxylate moieties preserved as stimuli-responsive sensors. The molecular structure of the hydrogel was confirmed by cross-polarization magic-angle spinning ^{13}C solid state NMR, and reaction parameters affecting the polymer synthesis, including reactant, catalyst concentrations, and solvent composition, were characterized by gel equilibrium swelling. The acetalization reaction can be thermodynamically controlled, offering fine-tuned control of gel swelling and pore properties. In addition, SNAP demonstrated pronounced swelling at alkaline pH and contraction in acidic environment with oscillatory response to repeated pH-stimuli, yielding a potential pulsatile, oral drug delivery vehicle. Through selection of reaction conditions, gel swelling, pore size and stimuli-responsive characteristics can be specifically tailored for applications such as tissue scaffold in regenerative medicine, as targeted delivery vehicle, and as superabsorbent in environmental clean-up.

4.1 Introduction

Natural polymers from plants, animals and microbes are of considerable interest for applications in the fields of biotechnology and biomedical engineering, and as biomaterials and pharmaceutical controlled release devices[1]. In recent decades, sophisticated and structurally diverse natural polymers such as alginate, chitosan, gelatin and collagen have been readily purified in significant quantities. The benefits in the use of natural polymers are substantial due to biodegradability, biocompatibility, natural abundance, and unique chemical structures and physico-chemical/biological properties[2-7]. However, applications are limited because natural materials have fixed structures, and thus there is limited flexibility to modify polymer properties. Natural polymers may be utilized as starting materials/building blocks in semisynthesis of new classes of polymers, chemically tailored to match, improve, and offer unique physical, chemical, and in some cases biological functionalities for a desired end use by manipulation of chemical reaction and kinetics.

Alginate, one of the most abundant polysaccharides, is extracted from brown seaweed, and used extensively in foods, pharmaceuticals, and regenerative medicine[4,5,7,8]. The mucoadhesive property of alginate has made it one of the favoured formulation excipients in the pharmaceutical industry[9]. In addition, alginate can act as a smart macroaffinity ligand for pectinase, α-amylase, phospholipase D, and lipases, and has been applied in bioseparation processes [10-12]. Alginate consists of block co-polymer of β-D-mannuronic (M) and α-L-guluronic acid (G) in varying sequential arrangements and

proportions. Alginate undergoes supramolecular assembly in acid at a pH below 3, forming acid gel[13] or forms ionotropic physical gel by cooperative binding with multi-valent cations, typically Ca^{2+}. Alginate hydrogels which contain carboxylate anions on their hydrophilic surface may mimic the characteristics of the cell surface in vertebrates, minimizing immunogenic effects, improving biocompatibility[14]. In addition, because of high water content and structural and mechanical similarity to the macromolecular-based components in natural tissue[15,16], alginate hydrogels have been used as biomimetic extracellular matrix for cell attachment in tissue engineering applications, as sustained delivery system for active biomacromolecules, and as biomaterial for protein/cell encapsulation[4,7,17-19]. Alginate has been studied for many years in an effort to relate composition of the polymer to its physical properties[5,20-22]. Due to spatial arrangement of the ring and hydroxyl oxygen atoms of the guluronic acid monomers, only poly-guluronate (GG block) can form a stronger type of ionic bonding with divalent cations[5]. Therefore, the affinity with cations and the consequent gelling capacity is a direct function of the G-block size and quantity, and the availability of cations[5]. Researchers have looked to various natural sources that can provide differences in molecular weight (~8-1000 kDa) or distribution or concentration of one or both of the two monomers making up the polymer (pure M or G or alternative MG alginate polymer)[21, 23]. However, flexibility in polymer selection is limited, as is control of the final properties of the polymer constructs.

Alternatively, alginate gel can be semi-synthesized by reacting alginate hydroxyls with bi-functional glutaraldehyde via acid-catalyzed acetalization reaction, forming an

acetal-linked network hydrogel[24-26]. Since the carboxylate moieties in alginate were not involved in the reaction and are thus preserved, the resultant network hydrogel exhibits pH-responsive swelling/contraction properties. The kinetics of acetalization were found to undergo zero and second-order reaction with respect to alginate and glutaraldehyde, respectively. With the determined rate constant of 19.06 $\mu L \cdot mole^{-1} \cdot s^{-1}$ at 40^{o}C and activation energy of 78.58 $kJ \cdot mol^{-1}$, the crosslinking density of the network polymer can be kinetically controlled (rate of reaction), providing specific polymer properties[26]. However, glutaraldehyde undergoes parallel oxidative degradation forming non-reactive glutaric acid and aldol-polymerization forming poly(glutaraldehyde), competing with the monomeric glutaraldehyde for acetalization reaction[27-30]. Since the rates of the side reactions increase as the temperature and pH increase, at low glutaraldehyde or acid catalyst concentrations, the competitive side reactions can often overshadow the acetalization reaction (crosslinking reaction), deviating the actual crosslinking density away from the predictive one[26]. In this study, we systematically studied the effect of reactant concentrations and addition of co-solvent on the crosslinking reaction, and allowed the reaction to approach equilibrium, providing rate information for thermodynamic/equilibrium control of the reaction. The dynamic and stimuli-responsive swelling properties of the semi-synthetic network alginate polymer (SNAP) and the influence of the ionic environment were characterized. This new class of biomaterial based on semisynthesis from natural polysaccharide is pH-responsive, is mechanically stable in aqueous ionic environment, has demonstrated absorption/swelling properties, and can be considered as a potential oral delivery vehicle for a wide range of molecular

sizes of protein therapeutics, as superabsorbent for environmental clean-up application or as scaffold for tissue engineering applications.

4.2 Materials and methods

4.2.1 Semisynthesis of network alginate hydrogel

Sodium alginate solution (SF120, FMC Biopolymer, Drammen, Norway, M_W = 325,000, $[\eta]_{0.1\ M\ NaCl}$ (dL/g) 8.63, $F_G = 0.72$, $F_{GG} = 0.60$) of 4 g/dL was extruded dropwise via an automatic liquid dispenser (EFD, Model 1000XL, East Providence, USA) into 0.05 M HCl, resulting in 2.9 ± 0.1 mm alginic (polyhexuronic) acid gel beads. Beads were incubated in the supernatant solutions for 4 h prior to use. Glutaraldehyde (1,5-pentanedial) in water of 25% w/w was purchased from Sigma-Aldrich (Oakville, Canada). The absorbance ratio measured for polymeric to monomeric form of pentanedial was no greater than A_{235}/A_{280} = 0.3. Acid gel beads were suspended in crosslinking reaction medium containing 1.58 M glutaraldehyde and 0.38 M HCl at 40^{o}C, unless otherwise specified. The mass ratio of beads to reaction medium was 0.30 and accounting for the water content inside gel beads, the initial reactant concentrations were 0.38 M hydroxyls (or 0.19 M hexuronic acid residue) and 3.16 M aldehyde which was about 10 fold greater than that of hydroxyls from alginate.

4.2.2 Solid state nuclear magnetic resonance spectroscopy of alginate gel

SNAP was formed by reacting alginic acid gel of 4% with 3.6 M glutaraldehyde and 1.5 M HCl as catalyst at 40^{o}C for 10 h. Resultant beads were subsequently washed with 0.1 M pH 7.8 NaCl solution, followed by incubation in pH 2 acid solution to allow trace residual glutaraldehyde to react further with available hydroxyls inside the gel beads or diffuse out to the acid supernatant. The suspended solution was changed frequently until the absorbance measured spectrophotometrically was less than 0.05 at wavelength between 235 and 280 nm. Both gel beads were dried by lyophilization and ground into fine powder for the nuclear magnetic resonance (NMR) study.

The molecular structure of the native alginate polymer and chemically modified SNAP was characterized by cross-polarization magic angle spinning (CP-MAS) solid state ^{13}C-NMR on a Bruker 600 MHz Avance spectrometer with a spinning rate of 14050 Hz, contract time of 2 ms, and a relaxation delay of 2 s. Carbon-1 (carbon atom that links to two oxygens in the alginate polymer) in guluronic acid-rich alginate has resonance signal peak ~106 ppm which may overlap with the signal due to acetal bond formed between hydroxyls and glutaraldehyde (~105 ppm). Therefore, mannuronic acid-rich alginate (Kelton HVCR supplied by ISP Alginate Inc, Fraction of guluronic acid = 0.31, Mw = 308 kDa), which has characteristic signal peak of C1 at 107 ppm, was used instead to characterize the acetalization reaction in alginate modified gel. Although resonance signals differed between alginate samples, the characteristic signal peaks of the carbon atoms in alginate were observed to be within 1-2 ppm. The use of mannuronic acid-rich alginate was intended to reveal the individual signal generated due to newly formed acetal

bond and the existing acetals in the native polymer chains. The spectrum of the SNAP based on mannuronic acid-rich alginate revealed similar structural configuration as the guluronic acid-rich alginate.

4.2.3 Equilibrium swelling

The extent of crosslinking reaction was characterized by equilibrium gel swelling. Beads sampled from the reaction medium were washed with 4^{o}C, 40% ethanol, and then submerged in the swelling medium containing 0.1 M NaCl at pH 7.8 for 72 hours. To provide an infinite sink, the solution was constantly replaced with fresh medium. The critical gelation point was monitored by suspending 3 reacted beads in 30 mL of swelling medium for 24 h and the supernatant was used to determine non-crosslinked polymer sol fraction by phenol-sulphuric acid total carbohydrate assay[31]. At the critical gelation point, a stable, maximum attainable gel volume was obtained, and the sol carbohydrate content was less than 5% of the total initial soluble polymer which was considered to be within experimental error of the assay. The equilibrium swelling volume of the gel beads, V_s, was calculated from the bead diameter in aqueous solution determined under Leica stereomicroscope (D3, Germany) with the assumption of a perfect sphere. The corresponding equilibrium swelling ratio was calculated with respect to the initial compact volume of polymer according to Equation 1:

$$Equilibrium \quad Swelling \quad ratio = \frac{V_s}{\bar{\upsilon} m_p} \text{ --Equation 1}$$

where $\bar{\upsilon}$ and m_p are the specific density (0.8 cm^3/g) and the mass of the polymer. Sample mean and standard deviation were calculated based on 3 beads for each experiment. All data reported were the pooled mean and standard deviation of three repeated experiments.

4.2.4 Surface morphological characterization using scanning electron microscopy

The surface morphology of alginate hydrogel was characterized using scanning electron microscopy. SNAP gel beads were allowed to reach their equilibrium state in pH 1.2 HCl acid solution and pH 7.8, 20 mM phosphate buffered saline. The samples were lyophilized and mounted on metal stubs, followed by gold coating by pulse-spraying for 20 min under vacuum. The samples were examined in a JEOL JSM-840 SEM (10 kV, Japan).

4.2.5 Step-wise pH-stimulus swelling

Preformed 4% SF120 alginate acid gel beads underwent crosslinking reaction with 1.65 M glutaraldehyde in the presence of 1.71 M HCl at 40^oC for 8 h. The chemically modified gel beads were separated and washed with NaCl saline (pH 7.8, I = 0.1 M) to remove residual glutaraldehyde. The diameter of the gel beads at this initial condition was

measured to determine the reference gel bead volume, $V_{relaxed}$. The oscillatory swelling behaviour of the resulting semi-synthetic gel beads was investigated by immersing the gel beads in a solution of pH 1.2, and alternating them between pH 7.8 (0.1 M, phosphate saline buffer) and pH 1.2 every 60 h. The supernatant was changed frequently to maintain a constant ionic strength and pH. The swollen and contracted gel bead diameters were measured at various time intervals and the corresponding gel bead volumes ($V_{swelled}$) were used to calculate the swelling ratio ($V_{swelled}/V_{relaxed}$) . The repeated step-wise change was continued for 3.5 cycles.

4.2.6 Data collection and analysis

Sample mean and standard deviation were calculated based on 10 samples in each experiment. All data reported were the pooled mean and standard deviation of three repeated experiments, unless otherwise specified. The sample means and standard deviations of the three repeated experiments were pooled using equation 2. The data points presented in this work refer to the pooled means and standard deviations of the corresponding data sets unless otherwise specified.

$$\text{Pooled mean} = \left(\sum_{i=1}^{k} \mu_i \right) / N \qquad \text{(Eq. 2a)}$$

$$\text{Pooled standard deviation} = \frac{\sum_{i=1}^{k} \left((n_i - 1) s_i^{\,2} \right)}{\left(\sum_{i}^{k} n_i \right) - N} \qquad \text{(Eq. 2b)}$$

where n is the number of the replicates in each experiment and N is the total experiments , μ is the sample mean, and s is the sample standard deviation.

4.3 Results and Discussion

4.3.1 Semisynthesis of pH-responsive network alginate gel

Uronic acid monomer in alginate has reactive carboxylic acid and hydroxyls available for chemical modification. To preserve the carboxylate moieties for greater pH-sensitive response, the hydroxyl functional groups are the preferred reaction targets. Glutaraldehyde is an effective bi-functional chemical crosslinker consisting of two terminal aldehydes which can react with four alcohols in the presence of an acid catalyst to yield two 1,1-geminal diethers which are known as acetals, $R_2C(OR')_2$. A proposed crosslinking reaction between glutaraldehyde and alginate is shown in Figure 4-1. In the presence of HCl, the oxygen lone-pair electrons on the –OH group from alginate (1) can readily attack the polarized carbonyl groups (2), resulting in rapid nucleophilic addition to the aldehyde, forming monacetal (4). The adjacent aldehyde in the glutaraldehyde molecule follows similar reaction mechanism to react with hydroxyls of alginate polymer (4) in near proximity. As result, the formation of bis-acetal crosslinking structure (5) between two uronic acid monomers from adjacent polymer chains leads to intermolecular crosslinking, forming three-dimensional gel structure. Concurrently, monomeric glutaraldehyde can also undergo oxidative degradation and aldol-condensation, resulting in glutaric acid (6), poly-cyclic (7) and α,β-unsaturated poly-glutaraldehyde (8)[28, 30] at elevated temperature and in the presence of oxygen. The cyclic or linear polymeric glutaraldehyde possesses different reactivity as compared to the monomeric form, possibly reacting further with alginate to form complex network structures.

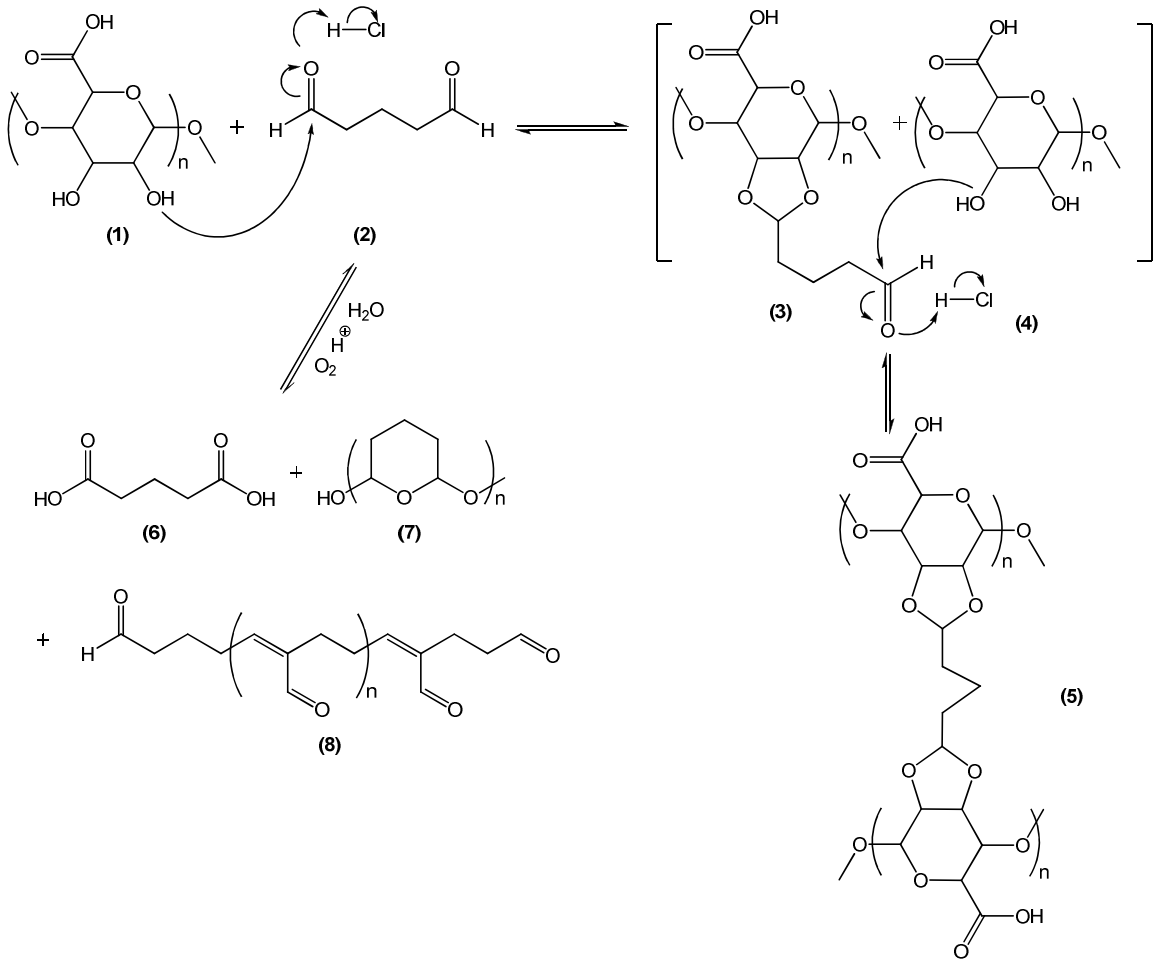

Figure 4-1. Semisynthesis of acetal-linked network alginate with glutaraldehyde as crosslinker.

Solid state ^{13}C-NMR was performed to characterize the molecular structure of the semi-synthetic network alginate polymer (SNAP) by comparing its spectra to the native alginate polymer in Figure 4-2. Resonance signals corresponding to the carbon atoms of linear alginate were assigned according to Grasdalen et al.[32] In the liquid state NMR, 8 narrow resonance peaks (line width) generally appear between 60-90 ppm, representing carbons numbered 2-5 in mannuronic (M) and guluronic acids (G). However, due to

limitations in signal sensitivity in the solid state, only 5 broader signal peaks are observed. Carbon 2 and 3 in mannuronic acid (M2, M3) and carbon 3 in guluronic acid (G3) are merged together and appear as one broad peak in the spectrum at 75 ppm. The signals of carbon 4 and 5 in mannuronic acid (M4, M5) are also inseparable, forming one broad peak at 83 ppm. Spectrum signals of carbon 1 in mannuronic (M1) and guluronic acid (G1), which only differed by approximately 1 ppm in the liquid state C-NMR, are inseparable in the solid state ^{13}C-NMR with one single peak at 107 ppm and wide line base ranging from 90 to 110 ppm.

The ^{13}C-NMR spectrum of the modified alginate is similar to that of the native polymer, except for the signal amplitude of two peaks at 68 and 75 ppm (corresponding to G2, and M3, M2, and G3 as marked with arrows) which appear to decrease relative to G5 signal. The decrease in relative signal intensities are likely the result of crosslinking of the two hydroxyls at carbon 2 and 3 in mannuronic and guluronic acids with glutaraldehyde, forming acetal linkage, $R_2C(OR')_2$, which has a characteristic peak at 105 ppm (identified by a star in the figure). G2, G3, M2 and M3 are being converted from hydroxyl-bearing carbons to ether-bearing carbons which results in a small chemical shift change and hence a broadening of the collective signals for these carbons relative to G5, G6, M5 and M6.

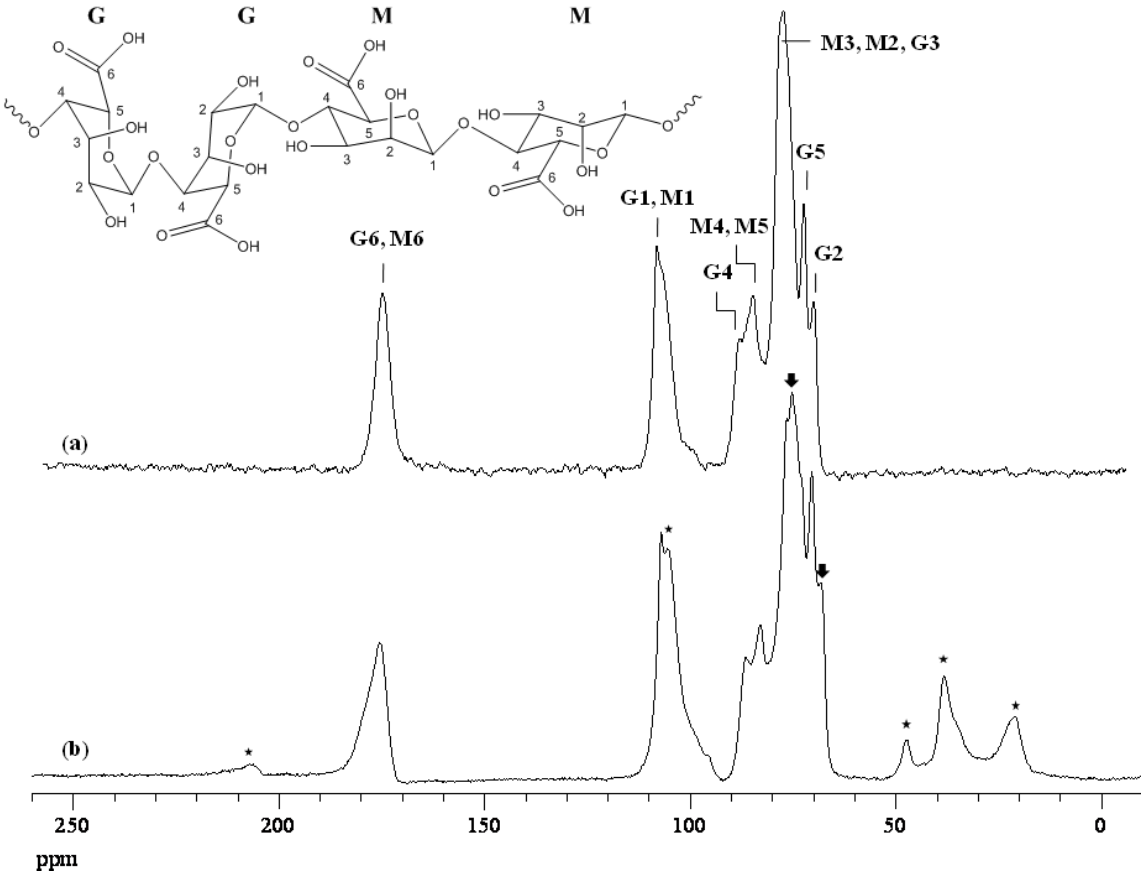

Figure 4-2. CP-MAS ^{13}C-NMR spectra of native alginate polymer (a) and SNAP (b) with the star and arrows denoting the new resonance signals (*) and reduction in signal intensity (↓) relative to G5 signal due to chemical modification of native polymer.

The modified, crosslinked polymer shows upfield signals at about 20, 35 and 45 ppm, and a downfield signal about 207 ppm. Highly concentrated glutaraldehyde was used to produce the highest possible acetal linkage, so the relative signal strength to other carbons in the network polymer is sufficiently large to be identifiable in the NMR spectrum. Such high aldehyde concentration was only used for the preliminary study. In practice, high reaction conversion (high crosslinking density) can be achieved through parameter and formulation optimization. The signals at 20 and 35 ppm are likely due to

the 3 (CH_2) groups between the acetals of the bis-acetal crosslinking structure (structure **5** in Figure 4-1), with the two CH_2 groups adjacent to the acetal rings having the larger chemical shift (35 ppm). However the other signals at around 45 and 207 ppm are likely due to the CH_2 group next to the aldehyde of glutaraldehyde that has formed only one acetal group (the monoacetal structure **3** in Figure 4-1) as well as the carbonyl group carbon, respectively. Since the polymer chain mobility decreases as the crosslinks form, the aldehyde on the glutaraldehyde monoacetal may not be able to react further with hydroxyls due to this lack of mobility. In addition, the monoacetal is covalently bounded to the polymer and thus is not removed from the beads by washing, while free glutaraldehyde is removed through washing.

Solid state ^{13}C-NMR confirms the proposed acetal formation, chemically modifying linear alginate into network structure. The present study was directed toward formulation of SNAP hydrogel by thermodynamically controlled reaction in which the desired gel properties were obtained with the pre-selected initial reactant and catalyst concentrations and allowing the reaction to approach equilibrium.

4.3.2 Thermodynamic control in synthesis of SNAP hydrogel

4.3.2.1 Influence of glutaraldehyde concentration on the reaction kinetics

The effect of initial glutaraldehyde concentration on the rate of acetal formation was examined by suspending 4% alginic acid beads in 0.43 M HCl acid catalyst and glutaraldehyde at concentrations ranging from 0.44 to 1.65 M, equivalent to 0.88 to 3.30

M of reactive aldehyde. The time course of the crosslinking reaction was studied by equilibrium swelling and is presented in Figure 4-3.

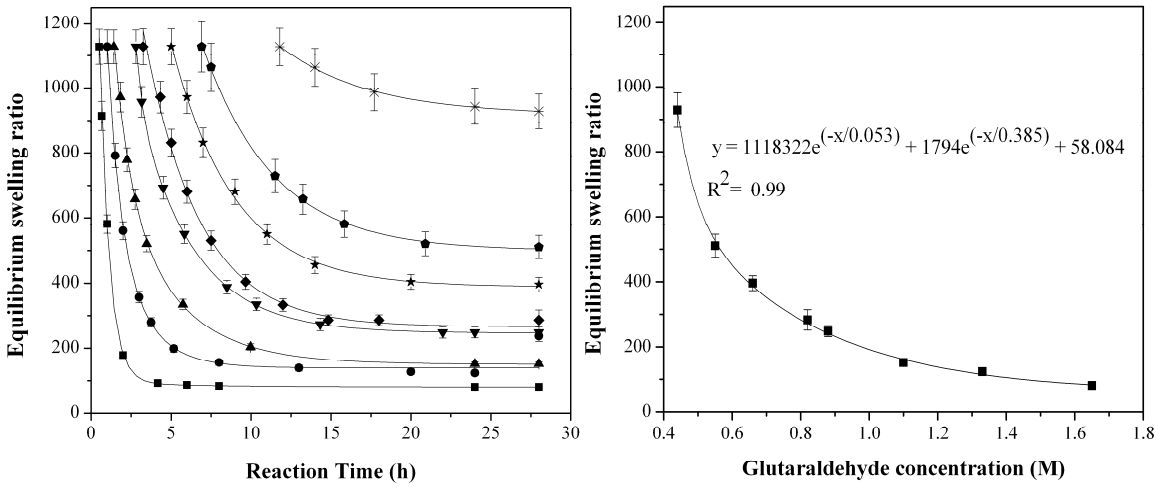

Figure 4-3. Equilibrium swelling ratio of the SNAP gel beads formulated by suspending alginic acid gel beads of 4% w/v in the reaction mediums containing 0.43 M HCl and 0.44(*), 0.55(⬟),0.66(★),0.82(◆),0.88(▼),1.10(▲),1.33(●),and 1.65 M (■) initial glutaraldehyde (left-side figure). The equilibrium swelling ratio of the reacted beads formulated in various initial glutaraldehyde concentrations after 28 h of reaction time are illustrated in the right-side figure.

As can be seen, gel swelling decreased as the reaction proceeded and reached a minimum between 80 to 1000 times of the dry compact volume. Depending on initial glutaraldehyde concentration, the reaction approached a maximum, reaching equilibrium after 8 to 25 h. Previously, it was found that formation of acetals requires high activation energy of 78.58 kJ/mol[26]. Therefore, the concentration of the acetal products which affects gel swelling can be equilibrium controlled (thermodynamically driven) by the initial reactant concentrations[26]. The relationship between initial glutaraldehyde concentration (x) and equilibrium swelling ratio of the gel beads with maximum achievable crosslink density (y) can be described by the second order exponential decay

function illustrated. This expression can be used to semi-synthesize alginate gel with preferred swelling properties by controlling the initial glutaraldehyde concentration and allowing the reaction to approach equilibrium.

4.3.2.2 Influence of acid catalyst concentration on reaction kinetics

The effect of acid catalyst on the crosslinking reaction was also characterized via equilibrium swelling ratio. A faster reaction was observed at higher acid catalyst concentration as seen in Figure 4-4. Under acidic conditions, the carbonyl oxygen is protonated, strongly polarizing the carbonyl group for rapid addition of weak nucleophilic alcohols. Therefore, increased HCl concentration promoted reactivity of the carbonyl group toward hydroxyls in alginate. In addition, the time to reach equilibrium (minimum equilibrium swelling ratio of each curve) was reduced from about 30 to less than 8 h when the acid concentration increased from 0.014 to 1.714 M. The equilibrium swelling ratio of the reacted beads obtained after 30 h (y) when the crosslinking reaction approached equilibrium, can be controlled by acid catalyst concentration (x) using the mathematical expression illustrated.

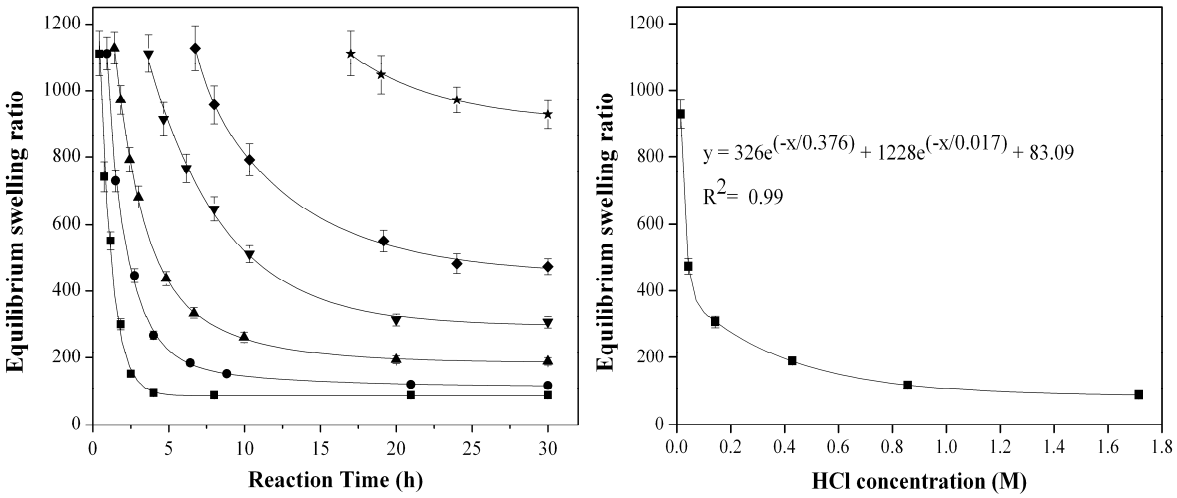

Figure 4-4. Effect of HCl concentration on crosslinking kinetics of the SNAP gel beads. Alginic acid gel beads were suspended in the reaction solution containing 1.65 M glutaraldehyde and 0.014 (★), 0.043 (◆),0.143 (▼),0.429 (▲),0.857 (●), and 1.714 M (■) HCl as catalyst. The equilibrium swelling ratio of the reacted beads formulated in various HCl concentrations after 30 h of reaction time is shown in the right-side figure.

4.3.2.3 Influence of alginate concentration on the reaction kinetics

Five gels were prepared with initial alginate concentrations ranging from 1.5 to 5% and reacted with excess glutaraldehyde which was at least 80 fold higher than hydroxyl concentration. Previously[26] , it was shown that alginate followed a zero-order reaction, in which alginate concentration did not affect the overall rate of reaction. However, the critical gel time, which is the time required to form sufficient crosslinks in the gel (gel point) so as to no longer be soluble in the aqueous swelling medium, decreased with increasing alginate concentration as observed in Figure 4-5.

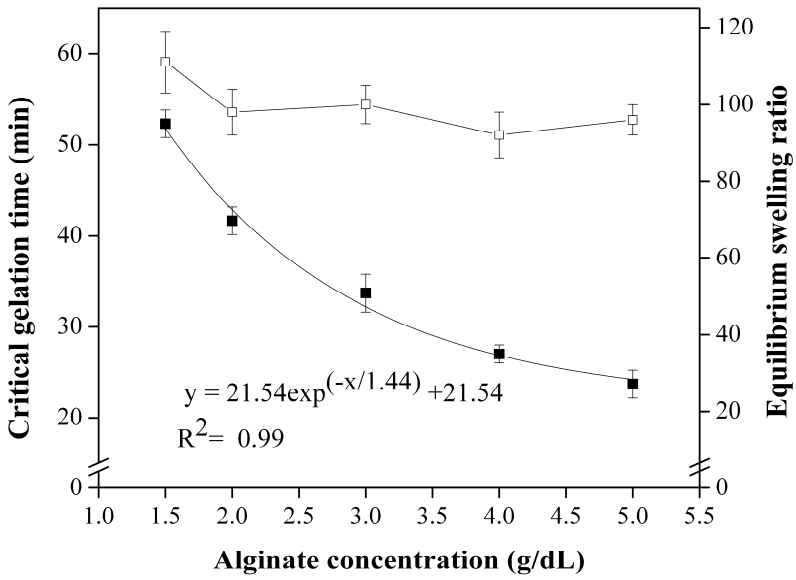

Figure 4-5. Critical gelation time (left-side ordinate, ■) in synthesis of SNAP hydrogel and the equilibrium swelling ratio of the SNAP hydrogel obtained at reaction equilibrium (right-side ordinate, □) as a function of polymer fraction.

The critical gel time decreased from 52 to 25 min with increasing alginate concentration from 1.5 to 5%, and follows a first order exponential decay curve. Since gel network formation is based on the probability of reactants colliding and forming crosslinked product, increased polymer fraction which subsequently increases the concentration of active hydroxyls, improves the probability of contact with available di-aldehyde, forming acetal bond linkages. Therefore, a longer reaction time was required to achieve the gel point for the lower concentration of 1.5% alginic acid gels.

Although alginate concentration affected the critical gel time, the equilibrium swelling ratios of all polymer samples obtained at the reaction equilibrium were similar, indicating the maximum crosslinking density was achieved, regardless of the initial polymer concentrations.

4.3.2.4 Effect of solvent composition on the reaction kinetics

Synthesis of SNAP gel beads was carried out in water-based media in which the solvent solvates the polymer and chemical crosslinkers to facilitate molecular collisions. Alginate is hydrophilic in the aqueous environment and its solution can tolerate the addition of 10-20% of water-miscible organic solvents such as alcohols and ketones without precipitating. To study the effect of water-miscible solvents on reaction kinetics, 20% v/v of various polar protic solvents, and polar aprotic solvents were added to the reaction medium composed of 1.05 M glutaraldehyde and 0.38 M HCl. The added solvent effect on the rate of crosslinking reaction characterized via equilibrium swelling is presented in Figure 4-6.

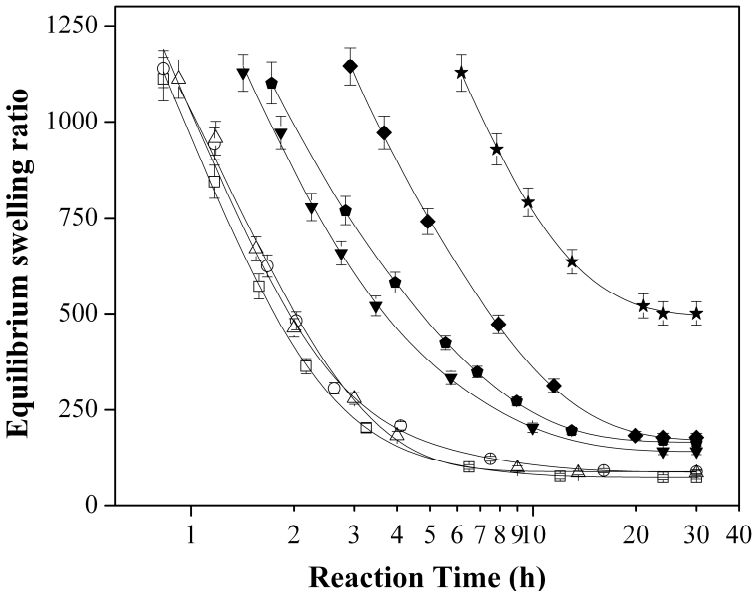

Figure 4-6. Equilibrium swelling of SNAP gel beads synthesized in water-based medium containing no added solvent (▼) or 20% v/v aprotic solvents: acetone (□), dioxane (○), DMSO (△) or protic solvents: 1-propanol (⬟), ethanol (◆), or methanol (★).

Reaction media containing aprotic solvents favored the crosslink formation (acetals), demonstrating the fastest rate of decrease in equilibrium swelling ratio as compared to the reactions performed in pure water and with added protic solvents. In addition, the effect of acetone, dioxane and DMSO on the reaction kinetics was observed to be similar, with the three reaction curves almost coinciding. As compared to the case in which the reaction was performed without added solvent, this greater rate of reaction may be due to the differential solubility of glutaraldehyde between the external solution and that within the gel beads. Since the dielectric constants of the external mixtures which contained 30% v/v water micible solvent were around 57-60, while the dielectric constant of pure water inside the preformed acid gel was about 81, glutaraldehyde (polar compound) is likely to partition from the less polar external medium (ie. mixture had lower dielectric constant) into the gel beads. The concentration sink inside the gel bead potentially increased the local glutaraldehyde concentration for reaction with hydroxyls, increasing rate of reaction. In addition, in the system consisting of 3 phases: external medium (liquid), internal medium (liquid) and polymer (solid), the crosslinking reaction requires glutaraldehyde to partition between the two liquid phases and the solid phase, where crosslinking takes place. The polar aprotic solvents may increase solubility of the di-aldehyde in the solid polymer phase, and hence accelerate the reaction.

Although the addition of protic solvent also lowers the polarity of the external and internal solution, the ability of the protic solvents to be competitive nucleophiles with the hydroxyl groups of alginate may hinder the nucleophilic addition reaction, retarding acetal linkage formation. Since alcohols can react with glutaraldehyde to form acetals, the

addition of protic solvent may result in competitive side reaction, leaving less chemical crosslinker for crosslinking reaction. Therefore, alcohol of higher reactivity is expected to lead to slower rate of reaction. The time to reach the gel point (time for the formation of stable network) in an ascending order for reactions carried out with added protic solvents was 1-propanol < ethanol < methanol, indicating a probable increase in alcohol reactivity as the size of the alkyl groups decreased. This steric effect on the competitive reactivity would make 1-propanol less competitive than methanol. Therefore, less undesired competitive side reaction from alcohols with pentanedial subsequently increases the rate of crosslinking reaction.

4.3.3 Responsive swelling behavior of SNAP hydrogel

4.3.3.1 Oscillatory pH-responsive characteristics of SNAP hydrogel

To demonstrate the potential application of SNAP hydrogel in the development of transmucosal pharmaceutical formulations to deliver therapeutic agents, the pH-responsiveness of the new biomaterial in gastric acid environment (~pH 1.2) and in the targeted intestinal luminal region (~pH 7.8) was characterized. SNAP hydrogel was synthesized by reaction with 1.65 M glutaraldehyde in the presence of 1.71 M of HCl at 40^{o}C for 8 h was subjected to stepwise pH-stimuli and the dynamic swelling response is presented in Figure 4-7.

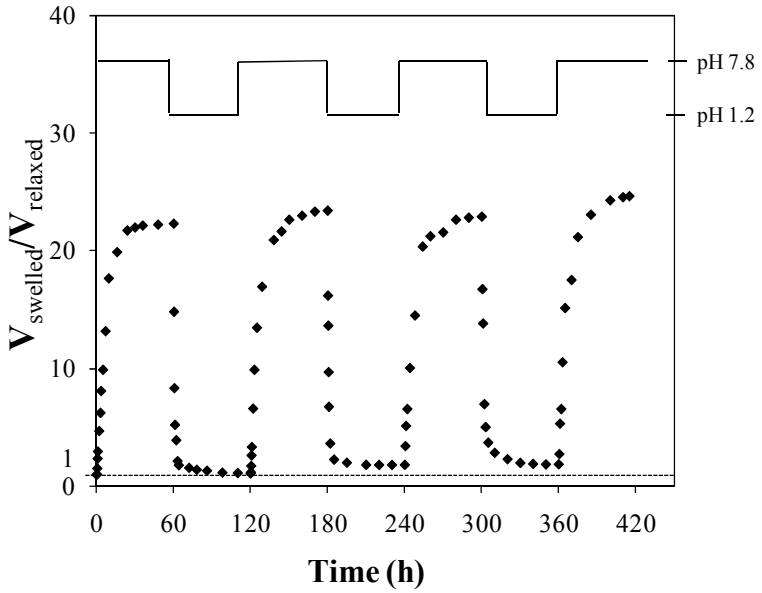

Figure 4-7. The oscillatory swelling response of SNAP hydrogel to step-wise alternating pH-stimulus.

In pH 7.8 solution, carboxylic acid moieties are deprotonated as the pK_a values of guluronic and mannuronic monomers are 3.65, and 3.38, respectively[33]. This increases polymer hydrophilicity and sets up an electrostatic repulsion which subsequently expands the gel network, leading to a swollen gel state. Alternatively at low pH, the pendant acids are protonated, resulting in uncharged polymer with limited solubility leading to rapid polymer rearrangement, expelling water out from the gel network and contracting to the original relaxed gel volume. In a pH-oscillating solution, SNAP hydrogel exhibits repetitive pulsatile swelling/contraction with a constant period and amplitude synchronized with the pH oscillation. The amplitude of the swelling, which is affected by the crosslinking density, can be specifically tailored for end application by controlling the reaction kinetics.

The change in pore size of the hydrogel due to responsive swelling behavior in acid/alkaline solutions is presented in Figure 4-8.

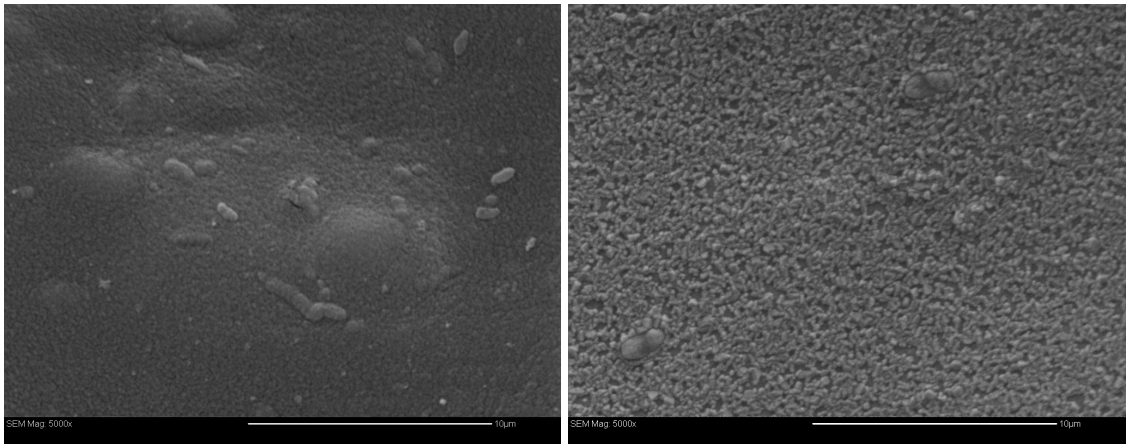

Figure 4-8. SEM micrographs of equilibrium swollen alginate gel in pH 1.2 HCl solution (left-side image) and pH 7.8 phosphate buffered saline (right-side image). Both images were taken at 5000 x magnification and scale bars represent 10 μm.

Distinct differences were observed in the SEM images in which the pores appeared tighter, smaller, and less than 0.1 μm for alginate in acid solution whereas the pores increased to close to 0.5 μm in alkaline solution. Since the pore size affects solute diffusion into and out from the hydrogel, with careful control of the crosslinking density (acetal concentration), the pore size can be tailored for desired diffusion and release rate.

4.3.4 Influence of ionic environment on gel swelling

The effect of the ionic environment on gel swelling was characterized by placing beads in NaCl solution of ionic strength (I) ranging from 0.01 to 2.0 M at 38^{o}C and pH 7.8. Beads of low, medium and high crosslinking density were obtained from equilibrium

reaction with increasing glutaraldehyde concentrations at 40°C. Equilibrium swelling in NaCl solution of various ionic strengths is plotted as a function of $1/\sqrt{I}$ in Figure 4-9. A linear relationship between equilibrium swelling ratio and $1/I^{0.5}$ was obtained with greater gel swelling in lower salt concentration, which corresponded with higher value of $1/I^{0.5}$. Sodium ions shield fixed negative charges on alginate, reducing electrostatic repulsion. In addition, when the dispersed solution contains high ion concentration (ie. high ionic strength), the chemical potential difference of water inside and the outside of the gel network is reduced and thus the magnitude of swelling is lowered compared to gel suspended in low ion concentration.

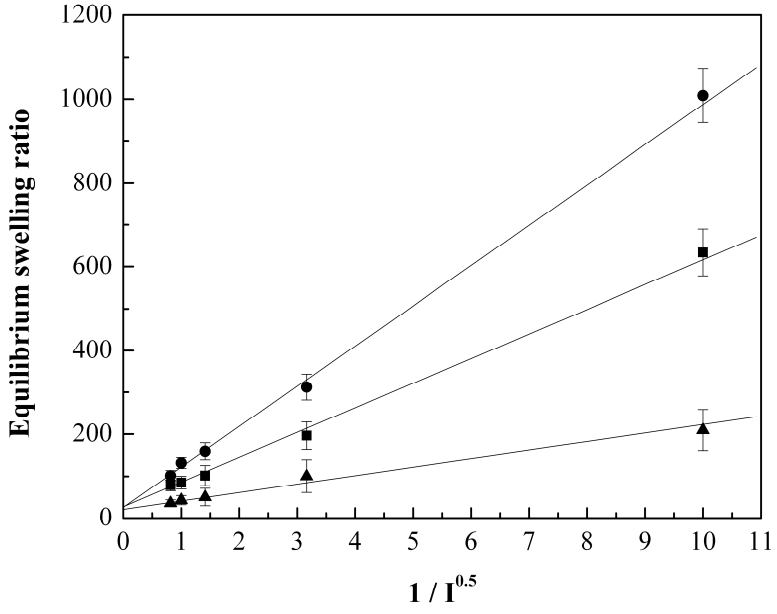

Figure 4-9. Equilibrium swelling of SNAP hydrogel in pH 7.8 NaCl solution of various ionic strengths at 38°C. Gel beads were synthesized by reaction with 0.82 M (●), 1.10 (■) and 1.65 M (▲) glutaraldehyde and 1.71 M HCl until the reaction approached equilibrium.

According to the equilibrium swelling model derived previously[26] for network alginate, the elastic retractive force exerted by the crosslinker restricts the gel from infinite swelling and the extent of swelling depends on the crosslinking density, external pH and ionic strength. As seen in the figure, densely crosslinked gel beads were less affected by external ionic strength compared to loosely crosslinked beads. Approximately 10-fold reduction in swelling was observed for loosely crosslinked gel beads when the solution ionic strength increased from 0.01 M to 2 M while only about 2-fold of swelling volume reduction was experienced for densely crosslinked beads. All sets of beads, each with different crosslink density, showed an equilibrium swelling of about 30 when extrapolated to infinite ionic strength ($I^{-0.5} \infty 0$), this corresponding to swelling at theta condition when the screening of the fixed charges on the polymers is so severe that the mutual repulsion between polymers was essentially removed, resulting in a behavior similar to that of neutral polymers.

In summary, natural polymers like alginate are of considerable interest in the fields of biotechnology and biomedical engineering due to their biodegradability, biocompatibility, natural abundance, and unique chemical structures and physico-chemical and biological properties. To enable the control of properties generally not possible with native polymer, SNAP was formed by acid-catalyzed reaction with glutaraldehyde, forming an acetal crosslinked network polymer. The extent of acetalization reaction, which affected the magnitude of the gel swelling, can be thermodynamically controlled (equilibrium controlled). The desired gel properties such as swelling and pore size can be obtained by pre-selected reaction conditions such as

glutaraldehyde and acid catalyst concentrations, and reaction solvent compositions, and by allowing the reaction to reach equilibrium. The correlation between the initial glutaraldehyde and acid catalyst concentrations used in semisynthesis and the resultant gel swelling in 0.1 M NaCl 7.8 solution can be described by a second order exponential decay models. The addition of aprotic solvent to the crosslinking medium enhanced the rate while the use of protic solvents retarded the rate of acetalization reaction.

SNAP hydrogel demonstrated pronounced, repeatable and programmable pH-responsive swelling in alkali, and would contract and remain in a compact state in acid medium. The extent of swelling can be as high as 1000 times the dry compact polymer volume for loosely crosslinked alginate, through thermodynamic controlled reaction with the use of low glutaraldehyde or acid catalyst concentrations, or with the addition of protic solvents such as ethanol. Since alginate consisted of ionizable carboxylate moieties, gel swelling is pH-responsive as well as ionic strength dependent. In ionic solution containing high salt concentration, the negative charged moieties are shielded by cations, reducing gel swelling significantly compared to low salt solutions. Loosely crosslinked gel tended to be influenced more than densely crosslinked alginate. However, SNAP is a permanent network hydrogel, and hence the mechanical stability was not compromised which is not the case for alginate gel formed by physical means such as is the case with Ca^{++} stabilized alginate gels which are unstable in high salt concentrations such as with NaCl, or with chelators such as sodium citrate or phosphate.

SNAP is pH-responsive, elastic, and mechanically stable. Through careful selection of the semisynthesis conditions such as reaction time, chemical crosslinker and

acid catalyst concentrations, and solvent composition, the permeability (ie. pore size) of the gel network can be modified and solute diffusion and release properties can be subsequently controlled. This new class of biomaterial can potentially be used as oral delivery vehicle for a wide range of molecular sizes of protein therapeutics, as superabsorbent for environmental clean-up application or as scaffold for tissue engineered implants.

4.4 Acknowledgements

The authors thank the Natural Sciences and Engineering Research Council of Canada for financial support.

4.5 Reference

1. Carraher, C. E. J., Derivatives of Natural Polymers. In *(Second Edition)*, 2 ed.; John Wiley & Sons, Inc.: 2003; pp 365-378.

2. Dang, J. M.; Leong, K. W., Natural polymers for gene delivery and tissue engineering. *Advanced Drug Delivery Reviews* **2006,** 58, (4), 487-499.

3. Ikada, Y.; Tsuji, H., Biodegradable polyesters for medical and ecological applications. *Macromolecular Rapid Communications* **2000,** 21, (3), 117-132.

4. Augst, A. D.; Kong, H. J.; Mooney, D. J., Alginate hydrogels as biomaterials. *Macromolecular Bioscience* **2006,** 6, (8), 623-633.

5. Draget, K. I.; SkjakBraek, G.; Smidsrod, O., Alginate based new materials. *International Journal of Biological Macromolecules* **1997,** 21, (1-2), 47-55.

6. Quignard, F.; Valentin, R.; Di Renzo, F., Aerogel materials from marine polysaccharides. *New Journal of Chemistry* **2008,** 32, (8), 1300-1310.

7. Orive, G.; Carcaboso, A. M.; Hernandez, R. M.; Gascon, A. R.; Pedraz, J. L., Biocompatibility evaluation of different alginates and alginate-based microcapsules. *Biomacromolecules* **2005,** 6, (2), 927-931.

8. Chan, G.; Mooney, D. J., New materials for tissue engineering: towards greater control over the biological response. *Trends in Biotechnology* **2008,** 26, (7), 382-392.

9. Bernkop-Schnurch, A.; Kast, C. E.; Richter, M. F., Improvement in the mucoadhesive properties of alginate by the covalent attachment of cysteine. *Journal of Controlled Release* **2001,** 71, (3), 277-285.

10. Smidsrod, O.; SkjakBraek, G., Alginate as Immobilization Matrix for Cells. *Trends in Biotechnology* **1990,** 8, (3), 71-78.

11. Sharma, A.; Sharma, S.; Gupta, M. N., Purification of wheat germ amylase by precipitation. *Protein Expression and Purification* **2000,** 18, (1), 111-114.

12. Sharma, S.; Gupta, M. N., Alginate as a macroaffinity ligand and an additive for enhanced activity and thermostability of lipases. *Biotechnology and Applied Biochemistry* **2001,** 33, 161-165.

13. Draget, K. I.; Stokke, B. T.; Yuguchi, Y.; Urakawa, H.; Kajiwara, K., Small-angle x-ray scattering and rheological characterization of alginate gels. 3. Alginic acid gels. *Biomacromolecules* **2003,** 4, (6), 1661-1668.

14. Smetana, K., Cell Biology of Hydrogels. *Biomaterials* **1993,** 14, (14), 1046-1050.

15. Lee, K. Y.; Mooney, D. J., Hydrogels for tissue engineering. *Chemical Reviews* **2001,** 101, (7), 1869-1879.

16. Jhon, M. S.; Andrade, J. D., Water and Hydrogels. *Journal of Biomedical Materials Research* **1973,** 7, (6), 509-522.

17. Kong, H. J.; Smith, M. K.; Mooney, D. J., Designing alginate hydrogels to maintain viability of immobilized cells. *Biomaterials* **2003,** 24, (22), 4023-4029.

18. McEntee, M. K. E.; Bhatia, S. K.; Tao, L.; Roberts, S. C.; Bhatia, S. R., Tunable transport of glucose through ionically-crosslinked alginate gels: Effect of alginate and calcium concentration. *Journal of Applied Polymer Science* **2008,** 107, (5), 2956-2962.

19. Sarmento, B.; Ribeiro, A.; Veiga, F.; Sampaio, P.; Neufeld, R.; Ferreira, D., Alginate/Chitosan nanoparticles are effective for oral insulin delivery. *Pharmaceutical Research* **2007,** 24, (12), 2198-2206.

20. Morch, Y. A.; Donati, I.; Strand, B. L.; SkjakBraek, G., Molecular engineering as an approach to design new functional properties of alginate. *Biomacromolecules* **2007,** 8, (9), 2809-2814.

21. Hartmann, M.; Dentini, M.; Draget, K. I.; Skjak-Braek, G., Enzymatic modification of alginates with the mannuronan C-5 epimerase AlgE4 enhances their solubility at low pH. *Carbohydrate Polymers* **2006,** 63, (2), 257-262.

22. Russo, R.; Malinconico, M.; Santagata, G., Effect of cross-linking with calcium ions on the physical properties of alginate films. *Biomacromolecules* **2007,** 8, (10), 3193-3197.

23. Lattner, D.; Flemming, H. C.; Mayer, C., C-13-NMR study of the interaction of bacterial alginate with bivalent cations. *International Journal of Biological Macromolecules* **2003,** 33, (1-3), 81-88.

24. Kulkarni, A. R.; Soppimath, K. S.; Aminabhavi, T. M.; Dave, A. M.; Mehta, M. H., Glutaraldehyde crosslinked sodium alginate beads containing liquid pesticide for soil application. *Journal of Controlled Release* **2000,** 63, (1-2), 97-105.

25. Kim, Y. J.; Yoon, K. J.; Ko, S. W., Preparation and properties of alginate superabsorbent filament fibers crosslinked with glutaraldehyde. *Journal of Applied Polymer Science* **2000,** 78, (10), 1797-1804.

26. Chan, A. W.; Whitney, R. A.; Neufeld, R. J., Kinetic controlled synthesis of pH-responsive network alginate. *Biomacromolecules* **2008,** 9, (9), 2536-45.

27. Jayakrishnan, A.; Jameela, S. R., Glutaraldehyde as a fixative in bioprostheses and drug delivery matrices. *Biomaterials* **1996,** 17, (5), 471-484.

28. Margel, S.; Rembaum, A., Synthesis and Characterization of Poly(Glutaraldehyde) - Potential Reagent for Protein Immobilization and Cell-Separation. *Macromolecules* **1980,** 13, (1), 19-24.

29. Purss, H. K.; Qiao, G. G.; Solomon, D. H., Effect of "'glutaraldehyde" functionality on network formation in poly(vinyl alcohol) membranes. *Journal of Applied Polymer Science* **2005,** 96, (3), 780-792.

30. Migneault, I.; Dartiguenave, C.; Bertrand, M. J.; Waldron, K. C., Glutaraldehyde: behavior in aqueous solution, reaction with proteins, and application to enzyme crosslinking. *Biotechniques* **2004,** 37, (5), 790-802.

31. Masuko, T.; Minami, A.; Iwasaki, N.; Majima, T.; Nishimura, S. I.; Lee, Y. C., Carbohydrate analysis by a phenol-sulfuric acid method in microplate format. *Analytical Biochemistry* **2005,** 339, (1), 69-72.

32. Grasdalen, H.; Larsen, B.; Smidsrod, O., C-13-Nmr Studies of Monomeric Composition and Sequence in Alginate. *Carbohydrate Research* **1981,** 89, (2), 179-191.

33. Smidsrod, O.; Haug, A., Dependence Upon Uronic Acid Composition of Some Ion-Exchange Properties of Alginates. *Acta Chemica Scandinavica* **1968,** 22, (6), 1989-1997.

Chapter 5

Tunable network alginate for absorptive encapsulation and controlled release of therapeutic proteins

Ariel W. Chan and Ronald J. Neufeld

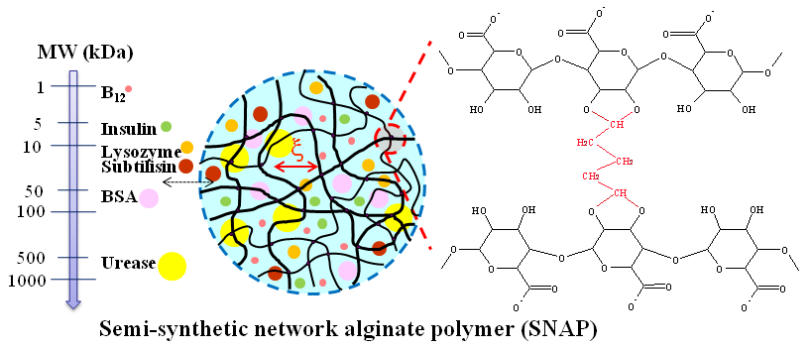

Keywords: alginate, glutaraldehyde, diffusion, pore size, insulin

Manuscript in Journal Submission

Abstract

Natural polymers may be utilized as building blocks for semisynthesis of tunable biomaterials, chemically tailored to match, improve, and offer unique physical, chemical, and biological functionalities for a desired end use. Semisynthetic network alginate polymer (SNAP) gel was formulated with desired pore diameter for absorptive encapsulation of proteins with wide ranging molecular sizes, achieving high protein payload and encapsulation yields. The diffusion characteristics of vitamin B_{12}, lysozyme, subtilisin, insulin, bovine serum albumin, urease and insulin into SNAP hydrogel were studied and compared to uptake by native polymer in the form of calcium alginate gels. Protein biomolecules were encapsulated via absorptive encapsulation approach whereby bead production was decoupled from protein loading, achieving high encapsulation yields and payloads. Drying was applied as a post-encapsulation mechanism to tailor protein diffusion/release properties. SNAP granules containing protein biomolecules demonstrated pH-responsive swelling, maintaining a compact state in acid solution while swelling pronouncedly to release active biomolecules in alkaline without burst release. SNAP as a new biomaterial can be fine-tuned to offer controlled diffusion/release properties and can be considered as a potential oral drug delivery vehicle for therapeutic proteins such as insulin.

Keywords: alginate, glutaraldehyde, diffusion, pore size, insulin

5.1 Introduction

Recent advances in recombinant DNA technology, protein engineering and tissue culture techniques have increased the number of available therapeutic biopharmaceuticals [1]. However, clinically proven biopharmaceuticals such as interferon-γ, interleukin-2 and insulin are still delivered intravenously due to protein instability caused by acid-induced hydrolysis and enzymatic degradation in the gastric and gastro-intestinal tract (GI) [2], resulting in low bioavailability when administering orally. Many attempts have been made to develop effective drug formulation for oral administration to avoid painful, invasive injection, improving patient compliance. One approach is to encapsulate acid-labile protein drugs within a pH-responsive polymeric matrix which has shown promising results in stabilizing and protecting protein therapeutics from acid and enzymatic degradation[3]. The concept of using pH as a trigger to release a drug at the intestinal absorptive site is based on varying pH down the GI tract. Gastric-irritating or pH-labile protein therapeutics can be protected by the collapsed/compact gel matrix in gastric environment (pH~1.2) while being released in the intestinal lumens (pH~7.8) through matrix swelling or erosion. In addition, encapsulation within mucoadhesive polymers was found to improve bioavailability after drug administration since contact between the drug and mucosal surface was enhanced, increasing the residence time at the site of drug absorption and reducing drug metabolism by luminal secreted proteases[4].

Alginate is considered a biocompatible, biodegradable and pH-responsive biopolymer consisting of (1→4)-O-glycosidic links of β-D-mannuronic (M) and α-L-guluronic acid residues (G) at varying sequential arrangements and proportions[5].

Alginate forms ionotropic physical gel by cooperative binding with multi-valent cations, typically calcium. Since the sol-gel transition is rapid yet gentle, calcium alginate has been used in wound dressing, dental impression, cell/protein encapsulation, and as tissue scaffold. In addition, the mucoadhesive property of alginate has made it one of the favoured formulation excipients in the pharmaceutical industry [4]. Typically, protein encapsulation within calcium-alginate gel involves dropwise extrusion of alginate sol containing protein therapeutic, into a calcium ion rich solution, forming instantaneous, reversible gel structure which interconnects through ionic interactions. Since alginate gel is porous, and due to the hydrophilic nature of most of proteins, poor protein retention within the gel matrix is normally encountered following the on-set of gelation, and in aqueous environment. Mass encapsulation yield of small peptides having molecular weight less than 20 kDa is often less than 0.1%[6, 7].

Alternative protein encapsulation approaches can be achieved by absorptive encapsulation whereby preformed alginate beads are loaded in bioactive concentrates[8]. The bead production system is decoupled from the encapsulation process, thus minimizing the loss of biologicals or biochemical activity. Subtilisin was previously loaded into calcium alginate with the resultant dry beads consisting of over 50% active subtilisin by mass and near zero loss in enzymatic activity, levels that are considerably higher than that achieved by most encapsulation technologies[8]. Nevertheless, large proteins such as bovine serum albumin (66.4 kDa) are unable to diffuse into 4% calcium alginate gel[6], due to size exclusion and inflexible ionic crosslinks. Although factors such as alginate concentration, fraction of guluronic acid and sequential arrangement, and

types of gelling cations (ie, calcium, barium, strontium) were found to affect the final alginate gel properties[5], the extent of modification possible to increase the pore size of the physical alginate gel is limited.

At this point, diffusion of large molecular weight proteins such as urease (~540 kDa) into alginate hydrogel has not been demonstrated. Since protein encapsulation by diffusional absorption into prefabricated "blank" gel beads showed promise in obtaining high encapsulation yield and protein payload, such a technology platform may be potentially suitable for encapsulating a wide range of molecular sizes of protein therapeutics and biologicals. To enable the control of matrix pore size, we proposed the use of chemical hydrogel instead of physical calcium alginate gel. Native alginate polymer was reacted with di-aldehyde, forming tetrafunctional acetal-linked network polymer gel, described as semisynthetic network alginate polymer (SNAP). The extent of crosslinking can be kinetically and thermodynamically controlled[9], and the pore size of SNAP hydrogel can be fine-tuned from a few nanometers to submicron through pre-selection of formulation conditions such as reaction temperature and duration, crosslinker concentration and/or solvent composition. In addition, since the polymer network of the chemical gel is interconnected covalently, permanent bonding can no longer be displaced by chelating or monovalent ions as in the case of physical calcium alginate, and thus the gel structure is mechanically stable in ionic or dilute solution. To effectively use this new class of biomaterial as an encapsulation matrix, the diffusional properties of SNAP hydrogel to a wide range of protein molecular sizes were characterized and compared to that of conventional calcium alginate. Seven model molecules ranging from 1 to 544 kDa

were selected. Two types of SNAP hydrogel were tested, one with crosslinking density similar to calcium alginate (highest achievable crosslinking density for SNAP, resulting in densely crosslinked gel) while another was moderately crosslinked with the resultant gel pore size larger than the hydrodynamic radius of the selected model biomolecules and proteins. Tunable SNAP hydrogel is pH-responsive, mechanically stable, and can be pre-designed with desired pore properties to capture and release a wide range of molecular sizes of biomolecules, and its potential use as a protective matrix for oral drug delivery is demonstrated.

5.2 Materials and methods

Pharmaceutical grade alginate, SF120 (MW = 325,000, $[\eta]_{0.1\ M\ NaCl}$ (dL/g) 8.63, F_G = 0.72, F_{GG} = 0.60) was provided by FMC Biopolymer (Drammen, Norway). Subtilisin ultrafiltrate, Purafect1 UF (lot L-20031), with protein concentration of 300 mg/mL and activity of 56 U/mg was provided by Genencor International (Palo Alto, USA). Peptide substrate N-succinyl-L-Ala-L-Ala-L-Pro-L-Phe-p-nitroanilide was purchased from Vega Biochemicals (Arizona, USA). Lysozyme from chicken egg white, urease from jackbean, bovine serum albumin, vitamin B_{12} and all other chemicals were purchased from Sigma-Aldrich, unless otherwise specified.

5.2.1 Preparation of alginic acid and calcium-alginate beads

Alginate solution of 4% was extruded dropwise via an automatic liquid dispenser (EFD, Model 1000XL, East Providence, USA) into 0.1 M HCl, forming acid gel beads or into 0.1 M $CaCl_2$, resulting in instantaneous calcium alginate gel beads. Bead sizes were controlled to 2.8 (± 0.2) mm by the inner diameter of the syringe needle and the coaxial airflow rate outside the syringe, and the distance between the tip of the needle and the capture solution. Gel beads were incubated in the supernatant solutions for 4 h prior to use.

5.2.2 Semisynthesis of tunable alginate based biomaterials

Glutaraldehyde (1,5-pentanedial) in water of 25% w/w was purchased from Sigma-Aldrich (Oakville, Canada) and used as the chemical crosslinker in semisynthesis of alginate gel. To ensure reproducibility, the absorbance ratio of polymeric to monomeric form of glutaraldehyde was verified as less than A_{235}/A_{280} = 0.3. Glutaraldehyde concentrations of 1.65 and 1.33 M were pre-selected to synthesize alginate gel with average pore sizes of 40 and 80 nm estimated by a previously derived equilibrium swelling equation[9]. Acid gel beads (SF 120) of 4% were reacted with glutaraldehyde in aqueous medium containing 0.38 M HCl acid catalyst at 40^{o}C for 10 h. The mass of acid gel beads to reaction medium was kept constant at ratio of 0.3 for synthesis of densely and moderate crosslinked alginate hydrogel. All concentrations reported accounted for water content inside gel beads. The resultant SNAP gel beads

were rinsed with 20% ethanol at 40°C, followed by incubation in 0.1 M NaCl, pH 7.8 to remove residual glutaraldehyde. The suspending solution was changed frequently until the absorbance measured spectrophotometrically was less than 0.05 at wavelength between 235 and 280 nm.

5.2.3 Pore size estimation

Thermoporometry was used to measure the median pore size of alginate hydrogels[10]. The shift in triple point temperature of water was determined by differential scanning calorimeter (DSC Q100, TA Instruments) equipped with a liquid nitrogen-cooling accessory. SNAP hydrogels were allowed to reach equilibrium swelling volumes in 20 mM phosphate buffered saline (PBS), pH 7.8, before measurement. Due to the reversible gel nature of calcium alginate, 20 mM of calcium chloride were included in PBS swelling medium to prevent gel dissolution. Samples weighing 10-20 mg were placed in a sealable aluminum pan and one drop of the solvent was added to prevent premature drying prior to the measurement. The samples were first equilibrated at -30°C, held for 10 min, followed by heating up to 15°C at a rate of 0.5°C/min and held for 10 min, and then cooled down from 15°C to -30°C. The median pore radius (R_p in nanometers) of the hydrogel can be estimated by equation 1.

$$R_p = \frac{-64.67}{\Delta T} + 0.57 \qquad (Eq.\ \ 1)\,[11]$$

where ΔT = T - 273.15 and T is the triple point depression temperature in Kelvin. The corresponding pore size distribution of the hydrogel can be determined by plotting the change of pore volume over pore size against pore size (Rp) using equation 2.

$$\frac{dV_p}{dR_p} = \frac{dQ}{dt}\frac{dt}{d(\Delta T)}\frac{d(\Delta T)}{dR_p}\frac{1}{m\Delta H_f(T)\rho(T)} \qquad (Eq.\ \ 2)$$

where $\Delta H_f(T) = 334.1 + 2119(\Delta T) - 0.00783(\Delta T)^2$ and

$\rho(T) = 0.917(1.032 - 1.17x10^{-4}T)$. dQ/dt is the heat flow recorded by differential scanning calorimeter (DSC), d(ΔT)/dt is the scanning rate of the DSC experiment, m is the mass of the porous material, $\Delta H_f(T)$ and ρ(T) are the temperature-dependent heat of fusion and density for the probe fluid, respectively.

5.2.4 Protein diffusion study and the absorptive encapsulation approach

The diffusion rates of vitamin B12, lysozyme, subtilisin, bovine serum albumin and urease were determined by suspending 200 alginate beads in 20 mM PBS at pH 7.8 containing biomolecules at concentrations of 100 mg/mL at 20°C. To prevent the dissolution of calcium alginate gel in the diffusion medium, 20 mM of calcium chloride was added. Insulin solutions from NovoRapid (monomeric insulin analogue, Novonordisk) and Novo GE Toronto (Zinc complexed insulin analogue, Novonordisk, Canada) were used which consisted of approximately 3.5 mg/mL, equivalent to 100 IU/mL. SNAP and calcium alginate gel beads were allowed to reach the equilibrium

swelling volume in the suspended solution prior to protein loading. The resultant calcium alginate and densely and moderate crosslinked SNAP bead sizes were 3.2, 4.6 and 5.5 mm, respectively. The diffusion rate into SNAP and calcium-alginate gel was determined by measuring the concentration in suspension medium at given time-interval. The absorptive encapsulation approach utilizes the porous nature of hydrogel whereby prefabricated "blank" SNAP gel beads with tailored pore properties and calcium alginate gel beads were suspended in protein solutions of 3.5 mg/mL. The volume ratio of beads to loading solution is 1% and the encapsulation was carried out at 4^{o}C for 36 h. After loading, beads were separated by filtration and dried forming granules.

The mass yields of all model biomolecules during each formulation step were determined. The biomolecules lost in the washing solvent were collected and the percentage of the mass loss was determined by taking the ratio with respect to the total encapsulated biomolecules present in the hydrogel beads determined from cumulative release over 72 h in pH 7.8, 20 mM PBS. The enzymatic activities of the free and cumulative released lysozyme, subtilisin and urease from the dried granules were measured. The corresponding activity yields were calculated with respect to the expected activity based on the cumulative activity of the released enzymes in PBS for 4 h. The bioactivity of insulin in the granules was determined using insulin enzyme-linked-immuno-sorbent assay developed by Mercodia, Sweden. The immunoassay is based on the sandwich technique, in which two monoclonal antibodies are directed against separate antigenic determinants on the insulin molecule. Only non-fragmented, active form of human insulin in the sample can react with anti-insulin antibodies bound to microtitration

wells and peroxidase-conjugated anti-insulin antibodies in the solution[12]. Therefore, the bioactivity of the insulin in this study can be determined by the solid phase two-site enzyme immunoassay.

5.2.5 Determination of protein concentration, enzymatic activity and insulin bioactivity

Protein concentration was determined by Bradford assay using BSA as reference. Vitamin B_{12} concentration was analyzed spectrophotometrically at 361 nm. Lysozyme, subtilisin and urease were assayed through the specific enzymatic activity assay. In brief, activity of urease in urea solution was determined with an autotitrator (Radiometer PHM82, Copenhagen). The activity was calculated from the rate of acid addition to maintain a set-point pH 7 as described by DeGroot [13]. For lysozyme, *Micrococcus luteus* was used as substrate. Activity was measured at 450 nm, pH 6.5 by tracking the decrease in optical density as the cell walls were hydrolyzed[14]. Subtilisin was assayed through the rate of formation of colorific product, *p*-nitroanilide at 410 nm, which is cleaved from *N*-succinyl-l-Ala-l-Ala-l-Pro-l-Phe-*p*-nitroanilide substrate [8]. The maximum slope from the time-absorbance profile was determined to calculate activity. Insulin bioactivity was determined by insulin enzyme-linked-immuno-sorbent assay (ELISA, Mercodia, Sweden) at 450 nm[15]. All data were the mean and standard deviations of three repeated experiments, unless otherwise specified. Three samples were obtained for each repeated experiment to generate a sample mean and a sample standard

deviation. The means and standard deviations were later pooled to generate a pooled mean and standard deviation.

5.2.6 Release of biomolecules from alginate granules under simulated gastrointestinal conditions

SNAP and calcium alginate granules were incubated in pH 1.2, HCl solution at 0.5% w/v granules to solution ratio for 2 h (t = 0-120 min). After 2 h in acid medium, granules were separated quickly from acid medium and suspended in 20 mM, pH 7.8 PBS for 5 h (t=120-420 min). Concentration and bioactivity of supernatant withdrawn at appropriate time intervals were determined and fresh medium was replenished to maintain sink conditions.

5.2.7 Mechanical stability of dried SNAP and calcium alginate granules

Dry SNAP and calcium alginate granules were obtained by acetone extractive drying of freshly prepared gel beads through the following method. SNAP alginate gel beads were incubated in 1 M NaCl solution at $4^{o}C$ and the suspension medium was changed frequently to exchange protons with Na^{+} prior to drying whereas calcium alginate granules were dried from the freshly prepared hydrogel beads. As for drying cycle 1, freshly prepared gel beads were immersed in acetone for 5 min and repeated 3 times. Residual acetone was evaporated resulting in dry granules, assisted if necessary by gentle air flow for 24 h on rotary shaker to maintain spherical morphology during drying. For drying cycle 2-4, the resultant granules were rehydrated in 0.1 M NaCl solution at pH

7.8 which was changed frequently to maintain constant ionic and pH environments for 72 h, followed by acetone extractive drying. Due to reversible nature of calcium alginate gel, 10 mM of $CaCl_2$ was included in the rehydration medium for freshly prepared calcium alginate gel experiment. The mass of the granules after each drying cycle was measured, and calculated with respect to the initial polymer mass obtained from drying the freshly prepared gel beads in oven overnight. The effect of drying on the mechanical stability of the gel structure was characterized after each drying for a total of 4 repeated cycles.

5.3 Results and discussion

5.3.1 Semisynthesis of network alginate polymer with desired pore properties

Semi-synthetic network alginate polymer (SNAP) was formulated by reacting hydroxyls in alginic acid with bi-functional glutaraldehyde, forming tetra-functional acetal-linked 3-D gel network. The kinetic of the acid-catalyzed acetalization reaction (formation of insoluble SNAP hydrogel) was previously described [9]. Through selection of the reaction conditions, the matrix pore size and swelling properties can be controlled.

Two SNAP hydrogels with desired average pore size of 40 (densely crosslinked) and 80 nm (moderate crosslinked) were produced using initial glutaraldehyde concentrations of 1.65 and 1.33 M respectively, and by allowing the reaction to approach equilibrium (~10 h of reaction time). Calcium alginate gel was also formulated for comparative purposes. The porous structure was characterized via thermoporometry [16]

based on the principle of liquid-solid transformation (ie. triple point temperature). Pore radius distribution curves are plotted in Figure 5-1 using equations 1 and 2.

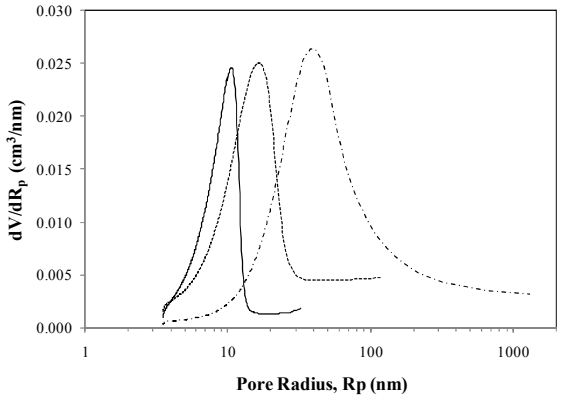

Figure 5-1. DSC thermograph (left-side figure) of calcium alginate (solid line), densely (short dash) and moderately crosslinked SNAP hydrogels (dash-dot), and corresponding pore radius distribution (right-side figure).

The curves of the densely and moderately crosslinked SNAP hydrogels were skewed to smaller pore size range with median pore diameters of 35 and 72 nm, respectively. The median pore diameters determined by DSC were similar to that of the predicted pore size, suggesting that the kinetic model determined previously appropriately described reaction conditions (reaction duration and reactant concentrations) to pre-select the pore properties of SNAP hydrogel. In contrast, the ability to control the pore properties of calcium alginate gel are limited because of its rapid gelation mechanism, and difficulty in manipulating the degree of ionic crosslink density. For calcium alginate gel, the median pore diameter was about 18 nm, even though both densely crosslinked SNAP and calcium alginate gels were formulated to achieve the highest possible crosslinking within the gel network. Since alginate polymer chains in SNAP hydrogel

were chemically interconnected by small molecular weight crosslinker, the chain mobility was greater than less mobile physical crosslinks in calcium alginate, allowing the gel network to expand without compromising the mechanical stability. Hence, the average pore sizes of SNAP hydrogel in aqueous environment were larger than physically gelled calcium alginate under comparable degree of crosslinking.

5.3.2 Characterization of protein diffusion into SNAP and calcium alginate hydrogel

Protein transport characteristics of SNAP and calcium alginate gels were studied by suspending beads in solution containing BSA. Absorption isotherms and model curves based on a Fick's second law of diffusion (Crank's model[17]) are presented in Figure 5-2. Model curves appeared a good-fit to the data, suggesting diffusion is the main mechanism of protein uptake. BSA (66.4 kDa) which has hydrodynamic radius of 3.6 nm diffused freely into both SNAP hydrogels, with approximately 30% of protein concentration reduction measured in the loading solution. However, only about 5% of initial protein was taken by calcium-alginate after 24 h, indicating a strong diffusion hindrance from the gel network.

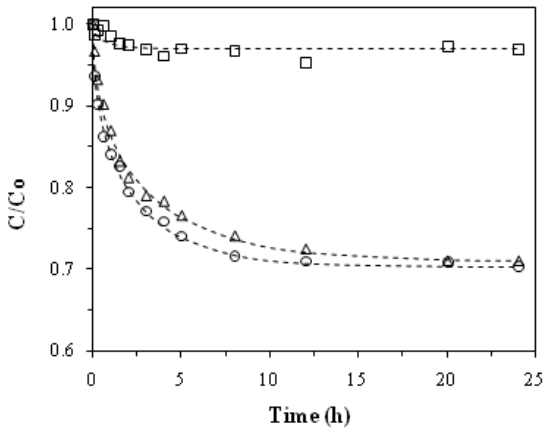

Figure 5-2. BSA diffusion into calcium alginate (square) and densely (triangle) and moderately crosslinked SNAP hydrogels (circle). Symbols and dashed lines represent experimental and calculated values from model simulation (Eq. 3), respectively.

From the absorption profiles, diffusion coefficients were estimated from the best fitted curves based on the diffusion model modified by Crank for spherical hydrogel beads (Eq. 5)[17]. The model assumes that the gel beads were homogenous and initially free of protein. When liquid film resistance was neglected in the well mixed system, the fraction of protein uptake by the beads at time t to the corresponding quantity after infinite time can be described by equation 5.

$$\frac{M_t}{M_\infty} = 1 - \sum_{n=1}^{\infty} \frac{6\alpha(\alpha+1)\exp(-Dq_n{}^2 t/a^2)}{9+9\alpha+q_n{}^2\alpha^2} \qquad \text{Eq. 5}$$

where M_t and M_∞ represent the protein mass in the gel beads at time t and at the equilibrium state, D is the diffusion coefficient of the protein to the gel matrix, and the values of q_n are the positive non-zero roots of

$$\tan q_n = \frac{3q_n}{3 + \alpha q_n^{\,2}} \qquad \text{Eq. 6}$$

and α represents the ratio of the protein solution volume to the beads as noted in equation 7.

$$\alpha = \frac{3V}{n4\pi a^3} \qquad \text{Eq. 7}$$

where V is the protein solution volume and a is the radius of the beads and n is the total number of beads.

From the non-linear regression analysis of the best fitted curve, the diffusion coefficients were estimated to be 0.52, 3.59 and 4.63 x 10^{-7} cm^2/s for calcium alginate, and densely and moderately crosslinked SNAP hydrogels, respectively. According to Tanaka *et al*, BSA showed no diffusion into, or out from 4% calcium alginate[6]. However, in our case, calcium alginate gel beads were swelled in PBS solution from an initial diameter of 2.8 mm to 3.2 mm, reducing the polymer fraction from 4 to 2.7%. Li et al.[18] determined the diffusion coefficient of BSA to be 0.2 x 10^{-7} cm^2/s for 3% alginate, comparable to results of diffusion into calcium alginate gel in the present study with 4% alginate.

Absorption of a wide molecular size range of biomolecules into SNAP hydrogel gels was demonstrated with gels fabricated with pre-selected pore sizes greater than the hydrodynamic radius of the model biomolecules. Tested materials included vitamin B_{12}, commercial insulin analogues in monomeric and hexameric form with zinc complex,

lysozyme, subtilisin, BSA and urease. The physical properties of these biomolecules including molecular weight, hydrodynamic radius (Stokes radius), and theoretical diffusion coefficient in water calculated from equation 9 are summarized in Table 5-1.

$$D_{water} = \frac{k_B T}{6\pi\eta r_H} \qquad (Eq.\ 9)$$

where k_B is Boltzmann's constant (1.38 x 10^{-23}J/K), T is the absolute temperature in Kevin, ηis the viscosity of water (1.06 x 10^{-3} Pa·s at 20°C) and r_H is the hydrodynamic radius of the solute in meters.

Table 5-1: Properties of model biomolecules in aqueous solution

Biomolecules/Proteins	Molecular weight (kDa)	Stokes radius (nm)	D_{water} [a] (x 10^6 cm^2/s)
Vitamin B_{12}	1.3	0.87 [19]	2.32
Insulin	5.8	1.11 [20]	1.82
Lysozyme	14.7	1.9 [21]	1.06
Subtlisin	27.3	2.5 [22]	0.81
Insulin (hexamer)	34.2	2.7 [20]	0.75
Bovine serum albumin	66.4	3.6 [23]	0.56
Urease	545.6	7.0 [24]	0.28

[a]. D_{water} was estimated using Stokes-Einstein equation at 20°C(Eq. 9)

The diffusion coefficients of the model biomolecules into SNAP and calcium alginate gels were characterized following the procedures described in Figure 5-2 for BSA, except for insulin. The initial insulin concentrations used in the diffusion study were about 30 times less than other model biomolecules. The ratios of diffusion

coefficients of model biomolecules in hydrogel (D_{gel}) to diffusivity in water (D_{water}, no viscosity effect or network barrier) were calculated and are presented in Figure 5-3.

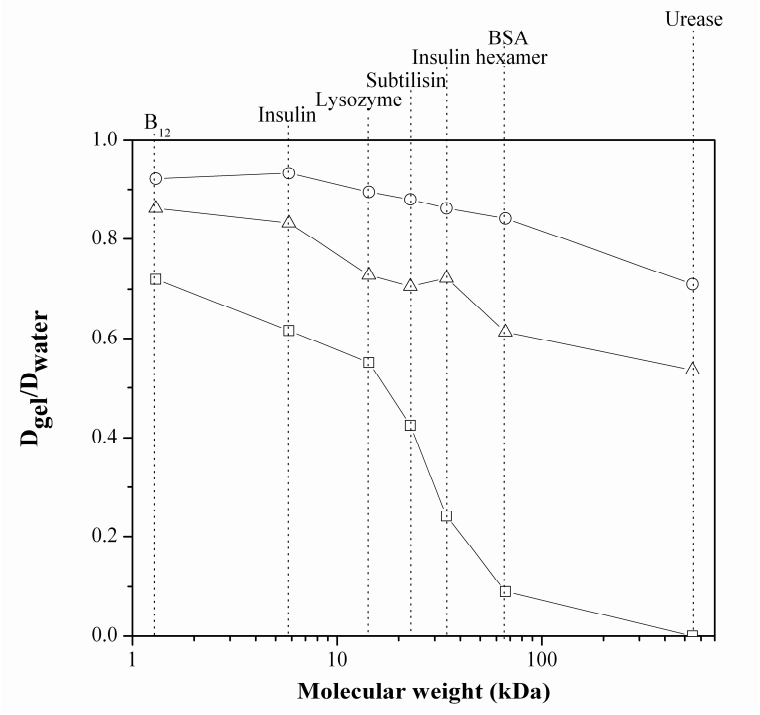

Figure 5-3. Ratio of diffusion coefficients in gel to water of vitamin B12 (1.3 kDa), monomeric insulin monomer (5.8 kDa), lysozyme (14.7 kDa), subtilisin (27.3 kDa), and hexameric insulin hexamer (34.2 kDa), BSA (66.4 kDa) and urease (545.6 kDa) into moderately (○) and densely crosslinked SNAP (△), and calcium alginate hydrogels (□).

Biomolecules ranging from 1 to 545.6 kDa with hydrodynamic radius between 1.7 to 14 nm appeared to diffuse freely into both moderate and densely crosslinked SNAP hydrogels, while experiencing transport resistance into calcium alginate gel. In addition, urease having radius of gyration of 12 nm (diameter of 24 nm) was larger than the pore size of the calcium-alginate gel matrix (pore diameters of calcium alginate were determined to be between 5-18 nm), and was excluded from calcium alginate. In contrast,

moderate and densely crosslinked SNAP hydrogel which had pore diameters of approximately 80 and 40 nm, allowed urease to readily diffuse into the hydrogel with about 30 and 40% rate reduction respectively, as compared to diffusion in water.

Since solute transport in polymer matrix can only occur when the size of an opening between the polymer chains (ξ, mesh pore diameter) is large enough to allow passage, diffusion data can be utilized in estimation of the mesh pore size of the gel network. According to Zhang and Amsden[25],

$$D_{gel} = D_{water} \exp\left[-\pi \left(\frac{r_H + r_f}{\xi + 2r_f} \right) \right] \quad (Eq. \quad 10)$$

where r_f is the cross-sectional radius of the polymer chain (0.83 for alginate) and r_H is the hydrodynamic radius. The estimated pore sizes for the three hydrogels, determined from the diffusion data of the model biomolecules are presented in Figure 5-4.

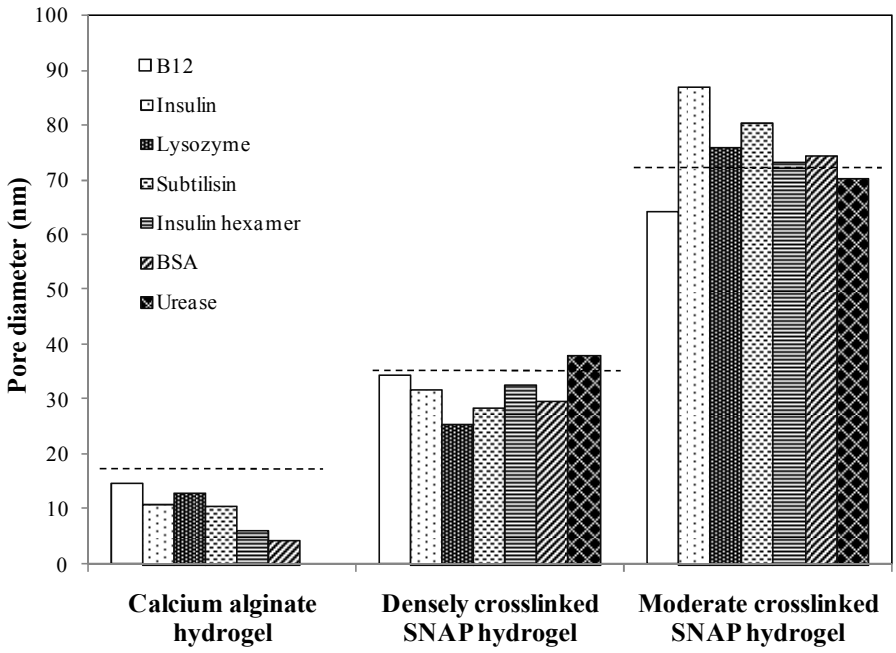

Figure 5-4. Pore diameters of alginate gels estimated from the diffusion data of the model proteins using obstruction-scaling diffusion model (Eq. 10) and the median pore diameter from DSC data (dotted horizontal line).

Pore diameters ranged between 4-14, 24-39 and 62-88 nm for calcium alginate, and densely and moderate crosslinked SNAP hydrogels respectively, which were similar to that determined using thermoporometry. In addition, the pore diameter of calcium alginate averaged from the diffusional transport data of 6 model biomolecules was around 11 nm which agrees with other published values of similarly crosslinked gel. For instance, Li *et al*[18] reported a pore diameter of 14.7 and 17 nm for 3 and 1.5% calcium alginate and Klein *et al*[26] found a pore size of approximately 16.6 nm for 3% alginate. Based on the literature and our determined values, the range of pore sizes of calcium alginate that can be manipulated was fairly narrow, generally between 10-20 nm. In

contrast, SNAP hydrogels can be formulated with larger window of tunable pore sizes, ranging from a few to a few hundred nanometers. Here, we demonstrated that biomolecules of wide range molecular sizes can diffuse into SNAP hydrogel and the diffusion rate can be controlled through the pre-selected pore sizes.

5.3.3 Influence of drying on mechanical stability, swelling and pH-responsiveness of alginate gels

5.3.3.1 Mechanical stability after repeated drying/rehydration cycle

Drying of hydrogel beads, forming dry granules allows the transformation of liquid product into solid dosage form, to facilitate storage, packaging and transport, and to stabilize for enhanced shelf-life. The mechanical stability of SNAP and calcium alginate gels was tested through several cycles of drying/rehydration. For drying cycle 1, freshly prepared alginate gel beads underwent acetone extractive drying, and the resultant dry granule mass was measured. For drying cycle 2, granules were rehydrated in 0.1 M NaCl, followed by acetone extractive drying. This was repeated for two additional cycles (cycle 3-4). For rehydration of freshly prepared calcium alginate gel, 10 mM of calcium ions were included in the swelling medium to stabilize the gel.

The percentage of the mass retained for SNAP and calcium alginate gels after each drying cycle was calculated with respect to the initial polymer mass and is presented in Figure 5-5.

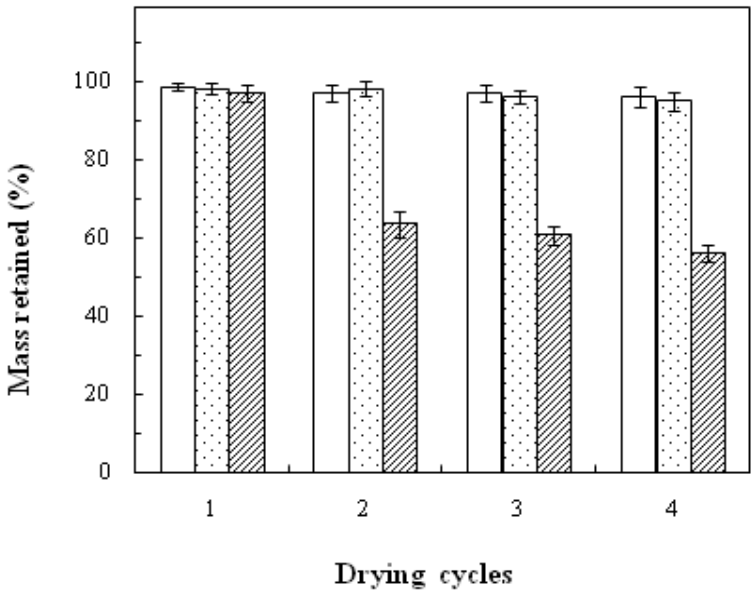

Figure 5-5. Mass retention of densely (clear bar) and moderately crosslinked SNAP (dotted bar) and calcium alginate granules (striped) after repeated drying cycles. The first drying cycle was applied to the fresh wet beads, forming dry granules, followed by repeated rehydration and acetone drying (drying cycles 2-4). Percentage of mass retained was calculated with respect to the initial polymer mass.

Near full mass retention was observed for both moderate and densely crosslinked SNAP hydrogels after 4 repeated drying treatments, whereas about 40% of polymer mass was lost after the first rehydration of the dry calcium alginate granules. Since calcium alginate was stabilized by Ca^{2+} through electrostatic interaction, acetone extractive drying in cycle 1 may partially remove Ca^{2+}, subsequently weakening the gel integrity and resulting in polymer dissolution during the rehydration and drying treatment in cycle 2. The lost Ca^{2+} may be regained from the rehydration medium, reestablishing the equilibrium calcium-polymer interaction, and therefore, the loss of polymer mass after drying cycle 3 and 4 was reduced. It is apparent that SNAP gels which are inter-linked by covalent bonds, are

much more stable during drying and rehydration, demonstrating superior mechanical stability as compared to ionically crosslinked calcium alginate gel.

5.3.3.2 Swelling kinetics of alginate granules

The effect of drying on the swelling kinetics of SNAP and calcium alginate granules was also characterized and compared with the corresponding swelling from the fresh gel beads. The volume ratio of the swelled gel from either freshly prepared beads or dry granules in 0.1 M NaCl solution was calculated with respect to the initial polymer volume and is presented in Figure 5-6.

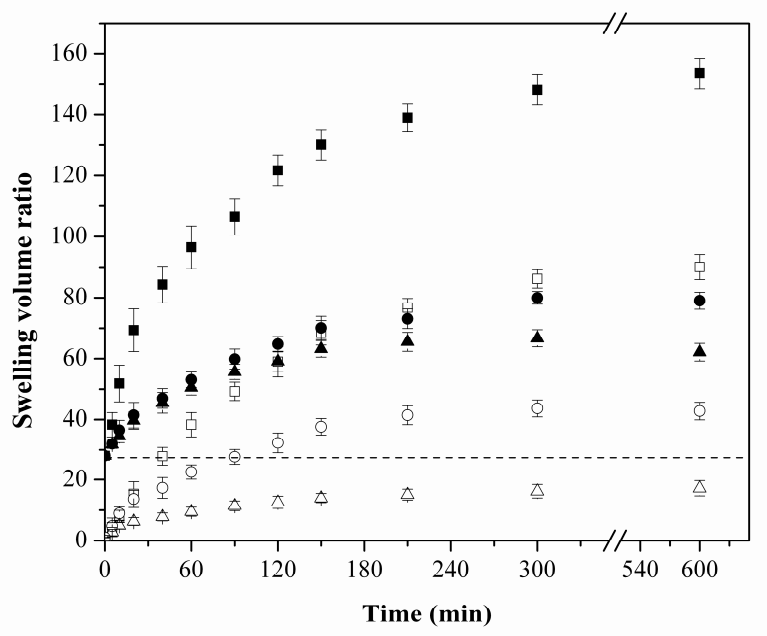

Figure 5-6. Swelling of moderate (■,□) and densely crosslinked SNAP (●,○) and calcium alginate (▲,△) from wet gel beads (closed symbols) and dry granules (open symbol) in 0.1 M NaCl, pH 7.8. The initial swelling volume ratio of the wet bead to its compact dry granules is represented by the dashed line.

Freshly prepared moderate and densely crosslinked SNAP hydrogels reached the equilibrium swelling volume after 10 h with approximately 150 and 80 times of the initial compact polymer volume, respectively. However, calcium alginate gel was unstable in presence of sodium ions and experienced partial disintegration after 6 h. The maximum achievable gel volume was about 60 times that of the initial polymer volume and the equilibrium swelling volume could not be established. In contrast to swelling from freshly prepared moderate and densely crosslinked SNAP and calcium alginate gel beads, the extent of swelling from dry granules was reduced by about 40-50 and 70%, respectively. As in the case of calcium alginate granules, drying significantly affected the extent of water absorption by the polymer, only regaining about 60% of the original freshly wet bead volume in swelling solution. In addition, calcium alginate granules were stable during rehydration without partial disintegration as observed in wet calcium alginate beads, possibly due to configurational rearrangement of the polymer network during drying, leading to different swelling behaviour. Drying the gel beads and forming dry granules may rearrange some amorphous polymers to form a more structured crystalline region and may promote hydrogen bonding between polymer chains [27, 28]. With these physical enforcements such as formation of ordered crystalline region and increasing hydrogen bonding between polymer chains, the pore sizes of the granules may be reduced, retarding water penetration and magnitude of water uptake during swelling.

5.3.3.3 pH-responsive swelling of alginate granules

The pH-responsive swelling of the alginate granules is plotted in Figure 5-7 against solution pH. The degree of polymer ionization at the corresponding solution pH was also calculated and plotted using Henderson-Hasselbalch equation assuming the pK_a values of guluronic and mannuronic monomers are 3.65, and 3.38, respectively[5] and constant irrespective of polymer molecular weight, solution pH and ionic strength.

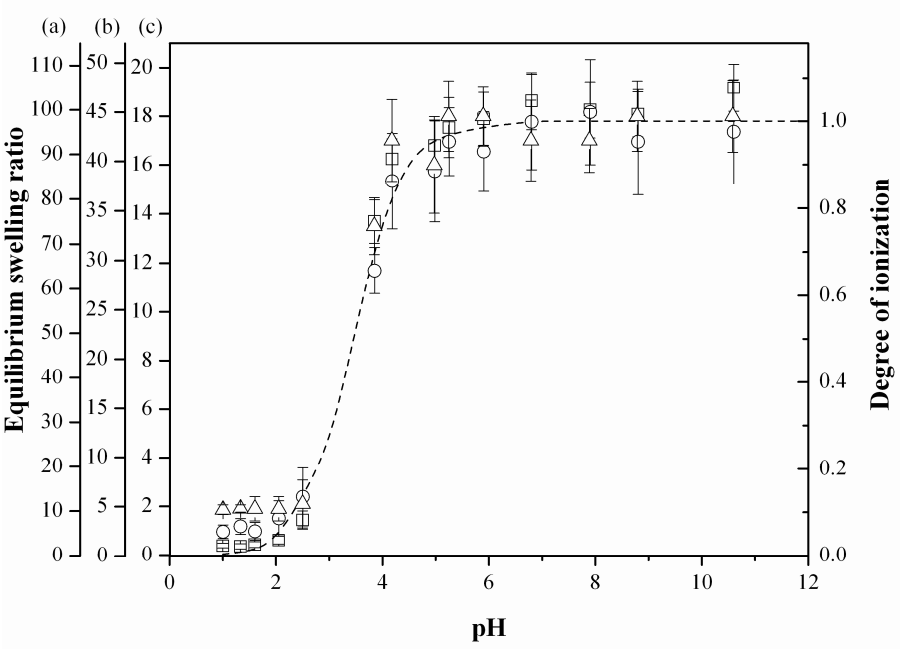

Figure 5-7. pH-dependent swelling (left side ordinate) of moderate (scale **a**, □) and densely crosslinked SNAP (scale **b**, ○) and calcium alginate granules (scale **c** , △) and corresponding degree of ionization (right side ordinate, dotted lines).

All three alginate granule samples followed the calculated ionization curves and only differed by the magnitude of the swelling. Alginate polymer consists of ionizable carboxylate moieties which are protonated (degree of ionization is low) in low pH,

resulting in limited solubility and thus the compact granule state was retained. When the pH-responsive moieties were deprotonated by an increased solution pH to around pH 4, the negatively charged carboxylate ions attached to the polymer chains increased the polymer hydrophilicity and set up an electrostatic repulsion which subsequently expanded the network, leading to the swollen hydrogel. The degree of ionization of the alginate polymer increased with solution pH and was expected to be completely ionized above pH 7. Consequently, the increased ionic carboxylate moieties increased hydrophilicity of the network and the electrostatic repulsions between the chains, resulting in greater swelling. The maximum equilibrium swelling volume was approached when the pH was greater than 7. Since the formation of SNAP granules involved hydroxyls from alginate and di-aldehyde, and left carboxylate moieties free for pH-responsive sensing, the swelling at alkaline pH was more pronounced as compared to calcium alginate which was formed through cooperative binding of carboxylate moieties with calcium ions, resulting in less available carboxylate moieties for pH-responsive swelling. The pH-dependent swelling behavior of SNAP granules which can swell pronouncedly at alkaline pH but less so under acidic conditions can potentially be utilized as oral drug delivery carrier.

5.3.4 SNAP granules as a potential oral delivery vehicle for therapeutic proteins

5.3.4.1 Absorptive encapsulation of biomolecules within SNAP granules

As a proof of concept biomaterial for encapsulation of a wide range of molecular sizes of biomolecules, SNAP hydrogel with 80 nm pore size was synthesized and

submerged in biomolecule solutions for absorptive loading of vitamin $B_{12,}$ insulin, lysozyme, subtilisin, BSA, and urease, followed by acetone extractive drying. The final payloads of biomolecules in the gel beads and dry granules, and the encapsulation efficiencies were determined and are presented in Table 5- 2. The encapsulation yields of BSA within calcium alginate were also characterized for comparison.

Table 5-2: Payload and encapsulation efficiency of biomolecules loaded into SNAP and calcium alginate granules

			SNAP				Ca-alginate
Model biomolecules	B_{12}	Insulin	Lysozyme	Subtilisin	BSA	Urease	BSA
Protein payload in gel beads (mg/g)[1]	5.18	4.24	7.78	5.41	6.60	3.53	2.87
Percent weight loss during drying (%)[2]	98.5	98.1	97.8	98.5	98.1	98.3	94.6
Protein loss during drying (%)[3]	37.5	33.3	34.5	30.4	28.4	29.7	5.6
Mass yield in granule (%)[4]	62.5	66.7	65.5	69.6	71.6	70.3	94.4
Activity yield in granule (%)[4]	N/A	53.8	60.5	61.5	N/A	64.8	N/A
Specific activity yield in parentheses (%)		(80.6)	(92.4)	(88.4)		(92.2)	
Protein payload in dry granules (mg/g)	272	246	370	327	352	222	48.8
Specific bioactivity in parentheses (U/mg)[1]		(4.53)	(8.03)	(15.19)		(17.56)	

[1]The standard deviations were less than ± 2.5 mg/g of the mean values for the protein payload in gel beads, and ± 11 mg/g in granules, and less than ± 3.7 U/mg of the mean values for activity.
[2]The standard deviations were less than ± 0.8% of the mean values
[3]The standard deviations were less than ± 5% of the mean values
[4]The standard deviations were less than ±5% of the mean values for both mass and activity yields.

The mass of biomolecules expelled from the gel beads during drying was measured and the mass yield calculated. Approximately 30% of biomolecules in the range

of 5.8-545.6 kDa were extracted by acetone out from the SNAP gel beads as shown in Table 5- 2, possibly caused by high osmotic pressure, pushing solutes out from large pores along with water before collapsing during drying. Due to small molecular size of vitamin B_{12} (1.3 kDa), 37% of the encapsulated mass in the gel bead was lost during drying. In contrast, only 5% of BSA encapsulated within calcium alginate gel was lost during drying as compared to 28% loss from SNAP gel beads, possibly due to smaller gel pore size which hinders protein transport out from the gel network during drying. Although the mass yield for encapsulation within calcium alginate was high with close to 95% for BSA, the payload in the dry granules was significantly lower by about 10-fold when compare to loading in SNAP granules in which 22-37% of active granules consisted of entrapped protein mass.

The specific bioactivities of insulin, lysozyme, subtilisin and urease were 22.8, 22.8, 23.6, 56.7, and 85.5 U/mg respectively, and the values were used to calculate the activity yield which was defined as the observed activity over the expected activity based on the determined protein payload in the granules. Over 90% of the encapsulated lysozyme, subtilisin and urease stayed in active state (ie. specific activity yield which was normalized with the mass of proteins encapsulated.). Since insulin may be more susceptible to denaturation/degradation when in contact with solvent, or through destruction of the zinc-insulin complex during drying, the activity is slightly lower with about 80% of specific activity retention. Absorptive encapsulation, whereby bead production was decoupled from the protein loading process, demonstrated good activity

retention and can be considered as a technology platform for encapsulating many therapeutic proteins or biologicals.

5.3.4.2 Controlled release of proteins from SNAP granules

The release profiles of vitamin $B_{12,}$ insulin, lysozyme, subtilisin, BSA and urease from SNAP granules in simulated GI conditions are plotted in Figure 5-8. The release of BSA from calcium alginate granules was included for comparison. The cumulative release was calculated with respect to the payloads presented in Table 5-2.

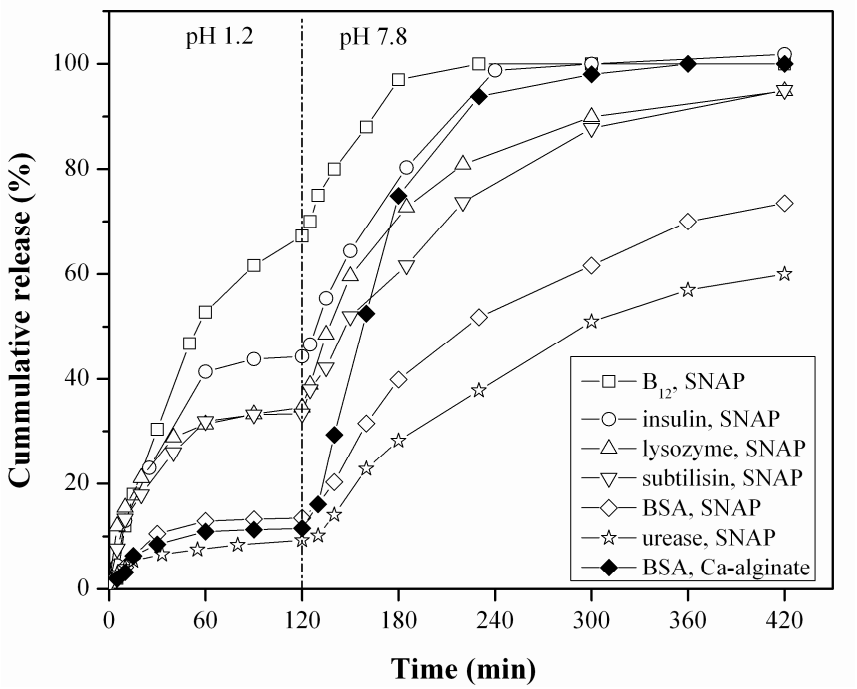

Figure 5-8. Release profiles of absorptive-encapsulated vitamin B_{12}, insulin, lysozyme, subtilisin, BSA and urease from SNAP, and BSA from calcium alginate granules in simulated GI condition in which the dry granules were placed in pH 1.2 solution for 120 min followed by 20 mM PBS, pH 7.8.

In acid condition, granules showed 10-40% of bioactive released during the transient period (between 20-60 min), reaching a plateau, except for vitamin B_{12} which released near 60% of the initial encapsulant into the external medium. The amount retained after the transient period increased with molecular size. The release-and-hold behavior may be due to the release of the entrapped biomolecules close to the polymer/solution interface, and re-establishment of the equilibrium of the dry beads in aqueous medium in which polymer rehydrated, relaxed and contracted again, known as overshooting-phenomenon[29].

The release-and-hold behavior may be explained by polymer overshooting effect in acidic medium[29]. Before the protonation of carboxylate moieties in acid medium, alginate granules swelled rapidly due to repulsive forces between the charged polymer chains, releasing biomolecules near the polymer/solution interface. With gradual protonation of carboxylate ions, the swelling decreased due to the formation of hydrogen bond crosslinking with the neighbouring polymer chains constituting protonated carboxylic acid groups. The continual increase in the protonation of carboxylate ions led to further increase in hydrogen bond crosslinking, subsequently the network contracted, expelling water until the new equilibrium was established and the entrapped biomolecules were sustained if the molecular size was larger than the new established matrix pore size. Since vitamin B_{12} may be smaller than the pore size of the swelled polymer matrix, slow release is observed even after the transient period toward equilibrium. Once equilibrium was established, biomolecules were fully retained within the granules in acid condition.

After 2 h of release in acid condition, granules were transferred to pH 7.8, PBS solution to simulate slight alkaline intestinal/colonic conditions. The SNAP granules swelled due to ionization of the carboxylate moieties in alginate, increasing hydrophilicity of the polymer and drawing water into the granules in response to the osmotic pressure build-up. As granules swelled, biomolecules were released with near first-order kinetics for about 2-3 h. The release rate (slope of the curve) increased as the molecular size of biomolecules increased, except for insulin. Insulin (hexameric insulin-zinc complex, 34.2 kDa) showed a faster release than subtilisin (27.3 kDa) in both acid and alkaline conditions, possibly due to the dissociation of hexameric insulin which complexes with zinc through ionic interaction into dimer or monomeric form during granule drying. Over 90% of the testing biomolecules were released from SNAP granules in about 36 h (or 5 h in alkaline pH) or less than 7 h for molecular size smaller than BSA. Due to electrostatic effect, approximately 5-10% of lysozyme still remained trapped within SNAP granules after 3 days of release in alkaline pH. In contrast, calcium alginate granules started to disintegrate after 20 min in PBS solution, and completely dissolved in less than 2 h due to ion exchange with surrounding phosphate ions, burst releasing BSA at less controllable rate.

The percentage of bioactive insulin, lysozyme, subtilisin and urease released from SNAP granules into simulated intestinal/colonic environment (t=120-420 min) was measured every hour for a course of 5 h and the averages are summarized in Table 5- 3.

Table 5-3: Bioactivity of released proteins

Protein	% Bioactivity at t=120-420 min
Insulin	58.7 ± 6.5
Lysozyme	83.2 ± 7.6
Subtilisin	90.1 ± 6.5
Urease	84.1 ± 8.1

The bioactivities of the proteins released from SNAP granules were fairly constant throughout the 5 h of suspension in alkaline medium. Encapsulated lysozyme, subtilisin and urease were well protected by the polymer matrix after 2 h of contact with acid with 83% of the released enzymes in the simulated intestinal/colonic alkaline condition remaining active. In addition, about 60% of the insulin released was bioactive, demonstrating the potential use of SNAP hydrogel/granules for oral delivery of therapeutic protein.

In summary, SNAP hydrogels were synthesized by reaction of native alginate with di-aldehyde, forming acetal-linked 3D gel network. The desired pore size can be fine-tuned by the pre-selected formulation condition. Two types of SNAP hydrogels were prepared: one was densely crosslinked with crosslinking density similar to that of calcium alginate while another was moderately crosslinked to produce pore diameter of 80 nm, about two times larger than densely crosslinked SNAP hydrogel (40 nm). The diffusion of 7 model biomolecules including vitamin B_{12}, two types of insulin analogues (monomer and hexamer-zinc complex), lysozyme, subtilisin, BSA and urease into SNAP hydrogels was characterized and compared to diffusing into calcium alginate and in water. Model

biomolecules ranging from 1.3 to 545.6 kDa with the corresponding hydrodynamic radius of 0.87 to 7 nm can diffuse freely into both moderate and densely crosslinked SNAP hydrogels. For large size protein like urease, the diffusion rate in moderate and densely crosslinked SNAP hydrogels was about 73 and 55% of that diffusing in water, whereas near zero diffusion was observed for calcium alginate due to size-exclusion of matrix pore size (pore diameter is around 18 nm as determined by thermoporometry). The diffusion data of the model biomolecules were also used to predict the gel pore sizes based on the obstruction-scaling model[25] and the values were similar to that estimated by thermoporometry and the equilibrium swelling study.

SNAP hydrogel was mechanically stable under repeated drying and rehydration in ionic solutions containing sodium or phosphate ions whereas calcium alginate gel lost about 40% of calcium ions (data not shown) during drying, and disintegrated upon rehydration in ionic solutions. Drying can cause polymer rearrangement, inducing the formation of hydrogen bonding, and about 40% of reduction in swelling was observed when compared to swelling from hydrogel without drying treatment. Therefore, drying may allow for post-fabrication or post-encapsulation treatment to obtain addition modification to the polymeric network.

SNAP hydrogel was used for absorptive encapsulation of a wide range of molecular sizes of biomolecules. Since the absorptive encapsulation decoupled bead production from loading, high encapsulation yields and payload were obtained with over 80% of encapsulated proteins remaining active and over 20% of granule mass consisting of loaded biomolecules. SNAP hydrogel/ granules are pH-responsive maintaining

compact structure in acid, potentially protecting protein actives from acid denaturation in gastric environment, while swelling in alkaline solution, releasing active proteins to intestinal or colonic sites, so is under consideration as a potential oral drug carrier for protein therapeutics such as insulin. In this study, over 80% of the released lysozyme, subtilisin and urease from SNAP granules remained active after exposed in acid solution for 2 h. Close to 60% of insulin released was bioactive. Since many physical properties of SNAP hydrogel/granules such as swelling and pore size can be fine-tuned to control the solute diffusional and transport properties, the encapsulation efficiency and bioactivity of insulin can be further improved. SNAP as a new class of biomaterial together with the absorptive encapsulation technique demonstrated the potential for application in oral delivery of protein therapeutics.

5.4 Acknowledgements

The authors thank the Natural Sciences and Engineering Research Council of Canada for financial support.

5.5 References

1. Larrick JW, Thomas DW. Producing proteins in transgenic plants and animals. Current Opinion in Biotechnology 2001 Aug;12(4):411-418.

2. Borges O, Cordeiro-Da-Silva A, Romeijn SG, Amidi M, de Sousa A, Borchard G, et al. Uptake studies in rat Peyer's patches, cytotoxicity and release studies of alginate coated chitosan nanoparticles for mucosal vaccination. J Control Release 2006 Sep 12;114(3):348-358.

3. Babu VR, Patel P, Mundargi RC, Rangaswamy V, Aminabhavi TM. Developments in polymeric devices for oral insulin delivery. Expert Opinion on Drug Delivery 2008 Apr;5(4):403-415.

4. Bernkop-Schnurch A, Kast CE, Richter MF. Improvement in the mucoadhesive properties of alginate by the covalent attachment of cysteine. J Control Release 2001 APR 28;71(3):277-285.

5. Draget KI, SkjakBraek G, Smidsrod O. Alginate based new materials. Int J Biol Macromol 1997 AUG;21(1-2):47-55.

6. Tanaka H, Matsumura M, Veliky IA. Diffusion Characteristics of Substrates in Ca-Alginate Gel Beads. Biotechnol Bioeng 1984;26(1):53-58.

7. Gehrke SH, Uhden LH, McBride JF. Enhanced loading and activity retention of bioactive proteins in hydrogel delivery systems. J Control Release 1998 Oct 30;55(1):21-33.

8. Chan AWJ, Becker T, Neufeld RJ. Subtilisin absorptive encapsulation and granulation. Process Biochem 2005 APR;40(5):1903-1910.

9. Chan AW, Whitney RA, Neufeld RJ. Kinetic controlled synthesis of pH-responsive network alginate. Biomacromolecules 2008 Sep;9(9):2536-2545.

10. Boontheekul T, Kong HJ, Mooney DJ. Controlling alginate gel degradation utilizing partial oxidation and bimodal molecular weight distribution. Biomaterials 2005 May;26(15):2455-2465.

11. Landry MR. Thermoporometry by differential scanning calorimetry: experimental considerations and applications. Thermochimica Acta 2005 Aug 1;433(1-2):27-50.

12. Lindstrom T, Hedman CA, Arnqvist HJ. Use of a novel double-antibody technique to describe the pharmacokinetics of rapid-acting insulin analogs. Diabetes Care 2002 Jun;25(6):1049-1054.

13. DeGroot AR, Neufeld RJ. Encapsulation of urease in alginate beads and protection from alpha-chymotrypsin with chitosan membranes. Enzyme Microb Tech 2001 OCT 4;29(6-7):321-327.

14. Srinivasan C, Katare YK, Muthukumaran T, Panda AK. Effect of additives on encapsulation efficiency, stability and bioactivity of entrapped lysozyme from biodegradable polymer particles. Journal of Microencapsulation 2005 Mar;22(2):127-138.

15. Reis CP, Veiga FJ, Ribeiro AJ, Neufeld RJ, Damge C. Nanoparticulate Biopolymers Deliver Insulin Orally Eliciting Pharmacological Response. J Pharm Sci-Us 2008 Dec;97(12):5290-5305.

16. Iza M, Woerly S, Danumah C, Kaliaguine S, Bousmina M. Determination of pore size distribution for mesoporous materials and polymeric gels by means of DSC measurements: thermoporometry. Polymer 2000 Jul;41(15):5885-5893.

17. Crank J. Diffusion in a sphere. The Mathematics of Diffusion. 2 ed. New York: Oxford University Press, 1998.

18. Li RH, Altreuter DH, Gentile FT. Transport characterization of hydrogel matrices for cell encapsulation. Biotechnol Bioeng 1996 May 20;50(4):365-373.

19. Cho SM, Kim SY, Lee YM, Sung YK, Cho CS. Synthesis, properties, and permeation of solutes through hydrogels based on poly(ethylene glycol)-co-poly(lactones) diacrylate macromers and chitosan. J Appl Polym Sci 1999 Sep 12;73(11):2151-2158.

20. Hovgaard L, Jacobs H, Mazer NA, Kim SW. Stabilization of insulin by alkylmaltosides .A. Spectroscopic evaluation. International Journal of Pharmaceutics 1996;132(1-2):107-113.

21. Grigsby JJ, Blanch HW, Prausnitz JM. Diffusivities of lysozyme in aqueous MgCl2 solutions from dynamic light-scattering data: Effect of protein and salt concentrations. J Phys Chem B 2000;104(15):3645-3650.

22. Bakhtiar S, Vevodova J, Hatti-Kaul R, Su XD. Crystallization and preliminary X-ray analysis of an alkaline serine protease from Nesterenkonia sp. Acta Crystallographica Section D-Biological Crystallography 2003 Mar;59:529-531.

23. Fincham AG, Leung W, Tan J, Moradian-Oldak J. Does amelogenin nanosphere assembly proceed through intermediary-sized structures? ; 1998: Gordon Breach Sci Publ Ltd; 1998. p. 237-240.

24. Follmer C, Pereira FV, da Silveira NP, Carlini CR. Jack bean urease (EC 3.5.1.5) aggregation monitored by dynamic and static light scattering. Biophysical Chemistry 2004;111(1):79-87.

25. Zhang Y, Amsden BG. Application of an obstruction-scaling model to diffusion of vitamin B-12 and proteins in semidilute alginate solutions. Macromolecules 2006 Feb 7;39(3):1073-1078.

26. Klein J, Stock J, Vorlop KD. Pore-Size and Properties of Spherical Ca-Alginate Biocatalysts. European Journal of Applied Microbiology and Biotechnology 1983;18(2):86-91.

27. Lin SY, Chen KS, Run-Chu L. Drying methods affecting the particle sizes, phase transition, deswelling/reswelling processes and morphology of poly(N-isopropylacrylamide) microgel beads. Polymer 1999 Nov;40(23):6307-6312.

28. Vehring R. Pharmaceutical particle engineering via spray drying. Pharmaceut Res 2008 May;25(5):999-1022.

29. Yin YH, Ji XM, Dong H, Ying Y, Zheng H. Study of the swelling dynamics with overshooting effect of hydrogels based on sodium alginate-g-acrylic acid. Carbohyd Polym 2008 Mar 7;71(4):682-689.

Chapter 6

Modeling the controllable pH-responsive swelling and pore size of networked alginate based biomaterial

Ariel W. Chan and Ronald J. Neufeld

Key words: Alginate; Hydrogel; Cross-linking; Modeling; Swelling; Porosity

Manuscript in Journal Submission

Abstract

Semi-synthetic network alginate polymer (SNAP), synthesized by acetalization of linear alginate with di-aldehyde, is a pH-responsive tetrafunctionally-linked 3D gel network, and has potential application in oral delivery of protein therapeutics and active biologicals, and as tissue bioscaffold for regenerative medicine. A constitutive polyelectrolyte gel model based on non-Gaussian polymer elasticity, Flory-Huggins liquid lattice theory, and non-ideal Donnan-membrane equilibria was derived, to describe SNAP gel swelling in dilute and ionic solutions containing uni-univalent, uni-bivalent, bi-univalent or bi-bi-valent electrolyte solutions. Flory-Huggins interaction parameters as a function of ionic strength and characteristic ratio of alginates of various molecular weights were determined experimentally to numerically predict SNAP hydrogel swelling. SNAP hydrogel swells pronouncedly to 1000 times in dilute solution, compared to its compact polymer volume, while behaving as a neutral polymer with limited swelling in high ionic strength or low pH solutions. The derived model accurately describes the pH-responsive swelling of SNAP hydrogel in acid and alkaline solutions of wide range of ionic strength. The pore sizes of the synthesized SNAP hydrogels of various crosslink densities were estimated from the derived model to be in the range of 30-450 nm which were comparable to that measured by thermoporometry, and diffusion of bovine serum albumin. The derived equilibrium swelling model can characterize hydrogel structure such as molecular weight between crosslinks and crosslinking density, or can be used as predictive model for swelling, pore size and mechanical properties if gel structural

information is known, and can potentially be applied to other point-link network polyelectrolytes such as hyaluronic acid gel.

6.1 Introduction

Hydrogels consist of three-dimensional, hydrophilic, polymeric networks which have been used in many biotechnological, medical and pharmaceutical applications. High water content and structural and mechanical similarities to macromolecular-based components in natural tissues, enable use in biosensors and drug delivery devices, as cell encapsulation matrices, or as tissue scaffold for transplantation. Hydrogels can be classified as physical or chemical gels based on the manner of gel formation. Physical gels are polymer complexes formed by polymer entanglement or electrostatic interaction such as dipole-dipole interaction, hydrogen bonding or van der Waals forces. In contrast, chemical gels are three-dimensional network polymers formed by covalent crosslinking of water-soluble polymers into point-like junctions resulting in permanent, irreversible hydrogels. Since the formation of chemical gels is time-dependent and not instantaneous or rapid as is the case with physical gels, the gel properties such as pore size, swelling, or elasticity can be readily controlled kinetically and thermodynamically, enabling the tailoring, improvement or matching of the polymer network for desired end use.

Alginate, a linear polysaccharide consisting of anionic block copolymer of β-D-mannuronic acid (M) and α-L-guluronic acid (G) residues, can form physical gels by cooperative binding with divalent cations such as calcium, or form chemical gels by reacting the hydroxyl functional groups with a di-aldehyde via acid-catalyzed acetalization[9, 27], with an epoxide via base-catalyzed ring-opening polymerization [28], or by an amine reaction targeting the carboxylic acid functional site, forming imide or amide bond linkages[29, 30]. Semisynthetic network alginate polymer (SNAP) hydrogel

formed by reaction of hydroxyl functional sites with glutaraldehyde, is stable in ionic media containing chelating agents or monovalent ions such EDTA, citrates, sodium and potassium. In contrast, calcium alginate hydrogels are unstable under these conditions. In addition, SNAP hydrogel is pH-responsive, swelling in alkaline and contracting in acid solutions, exhibiting oscillatory swelling/contraction response under alternating pH step change between 1.2 and 7.8 [27]. SNAP hydrogel has potential applications as biosensors, and as encapsulation matrices for wide range molecular sizes of biologicals and as an oral drug delivery vehicle for protein therapeutics such as insulin.

The most important considerations for the use of hydrogel in applications such as drug delivery or as tissue scaffolds, are the network permeability and the transport properties of solvents and ions through the polymer network. Although the polymeric network provides a structural framework that holds the liquid in place, water molecules are free to migrate when redistributed in aqueous solution resulting in gel swelling or contraction. The extent of swelling of a polyelectrolyte gel such as SNAP which consists of ionisable carboxylate moieties, depends on the delicate balance between the swelling potential due to the compatibility of the polymer with the molecules of the surrounding fluid (mixing potential) and the osmotic effect of Donnan membrane equilibria due to mobile ion distributions inside and outside of the gel, and the counter swelling potential generated from the elastic retractive reaction of the polymers[31]. One of the most commonly used swelling models for pH-sensitive hydrogel is that of Brannonpeppas and Peppas [32] which is based on Flory-Rehner rubber elasticity, Flory-Huggins polymer-solvent lattice theory and Gibbs-Donnan equilibrium. However, since Flory-Rehner

rubber elasticity rests on the assumption that the network consists of Gaussian chains, which is generally not valid for polysaccharide networks, and particularly not for alginate networks[33], limitations in adequately estimating the crosslinking density in high ionic strength solutions or extremely diluted solution environment is expected. In addition, there is no simple, generalized equation which accommodates gel swelling in both salt-free and high ionic concentration environments. To address the limitation of the existing models in describing SNAP gel swelling, we developed an equilibrium swelling equation which accounts for the effect of non-ideal Gaussian network stress, a non-ideal Donnan ionic effect, and a solvent-polymer volume exclusion effect. The Flory-Huggins interaction parameter, χ, was determined from rheological data of alginate in salt-free and NaCl aqueous media of various ionic strengths, and was incorporated into the swelling model. The derived model can ultimately be used to estimate the molecular weight between crosslinks, M_c, or crosslinking density and pore sizes of SNAP hydrogel from the known equilibrium swelled gel volume. The adequacy of the swelling model will be evaluated by comparing with pore sizes determined through thermoporometry, and diffusion of bovine serum albumin into SNAP hydrogel of various crosslinking densities.

6.2 Derivation of equilibrium swelling equation for polyelectrolyte hydrogels

The fundamental concept of swelling behaviour of neutral polymer such as vulcanized rubber has been described in the early work of Flory and Rehner as resulting

from the mixing of pure solvent with the initially pure, unstrained polymeric network, $(\Delta\mu_1)_{mix}$ and the elastic free energy consequential to the expansion of the network structure, $(\Delta\mu_1)_{el}$ [34, 35]. Symbolically, the chemical potential of the solvent molecule inside the gel, μ_1, relative to its chemical potential in the pure liquid, μ_1^0, can be expressed as:

$$\mu_1 - \mu_1^0 = (\Delta\mu_1)_{mix} + (\Delta\mu_1)_{el} \qquad \text{--Eq. 1}$$

If the polymeric network contains charged moieties such as carboxylic acids, the swelling becomes more complex in which the swelling pressure may be greatly enhanced as a result of the localization of charge moieties, setting up an electrostatic repulsion between charged polymers. Since soluble polymers are now interconnected covalently, the mobility of fixed charge moieties on the polymer backbone is hindered and cannot diffuse freely into the outer solution. Hence, counterions (original bounded cations) released from the polymer chains are confined inside the gel due to electroneutrality effect. Consequently, the total mobile ion concentration inside the gel will exceed that in the external solution, leading to an osmotic pressure difference which tends to drive solvent into the gel from the less concentrated external solution. If the network structure is permanent, through covalently interlinking polymeric chains with chemical crosslinker, a state of equilibrium swelling may be attained. Flory considered the Donnan-type effect on the swelling pressure and reestablished the expression for equilibrium swelling of network polyelectrolyte[31]. For highly swollen gel, the chemical potential can be assumed to be simple additive of the changes due to mixing of solvent with analogy to

linear polymer, $(\Delta\mu_1)_{mix}$, to the mixing with the ionic constituents, $(\Delta\mu_1)_i$, and to the elastic retractive energy arising from the swelling process, $(\Delta\mu_1)_{el}$:

$$\mu_1 - \mu_1^0 = (\Delta\mu_1)_{mix} + (\Delta\mu_1)_i + (\Delta\mu_1)_{el} \qquad \text{--Eq. 2}$$

At the equilibrium swelling, the chemical potential in the external solution comprising mobile electrolytes, μ_1^*, must be equal to that inside the gel solution. With the fulfillment of the condition, $\mu_1 = \mu_1^*$ and substituting $(\Delta\mu_1^*)_i = \mu_1^* - \mu_1^0$, Eq. 2 can be rearranged and rewritten as:

$$(\Delta\mu_1^*)_i - (\Delta\mu_1)_i = (\Delta\mu_1)_{mix} + (\Delta\mu_1)_{el} \qquad \text{--Eq. 3}$$

6.2.1 Mixing potential of the polymer solution, $(\Delta\mu_1)_{mix}$

The partial molar quantity of chemical potential from mixing polymer with solvent can be obtained by differentiating the free energy of mixing, ΔG_{mix}, with respect to the number of solvent molecules, n_1, and multiplying by Avogadro's number, *N*:

$$\mu_1 - \mu_1^0 = N\left(\partial\Delta G_{mix} / \partial n_1\right)_{T,P} \qquad \text{--Eq. 4}$$

where the change of Gibbs free energy on mixing comprises the entropy of mixing, ΔS_{mix}, and the heat of mixing, ΔH_{mix}:

$$\Delta G_{mix} = \Delta H_{mix} - T\Delta S_{mix}$$ --Eq. 5

Based on the liquid lattice theory, solvent molecules and long chain polymers consisting of *x* monomer molecules (ie. degree of polymerization), each of which is assumed to be equal in size to a solvent molecule, are arranged with regularity as represented by a lattice [36]. If the pure components may be arranged in the respective lattices in only one way, the total configurational entropy due to mixing as described by Boltzmann's statistical thermodynamics is,

$$S_c = k \ln \Omega$$ --Eq. 6

where k is Boltzmann's constant and Ω is the total number of arrangements possible in the solution. According to Flory and Huggins, the configurational entropy for the system of n_1 solvent molecules and xn_2 polymer submolecules can be computed [31, 36]:

$$\Delta S_{mix} = -k\left(n_1 \ln v_1 + n_2 \ln v_2\right)$$ --Eq. 7

where $v_1 = \dfrac{n_1}{n_1 + xn_2}$ and $v_2 = \dfrac{xn_2}{n_1 + xn_2}$ are the volume fractions of solvent and solute.

To estimate the enthalpy of mixing or heat of mixing under constant pressure, ΔH_{mix}, Flory and Huggins derived an expression based on the van Laar equation for heat of mixing in a binary system, assuming a liquid lattice model with each cell able to accommodate either a solvent or a polymer segment molecule [31, 36]:

$$\Delta H_{mix} = kT\chi_1 n_1 v_2$$ --Eq. 8

where χ_1 is known as Flory-Huggins interaction parameter, which represents the difference in energy of a solvent molecule surrounded by polymer molecules (ie. $v_2 \approx 1$), compared with the pure solvent environment (ie. $v_1 = 1$). In the present study, the Flory-Huggins interaction parameter was estimated via viscosity measurement of known molecular weight polymers using Stockmayer-Fixman hydrodynamic solution theory. Combining Eq. 7 and 8, the Gibbs free energy on mixing can then be expressed as:

$$\Delta G_{mix} = \Delta H_{mix} - T\Delta S_{mix} = kT\left[n_1 \ln v_1 + n_2 \ln v_2 + \chi_1 n_1 v_2\right] \qquad \text{--Eq. 9}$$

Taking the derivative of Eq. 9 with respect to n_1, and recalling that v_1 and v_2 are functions of n_1 and $v_1+v_2=1$, the mixing potential of polymer solution can be calculated as:

$$(\Delta\mu_1)_{mix} = N(\partial\Delta G_{mix}/\partial n_1) = RT[\ln(1-v_2) + (1-1/x)v_2 + \chi_1 v_2^2] \qquad \text{--Eq. 10}$$

Since the influence of the degree of polymerization or chain length, x , on the mixing potential vanishes with high molecular weight polymer, for network polymer in which the final molecular weight after crosslinking approaches infinity, it is permissible to approximate the chemical potential of the solvent with:

$$(\Delta\mu_1)_{mix} = RT[\ln(1-v_2) + v_2 + \chi_1 v_2^2] \qquad \text{--Eq. 10b}$$

6.2.2 Chemical potential of the elastic reaction, $(\Delta\mu_1)_{el}$

As the network is progressively expanded during swelling, the polymer chains are expected to take on a more elongated configuration. Depending on the existence of a permanent network structure, an opposite force analogy to rubber retractive reaction will develop in accordance with the swelling potential. Thermodynamically, the chain configurational entropy of the polymeric network is therefore reduced as opposed to an increase in entropy of mixing of solvent with polymer. For ideal rubber behaviour aside from the actual mixing with solvent molecules, the energy of intermolecular interaction is assumed to be affected negligibly by deformation (ie. $\Delta H = 0$). Therefore, the change of free energy of the elastic body, ΔG_{el}, may be equated to the entropy change at given temperature, $-T\Delta S_{el}$, before and after the deformation.

$$\Delta G_{el} = -T\Delta S_{el} \qquad \text{--Eq. 11}$$

Flory and Rehner developed one of the most widely used conceptual templates to estimate the configurational entropy of the elastic network based on the tetrahedral model, known as the phantom network. The phantom network comprises four portions of the structure extending from a crosslink point to the next point, occurring along the given primary molecules, (*f =4*). It is assumed that all of the chains are the same contour length, and the primary polymers prior to crosslinking, follow Gaussian distribution [34]. However, this overly restrictive assignment of the crosslinkages to definite positions in space (affined network model) tends to underestimate the entropy of the elastic reaction of the swollen network [37]. This model was later modified by Flory to include the entropy arising from fluctuations of the sub-system (portion of the polymer chains

between crosslinks) and network of any connectivity greater than 2 (f > 2) [37, 38]. Assuming isotropic swelling, the entropy change involved in deformation, obtained by taking the difference in entropy at deformed and relaxed states (ie. $\alpha_x = \alpha_y = \alpha_z = 1$) can be stated as

$$\Delta S_{el} = -(kv_e / 2)[3\alpha_s^2 - 3 - \frac{4}{f}\ln(\alpha_s^3)] \qquad \text{--Eq. 12}$$

where $\alpha_x\alpha_y\alpha_z = \alpha_s^3 = V_s / V_r$ --Eq. 13

and *s* and *r* denote swollen state and relaxed, non-deformed network formed right after the vulcanization and prior to the swelling process, respectively. The effective number of chains, v_e, is used to account for the imperfect network formation due to intramolecular connections and chain entanglement which do not contribute to the elastic retraction of the network structure, and for the influence of the terminal chains in the primary molecules that are not infinitely long in reality [38].

$$v_e = v_0\left[1 - \left(\frac{M_c}{M_0}\frac{f}{(f-2)}\right)\right] \qquad \text{--Eq. 14}$$

where M_o and $\bar{\upsilon}$ are the primary molecular weight and specific density of the polymer, M_c is the molecular weight between two crosslinking points, V_r is the volume of the network polymer after crosslinking and before deformation or swelling process, and f is the functionality of a structural unit which defines as f number of sub-chains extending from

one crosslink point. The Gibbs free energy change on elastic reaction in molar quantity can be written as:

$$\Delta G_{el} = -T\Delta S_{el} = \left(\frac{kTv_e}{2}\right)\left(3\alpha_s^2 - 3 - \frac{4}{f}\ln\alpha_s^3\right) \qquad \text{--Eq. 15}$$

For natural rubber, it is reasonable to assume unaltered polymer configuration before and after vulcanization which proceeds in the absence of diluent or swelling agent. However, this is not normally the case for hydrogels, where polymer chains absorb substantial quantity of solvent (diluent) prior to crosslinking, encouraging the formation of intramolecular crosslinkage due to greater separation of the chains with diluent. Bray and Merill [39] redefined Eq. 13 using the molar volume of solvent, V_1 , and dry polymer volume, V_p , which is the product of the dry polymer mass, m_p , and its specific volume, $\bar{\upsilon}$.

$$\alpha_s^3 = \frac{V_s}{V_r} = \frac{V_P + n_1 V_1 / N}{V_r} \qquad \text{--Eq. 16}$$

Substituting Eq. 16 back to 15, the chemical potential due to the elastic reaction can be calculated by taking the first derivative of ΔG_{el} with respect to number of solvent molecules and multipling by Avogadro's number, N:

$$(\Delta\mu_1)_{el} = N\left(\frac{\partial\Delta G_{el}}{\partial\alpha}\right)_{T,P}\left(\frac{\partial\alpha}{\partial n_1}\right)_{T,P} \qquad \text{--Eq. 17}$$

$$(\Delta\mu_1)_{el} = RTv_e \frac{V_1}{V_r}\left[\left(\frac{V_r}{V_s}\right)^{1/3} - \frac{2}{f}\frac{V_r}{V_s}\right] \qquad \text{--Eq. 17a}$$

With introduction of polymer volume fraction of the relaxed gel (formed right after crosslinking prior to swelling) and swollen gel, $v_{2,s}$ and $v_{2,r}$ respectively, the elastic potential based on Gaussian model can be expressed by Eq. 17b:

$$(\Delta\mu_1)_{el}^{\ Gaussian} = RTv_e \frac{V_1}{V_r}\left[\left(\frac{v_{2,s}}{v_{2,r}}\right)^{1/3} - \frac{2}{f}\frac{v_{2,s}}{v_{2,r}}\right] \qquad \text{--Eq. 17b}$$

where $v_{2,s} = v_2 = \frac{V_p}{V_s} = \frac{m_p\bar{\upsilon}}{V_s}$ and $v_{2,r} = \frac{V_p}{V_r} = \frac{m_p\bar{\upsilon}}{V_r}$.

However, Eq. 17b is based on the Gaussian coil assumption which may not be able to capture the changes in the small or large deformation/swelling regime of polymer behaviour [40, 41]. To improve the model applicability to polymers such as polyelectrolytes under conditions which can lead to extension of the polymer chains far beyond their average configuration, we modified Eq. 17b with the incorporation of the modified-Gaussian model developed by Kovac [42] for stiff polymer chains, into the swelling equation as presented in Eq. 17c.

$$(\Delta\mu_1)_{el} = RTv_e \frac{V_1}{V_r}\left[\left(\frac{v_{2,s}}{v_{2,r}}\right)^{1/3} - \frac{v_{2,s}}{v_{2,r}}\right]\left[1+\frac{v_{2,s}^{1/3}}{N}\right]^2\left[1-\frac{v_{2,s}^{2/3}}{N}\right]^{-3} \qquad \text{--Eq. 17c}$$

where N is the number of links between two crosslink points, $N = fM_c / M_r$, and f is the number of links per repeating unit. The general elastic term for non-Gaussian network of f-functionality can be expressed as:

$$\Delta(\mu_1)_{el} = RT\frac{V_1}{\upsilon M_c} v_{2,r}\left[1-\left(\frac{M_c}{M_0}\frac{f}{(f-2)}\right)\right]\left[\left(\frac{v_{2,s}}{v_{2,r}}\right)^{1/3} - \frac{2}{f}\frac{v_{2,s}}{v_{2,r}}\right]\left[1+\frac{v_{2,s}^{1/3}}{fM_c/2M_r}\right]^2\left[1-\frac{v_{2,s}^{2/3}}{fM_c/2M_r}\right]^{-3}$$

--Eq. 17d

The modified Gaussian model developed by Kovac incorporates assumptions other than those used in the statistical theory (e.g., nonaffined deformation) but still retains Gaussian statistics for the individual chains, therefore Eq. 17c can be applied to networks at small extension, and to finite extensibility[42].

6.2.3 Chemical potential of the ionic terms, $(\Delta\mu_1^*)_i - (\Delta\mu_1)_i$

Due to concentration gradient and electroneutrality, mobile ions diffuse from the external solution into the gel to establish individual ion equilibrium between the two phases, resulting in osmotic pressure difference which can be calculated using van't Hoff's equation, $\Pi = \sum_i^n c_i RT$ where Π is the osmotic pressure, c is the concentration of the mobile ions, R is the gas constant and T is the temperature. The corresponding chemical potential difference of the solvents inside and outside of the gel compartment due to this pressure difference can be estimate from the thermodynamic relationship: $\pi = -(\mu_1 - \mu_1^0)/V_1$:

$$(\Delta\mu_1^*)_i - (\Delta\mu_1)_i = V_1 RT \sum_i (c_i - c_i^*) \qquad \text{--Eq. 18}$$

where the asterisk indicates external solution compartment and the summation combines the concentration of all ionic solute species, c_i. Swelling of point-like crosslinked SNAP gel in ionic/electrolyte solution and the parameters used in the swelling model derivation are illustrated in Figure 6-1.

The concentrations of the mobile ions inside the swollen gel, c_+ and c_-, can be estimated from known conditions at the state of equilibrium. If the external swelling solution can be considered an infinite sink and contains simple electrolyte which dissociates completely to give concentration c^*, the concentrations of all mobile ions must follow the expressions to fulfill the electroneutrality conditions for anionic network polymer as shown in Table 6-1 (Eq. 19a-i).

Table 6-1: The electroneutrality conditions for anionic network polymer in electrolyte medium at state of equilibrium and assumed ideal Donnan equilibrium (activity coefficients of ionic species =1)

Electrolyte	Equilibrium condition	
Uni-univalent (1:1)	$c_+ = c_- + X_f = c_- + \phi i c_2$	(Eq. 19a)
	$c_+^* = c_-^* = c^*$	(Eq. 19b)
	$c_+ c_- = c^{*2}$	(Eq. 19c)
Di-univalent (1:2)	$c_+ = 2c_- + X_f = 2c_- + \phi i c_2$	(Eq. 19d)
	$c_+^* = c^*, \quad c_-^* = 2c^*$	(Eq. 19e)
	$(2c_+)^2 c_- = (c^*)(2c^*)^2$	(Eq. 19f)
Uni-divalent (2:1)	$c_+ = c_- + X_f / 2 = c_- + \phi i c_2 / 2$	(Eq. 19g)
	$c_+^* = 2c^*, \quad c_-^* = c^*$	(Eq. 19h)
	$c_+ (2c_-)^2 = (2c^*)^2 (c^*)$	(Eq. 19i)
Di-divalent (2:2)	$c_+ = c_- + X_f / 2 = c_- + \phi i c_2 / 2$	(Eq. 19j)
	$c_+^* = c_-^* = c^*$	(Eq. 19k)
	$c_+ c_- = c^{*2}$	(Eq. 19l)

where X_f and ϕ are the concentration and fraction of osmotically active counterions in the swollen gel network. Subscripts "+" and "-"denote positive and negative ions, respectively, and i is the degree of ionization of alginate which can be approximated using the Henderson-Hasselbalch equation in Eq. 20a, and c_2 is the molar concentration of the uronic acid monomers in the swollen gel network which can be calculated from Eq. 20b.

$$c_2 = \frac{v_{2,s}}{\bar{\upsilon} M_r} \qquad \text{--Eq. 20a}$$

$$i = \frac{[RCOO^-]}{[RCOOH] + [RCOO^-]} = \frac{10^{-pK_a}}{10^{-pH} + 10^{-pK_a}} \qquad \text{--Eq. 20b}$$

where K_a is the acid dissociation constant which is 2.51 x 10^{-4} M for alginate consisting of 72% guluronic acid fraction. K_a was calculated from the proportion and pK_a values of the two uronic acid monomers (pK_a = 3.38 for mannuronic acid and 3.65 for guluronic acid [5]), assuming similar pK_a value for the polymer.

According to Manning [43], when the polyelectrolyte is strongly charged, the electrostatic potential on the chain is large and some of the dissociated counterions remain bound to the chain. This phenomenon is known as ion-pairing or counterion condensation. The effective charge is lower than the nominal charge of the monomers, and counterion condensation can be effective even at infinite dilution and reduces the electrostatic interactions between monomers. To address the ion-pairing effect which is especially crucial at low polymer concentrations (or highly swollen network gel), an effective charge concentration of alginate (ϕic_2) that is less than the analytical value is introduced. Ionic activities are used instead of concentration to capture the non-ideal Donnan equilibrium (fraction of osmotically active counterions≠100%, activity coefficients≠1). As a further condition of equilibrium, the Donnan equilibrium relationship of mobile uni-valent, uni-bivalent, bi-univalent and bi-bivalent can be expressed as:

1:1 electrolyte $(c_- + \phi ic_2)c_- = \frac{\gamma_+^* \gamma_-^*}{\gamma_+ \gamma_-} c^{*2}$ --Eq. 21

1:2 electrolyte $(2c_- + \phi ic_2)^2 c_- = \frac{\gamma_+^{*2} \gamma_-^*}{\gamma_+^2 \gamma_-} 4c^{*3}$ --Eq. 21a

2:1 electrolyte $(c_- + \frac{\phi i c_2}{2})(2c_-)^2 = \frac{\gamma_+^* \gamma_-^{*2}}{\gamma_+ \gamma_-^2} 4c^{*3}$ --Eq. 21b

2:2 electrolyte $(c_- + \frac{\phi i c_2}{2})c_- = \frac{\gamma_+^* \gamma_-^*}{\gamma_+ \gamma_-} c^{*2}$ --Eq. 21c

where γ is the activity coefficient and ϕ is the fraction of osmotically active counterions. Assuming the only effect in the activity coefficients ratio of Eq. 21 is due to the ion-pairing phenomenon, and if the numerical value of association constant (K_{ass}) can be determined by an independent method, then the activity coefficient ratio can be estimated from combining Eq. 21 and Eq. 19 as expressed in Eq. 22.

$$K_{ass\,1:1\,or\,2:1} = \frac{X_b}{X_f c_+} \quad \text{--Eq. 22a}$$

$$K_{ass\,1:2\,or\,2:2} = \frac{X_b}{X_f^2 c_+} \quad \text{--Eq. 22b}$$

where subscript 1:1, 1:2, 2:1 and 2:2 denote electrolyte type, $X_b=(X-X_f)$ is the counterion-polymer-fixed ion pairs, and $X_f=(\phi i c_2)$ is the free charge groups (effective fixed charge concentration) on the polymer network and $\phi = X_f/X$ (see Figure 6-1 of schematic illustration).

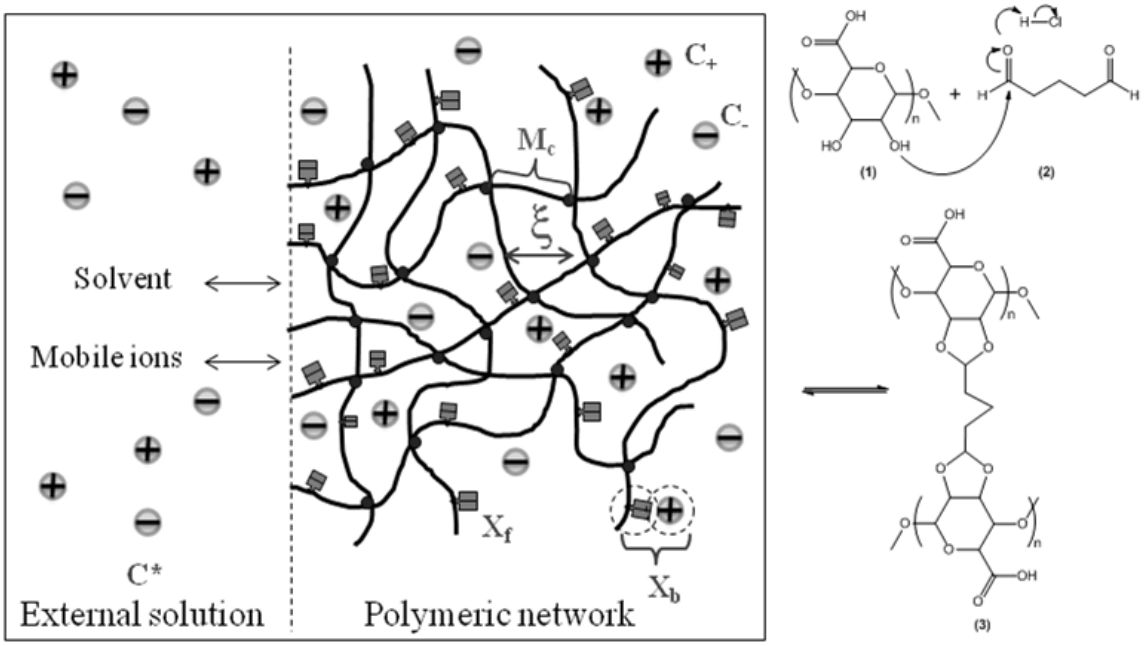

Figure 6-1. Illustration of swelling of point-like crosslinked alginate in ionic solution where the negative fixed charges represent carboxylate anions, solid circles represent point-link crosslinks, solid lines represent linear alginate and a dashed line represents the solvent-gel interface (left-side scheme) and the reaction mechanism of the network alginate hydrogel where structures (1), (2), and (3) are linear alginate, bi-functional glutaraldehyde as crosslinker, and the acetal product of tetrafunctional linked alginate hydrogel (right side scheme). The symbols M_c and ζ are molecular weight between two crosslinks and the mesh pore size, respectively, c_+, c_- are counterions and co-ion concentrations inside the network, and c* is the mobile ion concentration outside the network polymer. The concentrations of counterion-polymer-fixed ion pairs and free effective fixed charges are denoted by X_b and X_f, respectively.

For strong electrolyte, the external ionic activity coefficient can be assumed to be equal to mean ionic activity of the electrolyte, $\gamma_+^* = \gamma_-^* = \gamma_\pm^*$. Since co-ions (c_-) should be in regions far away from the fixed charge moieties and do not participate in the ion-pairing phenomenon, we can assume that the ionic activity coefficient of co-ions is similar to that of external anions, $\gamma_- \approx \gamma_-^* = \gamma_\pm^*$. With these assumptions, the counterion activity coefficient can be readily expressed as:

$$\gamma_{+1:1 or 2:1} \approx \frac{\gamma_{\pm}^{*}}{1 + K_{ass}\phi i c_2} \qquad \text{--Eq. 23a}$$

$$\gamma_{+2:1 or 2:2} \approx \frac{\gamma_{\pm}^{*}}{1 + \frac{1}{2}K_{ass}(\phi i c_2)^2} \qquad \text{--Eq. 23b}$$

With rearrangement of Eq. 21, the co-ion concentration inside the gel for uni-bi, bi-uni and bi-bi electrolyte solutions can be estimated from the empirical relationship:

For 1:1 electrolyte, $c_{-1:1} = \left[a_{1:1} c^{*2} + \left(\frac{\phi i c_2}{2} \right)^2 \right]^{1/2} - \frac{\phi i c_2}{2}$ --Eq. 24

For 1:2 or 2:1 electrolytes, $c_{-1:2 or 2:1} = A_{1:2 or 2:1} + \frac{(\phi i c_2)^2}{A_{1:2 or 2:1}} - \frac{1}{3}(\phi i c_2)$ --Eq. 25

where $A_{1:2} = \left\{ \left(\frac{1}{6}\phi i c_2 \right)^3 + \frac{1}{2} a_{1:2} c^{*3} + \left[216 \left(\phi i c_2 c^{*} \right)^3 a_{1:2} + \left(1089 a_{1:2} c^{*3} \right)^2 \right]^{1/2} \right\}^{1/3}$ --Eq. 25a

$$A_{2:1} = \left\{ \left(\frac{1}{6}\phi i c_2 \right)^3 + 2 a_{2:1} c^{*3} + \left[864 \left(\phi i c_2 c^{*} \right)^3 a_{2:1} + \left(432 a_{2:1} c^{*3} \right)^2 \right]^{1/2} \right\}^{1/3} \qquad \text{--Eq. 25b}$$

For 2:2 electrolyte, $c_{-2:2} = \left[a_{2:2} c^{*2} + \left(\frac{\phi i c_2}{4} \right)^2 \right]^{1/2} - \frac{i c_2}{4}$ --Eq. 26

When combining equations 10b, 17d, and 18, a general swelling expression for point-linked network polymer gel in electrolyte solution can be recast as:

$$V_1\left[\phi i c_2 + 2\left(c_- - c^*\right)\right] - \left[\ln\left(1-v_2\right) + v_2 + \chi_1 v_2^2\right] =$$
$$\frac{V_1}{\bar{\upsilon} M_c} v_{2,r}\left[1-\left(\frac{M_c}{M_0}\frac{f}{(f-2)}\right)\right]\left[\left(\frac{v_{2,s}}{v_{2,r}}\right)^{1/3} - \frac{2}{f}\frac{v_{2,s}}{v_{2,r}}\right]\left[1+\frac{v_{2,s}^{1/3}}{fM_c/2M_r}\right]^2\left[1-\frac{v_{2,s}^{2/3}}{fM_c/2M_r}\right]^{-3} \text{--Eq. 27}$$

where c- can be expanded by Eq. 24-26.

For SNAP hydrogel which was synthesized by reacting four hydroxyl groups with di-aldehyde, forming two acetal linkages between two hexuronic acid monomers from adjacent polymer chains, 4 sub-chains were extended from each crosslink point, f=4 [27]. Therefore, Eq. 27 can be further simplified for SNAP hydrogel swelling:

$$V_1\left[\phi i c_2 + 2\left(c_- - c^*\right)\right] - \left[\ln\left(1-v_2\right) + v_2 + \chi_1 v_2^2\right] =$$
$$\frac{V_1}{\bar{\upsilon} M_c} v_{2,r}\left[1-\left(\frac{2M_c}{M_0}\right)\right]\left[\left(\frac{v_{2,s}}{v_{2,r}}\right)^{1/3} - \frac{1}{2}\frac{v_{2,s}}{v_{2,r}}\right]\left[1+\frac{v_{2,s}^{1/3}}{2M_c/M_r}\right]^2\left[1-\frac{v_{2,s}^{2/3}}{2M_c/M_r}\right]^{-3} \quad \text{--Eq. 27a}$$

The left-hand side of the equation represents swelling potential while the right-hand side is the opposing elastic retractive potential acting against the expansion of the network during swelling. The equilibrium swelling gel volume is reached when the two sides of the equation are equal. Through measurement of the gel equilibrium volume in known ionic and pH environments, the extent of crosslinking characterized by molecular weight between crosslinks, M_c, can be estimated. The gel pore size, ξ, can be subsequently approximated using Eq. 28[44]:

$$\xi = v_{2,s}^{-1/3}\left[C_n\left(\frac{2\overline{M_c}}{M_r}\right)\right]^{1/2} l \qquad \text{--Eq. 28}$$

where C_n is the characteristic ratio which can be estimated from the intrinsic viscosity of the polymer at theta condition, $[\eta_\theta]$, l is carbon-carbon bond length of monomer unit (ie. uronic acid residue has bond length of 5.15 Å)[45] , M_r is monomer molecular weight (198 g/mol), and Φ is the Flory viscosity constant. Equation 28 which was originally derived by Flory[31] for calculation of the mean square end-to-end distance of a Gaussian polymer, has been extended by Canal and Peppas[44] to approximate the network mesh pore size (correlation length). In dilute solution or salt-free environment, the charges attached to the polyelectrolyte chain may be sufficient to cause the polymer to extend almost to full length, resulting in a rod-like conformation[46], hence having greater end-to-end distance than neutral Gaussian polymer. Treatment in accounting for the non-Gaussian coil behavior can be found in the work of Fixman and Kovac [47]. Therefore further modification to accurately account for the non-Gaussian polymer effect should be considered for rod-like, inflexible polyelectrolyte gels.

6.3 Materials and methods

Pharmaceutical grade sodium alginate, SF120 (470 kg/mol and F_G=0.22) was supplied by FMC Biopolymer (Drammen, Norway). Alginate of sample SF120 was degraded at pH 4, 30^{o}C and time course samples lyophilized to give alginates of different molecular weights of 66, 120, and 288 determined from light scattering (Zetasizer Nano ZS, Malvern Instrument) for the viscosity study.

6.3.1 Determination of the intrinsic viscosity at theta condition, $[\eta]_\theta$, and characteristic ratio C_n

Various alginate concentrations of less than 0.2% w/v in NaCl solution were prepared from isoionic dilution experiments [48]. The efflux times of alginate solutions at specific ionic strength through an Ubbelohde type glass viscometer (No. 0B, Cannon Instrument Company) were measured and used in constructing both Huggins ($\eta_{reduced}/c$ vs c) and Kraemer plots ($\ln(\eta/\eta_o)/c$ vs. c). The intrinsic viscosity of alginate at specific ionic strength was obtained by extrapolated the best fitted lines to zero concentration.

The intrinsic viscosity at theta condition was determined following procedures described in Amsden and Turner [49]. In brief, the intrinsic viscosities (dL/g) of alginate in NaCl solution of various ionic strengths were measured and plotted against $I^{-1/2}$. The intrinsic viscosity at theta condition, $[\eta]_\theta$, was obtained by extrapolating the best fitted line to an infinite ionic strength. The corresponding characteristic ratios of various molecular weight alginates determined from Eq. 31 can be calculated using Eq. 29.

$$C_n = \left(\frac{[\eta]_\theta}{\Phi} \right)^{2/3} \frac{M_r}{M_0^{1/3} l^2} \qquad \text{--Eq. 29}$$

where l is carbon-carbon bond length of monomer unit (ie. uronic acid residue has bond length of 5.15 Å)[45] and M_r is monomer molecular weight (198 g/mol).

6.3.2 Synthesis of chemically networked polyhexuronic acid gel

Sodium alginate solution of 4 g/dL was extruded dropwise via an automatic liquid dispenser (EFD, Model 1000XL, East Providence, USA) into 0.05 M HCl, resulting in 2.9 ± 0.1 mm alginic (polyhexuronic) acid gel beads. Beads were incubated in the supernatant solutions for 4 h prior to use. Glutaraldehyde in water of 25% w/w was purchased from Sigma-Aldrich (Oakville, Canada). The absorbance ratio measured for polymeric to monomeric form of pentanedial was no greater than $A_{235}/A_{280} = 0.3$. Four SNAP gel samples were synthesized by suspending preformed acid gel beads (from extruding a 4 g/dL Protanal SF 120 alginate in acid capture solution) in crosslinking reaction medium containing 0.8, 1.1, 1.3 and 1.6 M glutaraldehyde and 0.4 M HCl at 40^{o}C. The mass ratio of beads to reaction medium was 0.30 and accounting for the water content inside gel beads, the initial hydroxyl concentration was 0.38 M. The reaction was allowed for 8-20 h until approaching equilibrium following the kinetics characterized previously [27].

6.3.3 Equilibrium swelling measurement of SNAP gels

SNAP gel beads obtained from the various reaction conditions were washed with 4^{o}C, 40% ethanol, and then submerged in the swelling medium containing 0.1 M NaCl at pH 7.8 for 72 hours. To provide an infinite sink, the solution was constantly replaced with fresh medium. The equilibrium swelling volume of the gel beads, V_s, was calculated from the bead diameter in aqueous solution determined under Leica stereomicroscope (D3,

Germany) with the assumption of a perfect sphere. The corresponding equilibrium swelling ratio ($v_{2,s}^{-1}$) was calculated with respect to the initial compact volume of polymer ($m_p\bar{\upsilon}$) where m_p is the mass of dried alginate polymer and $\bar{\upsilon}$ is the specific volume of alginate which is 0.8 cm^3/g determined from differential sedimentation [50]. The bead volume measured microscopically was compared with volume displacement in paraffin oil. The difference between the two volume measurements was less than 5% for beads formed at the critical gelation point and less than 8% for beads prior to the swelling test. All bead volumes were measured microscopically.

The equilibrium swelling data of the four SNAP gel samples were used in the calculation of the molecular weight between crosslinks, M_c, and the corresponding pore sizes, ξ, using equations 27a and 28 with characteristic parameters of C_n= 27.33, ϕ=0.4, M_o =470 kg/mol, M_r=198 g/mol, and V_1=18 cm^3/mol. The sample mean and standard deviation were calculated based on 3 beads for each experiment. All data reported were the pooled mean and standard deviation of three repeated experiments.

6.3.4 Protein diffusion study and the absorptive encapsulation approach

The diffusion rates of bovine serum albumin (BSA) were determined by suspending 200 SNAP gel beads in 0.1 M NaCl at pH 7.8 containing BSA at 100 mg/mL at 20°C. The protein concentration change of the loading solution was determined by Bradford assay and used to construct the absorption profiles for BSA into SNAP

hydrogel. The diffusion coefficients were estimated from the best fitted curves based on the diffusion model modified by Crank for spherical hydrogel beads (Eq. 30) [17].

$$\frac{M_t}{M_\infty} = 1 - \sum_{n=1}^{\infty} \frac{6\alpha(\alpha+1)\exp(-Dq_n{}^2 t/a^2)}{9+9\alpha+q_n{}^2\alpha^2} \qquad \text{--Eq. 30}$$

where M_t and M_∞ represent the protein mass in the gel beads at time t and at the equilibrium state, D is the diffusion coefficient of the protein to the gel matrix, q_n are the positive non-zero roots of $\tan q_n = \frac{3q_n}{3+\alpha q_n{}^2}$, α represents the ratio of the protein solution volume to the beads $\alpha = \frac{3V}{n4\pi a^3}$ and *a* is the radius of the gel bead.

The diffusion coefficient of BSA in water was calculated from Eq. 31.

$$D_{water} = \frac{k_B T}{6\pi\eta r_H} \qquad \text{--Eq. 31}$$

where k_B is Boltzmann's constant (1.38 $x10^{-23}$J/K), T is the absolute temperature in Kevin, ηis the viscosity of water ($1.31x10^{-3}$ Pa·s at 20°C) and r_H is the hydrodynamic radius of the solute in meters (molecular weight of BSA is 66.4 kDa and hydrodynamic radius is 3.5 nm [51]).

6.3.5 Pore size measurement by differential scanning calorimeter

Thermoporometry technique was used to approximate the pore size of alginate hydrogels [10]. Through measuring the shift in equilibrium temperature (ΔT) of the liquid-solid transformation, we can approximate the average pore radius (R_p in nanometers) of the hydrogel using Eq. 32 derived by Iza et al[16].

$$R_p = -273.15\left(\frac{0.25}{\Delta T} + 0.023\right) \qquad \text{--Eq. 32}$$

where $\Delta T = T - 273.15$ and T is the triple point depression temperature in Kelvin. The shift in freezing and melting temperature of water was determined by differential scanning calorimeter (DSC Q100, TA Instruments) equipped with a liquid nitrogen-cooling accessory. Samples weighing 10-20 mg were placed in a sealable aluminum pan and one drop of the solvent was added to prevent premature drying prior to the measurement. The samples were first equilibrated at -30^{o}C, held for 10 min, followed by heating up to 15^{o}C at a rate of 2.0^{o}C/min and held for 10 min, and then cooled down from 15^{o}C to -30^{o}C at a rate of 2.0^{o}C/min.

6.4 Results and discussion

6.4.1 Rheological properties of alginate

6.4.1.1 Measurement of Flory-Huggins interaction parameter, χ, by Stockmayer-Fixman equation

The Flory-Huggins interaction parameter was experimentally measured using Flory viscosity theory and Stockmayer-Fixman relationship[52] in various ionic strength NaCl pH 7 solution. Intrinsic viscosity, [η], of various molecular weight alginates, M_0, at specific ionic strength was measured with Ubbelohde type glass viscometer. The viscosity data were then used in constructing plots of $M_0^{1/2}$ versus $[\eta]M_0^{-1/2}$ of which the slopes determined from the best fitted lines were used to calculate the Flory-Huggins interaction parameter, χ from Eq. 33. $\frac{[\eta]}{M_0^{\frac{1}{2}}} = k_\theta + 0.51\Phi B M_0^{\frac{1}{2}}$ and $B = \frac{2\bar{\upsilon}^2\left(\frac{1}{2}-\chi\right)}{N_A V_1}$ --Eq. 33

where k_θ is the unperturbed parameter (mLg^{-1}), $\bar{\upsilon}$ is the specific density of alginate (0.8 cm^3g^{-1}), V_1 is molar volume of the solvent (cm^3g^{-1}), N_A is Avogadro number, M_0 is the primary molecular weight of alginate and Φ is the Flory viscosity constant (which is1.21 $x10^{21}$ mol^{-1} in 0.1 M NaCl solution approximated using data from Smidsrod [45]). The interaction parameter as function of ionic strength is presented in Figure 6-2.

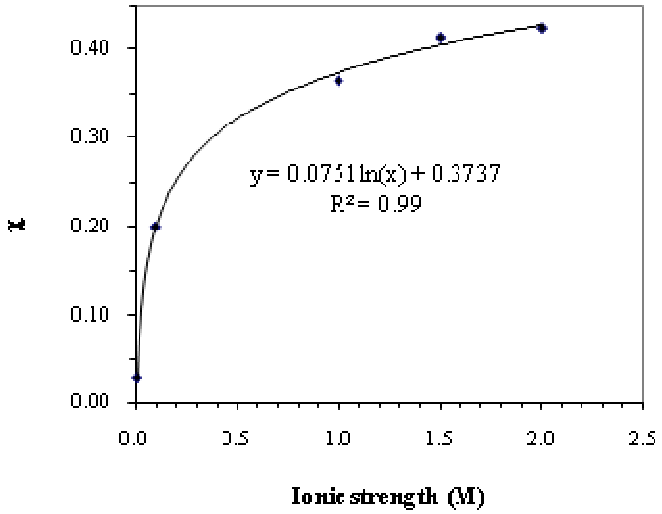

Figure 6-2. Flory-Huggins interaction parameters as function of solution ionic strength determined from intrinsic viscosity and molecular weight of alginate samples using equation 33.

If 2:1 or 2:2 electrolytes such as calcium chloride, barium chloride, or magnesium sulfate, were used as suspension mediums, white precipitate forms. Higher valency electrolyte solutions behave like poor solvents with $\chi \approx 0.5$ (data not shown). In addition, alginate precipitates in acid solutions at pH less than 3-3.5, therefore χ was approximated to be around 0.5. For suspension medium with pH greater than 4, the χ values are similar to the function obtained in Figure 6-2.

6.4.1.2 The intrinsic viscosity at theta condition, $[\eta]_\theta$, and characteristic ratio, C_n, of alginate

As alginate is a polyelectrolyte, its intrinsic viscosity at theta condition in which the coil expansion due to intramolecular electrostatic repulsion is suppressed [45], was

measured at various ionic strengths and extrapolated to infinite ionic strength. The intrinsic viscosity of various molecular weight alginates at theta condition, $[\eta]_\theta$, and the corresponding characteristic ratios determined from Eq. 29 are plotted in Figure 6-3.

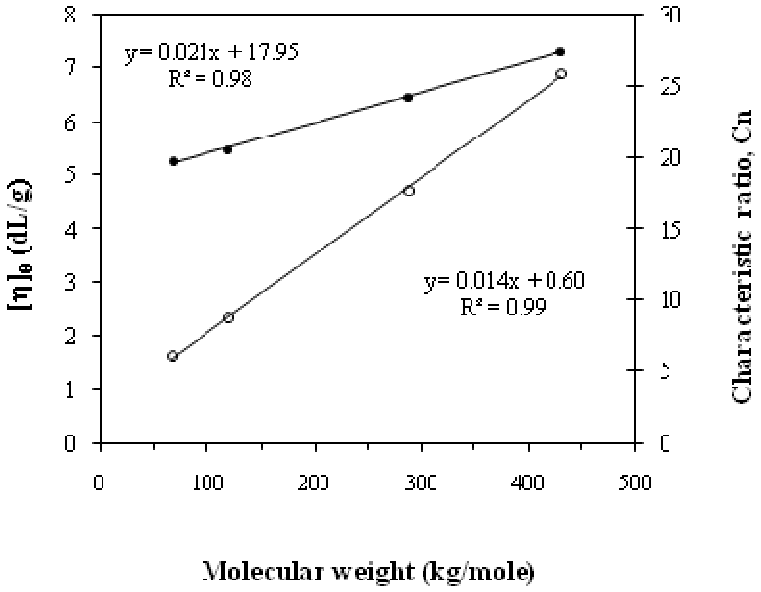

Figure 6-3. Intrinsic viscosity of various molecular weight alginates at theta concentration (open symbol, right-side ordinate) and the corresponding characteristic ratio (closed symbol, left-side ordinate) determined from Equation 34.

Linear relationships were observed for both $[\eta]_\theta$ and C_n with respect to alginate molecular weight in the range of 50-500 kDa. The greater characteristic ratio was obtained for higher molecular weight alginate which has a more rigid and extended polymer structure. Since the parameters of intrinsic viscosity at theta condition and characteristic ratio are measures of the dimension of a polymer in its real and unperturbed state, with determined equilibrium swelling gel volume, the pore size can be estimated using Eq. 29.

6.4.2 Numerical evaluation of the swelling model for SNAP hydrogel

6.4.2.1 Swelling potentials of solvent in SNAP hydrogel

From numerical evaluation of the swelling potentials as a function of swollen gel volume which consisted of mixing and ionic terms as expressed by equations 10b and 26, it is apparent that at ionic strengths below 0.01 M, the chemical potential due to the ionic effect is the most significant term contributing to the swelling pressure of SNAP gel as seen in Figure 6-4. Moe et al. at the equilibrium swelling, the ionic part ($\Delta\pi_{ion}$) has been shown to contribute approximately 90% of the overall swelling pressure in a crosslinked sodium-alginate gel [28]. However, with an increase in ionic strength to above 0.1 M, positive sodium ions shield negative carboxylate anions on alginate, reducing electrostatic repulsion. In addition, the chemical potential difference due to mobile concentration difference between inside and the outside of the gel network is reduced. Therefore, at high ionic strength, the screening of the fixed charges on the polymers is so severe that the charged polymer network behaves similarly to neutral polymers and thus the mixing potential dominants during swelling.

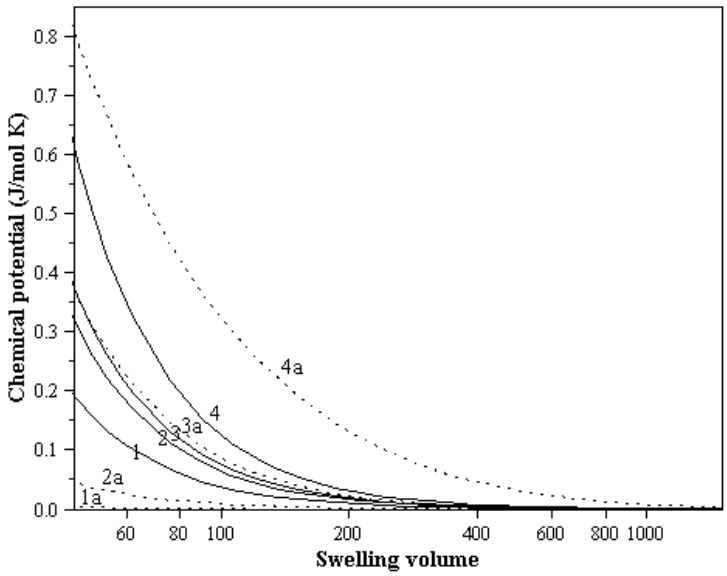

Figure 6-4. Numerical evaluation of chemical potential of the solvent due to mixing term (solid line) and Donnan membrane effect (dotted line) as a function of swelling volume in 1 (1, 1a), 0.1 (2, 2a), 0.01 (3, 3a), and 0.001 M (4, 4a) NaCl solution, pH 7, and ϕ=0.4.

6.4.2.2 Swelling model accounts for non-Gaussian elastic effect

Elastic potentials of SNAP hydrogel of various crosslinking densities were numerically evaluated using Eq. 17d and the corresponding swelling potentials due to polymer mixing effect and Donnan ionic effects were calculated from equations 10b and 26 and plotted in Figure 6-5. The intercept of the swelling and elastic potential functions indicates the equilibrium swelling volume of SNAP hydrogel. According to Moe et al[33], alginate is non-Gaussian, however as can be seen in Figure 6-5, the curve of chemical potential calculated using the network model (Eq. 17b) based on Gaussian coil assumption, nearly coincide with the curves calculated with the modified model (Eq. 17c), suggesting networked alginate polymer behaves more like a Gaussian polymer.

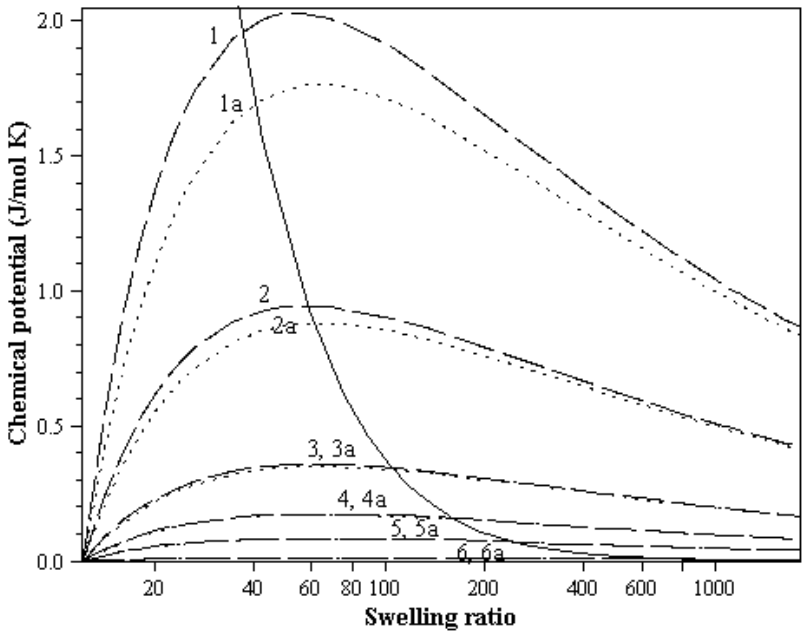

Figure 6-5. Chemical potential of the elastic reaction calculated from the modified non-Gaussian (Eq. 17d, long dash) and ideal-Gaussian elastic network models (Eq 17b, dotted line), and the swelling potential due to mixing and Donnan ionic effect (Eq 23, $-\Delta\mu_{ion}$, solid line) as a function of equilibrium swelling ratio of network alginate in 0.1 M NaCl pH 7.8 solution. The simulation of the elastic potential was based on molecular weight between crosslinks, M_c, of 500 (1, 1a), 1,000 (2, 2a), 2,500 (3, 3a), 5,000 (4, 4a), 10,000 (5, 5a), and 50,000 g/mol (6, 6a). The equilibrium swelling of the network hydrogel was reached when swelling potential was equal to the opposite elastic retractive potential (interception of solid and dash or dotted lines). Simulation was constructed with ϕ=0.4.

In addition, equilibrium swelling of SNAP hydrogels as a function of molecular weight between crosslinks, M_c , was calculated from Eq. 27 and also calculated with the Gaussian polymer assumption using Eq. 17c, and plotted in Figure 6-6. The results show little or no difference between the lines, indicating that network alginate polymer behaves as a Gaussian polymer. It is therefore reasonable to utilize Eq. 28 for pore size characterization for SNAP hydrogels.

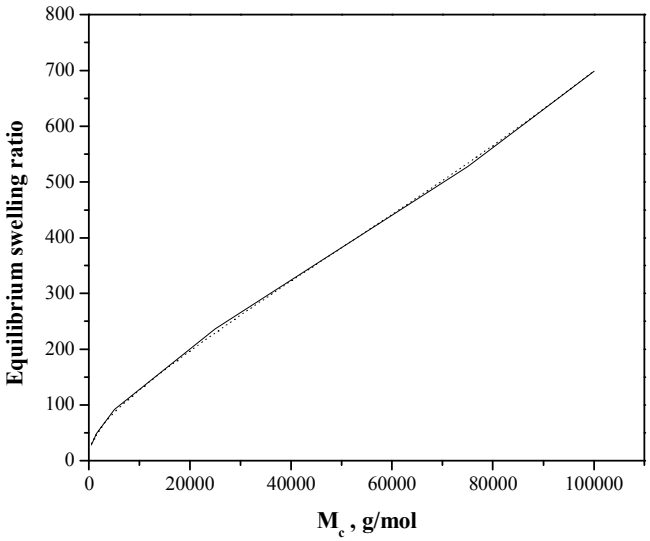

Figure 6-6. Numerical evaluation of equilibrium swelling of SNAP hydrogels from Eq. 27 accounting for non-Gaussian elastic behavior (solid line) and considering Gaussian polymer assumption(dotted line).

6.4.2.3 Simulation of equilibrium swelling with pre-determined Flory-Huggins interaction parameters as function of ionic strength and pH

SNAP hydrogel of various crosslinking densities was synthesized and the corresponding equilibrium swelling gel volume in 0.1 M NaCl, pH 7 solution determined for subsequent calculation of molecular weight between crosslinks, M_c, using equation 27a. From the determined equilibrium swollen gel volumes, the M_c of SNAP hydrogels were estimated to be 1500, 5000, 25000, and 75000, and the corresponding pore sizes determined from equation 28 were 37, 104, 225, 442 nm, respectively. Equilibrium swelling of SNAP gels was numerically evaluated as a function of ionic strength using

constant and pre-determined χ values. The simulation data is plotted in Figure 6-7 along with the experimentally determined swelling measurement in various ionic media.

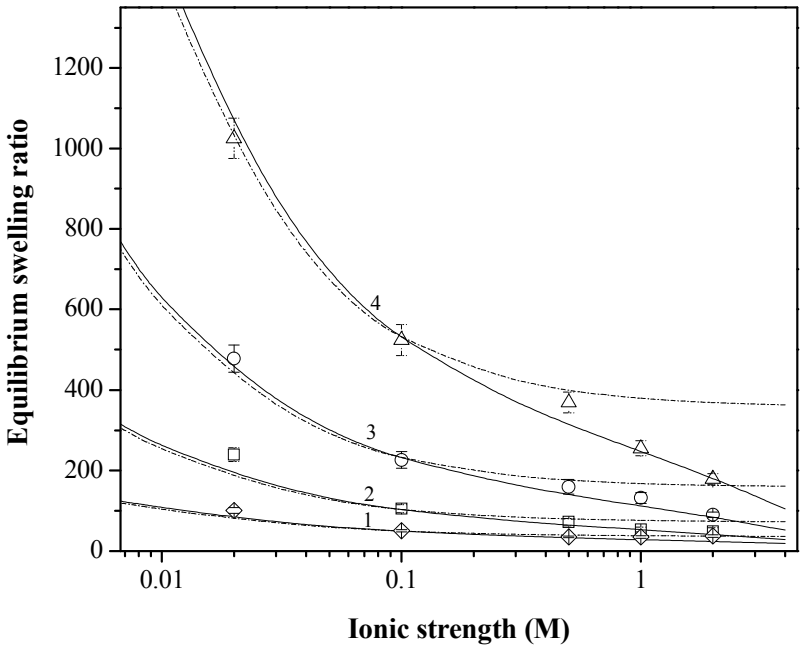

Figure 6-7. The experimentally determined (symbols) and simulation (lines) of equilibrium swelling of SNAP hydrogels having molecular weight between crosslinks of (◇, curve 1), 5,000 (□, curve 2), 25,000 (○, curve 3), and 75,000 (△, curve 4) in NaCl solutions of various ionic strength (pH 7). Simulation was conducted with constant χ determined at 0.1 M (dotted line) and χ as function of ionic strength (solid line), and ϕ=0.4.

Flory-Huggins interaction parameters,χ, vary according to the ionic environment of the suspension solution as seen in Figure 6-2. However, due to lack of rheological data on alginates, molecular weight between crosslinks or crosslinking density have been previously estimated from the swelling model using constant χ [28, 53]. As can been seen in Figure 6-7, approximately 10-fold reduction in swelling was observed for loosely

crosslinked gel beads (estimated M_c=75000) when the solution ionic strength increased from 0.02 M to 2 M. This swelling behaviour was better captured by the model simulated with variable χ values. In addition, an equilibrium swelling ratio of about 30 when extrapolated to infinite ionic strength was obtained for SNAP hydrogels of various crosslinking densities predicted using variable χ values. This equilibrium swelling ratio corresponds to swelling at theta condition when the screening of the carboxylate charges by sodium ions is so strong that the mutual repulsion between polymers is essentially removed, resulting in a behavior similar to that of neutral polymers. Since the simulated data showed good fit to the experimental data, the derived swelling model is considered to be adequate and can accurately describe SNAP hydrogel swelling in ionic media.

The equilibrium swelling of the four synthesized SNAP hydrogels in various pH solutions was numerically evaluated with variable and constant Flory-Huggins interaction parameter, χ. The simulation data is plotted along with the experimentally determined values in Figure 6-8. As can be seen, SNAP hydrogel demonstrated pH-responsive swelling when the pH was greater than 3.5, while remaining in a compact state in acid media with pH less than 3. This swelling behavior was better described by a model simulated with variable χ values instead of a constant value. The equilibrium swelling ratio of loosely crosslinked SNAP hydrogel (simulated with M_c=75000) in pH 1 solution was predicted to be around 350 using the model with constant χ values. In contrast, the simulation with variable χ values showed near minimum swelling at pH less than 2 and equilibrium swelling ratio of less than 50 in pH 1. Therefore, if a fixed χ value is used without accounting for the effect of the suspended electrolyte environment, discrepancy

in estimation of equilibrium swelling or crosslinking density from the derived swelling model may be experienced

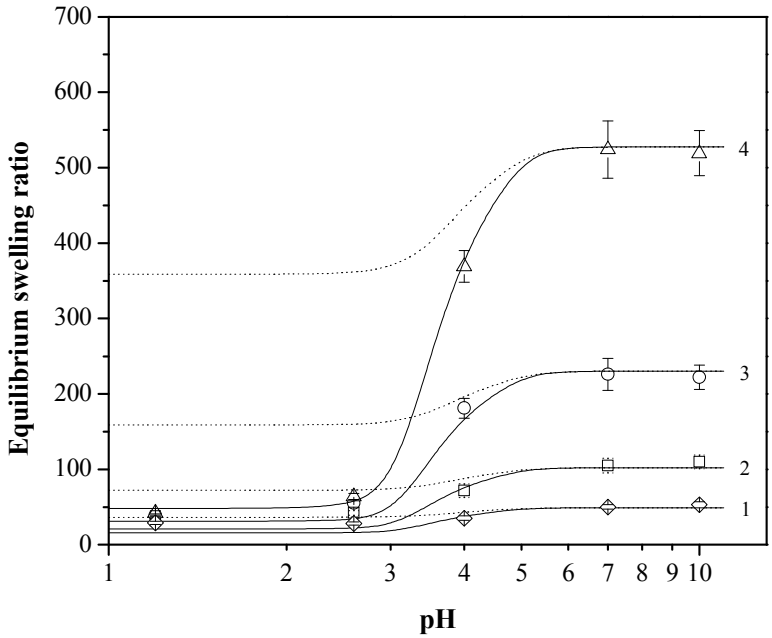

Figure 6-8. The experimentally determined (symbols) and simulation (lines) of equilibrium swelling of SNAP hydrogels having molecular weight between crosslinks of of 1,500 (◇, curve 1), 5,000 (□, curve 2), 25,000 (○, curve 3), and 75,000 (△, curve 4) in various pH solutions containing 0.1 M NaCl. Simulation with constant χ determined at 0.1 M (dotted line) and χ as function of ionic strength (solid line), and ϕ=0.4.

The swelling model derived in this study (Eq. 27) was based on the ideal Donnan equilibrium extended to account for the ion pairing effect within the results obtained from a thermodynamic model that uses ionic activities rather than concentrations. The model no longer assumed the activity coefficients to be equal to unity ($\frac{\gamma_+^* \gamma_-^*}{\gamma_+ \gamma_-} \neq 1$) and no ion pairing effect (a.k.a condensed ion or ion fixation effect). The importance of accounting for the ion pairing effect in dilute solution was demonstrated in Figure 6-9.

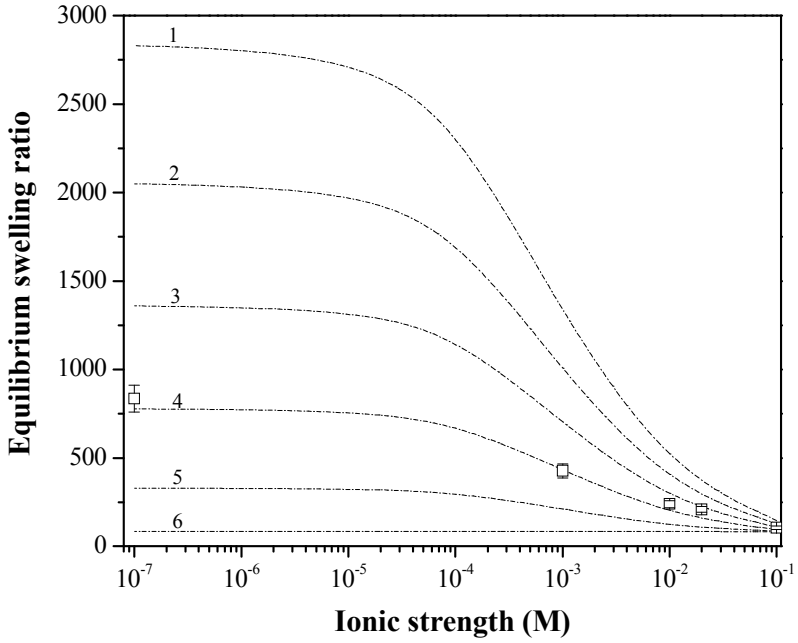

Figure 6-9. Computation of equilibrium swelling ratio of SNAP hydrogel with 0 (curve 1), 20 (curve 2), 40 (curve 3), 60 (curve 4), 80 (curve 5), and 100% (curve 6) of condensed ions in pH 7 NaCl solution. The experimentally determined swelling of SNAP hydrogels of M_c=5000 are represented by the data points. Simulation was conducted with χas a function of ionic strength and M_c=5000.

Since the maximum attainable swelling volume of SNAP hydrogel in de-ionized water was experimentally observed to be less than 1000 times its compact volume (data points in Figure 6-9), the simulation without considering the appropriate ion pairing effect such as the case with curves 1-3, appeared to overestimate the swelling behavior. According to Katchalsky [54], the ion-pairing effect for alginate in solutions of 0.005~0.1 M NaCl was severe, and only about 40% of the carboxylate charge groups remained unbounded (fraction of the osmotically active charge, ϕ=0.4). Therefore, in dilute solution environment, it is reasonable to assume ϕ=0.4 in the derived model. At high ionic concentration, the chemical potential due to mobile ion distribution inside and outside of

the gel diminishes, and ϕ approaches zero, making anionic polymers behave similar to neutral polymers. With the inclusion of the ion-pair effect in the derived model, SNAP gel swelling in solutions of wide range ionic strengths, including in de-ionized water, can be appropriately modeled.

In addition, in dilute solution where the charged ion concentration within the gel network is generally greater than that of external suspending solution, the ideal Donnan equilibrium effect is no longer valid as the activity coefficients of the mobile ions within the gel network are generally greater than that of the external electrolyte environment. The simulation of gel swelling in various ionic strength solutions with the use of different activity coefficients is presented in Figure 6-10. The estimated equilibrium swelling ratio for SNAP gel using the association constant for sodium and carboxylate ions of 90 M^{-1} [55] and the corresponding calculated activity coefficient of $\frac{\gamma_+^* \gamma_-^*}{\gamma_+ \gamma_-} = 0.8$ was about 150 (line 1 in Figure 6-10). If the activity coefficient used for simulation increases from 0.8 to 1.15 (line 6 in Figure 6-10), the estimated swelling gel volume will increase by 2 fold in 0.01 M NaCl, indicating a strong correlation between activity coefficients and the resultant swelling volume at low ionic concentration. However, at extremely low ionic environment (lower than 1 x 10^{-5} M), ion pairing effect becomes significant and most of the counterions are confined within the gel, leading to low concentrations of the mobile ions moving between gel and external environments. Therefore, the effect of assuming non-ideality of the gel environment becomes insignificant.

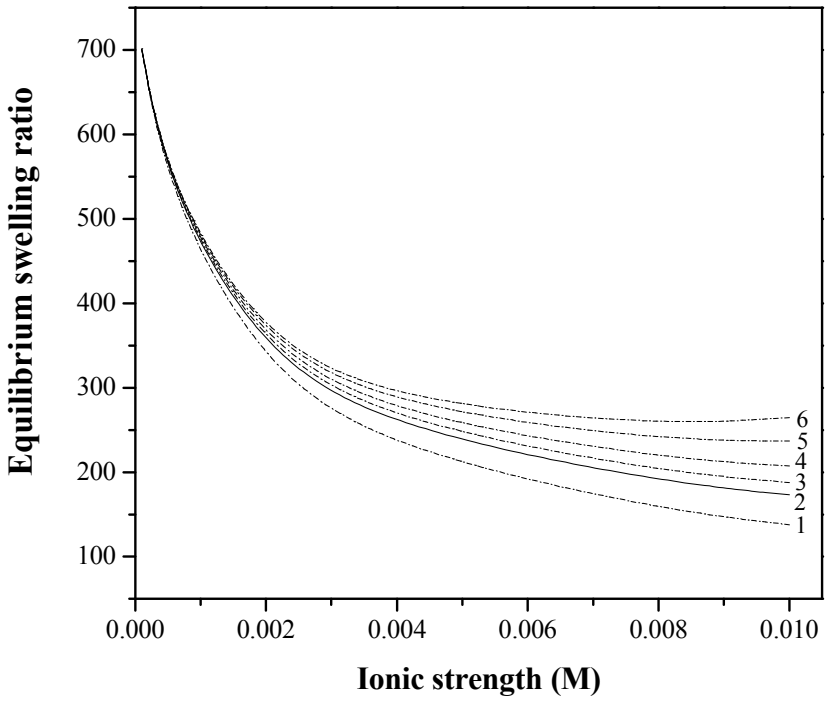

Figure 6-10. Computation of equilibrium swelling ratio of network alginate with activity coefficient of 0.8 (curve 1), 1 (curve 2), 1.05 (curve 3), 1.1 (curve 4), 1.15 (curve 5), and 2 (curve 6) in pH 7 NaCl solution. Simulation was conducted with ϕ=0.4, χ as a function of ionic strength and M_c=5000.

6.4.3 Adequacy of the swelling model in estimation of the gel pore size

6.4.3.1 Gel pore size estimate from the diffusion data of BSA into SNAP of various crosslinking densities

The diffusion coefficient of SNAP gel beads was studied with beads of various crosslinking densities in BSA solution. Absorption isotherms and model curves based on a Fick's second law of diffusion (Crank's model[17]) were used to estimate diffusion coefficients. Since solute transport into hydrogel requires that the size of an opening

between the polymer chains (ξ, mesh pore diameter) be large enough to allow passage, diffusion data can be utilized in estimation of the pore size of the gel network according to Zhang and Amsden [22] using Eq. 34,

$$D_{gel} = D_{water} \exp\left[-\pi \left(\frac{r_H + r_f}{\xi + 2r_f} \right) \right] \qquad \text{--Eq. 34}$$

where r_f is the cross-sectional radius of the polymer chain (0.83 nm for alginate which is estimated from chain radius of 0.55 nm characterized by small-angle X-ray scattering (SAXS) [56], plus a water layer of 0.28 nm (van der Waals radius of water is 0.14 nm) [57]) and r_H is the hydrodynamic radius of BSA which was determined to be 3.5 nm [51].

The gel pore sizes were also estimated using thermoporometry which is based on the principle of liquid-solid transformation. The pore sizes of SNAP gels obtained from various reaction conditions were determined from the derived swelling model, diffusion study and thermoporometry, and the results are presented in Table 6- 2 along with the necessary parameter values used for each characterization method. The pore sizes determined from the derived model were comparable to that obtained from both diffusion and thermoporometry methods, demonstrating the adequacy in the use of the swelling equation in estimation of SNAP gel pore size.

6.5 Conclusions

An equilibrium swelling model was derived for SNAP hydrogel which accounts for non-Guassian behavior of the gel network and non-ideality of the ionic environment during gel swelling. The Flory-Huggins interaction parameter was determined and incorporated into the swelling equation to consider the hydrophilicity and solubility of the polymer in the swelling medium. We also included ion-pairing and non-ideal Donnan ionic effects, allowing the derived swelling model to be used in extreme dilute solution environment (mobile ion concentration inside the gel is greater than external ion concentration) and various ionic strength of uni-univalent, uni-bivalent, bi-univalent or bi-bivalent electrolyte media. Network alginate polymer was assumed to behave like a Gaussian polymer throughout the study. Such an assumption was considered reasonable, based the similar elastic potential of network alginate polymer when calculated using the Gaussian model (Eq. 17b) and modified Gaussian polymer model (Eq. 17c). Experimental swelling results of SNAP hydrogels of various crosslink densities showed good agreement between model simulation. This swelling model adequately estimated the pore diameters of the SNAP hydrogel with results similar to those characterized by diffusion and thermoporometry techniques. The generalized equilibrium swelling model in Eq. 27 can readily estimate molecular weight between two consecutive crosslinks, or pore sizes from the determined swollen gel volume without the need for sophisticated instrumentation, and can potentially be applied to any point-link network polyelectrolyte gels such as hyaluronic acid gels, chemically crosslinked chitosan, starch and agarose gels. The derived model can also serve as a predictive model in obtaining desired gel

properties (swollen gel volume, pore size) through controlling the crosslinking density via manipulation of reaction kinetics.

6.6 Acknowledgements

The authors thank the Natural Sciences and Engineering Research Council of Canada for financial support.

6.7 References

1. Larrick JW, Thomas DW. Producing proteins in transgenic plants and animals. Current Opinion in Biotechnology 2001 Aug;12(4):411-418.

2. Borges O, Cordeiro-Da-Silva A, Romeijn SG, Amidi M, de Sousa A, Borchard G, et al. Uptake studies in rat Peyer's patches, cytotoxicity and release studies of alginate coated chitosan nanoparticles for mucosal vaccination. J Control Release 2006 Sep 12;114(3):348-358.

3. Babu VR, Patel P, Mundargi RC, Rangaswamy V, Aminabhavi TM. Developments in polymeric devices for oral insulin delivery. Expert Opinion on Drug Delivery 2008 Apr;5(4):403-415.

4. Bernkop-Schnurch A, Kast CE, Richter MF. Improvement in the mucoadhesive properties of alginate by the covalent attachment of cysteine. J Control Release 2001 APR 28;71(3):277-285.

5. Draget KI, SkjakBraek G, Smidsrod O. Alginate based new materials. Int J Biol Macromol 1997 AUG;21(1-2):47-55.

6. Tanaka H, Matsumura M, Veliky IA. Diffusion Characteristics of Substrates in Ca-Alginate Gel Beads. Biotechnol Bioeng 1984;26(1):53-58.

7. Gehrke SH, Uhden LH, McBride JF. Enhanced loading and activity retention of bioactive proteins in hydrogel delivery systems. J Control Release 1998 Oct 30;55(1):21-33.

8. Chan AWJ, Becker T, Neufeld RJ. Subtilisin absorptive encapsulation and granulation. Process Biochem 2005 APR;40(5):1903-1910.

9. Chan AW, Whitney RA, Neufeld RJ. Kinetic controlled synthesis of pH-responsive network alginate. Biomacromolecules 2008 Sep;9(9):2536-2545.

10. Boontheekul T, Kong HJ, Mooney DJ. Controlling alginate gel degradation utilizing partial oxidation and bimodal molecular weight distribution. Biomaterials 2005 May;26(15):2455-2465.

11. Landry MR. Thermoporometry by differential scanning calorimetry: experimental considerations and applications. Thermochimica Acta 2005 Aug 1;433(1-2):27-50.

12. Lindstrom T, Hedman CA, Arnqvist HJ. Use of a novel double-antibody technique to describe the pharmacokinetics of rapid-acting insulin analogs. Diabetes Care 2002 Jun;25(6):1049-1054.

13. DeGroot AR, Neufeld RJ. Encapsulation of urease in alginate beads and protection from alpha-chymotrypsin with chitosan membranes. Enzyme Microb Tech 2001 OCT 4;29(6-7):321-327.

14. Srinivasan C, Katare YK, Muthukumaran T, Panda AK. Effect of additives on encapsulation efficiency, stability and bioactivity of entrapped lysozyme from biodegradable polymer particles. Journal of Microencapsulation 2005 Mar;22(2):127-138.

15. Reis CP, Veiga FJ, Ribeiro AJ, Neufeld RJ, Damge C. Nanoparticulate Biopolymers Deliver Insulin Orally Eliciting Pharmacological Response. J Pharm Sci-Us 2008 Dec;97(12):5290-5305.

16. Iza M, Woerly S, Danumah C, Kaliaguine S, Bousmina M. Determination of pore size distribution for mesoporous materials and polymeric gels by means of DSC measurements: thermoporometry. Polymer 2000 Jul;41(15):5885-5893.

17. Crank J. Diffusion in a sphere. The Mathematics of Diffusion. 2 ed. New York: Oxford University Press, 1998.

18. Li RH, Altreuter DH, Gentile FT. Transport characterization of hydrogel matrices for cell encapsulation. Biotechnol Bioeng 1996 May 20;50(4):365-373.

19. Cho SM, Kim SY, Lee YM, Sung YK, Cho CS. Synthesis, properties, and permeation of solutes through hydrogels based on poly(ethylene glycol)-co-poly(lactones) diacrylate macromers and chitosan. J Appl Polym Sci 1999 Sep 12;73(11):2151-2158.

20. Bakhtiar S, Vevodova J, Hatti-Kaul R, Su XD. Crystallization and preliminary X-ray analysis of an alkaline serine protease from Nesterenkonia sp. Acta Crystallographica Section D-Biological Crystallography 2003 Mar;59:529-531.

21. Brode PF, Erwin CR, Rauch DS, Lucas DS, Rubingh DN. Enzyme Behavior at Surfaces - Site-Specific Variants of Subtilisin Bpn' with Enhanced Surface Stability. J Biol Chem 1994 Sep 23;269(38):23538-23543.

22. Zhang Y, Amsden BG. Application of an obstruction-scaling model to diffusion of vitamin B-12 and proteins in semidilute alginate solutions. Macromolecules 2006 Feb 7;39(3):1073-1078.

23. Klein J, Stock J, Vorlop KD. Pore-Size and Properties of Spherical Ca-Alginate Biocatalysts. European Journal of Applied Microbiology and Biotechnology 1983;18(2):86-91.

24. Lin SY, Chen KS, Run-Chu L. Drying methods affecting the particle sizes, phase transition, deswelling/reswelling processes and morphology of poly(N-isopropylacrylamide) microgel beads. Polymer 1999 Nov;40(23):6307-6312.

25. Vehring R. Pharmaceutical particle engineering via spray drying. Pharmaceut Res 2008 May;25(5):999-1022.

26. Yin YH, Ji XM, Dong H, Ying Y, Zheng H. Study of the swelling dynamics with overshooting effect of hydrogels based on sodium alginate-g-acrylic acid. Carbohyd Polym 2008 Mar 7;71(4):682-689.

27. Chan AW, Whitney RA, Neufeld RJ. Semisynthesis of a Controlled Stimuli-Responsive Alginate Hydrogel. Biomacromolecules 2009 Mar;10(3):609-616.

28. Moe ST, Skjakbraek G, Elgsaeter A, Smidsrod O. Swelling of Covalently Cross-Linked Alginate Gels - Influence of Ionic Solutes and Nonpolar-Solvents. Macromolecules 1993 JUL 5;26(14):3589-3597.

29. Leone G, Torricelli P, Chiumiento A, Facchini A, Barbucci R. Amidic alginate hydrogel for nucleus pulposus replacement. Journal of Biomedical Materials Research Part A 2008 Feb;84A(2):391-401.

30. Xu JB, Bartley JP, Johnson RA. Preparation and characterization of alginate hydrogel membranes crosslinked using a water-soluble carbodiimide. J Appl Polym Sci 2003 OCT 17;90(3):747-753.

31. Flory PJ. Principles of polymer chemistry. New York: Ithaca, 1953.

32. Brannonpeppas L, Peppas NA. Equilibrium Swelling Behavior of Ph-Sensitive Hydrogels. Chem Eng Sci 1991;46(3):715-722.

33. Moe ST, Draget KI, Skjakbraek G, Smidsrod O. Temperature-Dependence of the Elastic-Modulus of Alginate Gels. Carbohyd Polym 1992;19(4):279-284.

34. Flory PJ, John Rehner J. Statistical Mechanics of Cross-Linked Polymer Networks I. Rubberlike Elasticity. The Journal of Chemical Physics 1943;11(11):512-520.

35. Flory PJ, John Rehner J. Statistical Mechanics of Cross-Linked Polymer Networks II. Swelling. The Journal of Chemical Physics 1943;11(11):521-526.

36. Huggins ML. Some Properties of Solutions of Long-chain Compounds. J Phys Chem 1942;46(1):151-158.

37. Flory PJ. Statistical Mechanics of Swelling of Network Structures. J Chem Phys 1950;18(1):108-111.

38. Flory PJ. Network Structure and the Elastic Properties of Vulcanized Rubber. Chem Rev 1944;35(1):51-75.

39. Bray JC, Merrill EW. Polyvinyl-Alcohol) Hydrogels - Formation by Electron-Beam Irradiation of Aqueous-Solutions and Subsequent Crystallization. J Appl Polym Sci 1973;17(12):3779-3794.

40. Erman B, Flory PJ. Rubber Elasticity in Range of Small Uniaxial Tensions and Compressions - Results for Poly(Dimethylsiloxane). J Polym Sci Pol Phys 1978;16(6):1115-1121.

41. Arruda EM, Boyce MC. A 3-Dimensional Constitutive Model for the Large Stretch Behavior of Rubber Elastic-Materials. J Mech Phys Solids 1993 FEB;41(2):389-412.

42. Kovac J. Modified Gaussian Model for Rubber Elasticity. Macromolecules 1978;11(2):362-365.

43. Manning GS. Counterion condensation on charged spheres, cylinders, and planes. J Phys Chem B 2007 Jul 26;111(29):8554-8559.

44. Canal T, Peppas NA. Correlation between Mesh Size and Equilibrium Degree of Swelling of Polymeric Networks. J Biomed Mater Res 1989 OCT;23(10):1183-1193.

45. Smidsrod O. Solution Properties of Alginate. Carbohyd Res 1970;13(3):359-372.

46. Maurstad G, Danielsen S, Stokke BT. Analysis of compacted semiflexible polyanions visualized by atomic force microscopy: Influence of chain stiffness on the morphologies of polyelectrolyte complexes. J Phys Chem B 2003 Aug 14;107(32):8172-8180.

47. Fixman M, Kovac J. POLYMER CONFORMATIONAL STATISTICS .3. MODIFIED GAUSSIAN MODELS OF STIFF CHAINS. J Chem Phys 1973;58(4):1564-1568.

48. Yamanaka J, Yamada S, Ise N, Yamaguchi T. Revisit to the Intrinsic Viscosity-Molecular Weight Relationship of Ionic Polymers .7. Examination of the Pals-Hermans Dilution Method with Reference to the Viscosity Behavior of Dilute Aqueous Dispersion of Ionic Polymer Latex. J Polym Sci Pol Phys 1995 Jul 30;33(10):1523-1526.

49. Amsden B, Turner N. Diffusion characteristics of calcium alginate gels. Biotechnol Bioeng 1999 DEC 5;65(5):605-610.

50. Martin WG, Cook WH, Winkler CA. The Determination of Partial Specific Volumes by Differential Sedimentation. Canadian Journal of Chemistry-Revue Canadienne De Chimie 1956;34(6):809-814.

51. Meechai N, Jamieson AM, Blackwell J. Translational diffusion coefficients of bovine serum albumin in aqueous solution at high ionic strength. Journal of Colloid and Interface Science 1999 Oct 1;218(1):167-175.

52. Kashyap AK, Kalpagam V. Dilute-Solution Properties of Methyl Methacrylate-Acrylonitrile Random Co-Polymers .2. Stockmayer Fixman Relations. Makromolekulare Chemie-Macromolecular Chemistry and Physics 1981;182(4):1147-1152.

53. Moe ST, Elgsaeter A, Skjakbraek G, Smidsrod O. A New Approach for Estimating the Cross-Link Density of Covalently Cross-Linked Ionic Polysaccharide Gels. Carbohyd Polym 1993;20(4):263-268.

54. Katchalsky A, Upadhyay J, Wassermann A, Cooper RE. Counter-Ion Fixation in Alginates. Journal of the Chemical Society 1961(Dec):5198-5204.

55. Watanabe F, Yamagishi A. Electrometric Study on Association of Sodium Ion with Carboxylate Ion in Poly(a-L-Glutamic Acid)-Acridine Orange Complex. Biopolymers 1976;15(11):2291-2293.

56. Wang ZY, White JW, Konno M, Saito S, Nozawa T. A Small-Angle X-Ray-Scattering Study of Alginate Solution and Its Sol-Gel Transition by Addition of Divalent-Cations. Biopolymers 1995 Feb;35(2):227-238.

57. Halle B, Davidovic M. Biomolecular hydration: From water dynamics to hydrodynamics. Proceedings of the National Academy of Sciences of the United States of America 2003 Oct 14;100(21):12135-12140.

Chapter 7

General discussion

Stimuli-responsive or so called “smart” hydrogels undergo abrupt volume transition in response to external stimuli, such as pH or temperature. Alginate is a linear co-polymer of guluronic (G) and mannuronic acid residues (M) and exhibits pH-dependent swelling behavior, and so is under consideration for many biotechnology and biomedical applications such as oral delivery vehicle for protein therapeutics, tissue scaffold in regenerative medicine, and encapsulation matrix for a wide range of biologicals. In this PhD research, alginate was used as a building block in semisynthesis of a new class of networked biopolymer through covalent crosslinking with glutaraldehyde. Since alginate consists of carboxylic acid and hydroxyl reactive sites available for chemical modification, hydroxyl functional sites were proposed for cross-linking reaction to preserve ionizable carboxylic acid for stimuli-responsive swelling nature toward the change of pH and ionic external environment.

The reaction between an alcohol and aldehyde to form an acetal and water is a well characterized reaction used in producing perfumes, flavors, pharmaceuticals, plasticizers, rubbers and resins[1-3]. These reactions are carried out in organic solvent in which water is readily removed to favour acetal production, and involves small molecular weight alcohols such as ethanol, methanol, and uni-functional crosslinkers such as formaldehyde and acetaldehyde. The structure of the resultant acetal products are generally not complicated and can be confirmed by Infrared Spectroscopy (IR) and

Nuclear Magnetic Resonance (NMR). In addition, the reaction kinetics are readily characterized by monitoring the time-concentration profiles of reactant and products. However, this is not normally the case for network hydrogel formed by acetalization reaction such as acetal-linked alginate gel used in this study. Since the polysaccharide is hydrophilic, the acetalization reaction is carried out in water with HCl as catalyst. Therefore, high concentration of water can lead to a less thermodynamically favourable environment for acetal product formation, quickly reaching the chemical equilibrium. In addition, network hydrogel has extremely large molecular weight and does not dissolve in water, and di-aldehydes can undergo side reactions such as degradation and self-polymerization. Therefore, quantification of acetal product and real-time determination of the reactants consumed can be challenging, as is the analysis of molecular structure of the gel network, making the characterization of reaction kinetics more complicated and difficult.

To overcome these challenges while achieving the overall objective of developing a new alginate based biomaterial, this PhD research was approached from two separate directions:

1. Establishment of an analytical technique for quantifying the extent of the crosslinking reaction. A polyelectrolyte gel model was derived to estimate the molecular weight between crosslinks (ie. crosslinking density, acetal concentration) from equilibrium swelling data of the hydrogel.

2. Development of a detailed understanding of reaction mechanism and kinetics between alginate and glutaraldehyde and characterization of resultant networked polymer gels.

The two research focuses were integrated to enable the controlled synthesis of desired gel properties such as pore size, and the potential of the developed alginate gel in oral delivery of protein therapeutics and biomolecules was demonstrated.

7.1 Semisynthesis of alginate network polymer

Native alginate was chemically modified with di-aldehyde, forming an acetal-linked, semi-synthetic network alginate polymer (SNAP) with carboxylate moieties preserved as pH-responsive sensors. Since the formation of SNAP hydrogels is not instantaneous or rapid, as is the case with the formation of ionotropic hydrogel such as calcium-alginate, the time-dependent gelation kinetics allow a more predictable control for designing desirable gel properties. Therefore, research on the mechanism and kinetics of crosslinking reaction is required to control the extent of acetal bond formation (ie. crosslinking density). Other researchers have cross-linked alginate with small molecules, forming covalent-linked network alginate gel, but no one to this point has developed a detailed understanding of the reaction mechanism and kinetics nor characterized the resultant gel structure[4-7]. In particular, glutaraldehyde was used as a secondary crosslinker in these prior studies to improve the mechanical properties of calcium alginate gels. Most studies only characterized the effect of the exposure time to glutaraldehyde in

less than 30 min and the highest concentration of glutaraldehyde used was lower than 25 mM. In addition, no one has developed a predictive reaction model which may be used *a priori* to select reaction conditions providing specific polymer properties.

SNAP gel microspheres were produced by submerging alginic acid gel beads in chemical reaction medium consisting of glutaraldehyde as the crosslinker and hydrochloride acid as catalyst. The reaction mechanism for Bronsted-acid catalyzed acetalization between hydroxyls in hexuronic acid residues, and glutaraldehyde was proposed and the reaction kinetics were characterized through systematic variations in the copolymer composition (M and G) and reaction conditions including reactants and catalyst concentrations, solvent compositions, and temperatures. From measuring the time required to reach critical gel point by initial rate method and concentration of acetal formation through isolation method, glutaraldehyde and alginate were found to undergo second and zero order rate reactions with respect to overall acetalization reaction, respectively. The rate equation for the proposed reaction mechanism can be expressed by equation 1.

$$\frac{\Delta[R_2C(OR')_2]}{t} = k[R-OH]^0[R-CHO]^2 \text{ and } k = 7.6 \text{x} 10^6 e^{-78.58/RT} \qquad \textbf{(Eq. 1)}$$

where k is 19.06 x 10^{-6} L·mol^{-1}·sec^{-1} at 40^{o}C and 0.38 M acid solution and R is the gas constant and T is the reaction temperature. Due to the high activation energy, alginate chemical gel will not form in the absence of acid catalyst and from the kinetic study, the rate of acetalization was shown to increase with increasing HCl concentration. According

to the developed rate equation (Eq. 1), SNAP hydrogels of desired acetal concentration can be kinetically controlled through controlling the reaction time, producing network architecture with specific swelling and pore properties.

Alternatively, the acetalization reaction can be thermodynamically controlled in synthesizing SNAP hydrogel with fine-tuned physical properties. In oxygen-rich environment and at pH values over 3 and temperatures greater than -6^{o}C, the monomeric form of glutaraldehyde undergoes parallel oxidative degradation forming non-reactive glutaric acid and autopolymerizes via aldol condensation reaction, forming polyglutaraldehyde [8, 9]. The competitive side reactions can often make kinetic controlled synthesis difficult at lower glutaraldehyde concentration, deviating the actual crosslinking density away from the expected. In Chapter 4, the first available rate information for thermodynamic/equilibrium control of the reaction is provided, whereby the acetalization reaction was allowed to approach equilibrium, achieving the highest crosslinking density under the specific reaction condition. The correlation between initial glutaraldehyde concentration and equilibrium swelling can be described by the second order exponential decay function. A similar correlation was also observed for acid catalyst concentration and equilibrium swelling. The reaction can also be controlled by the use of co-solvent of specific di-electric constant. Through careful selection of initial reaction conditions, SNAP hydrogel can be produced with tighter material control via equilibrium controlled synthesis.

The acetalization reaction of alginate and glutaraldehyde is highly endothermic and the activation energy determined from Arrhenius kinetics is 78.58 kJ/mol,

comparable to that of the reaction of polyvinyl alcohol with formaldehyde which is 72.75 kJ/mol[10] and to the reaction of acetaldehyde and methanol which is 72.35 kJ/mol [2], indicating similar reaction mechanisms in the formation of acetal bonds and suggesting the adequacy of the developed rate equation. From the kinetic data, an acid catalyzed acetalization reaction may not take place at low temperature due to high activation energy as was the case at 4^{o}C. At room temperature (20-25^{o}C), more than 30 h of reaction time were required to form sufficient crosslinks for a stable SNAP hydrogel, capable of reaching equilibrium swelling state without disintegration. Therefore, without post-fabrication treatment such as drying which may induce hydrogen bonding and crystal formation, or suspension in calcium ion containing solution to introduce additional ionic crosslinks, alginate gel formed in reaction medium consisting of low glutaraldehyde concentration at room temperature for a few hours may not promote sufficient acetal formation, resulting in low crosslink density and disintegration upon swelling in aqueous medium. This was experienced if alginate beads were produced following the procedure described in Kulkarni et. al [5] in which alginate solution was extruded drop-wise into reaction medium containing low glutaraldehyde concentration and the reaction was carried out at room temperature for less than 30 min.

An experiment was carried out to produce chemically modified alginate beads by direct extrusion into medium containing crosslinker. These hydrogel beads were found to dissolve in 0.1 M NaCl solution within 1 h, suggesting insufficient crosslinks. In addition, it was observed that the alginate gel beads formed by direct extrusion were not spherical and appeared to have a long tail as illustrated in Figure 7-1a. The tail is formed when the

alginate droplet hits the solution resulting in droplet deformation. In contrast, alginate chemical gel prepared by immersion of the preformed gel beads in the reaction medium were more spherical since the shape of the granules was pre-determined by the preformed gel beads (Figure 7-1b). Hence, chemically modified alginate beads were produced by submerging the preformed acid gel beads in the glutaraldehyde solution throughout this PhD research.

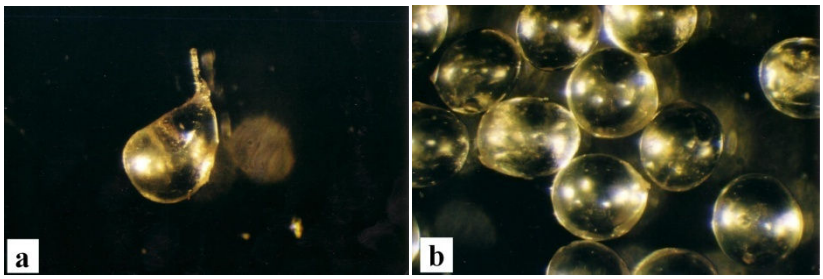

Figure 7-1. Chemically modified alginate beads produced by (a) droplet extrusion of alginate solution or (b) immersion of preformed acid gel in a reaction medium containing glutaraldehyde and acid catalyst.

The effect of using different preformed gel beads was also studied. SNAP gel beads were prepared using calcium alginate or alginic acid gel beads. The rate of crosslinking reaction was observed to be faster for alginic acid gel beads than calcium alginate reacting under the same chemical reaction conditions (data not provided). This may be explained by greater proton concentration inside alginic acid gel, accelerating the activation of carbonyl groups in glutaraldehyde for subsequent nucleophilic addition to hydroxyls in alginate polymers. Hence, alginic acid gel was used instead of calcium alginate gel in preparing SNAP hydrogels throughout the study.

In Chapter 3, it was shown that the rate of acetalization was not influenced by the chemical positions of alginate polymers (G and M sequential arrangement and concentrations) but only by alginate molecular weight. Similar reactivity between the two uronic acid isomers may allow some alginate types which do not form stable ionotropic gels to be used in the formation of chemically networked hydrogel, extending the spectrum of the gelling properties of alginates. In addition, the independence on the chemical composition can minimize variation between gel properties due to alginate sample source (ie. location, season) and preparation methods (ie. extraction) and enable control of gel properties by using alginate of specific molecular weight and reaction kinetics.

7.2 Characterization of semi-synthetic network alginate polymer

7.2.1 Structural analysis

Alginate is a polyhexuronic acid glycoside which consists of one acetal bond as result of (1→4)-O-glycosidic linkage between two sugar monomers. The inherent acetal bond appeared to have similar IR spectral signal as the acetal bond formed between glutaraldehyde and hydroxyls (unpublished data), making the identification between SNAP and native alginic acid gels difficult. Although there have been attempts by other researchers to use IR spectroscopy and X-ray diffractometery to show the structural change of the modified polymer as compared to the native polymer (demonstrating the effect of crosslinker concentration on the modified polymers), no one to this point has

proposed a possible network structure resulting from reacting glutaraldehyde and alginate, nor provided detailed structural information on alginate chemical hydrogel.

The first description of structural conformation of the semi-synthetic alginate modified with di-aldehyde and the possible reaction sites involved in the acetalization reaction were analyzed through the use of cross-polarization magic-angle spinning (CP/MAS) ^{13}C solid state NMR and are presented in Chapter 4. The NMR spectrum confirmed the predicted structure of SNAP hydrogel as described in Chapter 3, Figure 1, in which two hydroxyls in each uronic acid were reacted with one aldehyde, and two uronic acids from the adjacent polymers consumed one glutaraldehyde (di-aldehyde), generating a point-link network hydrogel with 4 sub-chain polymers of various lengths bound together in one tetrafunctional crosslink. Although solid state NMR spectrum can be used in reconstruction of the potential polymer structure, it is not quantitative for estimation of acetal concentration. In this study, acetal concentration was studied by equilibrium gel swelling using the model derived in Chapter 6, and will be discussed in a later section.

7.2.2 SNAP hydrogel as mechanically stable, pH-responsive superabsorbent polymer

The fundamental difference between molecular structures of calcium-alginate and SNAP hydrogels is that the long junction zones in calcium-alginate are substituted by discrete, covalent crosslinks between chains as illustrated in Figure 7-2. This leads to a gel with considerably more flexible elastic chains and with dramatically different

swelling behaviour. Skjak-Braek et al. patented a technology to synthesize alginate based superswelling hydrogel by crosslinking with epichlorohydrin, which can absorb water up to about 300 times its dry state volume [11, 12]. Loosely crosslinked SNAP hydrogel also demonstrated a pronounced water absorption capacity, swelling to 1000 times the dry polymer volume, equivalent to 0.1% of alginate polymer mass in the swollen gel. In addition, SNAP hydrogels are formed by interconnecting individual soluble alginate polymers through permanent acetal linkages, and thus are not stabilized/destabilized by the presence/removal of gelling ions, nor is the hydrogel affected by high concentrations of monovalent cations or chelating ions such as phosphate, citrate and EDTA, which can destabilize alginate physical gels. Hence, SNAP with superabsorbent/superswelling property may be used in environmental clean up applications and in personal hygiene products.

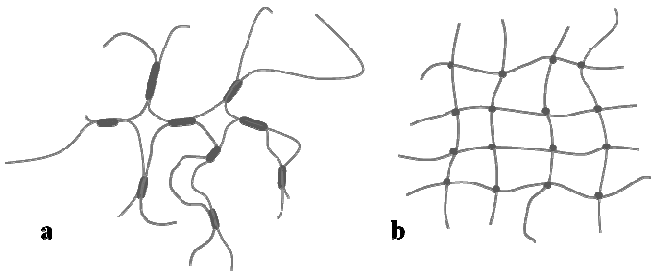

Figure 7-2. Two-dimensional representation of the molecular structure of (a) ionic crosslinked calcium-alginate and (b) covalently crosslinked SNAP hydrogels.

Owing to the nature of ionizable carboxylate moieties, SNAP hydrogel exhibits pH-responsive volume transition. SNAP hydrogel is of particular interest in the development of transmucosal pharmaceutical formulations for the delivery of therapeutic proteins. In acid environment, alginate gel contracts due to limited solubility of non-

ionized acid moieties and protects protein from enzymatic and acid degradation in the gastric environment of the stomach (~ pH 1.2) while swelling in alkaline media as a result of increased hydrophilicity of ionized carboxylate moieties, releasing active therapeutics in the intestinal lumen (~ pH 7.8). So called "smart" hydrogel can be specifically tailored by manipulating reaction kinetics, to produce desired pH-responsive swelling behavior for applications such as artificial muscle in regenerative medicine or as targeted pulsatile delivery vehicle.

7.2.3 Diffusion characteristics and pore properties of SNAP hydrogel

With pre-selected reaction conditions, the crosslinking density (ie. acetal concentration) of SNAP hydrogel can be manipulated, producing hydrogel with specific gel properties such that gel swelling can be fine-tuned in the range of 80-1000 times its dry polymer volume with the gel pore size ranging between 30 nm to 1 μm. Subsequently, the solute diffusion and release properties can be tailored as presented in Chapter 5.

Diffusion data for biomolecules ranging between 1.3 to 546 kDa and Stoke diameters ranging from 1.7 to 14 nm, were provided in Chapter 5. Biomolecules tested included vitamin B_{12}, lysozyme, subtilisin, insulin, bovine serum albumin (BSA), and urease, diffusing into and out from SNAP hydrogels with pre-designed gel swelling volumes and pore sizes. Based on the diffusion coefficients calculated from protein uptake experiments, the SNAP hydrogel with pre-designed pore size of 80 nm (confirmed

by differential scanning calorimetry, DSC) can allow urease to diffuse freely into the hydrogel. This is by far the biggest solute ever reported to diffusion into alginate based biomaterial. It is expected that solute biomolecules larger than urease can diffuse into SNAP hydrogels of greater pore sizes, making SNAP hydrogel a superporous biomaterial suitable for tissue engineering application such as bioscaffold for cell attachment/anchorage.

In contrast, native alginate as in the form of calcium-alginate is porous in nature with pore size at around 17 nm in diameter determined by DSC (Chapter 5) and approximately 14 nm from protein diffusion study. The ratio of diffusion coefficients in gel to water can be utilized in the estimation of the mesh pore size using the obstruction-scaling model (Eq. 7, Chapter 5) [13]. The radius of the hydrated alginate polymer, r_f, used in this study is 0.83 nm which is estimated from chain radius of 0.55 nm characterized by small-angle X-ray scattering (SAXS)[14], plus a water layer of 0.28 nm (van der Waals radius of water is 0.14 nm)[15]. This value was used for estimation of the pore size for both network alginate gel and calcium alginate gel. For calcium-alginate gel, the network pore structure is constructed with both linear portion of alginate chain and the zip-zag double chains. Therefore, the cross-sectional radius should be expected to be greater than 0.83 nm and less than 1.66 nm. Pore sizes estimated using the minimum and maximum values of r_f are shown in Table 7-1.

Table 7-1: Pore sizes estimated the Obstruction-Scaling model for two different values of polymer radius.

Solutes	ξ (nm) $r_f = 0.83$	ξ (nm) $r_f = 1.66$
BSA	4	4
Insulin hexamer	6	6
Subtilisin	11	12
Lysozyme	13	15
Insulin	11	14
B12	15	20

As can be seen from the table, doubling the value of r_f has a small, or no affect on the estimate of pore size. The deviation of pore size estimated using different molecular sizes of solutes is greater than the difference estimated using twice the r_f value for the same solute. Although 0.83 nm may not be the best measure for calcium alginate, the pore sizes estimated using this value in equation 7 (Chapter 5) were intended to provide a reference point (physical gel versus chemical gel) for comparison purpose with SNAP hydrogels.

Calcium alginate is porous in which the pore size is too large for encapsulation of small molecular size proteins or molecules, yet too small for large molecular weight solutes such as BSA and urease to diffuse into or out from the gel. Based on the literature [16-19] and determined values in the present study, the range of pore sizes of calcium alginate that can be manipulated was fairly narrow, generally between 10-20 nm, depending on the gel preparation conditions. Therefore, uses for the natural polymer are limited because natural materials have limited flexibility to modify properties, which is

more directly possible with semi-synthetic polymers derived from the same natural materials.

7.3 Drying as post-fabrication treatment to tailor gel structure

The gel swelling, pore size and mechanical properties can be further altered by drying after gel formation. Drying can serve as post-fabrication treatment which may induce polymer rearrangement, resulting in the formation of a more structured crystalline region promoting hydrogen bonding between polymer chains [20, 21]. With these physical enforcements (ie. crystalline structure, hydrogen bonding), the pore size of the granules may be reduced, retarding water penetration and magnitude of water uptake during swelling. In Chapter 5, the effect of drying was studied as post-fabrication treatment. Complete dehydration of SNAP gel beads, forming dry granules can reduce swelling by approximately 40-70% depending on the crosslinking density as compared to gel swelling without drying. Although drying can lower the reswelling ability of SNAP hydrogels, the pH-dependent contraction/swelling behavior was not affected. This pH-responsiveness was observed in atomic force micrographs shown in Figure 7-3 as the pores contract or swell corresponding to the external pH environment. In acid medium, the dry SNAP film remained in a compact state with almost no visible pore, whereas pores of 100-200 nm were evenly distributed throughout the hydrated film in alkaline solution. In addition, covalently crosslinked alginate gel is a permanent hydrogel which does not undergo reversible sol-gel transition like calcium alginate when physical crosslinks are removed. Therefore no mass loss was experienced for chemically modified

alginate gel during drying or rehydration or during repeated drying-rehydration cycles. However, this is not the case for calcium alginate, as drying destabilized the polymer due to significant loss of physical crosslinks (ie. Ca^{++}), resulting in polymer loss during rehydration in a calcium rich swelling medium.

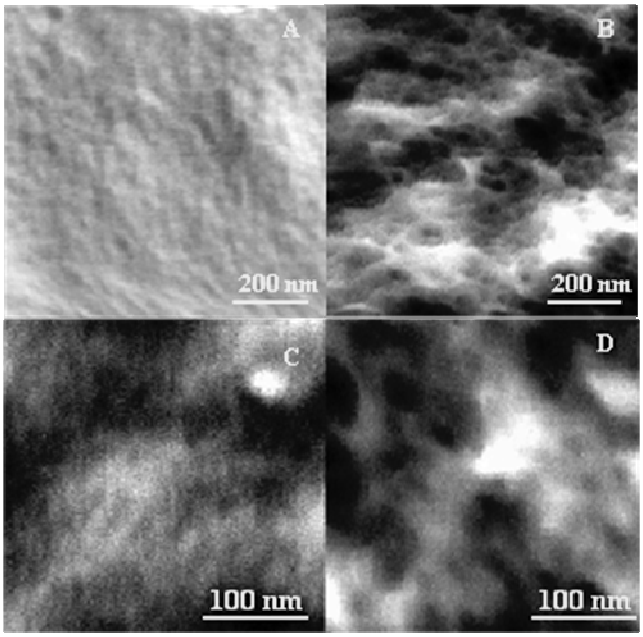

Figure 7-3. Tapping-mode AFM topographs of alginate films in pH 1.2 (A) and in pH 7.8 (B). (C) and (D) are images of higher magnification of a section of image A and B, respectively.

7.4 Absorptive protein encapsulation within SNAP granules for oral delivery application

Protein encapsulation within SNAP hydrogel/granules can be achieved by absorptive encapsulation which decouples bead or granule production from the subsequent encapsulation process, offering cost effective large scale bead production and

providing customized bead properties. In Chapter 5, the absorptive encapsulation technique was used to encapsulate a wide range of molecular sizes of proteins/biomolecules ranging between 1.3 - 546 kDa within pre-designed SNAP hydrogel of desired pore sizes. Due to mild loading conditions, high encapsulation efficiency was achieved with near full protein and enzyme bioactivities. Drying was applied as post-fabrication treatment to reduce network pore size. However, approximately 30% of the mass loss was experienced during drying, possibly caused by aggressive, rapid removal of water in which protein biomolecules were dissolved.

The potential of chemically modified alginate as oral drug delivery vehicle for protein therapeutics was demonstrated. The granules showed release-hold ability after transient period (~30 min), with near zero protein loss in acid environment, while triggered-release was subsequently observed with near first-order release kinetics in alkaline solution. Encapsulated enzymes were well protected by the polymer matrix after 2 h in acid with 83% of the released enzymes in the simulated intestinal/colonic alkaline condition remaining active. Insulin was used as a model therapeutic protein with 80% of the encapsulated insulin remaining bioactive after the loading and drying process. In simulated gastrointestinal pH, approximately 60% of the released insulin was bioactive. Since SNAP hydrogel used for insulin encapsulation had large pore sizes (~80 nm), designed to accommodate the diffusion of a wide range of molecular sizes of biomolecules, it is believed that higher encapsulation yield as well as bioactivity retention can be obtained if smaller pore size hydrogel of higher crosslink density were used instead. In addition, to improve bioavailability of insulin uptake by membranous

epithelial cells (M-cell) of the Peyer's patches in the gut-associated lymphoid tissue and enterocytes, smaller SNAP gel beads in the submicron to nanometer ranges can be attempted[22].

7.5 Development of equilibrium swelling model for *a priori* selection of gel properties

Networked polymer structure (ie. hydrogel) performs the multiple roles of solute, osmotic membrane, and pressure-generating device. In general, the crosslinking density (ie. the acetal linkage concentration) in network polymer gel is the only controllable parameter for most of the applications. Such information is critical for biomaterial design, especially in controlling the solute transport properties of the hydrogel. Therefore, many swelling models for polyelectrolyte have been derived to correlate crosslinking density with gel swelling, pore size and mechanical properties. These models are generally based on Flory's rubber elasticity and Donnan membrane equilibria theories and can be used to estimate molecular weight between two consecutive crosslinks or crosslinking density from the determined swollen gel volume. However these models may not be suitable for polyelectrolyte gels in which the polymer may be fully extended in dilute solution and Gaussian coil assumption is invalid, and when ideal solution environment is assumed as is the case with Flory's swelling model for polyelectrolyte gel. Another commonly used model from Brannonpeppas and Peppas [23] was modified from Flory's swelling model with the incorporation of the Henderson-Hasselbalch equation. The equation is simple to

use for prediction of gel swelling in uni-univalent solution environment with ionic strength comparable to that of fixed ions in the network polymer. In addition, most swelling equations in the literature were derived without consideration of ion-pairing effect (also known as Manning condensation phenomena). According to Manning[24], a fraction of dissociated counterions (ie. Na^+) remains in proximity to the polymer charged pendant groups (ie. carboxylate), reducing the concentration of osmotically active ions and thus lowering the gel swelling.

In Chapter 6, a generalized swelling model for polyelectrolyte gel was derived which can readily estimate molecular weight between two consecutive crosslinks, crosslinking density, or pore sizes from the determined swollen gel volume in both salt-free and high ionic concentration environment. The derived equilibrium swelling model which accounts for the effects of non-ideal Gaussian network stress, non-ideal Donnan equilibrium, ion-paring effect and solvent-polymer volume exclusion, accurately simulated SNAP gel swelling in dilute and ionic solutions containing uni-univalent, uni-bivalent, bi-univalent or bi-bi-valent simple electrolyte solutions. In addition, rheological properties including Flory-Huggins interaction parameters which measure the polymer configuration in the suspended solvent and characteristic ratio were determined experimentally as a function of ionic strength and incorporated into the swelling model. Therefore, the swelling model can closely describe gel swelling in aqueous media consisting of different ionic compositions, pH and ionic strength.

For simplicity of the equation, only the classical Henderson-Hasselbalch (H-H) equation was used in the present study with the assumption of constant pKa. However,

Haug [25] found that the pKa value of the alginate polymer differs slightly from those of the monomeric residues. In addition, for the effect of ionic strength, the pKa value for *L. digitata* alginate (F_G=0.42) drops from 3.92 in no salt solution to 3.42 when 0.1 N of salt is added. For *L. hyperborean* alginate (F_G=0.69), the pKa decreased from 4.41 to 3.74, so there is some effect of ionic strength on the pKa. Therefore, it is recommended for the future study that a modified H-H equation be used to account for the ionic effect, where the swelling equation can more precisely describe the swelling of a wider range of polyelectrolyte gels.

7.5.1 Pore size estimation from equilibrium swelling

Equation 28 (Chapter 6) which was originally derived by Flory[26] for calculation of the mean square end-to-end distance of a Gaussian polymer, has been extended by Canal and Peppas[27] to approximate the network mesh pore size (correlation length). A schematic diagram is presented below for a crosslinked structure of a hydrogel (Figure 7-4). Although this equation was derived based on Gaussian coil assumption, it has also been used by many researchers to estimate mesh pore size of pH-responsive hydrogels [28-33] due to the simplicity of the equation and readily obtained characteristic parameters in the equation.

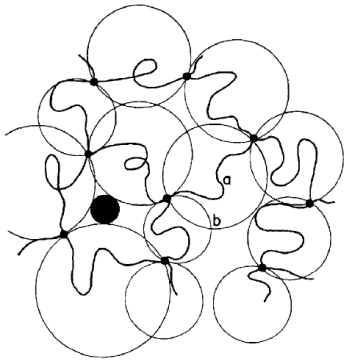

Figure 7-4: Crosslinked structure of a hydrogel, indicating the effective chains (a), confined within the circle (linear distance as mesh pore diameter), and a diffusing species represented by the solid circle [27].

In a good solvent, ξ can be calculated using equation 28a [27]:

$$\xi = \alpha(\overline{r_0^2})^{1/2} \qquad \text{--(Eq. 28 a)}$$

where α is the elongation ratio of the polymer chains in any direction and $(\overline{r_0^2})^{1/2}$ is the unperturbed, end-to-end distance of the polymer chains between two neighboring crosslinks. For isotropical swelling, the elongation ratio of the hydrogel can be expressed as:

$$\alpha_x\alpha_y\alpha_z = \alpha_s^3 = V_s / V_r = v_{2,s}^{-1}$$
$$\alpha = v_{2,s}^{-1/3} \qquad \text{--(Eq. 28b)}$$

where subscript x, y, z indicate the swelling direction, V_r and V_s represent the volume of polymer network at relaxed state formed right after the crosslinking reaction and at equilibrium swollen state respectively, and $v_{2,s}$ is the equilibrium swelling ratio (the corresponding inverse expression is the polymer volume fraction). Flory derived an

expression to estimate the unperturbed, mean-square end-to-end distance of the polymer chain[34]:

$$(\overline{r_0^2}) \cong C_n n l^2 (1-\cos\theta)/(1+\cos\theta) \qquad \text{--(Eq. 28c)}$$

where n is the number of repeating unit bonds between the crosslinks, $n=M_c/M_r$, and l is the bond length of the monomer unit (ie. uronic acid residue has bond length of 0.515 nm). For freely jointed, unrestricted chain, cos θ =0, $(\overline{r_0^2})^{1/2} \cong C_n n l^2$. For a tetrahedral bonded chain, the bond angle, $\theta=109.5^o$ (for glycosidic ether bond, $\theta=110^o$), and cos θ=-1/3, thus equation 28c can be written as:

$$(\overline{r_0^2}) \cong 2C_n n l^2 \qquad \text{--(Eq. 28d)}$$

Substituting equations 28b and 28d into 28a, the pore size can be estimated by the resulting equation 28.

$$\xi = \alpha(\overline{r_0^2})^{1/2} = v_{2,s}^{-1/3}\left[C_n\left(\frac{2\overline{M_c}}{M_r}\right)\right]^{1/2} l \qquad \text{--(Eq. 28).}$$

To estimate the distance between two consecutive crosslink points, ξ, from equation 28, molecular weight between crosslinks, M_c must be first determined. A better M_c approximation is essential to accurately calculate the pore size. In Chapter 6, I derived an equilibrium swelling model in which the M_c value can be obtained from the measured equilibrium swelling gel volume (Eq. 27, Chapter 6). In dilute solution or salt-free environment, the charges attached to the polyelectrolyte chain may be sufficient to cause the polymer to extend almost to full length, resulting in fully extended conformation[35], hence has greater end-to-end distance than neutral Gaussian polymer. Therefore, a

modified-Gaussian model was incorporated for polyelectrolyte swelling to closely capture the gel swelling at dilute solution environment, allowing for more precise estimation of molecular weight between crosslinks, M_c.

Although equation 28 was derived based on Gaussian coil assumption (Eq. 28a), according to Flory [26], the Gaussian approximation is acceptable for the treatment of rubber elasticity, swelling and the configuration of polymer molecules in solution, except for polyelectrolyte in media of very low ionic strength. Therefore, only under conditions leading to extension of the polymer chains far beyond their average configuration is necessary to resort to the more accurate formulas. Various approaches to approximate the mean square end-to-end distance of the stiff, polyelectrolyte in the dilute solution and salt-free environment can be found in the work of Dobrynin et al [36].

In general, network polyelectrolyte (forming network structural gels) exhibit different solution properties than its linear counterpart. Network polymer gel constrains linear polymers within finite gel volume due to physical or chemical crosslinks, therefore, mobility of the polymer chains is restricted and even at high dilution, polymer may never reach its fully extended configuration as in its linear, unrestrained analogue (assuming no dissolution or disintegration occurs during swelling and an equilibrium swelling gel volume, thus thermodynamic stable configuration is reached). Segeren et al[37] showed that the stress-strain curve of calcium alginate (polymer fraction of 9.4 kg/m^3, equivalent to 11 crosslinks per molecule) measured at a constant, low rate of shear, support Gaussian coil assumption. Kong et al[38] also demonstrated that ionically crosslinked calcium alginate gel of various swelling degree follow the Gaussian elastic network model. In

addition, since the elastic potential determined in the present study using both the modified-Gaussian model (Eq. 17c) and the classical Gaussian approximation (Eq. 17b) were almost identical, it may be concluded that the network alginate polymer behaves similarly to a Gaussian polymer. It is reasonable then to use equation 28 in estimating the network pore size.

7.5.2 Adequacy of the derived equilibrium swelling model

The derived model accuracy was demonstrated through comparison of the swelling data obtained at different experimental condition with the simulated values. In addition, I compared gel swelling prediction using the model derived in the present study, to the swelling model derived by Brannonpeppas and Peppas [23] for polymethacrylate gel in low ionic strength environment. Using the Brannonpeppas and Peppas model, the gel was predicted to swell to be about 4,500,000 times its dry polymer volume which is too high to be a reasonable result, suggesting that the model cannot accurately describe swelling of polyanionic gels in dilute solution. As a comparison, gel swelling predicted using the swelling model derived in the present study, with the parameters described by Brannonpeppas and Peppas [23], was only about 1200 times its dry polymer volume (simulation with the assumption of zero condensed ion fraction), significantly advancing the swelling simulation in dilute solution environment. In addition, the pore size data determined from the swelling model was used to compare to other experimental techniques. The comparison was not intended to provide a direct validation to the derived

swelling model. The pore size estimated from the polymer configuration model (Eq. 28) with the M_c determined from the developed swelling model and experimental swelling data (Eq. 27) were comparable to those determined by thermoporometry and protein diffusion.

The generalized equilibrium swelling model presented in Chapter 6 can readily estimate molecular weight between two consecutive crosslinks, or pore sizes from the determined swollen gel volume without the need for sophisticated instrumentation. The derived model can potentially be applied to any point-link network polyelectrolyte gels such as hyaluronic acid gels, chemically crosslinked chitosan, starch and agarose gels. The derived model can also serve as predictive model in obtaining desired gel properties (swollen gel volume, pore size) through controlling the crosslinking density via manipulation of reaction kinetics.

SNAP is a "semisynthetic" polymer derived from a natural polysaccharide, using formulation conditions and a crosslinking reagent which is extensively employed in fabricating tissue valves from bovine pericardium[39]. In the past decades, these valves have been implanted into patients with very high degree of clinical success. In addition, human serum albumin microspheres prepared using glutaraldehyde crosslinking have been approved by US Food and Drug Administration for clinical use[40]. Although glutaraldehyde is regarded as cytotoxic, unreacted reagent can be readily removed through washing and the residual content can be quenched with amino acids or ethanol. In addition, the acetal bonds are stable and the high activation energy of acetalization does not favour reverse reaction in forming initial glutaraldehyde once the bond is formed.

Nevertheless future research on biocompatibility is required to enhance the utility of SNAP hydrogel in many biologically related applications.

7.6 References

1. Gillies, E. R.; Goodwin, A. P.; Frechet, J. M. J., Acetals as pH-sensitive linkages for drug delivery. *Bioconjugate Chemistry* **2004,** 15, (6), 1254-1263.

2. Gandi, G. K.; Silva, V. M. T. M.; Rodrigues, A. E., Process development for dimethylacetal synthesis: Thermodynamics and reaction kinetics. *Industrial & Engineering Chemistry Research* **2005,** 44, (19), 7287-7297.

3. Aumo, J.; Lilja, J.; Maki-Arvela, P.; Salmi, T.; Sundell, M.; Vainio, H.; Murzin, D. Y., Hydrogenation of citral over a polymer fibre catalyst. *Catalysis Letters* **2002,** 84, (3-4), 219-224.

4. Kulkarni, A. R.; Soppimath, K. S.; Aminabhavi, T. M.; Dave, A. M., Polymeric sodium alginate interpenetrating network beads for the controlled release of chlorpyrifos. *Journal of Applied Polymer Science* **2002,** 85, (5), 911-918.

5. Kulkarni, A. R.; Soppimath, K. S.; Aminabhavi, T. M.; Dave, A. M.; Mehta, M. H., Glutaraldehyde crosslinked sodium alginate beads containing liquid pesticide for soil application. *Journal of Controlled Release* **2000,** 63, (1-2), 97-105.

6. Park, J. K.; Jin, Y. B.; Chang, H. N., Reusable biosorbents in capsules from Zoogloea ramigera cells for cadmium removal. *Biotechnology and Bioengineering* **1999,** 63, (1), 116-121.

7. Yeom, C. K.; Lee, K. H., Characterization of sodium alginate membrane crosslinked with glutaraldehyde in pervaporation separation. *Journal of Applied Polymer Science* **1998,** 67, (2), 209-219.

8. McMurry, J., *Organic chemistry*. 4 ed.; Brooks/Cole Publishing Company: Pacific Grove, 1996.

9. Jayakrishnan, A.; Jameela, S. R., Glutaraldehyde as a fixative in bioprostheses and drug delivery matrices. *Biomaterials* **1996,** 17, (5), 471-484.

10. Kormanovskaya, G. N.; Vlodavets, I. N., Kinetics of acetalization of poly(vinyl alcohol) with aliphatic aldehydes in aqueous solutions. *Russian Chemical Bulletin* **1965,** 14, (4), 718-720.

11. Moe, S. T.; Skjakbraek, G.; Elgsaeter, A.; Smidsrod, O., Swelling of Covalently Cross-Linked Alginate Gels - Influence of Ionic Solutes and Nonpolar-Solvents. *Macromolecules* **1993,** 26, (14), 3589-3597.

12. Skjak-Braek, G.; Moe, S. T. Alginate gels. 5144016, 1992.

13. Mofidi, N.; Aghai-Moghadam, M.; Sarbolouki, M. N., Mass preparation and characterization of alginate microspheres. *Process Biochemistry* **2000,** 35, (9), 885-888.

14. Li, R. H.; Altreuter, D. H.; Gentile, F. T., Transport characterization of hydrogel matrices for cell encapsulation. *Biotechnology and Bioengineering* **1996,** 50, (4), 365-373.

15. Klein, J.; Stock, J.; Vorlop, K. D., Pore-Size and Properties of Spherical Ca-Alginate Biocatalysts. *European Journal of Applied Microbiology and Biotechnology* **1983,** 18, (2), 86-91.

16. Stewart, W. W.; Swaisgood, H. E., Characterization of Calcium Alginate Pore Diameter by Size-Exclusion Chromatography Using Protein Standards. *Enzyme and Microbial Technology* **1993,** 15, (11), 922-927.

17. Lin, S. Y.; Chen, K. S.; Run-Chu, L., Drying methods affecting the particle sizes, phase transition, deswelling/reswelling processes and morphology of poly(N-isopropylacrylamide) microgel beads. *Polymer* **1999,** 40, (23), 6307-6312.

18. Vehring, R., Pharmaceutical particle engineering via spray drying. *Pharmaceutical Research* **2008,** 25, (5), 999-1022.

19. Pan, Y.; Zheng, J. M.; Zhao, H. Y.; Li, Y. J.; Xu, H.; Wei, G., Relationship between drug effects and particle size of insulin-loaded bioadhesive microspheres. *Acta Pharmacologica Sinica* **2002,** 23, (11), 1051-1056.

20. Brannonpeppas, L.; Peppas, N. A., Equilibrium Swelling Behavior of Ph-Sensitive Hydrogels. *Chemical Engineering Science* **1991,** 46, (3), 715-722.

21. Manning, G. S., Limiting Laws and Counterion Condensation in Polyelectrolyte Solutions .I. Colligative Properties. *Journal of Chemical Physics* **1969,** 51, (3), 924-933.

22. Benhameid, O.; Jamieson, W. R. E.; Castella, M.; Carrier, M.; Pomar, J. L.; Germann, E.; Pellerin, M.; Brownlee, R. T., CarboMedics mitroflow pericardial aortic Bioprosthesis performance in patients aged 60 years and older after 15 years. *Thoracic and Cardiovascular Surgeon* **2008,** 56, (4), 195-199.

23. Gupta, P. K.; Hung, C. T., Albumin Microspheres .2. Applications in Drug Delivery. *Journal of Microencapsulation* **1989,** 6, (4), 463-472.

Chapter 8

Conclusions

Alginate which consists of mannuronic and guluronic acid residues in varying sequential arrangements and proportions was chemically modified with di-aldehyde via acid-catalyzed acetalization, forming 3D network polymer gel. The controlled gel properties such as swelling and pore size were enabled through manipulation of reaction kinetics. The reaction mechanism and resultant network structure were confirmed by solid state NMR. The potential application of SNAP hydrogel as oral drug delivery vehicle for encapsulation and controlled release of a wide range of molecular sizes of biologicals was demonstrated. With the developed rate equation for the acetalization reaction and derived equilibrium swelling model for networked polyelectrolyte gel, the reaction conditions can be pre-selected to enable specific polymer properties.

The overall objectives stated in this study have been achieved and the specific conclusions arising out of this research are summarized below.

1. Alginate, a linear natural polysaccharide consisting of two hexuronic acid isomers in various sequential arrangements and proportions, was chemically modified with di-aldehyde, forming a tetrafunctional, pH-responsive, semi-synthetic network alginate polymer (SNAP).

2. The two hexuronic acid isomers, M and G, showed similar reactivity which will allow some alginate types which do not form stable ionotropic gels, to be used in the

formation of chemically networked hydrogel, extending the spectrum of the gelling properties of alginates.

3. The kinetics of acetalization measured through equilibrium swelling of the networked polymer, were found to undergo zero and second-order reaction with respect to di-aldehyde and alginate, respectively. With the determined rate constants of 19.06 $\mu L \cdot mole^{-1} \cdot s^{-1}$ at 40°C and activation energy of 78.58 $kJ \cdot mol^{-1}$, a proposed predictive reaction model (shown below) may be used *a priori* to select reaction conditions and achieve the desired acetal formation (crosslinking density) through time-evolution control, providing network architect with controlled swelling and pore properties.

$$\frac{\Delta[R_2C(OR')_2]}{t} = k[R-CHO]^2 \text{ and } k = 7.6 \text{x} 10^6 e^{-78.58/RT}$$

4. Through systematic variations in the reaction conditions including reactant and catalyst concentrations, and solvent composition, the kinetic information to thermodynamically/equilibrium control synthesis of network architect was obtained, offering alternative reaction control beside kinetically controlled synthesis to fine-tune gel swelling and pore properties by pre-selecting initial reactant and catalyst concentrations and allowing the reaction to approach equilibrium. The relationship between initial glutaraldehyde concentration and equilibrium swelling ratio of the gel beads with maximum achievable crosslink density fellow the second order exponential decay function. A similar exponential decay relationship was also obtained for the initial acid catalyst concentration. In addition, the rate of acetalization

reaction can be controlled by different solvent composition such as the addition of aprotic co-solvent (e.g. acetone) increasing the rate while protic solvents (e.g. methanol) retarded the reaction.

5. SNAP hydrogel can be synthesized via kinetic or thermodynamic control to obtain equilibrium gel swelling between 80-1000 times the volume of the compact dry polymer network, corresponding to about 1 - 0.1% of polymer fraction in the swollen gel and 30 nm -1 μm of pore diameters. At lowest crosslinking density, the molecular weight between consecutive crosslink points M_c, was calculated to be 71,319 g/mol, which represents 4 to 5 crosslinks in the primary polymer chain whereas at the maximum achievable crosslinking density, M_c, was down to 1050 g/mole, approximately 5 monomeric units between crosslink points. The time required to achieve critical gel point (ie. the minimum crosslinking density necessary to reach a stable, equilibrium swollen gel) ranged from 30 min to over 10 h depending on the concentrations of the aldehyde, catalyst, and temperature.

6. Acetalization reaction mechanism and SNAP gel structure were studied through the use of cross-polarization magic-angle spinning (CP/MAS) ^{13}C solid state NMR. From comparing the spectrum of modified alginate network polymer with native alginic acid polymer, the reaction site on the uronic acid was confirmed. The hydroxyls attached to carbon 2 and 3 from each uronic acid residue were involved in the formation of one acetal bond, two acetal bonds were formed per each glutaraldehyde molecule, linking two uronic acid units from the adjacent alginate polymers (a total of 4 hydroxyls from two uronic acids to form 2 acetals). As a result, the crosslink point

was tetrafunctional, linking four subchain polymers ($f = 4$). This information was used in the development of the swelling model for SNAP hydrogel.

7. SNAP hydrogel demonstrated pronounced swelling at alkaline pH and contraction in acidic environment with oscillatory response to repeated pH-stimuli. Since the modified alginate gel was connected by covalent acetal linkages, it demonstrated enormous water absorbing/superswelling ability while maintaining polymer structural stability in dilute and ionic solution containing monovalent cations or chelating ions, which can destabilize alginate physical gels. The magnitude of gel swelling depended on external solution pH and ionic strength, and the acetal concentration throughout the network hydrogel (ie. crosslinking density, molecular weight between crosslinks) which can be predicted from the derived equilibrium swelling model and specifically tailored through reaction kinetics for desired gel properties.

8. The potential use of SNAP hydrogels as oral drug delivery vehicle for a wide range of molecular sizes of therapeutic proteins such as insulin was demonstrated. The pore sizes of two SNAP hydrogels were fine-tuned to 40 and 80 nm, and the diffusion coefficients of vitamin B_{12}, lysozyme, subtilisin, bovine serum albumin (BSA), urease and insulin were measured. These biomolecules encountered little or no diffusion restriction into larger pore SNAP hydrogel whereas BSA and urease experienced substantial decrease in rate of diffusion into smaller pore hydrogel. This was the first study to report the diffusion of large biomolecules like urease into alginate based hydrogel.

9. Protein biomolecules were encapsulated via absorptive encapsulation whereby pre-formed SNAP gel beads were immersed in protein concentrates, achieving high encapsulation yields and payloads, followed by drying. Drying hydrogels, forming granules, reduced subsequent gel reswelling ability by 40-70%, an effective post-encapsulation mechanism to tailor solute diffusion/release.

10. SNAP granules showed pH-responsive swelling, maintaining a compact state in acid solution while swelling pronouncedly to release active biomolecules in alkaline without burst release. Encapsulated lysozyme, subtilisin and urease were protected by the polymer matrix after 2 h in acid with 83% of the released enzymes in the simulated intestinal/colonic alkaline condition remained active. In addition, about 60% of the insulin released was bioactive, demonstrating the potential use of SNAP hydrogel/granules for oral delivery of therapeutic protein.

11. A generalized swelling model for polyelectrolyte gel was derived which can be used to estimate molecular weight between two consecutive crosslinks, crosslinking density, or pore size from the determined swollen gel volume in both salt-free and high ionic concentration environments containing uni-uni, uni-bi, bi-uni, or bi-bivalent electrolytes. The derived equilibrium swelling model accounts for non-ideal elastic behavior of non-Guassian polymer and non-ideality of the ionic environment during gel swelling, and predicted the pore sizes of SNAP hydrogels with comparable results to those determined experimentally using AFM, SEM, DSC and protein diffusion. The derived equilibrium swelling model may be used to estimate

crosslinking density for other pH-responsive, point-link network polyelectrolytes (chemically crosslinked hydrogels).

12. Network alginate polymer behaves like a Gaussian polymer demonstrated through similar values of elastic potential calculated using the Gaussian model (Eq. 17b) and modified Gaussian polymer model (Eq. 17c).

Chapter 9

Recommendations for future work

This research has contributed to the field of material science by development of a new class of biopolymer based on chemical modification of native alginate, through exploring its potential application as oral delivery vehicle for protein therapeutics, and by the derivation of a mathematical model for subsequent characterization of the developed network alginate hydrogel. Recommended future experimentation involving material characterization and potential scale-up for modified polymer synthesis are listed below.

9.1 Viscoelastic property of the chemically modified alginate gel

Most tissues such as tendons and ligaments are viscoelastic materials, which exhibit both fluid- and solid-like properties and possess time-dependent or rate sensitive stress-strain relationships. Therefore, research on the viscoelastic response will enhance the utility of SNAP hydrogel in many bioengineering or tissue regeneration applications. Analytical techniques such as tensile and compression tests are commonly performed to characterize the mechanical properties of network polymer gels. The tensile test or extensometry involves deforming a material at a constant rate of elongation and recording the force required to maintain that rate of elongation. A stress versus strain chart can be obtained and used for determination of several mechanical parameters such as the Young's modulus, yield strength and ultimate tensile strength. In compression test, the

force to compress hydrogel between two plates and the amount of deformation are used to derive a stress versus strain graph, from which the compressive modulus and compressive strength can be determined. Other techniques including the rheological measurement of shear viscosity and elastic shear modules, and contact-force measurement using atomic force microscopy can be used to quantify the viscoelasticity of the hydrogels [1-3].

9.2 Mucoadhesive properties of the modified alginate gel

Oral administration of therapeutic protein-based drugs can avoid painful, invasive injection, improving patient compliance. The use of mucoadhesive polymers such as alginate in oral drug delivery can promote polymer binding to the intestinal mucosa, increasing residence time of the carrier at the delivery site, improving bioavailability of the therapeutic drug. There are various analytical tools that can be used to quantify the mucoadhesive properties of hydrogel such as texture analyzer and quartz crystal microbalance (QCM) [4]. Texture analyzer is a useful tool in studying the mechanical characteristics of mucoadhesiveness polymers [5]. Mucoadhesion is evaluated through the measurement of maximum force required to separate the polymer from mucosal tissues such as stomach tissue, bovine sublingual mucosa, bovine duodenal mucosa, and mucin gel under simulated gastric conditions. QCM measures the real-time shifts in frequency and losses of energy (also introduced as dissipation shifts) by the piezoelectric quartz as materials adsorb onto its surface, enabling the analysis of the interactions between polymer and mucin under various conditions (ie. kinetics of adhesion) and to make

comparison between the native alginate and the modified alginate gel. Mucoadhesive properties can also be quantified by the mucus glycoprotein assay whereby hydrogel is suspended in aqueous medium containing mucin and the adsorption isotherm determined.

9.3 Biocompatibility of the modified alginate gel

A biocompatibility study of the modified alginate gel is required for many *in vivo* biomedical applications. Biomaterials which govern the interaction of material surfaces with blood and tissue components in the physiological environment must be nontoxic, non-allergenic, non-carcinogenic, and non-mutagenic, and therefore considered as being biocompatible for specific applications. Although glutaraldehyde is cell toxic, complete removal of residual crosslinker and quenching reactive aldehyde with amino acids such as glycine or glutamic acid have proven successfully to improve biocompatibility of glutaraldehyde-crosslinked biomaterials, many of which have acquired FDA approval in applications such as heart valve and hip prosthesis [6, 7]. Therefore, to assess the biocompatibility of SNAP hydrogel as an oral drug carrier or as tissue scaffold, the *in vitro* cell based toxicity study of the SNAP hydrogel is the first step of a biocompatibility study, prior to any animal testing. Since SNAP hydrogel is considered as low density material, the direct contact method cell culture assay is proposed. In this assay, the test material is placed directly onto cells and incubated in a suitable condition. Cell viability and morphology are characterized during incubation. Leachable chemicals from the test material can diffuse into the culture medium and directly contact the cell layer. The test

material is considered cytotoxic if the chemicals released induce cell malformation, degeneration and lysis around the testing material. Elution cell culture assay is also suited for cytoxicity study. In this assay, extracts of the tested material using different extracting media and conditions according to actual use or exaggerated conditions are obtained and transferred to the cell layer and incubated. The cell toxicity effect is determined qualitatively, microscopically, and quantitatively by measuring cell death, inhibition of cell growth, cell proliferation or colony formation.

9.4 Scale-up experiment in semisynthesis of network alginate gels

SNAP hydrogels can find many applications in food, pharmaceutical and biotechnology industries. Therefore, it is of interest to scale-up the formulation process for commercial exploitation of the polymer gel. In this PhD research, semi-synthetic alginate gel was formed by producing the pre-formed acid gel beads through extruding alginate sol into acid solution, followed by reacting preformed beads with glutaraldehyde in aqueous medium. For scale up, a semi-batch emulsification polymerization method is proposed to prepare semi-synthetic alginate gel, whereby glutaraldehyde is pre-mixed with alginate solution, followed by emulsifying in oil suspension. Acid is added to the water-in-oil emulsion to trigger the crosslinking reaction. The reaction can be controlled kinetically by the duration of reaction time, or thermodynamically by controlling the initial glutaraldehyde concentration and allowing the reaction to reach equilibrium.

Preliminary research in the scale up process was carried out by emulsifying alginate sol of 4% containing glutaraldehyde crosslinkers in canola oil at a ratio of 1/4 (v/v of alginate sol to oil) for 15 min, followed by the addition of HCl, acetic acid and canola oil mixture (prepared at 1:1:10 ratio) at 1% v/v acid mixture to emulsion. Reaction was carried out at 40^{o}C for 8 h. At the end of reaction, pH 1.2 HCl solution was added to the slurry at 1:1 volume ratio to facilitate gel microsphere partitioning into the aqueous phase and allow for additional 30 minute of reaction. The oil supernatant was withdrawn and discarded. Resultant beads were washing with cold acetone-ethanol (80:20) mixture and dryed with pure acetone, forming granules. A micrograph from Leica stereomicroscope (D3, Germany) of the resultant granules is presented in Figure 9-1. Granules appeared spherical and discrete.

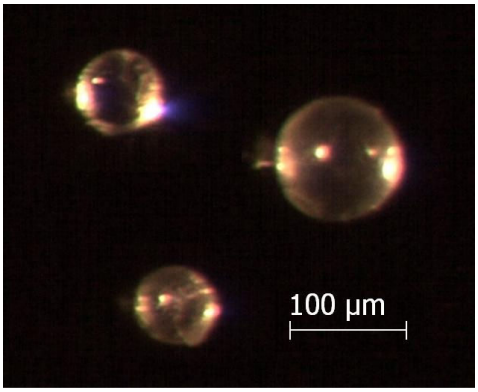

Figure 9-1. SNAP granules formed by scale-up emulsion polymerization method.

For future study in scale up, it is recommended that the reaction kinetics of the acetalization reaction be characterized to enable the manufacturing control of the hydrogel synthesized by the emulsion polymerization process. Another main challenge encountered for this production process is the bead separation after the reaction. Residual

oil can be readily removed from larger size beads by washing with ethanol-acetone mixture, however as size of beads decreased to submicron diameters, a large quantity of gel beads generally clustered at the oil-water interface, resulting in significant lost in bead recovery. Therefore, it is vital to investigate alternative bead separation/recovery methods or conduct research on alternative dispersed phases which can be readily removed after the bead production process. In addition, for successful use of SNAP gel in bio-related application, unreacted glutaraldehyde must be completely removed. It is recommended that glycine and ethanol are both added to aqueous acid medium during two-phase partitioning to further promote reaction with residual active aldehyde. The small crosslinked glycine-glutaraldehyde and ethanol-glutaraldehyde molecules are water soluble and removed during washing.

9.5 References

1. Lin, D. C.; Yurke, B.; Langrana, N. A., Use of rigid spherical inclusions in Young's moduli determination: Application to DNA-crosslinked gels. *Journal of Biomechanical Engineering-Transactions of the Asme* **2005,** 127, (4), 571-579.

2. Flanagan, L. A.; Ju, Y. E.; Marg, B.; Osterfield, M.; Janmey, P. A., Neurite branching on deformable substrates. *Neuroreport* **2002,** 13, (18), 2411-2415.

3. Yang, N.; Wong, K. K. H.; de Bruyn, J. R.; Hutter, J. L., Frequency-dependent viscoelasticity measurement by atomic force microscopy. *Measurement Science & Technology* **2009,** 20, (2), 1-9.

4. Chayed, S.; Winnik, F. M., In vitro evaluation of the mucoadhesive properties of polysaccharide-based nanoparticulate oral drug delivery systems. *European Journal of Pharmaceutics and Biopharmaceutics* **2007,** 65, (3), 363-370.

5. Thirawong, N.; Nunthanid, J.; Puttipipatkhachorn, S.; Sriamornsak, P., Mucoadhesive properties of various pectins on gastrointestinal mucosa: An in vitro evaluation using texture analyzer. *European Journal of Pharmaceutics and Biopharmaceutics* **2007,** 67, (1), 132-140.

6. Jayakrishnan, A.; Jameela, S. R., Glutaraldehyde as a fixative in bioprostheses and drug delivery matrices. *Biomaterials* **1996,** 17, (5), 471-484.

7. Migneault, I.; Dartiguenave, C.; Bertrand, M. J.; Waldron, K. C., Glutaraldehyde: behavior in aqueous solution, reaction with proteins, and application to enzyme crosslinking. *Biotechniques* **2004,** 37, (5), 790-802.

Appendix

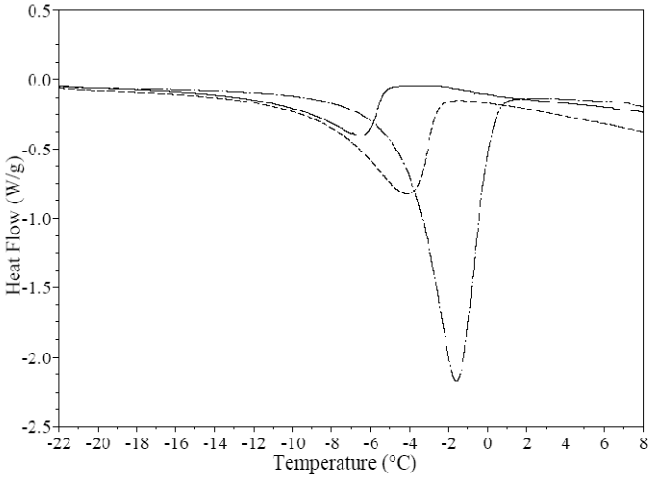

Figure A-1: DSC thermographs of loosely (dash-dotted), moderate (short dashed) and calcium alginate gel (solid). The triple point temperatures and heat flow data were used in the determination of the pore radius distribution shown in Figure 5-1.

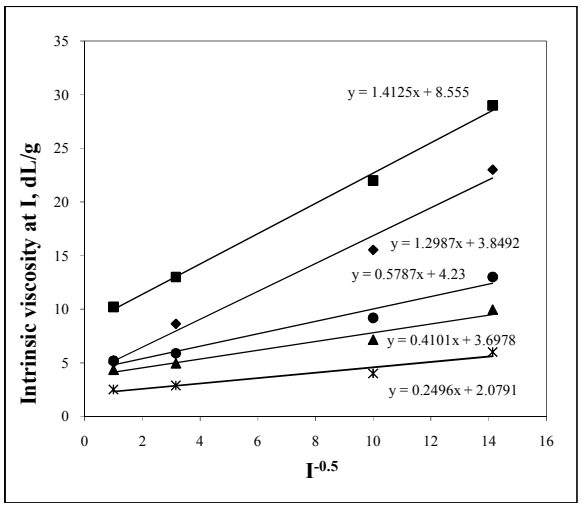

Figure A-3: Intrinsic viscosity of various alginate of MW=650 (square), 430 (diamond), 288 (circle), 144 (triangle), 68 kDa (star). Extrapolate to infinite ionic strength to obtain the intrinsic viscosity at theta condition.

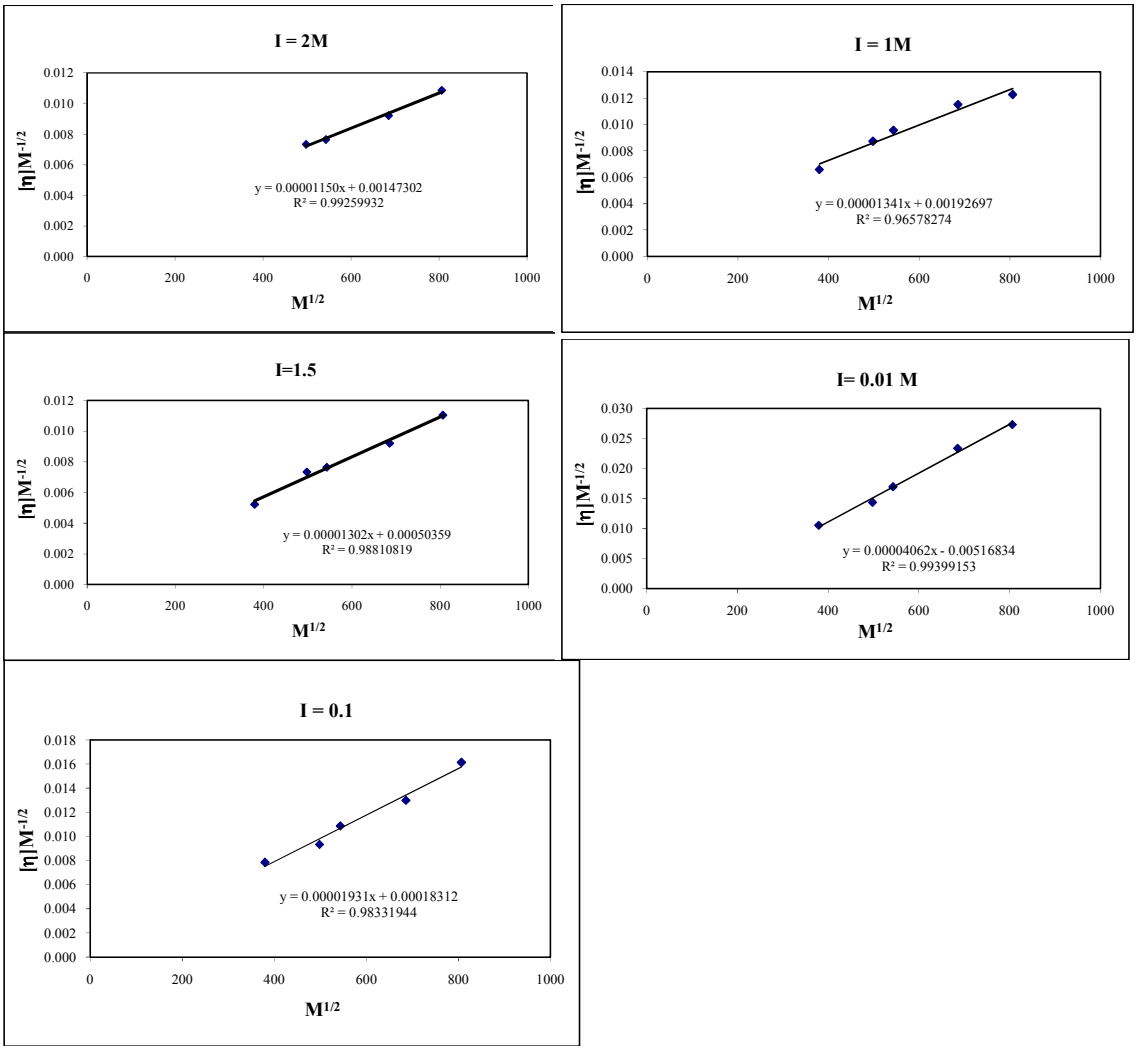

Figure A-2: Intrinsic viscosity of various molecular weight alginates in pH 7, NaCl solution. Slope of the best fitted line from each figure was used in the subsequent determination of Flory-Huggins interaction parameter using Eq. 33 (Chapter 6).

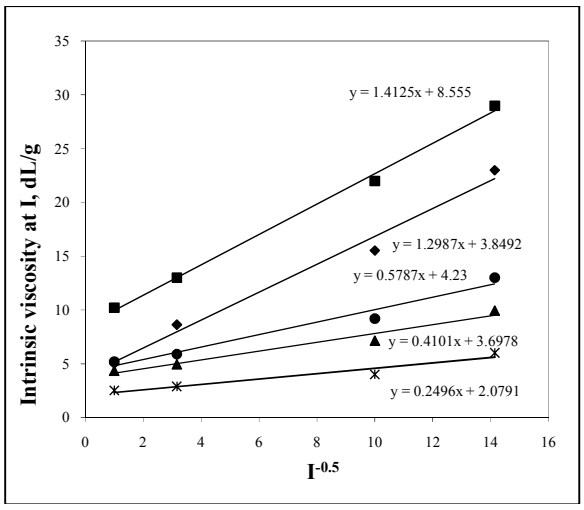

Figure A-3: Intrinsic viscosity of various alginate of MW=650 (square), 430 (diamond), 288 (circle), 144 (triangle), 68 kDa (star). Extrapolate to infinite ionic strength to obtain the intrinsic viscosity at theta condition.

Table A-1: Equilibrium swelling ratio and pore size of SNAP hydrogels predicted using the derived equilibrium swelling model with the incorporation of the modified Gaussian elastic equation (Eq. 17c) and with the classical Gaussian elastic equation Eq. 17b. Data was plotted in Figure 6-6.

Mc, g/mol	**Equilibrium swelling ratio**		**Pore size (nm)**	
	Modified-Gaussian[1]	Classic Gaussian[2]	Modified-Gaussian[3]	Classic Gaussian[4]
500	28	31	18	18
1500	49	50	37	38
5000	92	93	84	85
25000	236	237	258	258
75000	528	528	584	584
100000	699	699	741	741

[1] The equilibrium swelling ratio was evaluated with the elastic potential which accounts for non-Gaussian coil effect using Eq. 17c, Chapter 6.
[2] The equilibrium swelling ratio was evaluated with the elastic potential which assumes Gaussian coil polymer using Eq. 17b, Chapter 6.
[3] Pore sizes estimated using Mc values calculated from the swelling model that accounts for non-Gaussian coil effect.
[4] Pore sizes estimated using Mc values calculated from the swelling model that assumes ideal Gaussian coil polymer.

Table A-2: Pore sizes of the synthesized SNAP hydrogels estimated from the derived equilibrium swelling model which accounts for the non-Gaussian elasticity with Eq. 17c (modified Gaussian model) and the swelling model which assumes ideal Gaussian polymer (Eq. 17b). The pore sizes data estimated from the modified Gaussian model are presented in Table 6-2.

Mc, g/mol	**Pore size (nm)**	
	Modified-Gaussian	Classic Gaussian
1500	37.39	36.861
6800	104.07	99.99
20800	226.41	227.264
52500	443.37	449.776

Table A-3: Values of the positive non-zero roots, q_n, (Eq. 4, Chapter 5) used in the estimation of solute diffusion coefficients in SNAP and calcium-alginate hydrogels. The non-zero roots were solved by Maple.

n	moderate crx SNAP	densely crx SNAP	Ca-alginate
1	3.2919	3.2230	3.1681
2	6.3641	6.3251	6.2966
3	9.4795	9.4529	9.4337
4	12.6077	12.5875	12.5731
5	15.7411	15.7249	15.7133
6	18.8772	18.8637	18.8540
7	25.1535	25.1433	25.1361
8	28.2928	28.2837	28.2773
9	31.4325	31.4244	31.4186
10	34.5726	34.5652	34.5599
11	40.8535	40.8472	40.8427
12	43.9942	43.9883	43.9842
13	47.1350	47.1295	47.1256
14	53.4169	53.4120	53.4086
15	56.5579	56.5533	56.5501
16	62.8402	62.8361	62.8332
17	65.9814	65.9775	65.9747
18	69.1226	69.1189	69.1162

Table A-4: Diffusion of BSA into calcium alginate gel. Diffusion coefficient was determined from Eq. 3, Chapter 5 from the non-linear regression analysis. The best fitted curve was obtained when the error square was the smallest. Diffusion coefficient determined was used for plotting Figure 5-2 and Figure 5-3.

Time (h)	M_t (mg)	Experimental M_t/M_∞	Calculated M_t/M_∞	Error square
0.00	0.00	0.00	0.00	0.0000
0.08	131.12	0.44	0.08	0.1296
0.25	78.09	0.26	0.11	0.0230
0.58	18.31	0.06	0.15	0.0081
1.00	148.95	0.50	0.19	0.0953
1.50	232.74	0.78	0.22	0.3054
2.00	248.05	0.83	0.25	0.3291
3.00	304.66	1.02	0.30	0.5088
4.00	384.79	1.29	0.34	0.8846
5.00	294.64	0.98	0.38	0.3659
8.00	318.01	1.06	0.46	0.3618
12.00	467.91	1.56	0.54	1.0461
20.00	269.00	0.90	0.65	0.0616
24.00	299.37	1.00	0.69	0.0953

Table A-5: Diffusion of BSA into moderately crosslinked SNAP hydrogel.

Time (h)	M_t (mg)	Experimental M_t/M_∞	Calculated M_t/M_∞	Error square
0.00	0.00	0.00	0.00	0.0000
0.08	631.14	0.21	0.17	0.0020
0.25	978.32	0.33	0.27	0.0037
0.58	1378.95	0.47	0.39	0.0060
1.00	1584.68	0.53	0.48	0.0026
1.50	1733.30	0.58	0.57	0.0004
2.00	2048.02	0.69	0.63	0.0040
3.00	2285.37	0.77	0.72	0.0027
4.00	2409.85	0.81	0.78	0.0009
5.00	2590.88	0.87	0.83	0.0018
8.00	2837.76	0.96	0.92	0.0015
12.00	2897.94	0.98	0.97	0.0001
20.00	2905.03	0.98	1.00	0.0002
24.00	2964.89	1.00	1.00	0.0000

Table A-6: Diffusion of BSA into densely crosslinked SNAP hydrogel.

Time (h)	M_t (mg)	Experimental M_t/M_∞	Calculated M_t/M_∞	Error square
0.00	0.00	0.00	0.00	0.0000
0.08	331.08	0.11	0.15	0.0014
0.25	678.15	0.23	0.24	0.0001
0.58	978.84	0.34	0.35	0.0001
1.00	1300.87	0.45	0.44	0.0001
1.50	1673.30	0.58	0.52	0.0039
2.00	1874.96	0.65	0.58	0.0052
3.00	2097.82	0.72	0.66	0.0036
4.00	2164.75	0.75	0.73	0.0003
5.00	2338.91	0.81	0.78	0.0008
8.00	2589.31	0.89	0.88	0.0003
12.00	2749.42	0.95	0.94	0.0001
20.00	2894.72	1.00	0.99	0.0002
24.00	2895.04	1.00	0.99	0.0000

Table A-7: Diffusion of urease into moderately crosslinked SNAP hydrogel.

Time (h)	M_t (mg)	Experimental M_t/M_∞	Calculated M_t/M_∞	Error square
0.00	0.00	0.00	0.00	0.0000
0.08	201.15	0.09	0.12	0.0008
0.25	400.13	0.18	0.19	0.0000
0.58	651.02	0.30	0.27	0.0006
1.00	791.28	0.36	0.34	0.0003
1.50	929.29	0.42	0.41	0.0003
2.00	1098.77	0.50	0.46	0.0018
3.00	1278.36	0.58	0.54	0.0020
4.00	1398.12	0.64	0.60	0.0015
5.00	1499.05	0.68	0.65	0.0013
8.00	1687.52	0.77	0.75	0.0002
12.00	1894.23	0.86	0.84	0.0005
20.00	2001.89	0.91	0.93	0.0004
24.00	2190.92	1.00	0.96	0.0019

Table A-8: Diffusion of vitamin B12 into moderately crosslinked SNAP hydrogel.

Time (h)	M_t (mg)	Experimental M_t/M_∞	Calculated M_t/M_∞	Error square
0.00	0.00	0.00	0.00	0.0000
0.08	802.35	0.31	0.32	0.0002
0.25	1259.03	0.48	0.51	0.0007
0.58	1976.54	0.76	0.69	0.0044
1.00	2233.25	0.86	0.81	0.0020
1.50	2401.25	0.92	0.89	0.0008
2.00	2457.38	0.94	0.94	0.0000
3.00	2596.98	1.00	0.98	0.0003
4.00	2564.53	0.99	0.99	0.0001
5.00	2572.03	0.99	1.00	0.0001
8.00	2598.79	1.00	1.00	0.0000
12.00	2594.65	1.00	1.00	0.0000
20.00	2613.59	1.00	1.00	0.0000
24.00	2601.06	1.00	1.00	0.0000

Table A-9: Diffusion of insulin into moderately crosslinked SNAP hydrogel.

Time (h)	M_t (mg)	Experimental M_t/M_∞	Calculated M_t/M_∞	Error square
0.00	0.00	0.00	0.00	0.0000
0.08	737.28	0.24	0.29	0.0031
0.25	1296.45	0.42	0.47	0.0025
0.58	2131.22	0.68	0.64	0.0019
1.00	2498.56	0.80	0.76	0.0016
1.50	2694.36	0.87	0.85	0.0002
2.00	2803.05	0.90	0.90	0.0000
3.00	2934.57	0.94	0.96	0.0003
4.00	3036.99	0.98	0.98	0.0001
5.00	3121.01	1.00	0.99	0.0001
8.00	3142.25	1.01	1.00	0.0001
12.00	3172.48	1.02	1.00	0.0004
20.00	3103.22	1.00	1.00	0.0000
24.00	3112.29	1.00	1.00	0.0000

Table A-10: Diffusion of Lysozyme into moderately crosslinked SNAP hydrogel.

Time (h)	M_t (mg)	Experimental M_t/M_∞	Calculated M_t/M_∞	Error square
0.00	0.00	0.00	0.00	0.0000
0.08	898.36	0.24	0.23	0.0001
0.25	1497.78	0.39	0.37	0.0008
0.58	1898.32	0.50	0.52	0.0003
1.00	2308.01	0.61	0.63	0.0006
1.50	2684.95	0.71	0.72	0.0002
2.00	3011.68	0.79	0.79	0.0000
3.00	3237.65	0.85	0.87	0.0004
4.00	3519.05	0.93	0.92	0.0000
5.00	3579.71	0.94	0.95	0.0001
8.00	3800.06	1.00	0.99	0.0002
12.00	3741.25	0.99	1.00	0.0001
20.00	3781.96	1.00	1.00	0.0000
24.00	3792.66	1.00	1.00	0.0000

Table A-11: Diffusion of subtilisin into moderately crosslinked SNAP hydrogel.

Time (h)	M_t (mg)	Experimental M_t/M_∞	Calculated M_t/M_∞	Error square
0.00	0.00	0.00	0.00	0.0000
0.08	566.66	0.20	0.20	0.0000
0.25	900.08	0.31	0.32	0.0002
0.58	1434.74	0.50	0.46	0.0011
1.00	1597.02	0.55	0.57	0.0003
1.50	2004.68	0.69	0.66	0.0012
2.00	2102.21	0.73	0.72	0.0000
3.00	2317.98	0.80	0.81	0.0002
4.00	2492.99	0.86	0.87	0.0001
5.00	2653.98	0.92	0.91	0.0000
8.00	2891.05	1.00	0.97	0.0008
12.00	2892.33	1.00	0.99	0.0000
20.00	2889.79	1.00	1.00	0.0000
24.00	2897.12	1.00	1.00	0.0000

Table A-12: Diffusion of insulin hexamer into moderately crosslinked SNAP hydrogel.

Time (h)	M_t (mg)	Experimental M_t/M_∞	Calculated M_t/M_∞	Error square
0.00	0.00	0.00	0.00	0.0000
0.08	501.23	0.17	0.19	0.0007
0.25	888.98	0.29	0.31	0.0002
0.58	1386.79	0.46	0.44	0.0003
1.00	1702.35	0.56	0.55	0.0003
1.50	1896.46	0.63	0.64	0.0000
2.00	2036.69	0.68	0.70	0.0006
3.00	2436.99	0.81	0.79	0.0003
4.00	2554.23	0.85	0.85	0.0000
5.00	2702.81	0.90	0.89	0.0000
8.00	2831.22	0.94	0.96	0.0005
12.00	3002.00	1.00	0.99	0.0000
20.00	2989.26	0.99	1.00	0.0001
24.00	3014.11	1.00	1.00	0.0000

Table A-13: Diffusion of urease into densely crosslinked SNAP hydrogel.

Time (h)	M_t (mg)	Experimental M_t/M_∞	Calculated M_t/M_∞	Error square
0.00	0.00	0.00	0.00	0.0000
0.08	202.12	0.10	0.09	0.0001
0.25	289.98	0.14	0.14	0.0001
0.58	501.31	0.24	0.22	0.0004
1.00	612.35	0.29	0.28	0.0001
1.50	716.58	0.34	0.34	0.0000
2.00	886.96	0.42	0.39	0.0011
3.00	1002.32	0.47	0.46	0.0002
4.00	1112.35	0.53	0.52	0.0001
5.00	1232.35	0.58	0.57	0.0003
8.00	1399.98	0.66	0.67	0.0001
12.00	1624.32	0.77	0.77	0.0000
20.00	1797.71	0.85	0.88	0.0006
36.00	2115.12	1.00	0.96	0.0013

Table A-14: Diffusion of vitamin B12 into densely crosslinked SNAP hydrogel.

Time (h)	M_t (mg)	Experimental M_t/M_∞	Calculated M_t/M_∞	Error square
0.00	0.00	0.00	0.00	0.0000
0.08	674.36	0.30	0.29	0.0002
0.25	1105.68	0.50	0.48	0.0006
0.58	1535.45	0.69	0.66	0.0012
1.00	1769.36	0.80	0.78	0.0002
1.50	2022.35	0.91	0.87	0.0019
2.00	2002.05	0.90	0.92	0.0003
3.00	2178.69	0.98	0.97	0.0002
4.00	2143.02	0.97	0.99	0.0005
5.00	2177.12	0.98	1.00	0.0002
8.00	2143.25	0.97	1.00	0.0011
12.00	2199.85	0.99	1.00	0.0001
20.00	2205.07	1.00	1.00	0.0000
36.00	2215.69	1.00	1.00	0.0000

Table A-15: Diffusion of insulin into densely crosslinked SNAP hydrogel.

Time (h)	M_t (mg)	Experimental M_t/M_∞	Calculated M_t/M_∞	Error square
0.00	0.00	0.00	0.00	0.0000
0.08	706.58	0.23	0.26	0.0005
0.25	1184.98	0.39	0.42	0.0011
0.58	1796.45	0.59	0.60	0.0000
1.00	2096.23	0.69	0.72	0.0009
1.50	2377.69	0.78	0.81	0.0009
2.00	2695.41	0.89	0.87	0.0002
3.00	2799.87	0.92	0.94	0.0004
4.00	2902.03	0.95	0.97	0.0003
5.00	2995.21	0.98	0.99	0.0000
8.00	3013.21	0.99	1.00	0.0001
12.00	3022.32	0.99	1.00	0.0000
20.00	3003.58	0.99	1.00	0.0002
36.00	3042.00	1.00	1.00	0.0000

Table A-16: Diffusion of lysozyme into densely crosslinked SNAP hydrogel.

Time (h)	M_t (mg)	Experimental M_t/M_∞	Calculated M_t/M_∞	Error square
0.00	0.00	0.00	0.00	0.0000
0.08	612.00	0.17	0.18	0.0001
0.25	989.98	0.28	0.31	0.0009
0.58	1602.37	0.46	0.46	0.0000
1.00	1890.22	0.54	0.57	0.0007
1.50	2306.15	0.66	0.66	0.0000
2.00	2501.12	0.71	0.72	0.0001
3.00	2792.35	0.80	0.82	0.0004
4.00	2979.21	0.85	0.88	0.0007
5.00	3102.77	0.88	0.92	0.0009
8.00	3342.56	0.95	0.97	0.0004
12.00	3402.64	0.97	0.99	0.0006
20.00	3481.19	0.99	1.00	0.0000
36.00	3506.12	1.00	1.00	0.0000

Table A-17: Diffusion of subtilisin into densely crosslinked SNAP hydrogel.

Time (h)	M_t (mg)	Experimental M_t/M_∞	Calculated M_t/M_∞	Error square
0.00	0.00	0.00	0.00	0.0000
0.08	400.12	0.15	0.16	0.0001
0.25	687.63	0.26	0.27	0.0002
0.58	985.21	0.37	0.40	0.0009
1.00	1398.12	0.52	0.50	0.0005
1.50	1601.25	0.60	0.59	0.0001
2.00	1785.43	0.67	0.65	0.0003
3.00	1985.46	0.74	0.75	0.0000
4.00	2104.99	0.79	0.81	0.0005
5.00	2237.64	0.84	0.86	0.0004
8.00	2487.32	0.93	0.94	0.0001
12.00	2541.18	0.95	0.98	0.0008
20.00	2680.92	1.01	1.00	0.0001
36.00	2667.18	1.00	1.00	0.0000

Table A-18: Diffusion of insulin hexamer into densely crosslinked SNAP hydrogel.

Time (h)	M_t (mg)	Experimental M_t/M_∞	Calculated M_t/M_∞	Error square
0.00	0.00	0.00	0.00	0.0000
0.08	397.68	0.13	0.16	0.0005
0.25	701.26	0.23	0.26	0.0009
0.58	1096.76	0.37	0.39	0.0005
1.00	1519.32	0.51	0.49	0.0003
1.50	1799.64	0.60	0.58	0.0007
2.00	1984.56	0.66	0.64	0.0005
3.00	2197.63	0.74	0.73	0.0000
4.00	2403.01	0.80	0.80	0.0000
5.00	2502.23	0.84	0.85	0.0001
8.00	2705.89	0.91	0.93	0.0007
12.00	2870.64	0.96	0.98	0.0003
20.00	2940.22	0.98	1.00	0.0002
36.00	2989.23	1.00	1.00	0.0000

Table A-19: Diffusion of vitamin B12 into calcium alginate hydrogel.

Time (h)	M_t (mg)	Experimental M_t/M_∞	Calculated M_t/M_∞	Error square
0.00	0.00	0.00	0.00	0.0000
0.08	189.65	0.32	0.38	0.0040
0.25	300.12	0.50	0.60	0.0092
0.58	437.65	0.73	0.80	0.0041
1.00	516.79	0.86	0.91	0.0018
1.50	528.77	0.89	0.96	0.0062
2.00	549.65	0.92	0.99	0.0043
3.00	555.35	0.93	1.00	0.0047
4.00	575.59	0.96	1.00	0.0013
5.00	593.65	0.99	1.00	0.0000
8.00	558.69	0.94	1.00	0.0042
12.00	596.63	1.00	1.00	0.0000
20.00	592.65	0.99	1.00	0.0001
36.00	597.48	1.00	1.00	0.0000

Table A-20: Diffusion of insulin into calcium alginate hydrogel.

Time (h)	M_t (mg)	Experimental M_t/M_∞	Calculated M_t/M_∞	Error square
0.00	0.00	0.00	0.00	0.0000
0.08	345.68	0.35	0.38	0.0007
0.25	577.94	0.58	0.59	0.0000
0.58	789.96	0.80	0.79	0.0001
1.00	898.25	0.91	0.90	0.0001
1.50	964.36	0.98	0.96	0.0002
2.00	957.88	0.97	0.98	0.0002
3.00	985.06	1.00	1.00	0.0000
4.00	991.27	1.00	1.00	0.0000
5.00	1011.54	1.02	1.00	0.0005
8.00	998.69	1.01	1.00	0.0001
12.00	986.51	1.00	1.00	0.0000
20.00	990.02	1.00	1.00	0.0000
36.00	988.49	1.00	1.00	0.0000

Table A-21: Diffusion of lysozyme into calcium alginate hydrogel.

Time (h)	M_t (mg)	Experimental M_t/M_∞	Calculated M_t/M_∞	Error square
0.00	0.00	0.00	0.00	0.0000
0.08	382.21	0.26	0.28	0.0003
0.25	714.63	0.49	0.46	0.0015
0.58	944.44	0.65	0.64	0.0003
1.00	1095.68	0.76	0.76	0.0000
1.50	1199.87	0.83	0.85	0.0005
2.00	1306.54	0.90	0.91	0.0000
3.00	1398.79	0.97	0.96	0.0000
4.00	1416.52	0.98	0.99	0.0000
5.00	1455.54	1.01	0.99	0.0002
8.00	1467.82	1.02	1.00	0.0003
12.00	1453.35	1.01	1.00	0.0000
20.00	1432.99	0.99	1.00	0.0001
36.00	1444.01	1.00	1.00	0.0000

Table A-22: Diffusion of subtilisin into calcium alginate hydrogel.

Time (h)	M_t (mg)	Experimental M_t/M_∞	Calculated M_t/M_∞	Error square
0.00	0.00	0.00	0.00	0.0000
0.08	189.32	0.26	0.22	0.0012
0.25	289.96	0.39	0.36	0.0009
0.58	387.65	0.53	0.52	0.0001
1.00	473.66	0.64	0.64	0.0000
1.50	539.52	0.73	0.73	0.0000
2.00	595.12	0.81	0.80	0.0001
3.00	683.44	0.93	0.89	0.0019
4.00	695.25	0.95	0.93	0.0001
5.00	703.31	0.96	0.96	0.0000
8.00	724.12	0.98	0.99	0.0001
12.00	755.05	1.03	1.00	0.0007
20.00	748.91	1.02	1.00	0.0003
24.00	735.49	1.00	1.00	0.0000
36.00	2801.06	1.0000	0.7200	0.7287

Table A-23: Diffusion of insulin hexamer into calcium alginate hydrogel.

Time (h)	M_t (mg)	Experimental M_t/M_∞	Calculated M_t/M_∞	Error square
0.00	0.00	0.00	0.00	0.0000
1.69	101.11	0.13	0.17	0.0014
3.66	219.35	0.28	0.27	0.0001
4.83	289.98	0.37	0.40	0.0005
6.46	387.64	0.50	0.50	0.0000
7.71	462.40	0.59	0.58	0.0001
8.39	503.16	0.65	0.65	0.0000
9.63	577.61	0.74	0.74	0.0000
10.82	649.08	0.84	0.81	0.0006
11.31	678.89	0.87	0.86	0.0002
8.00	747.14	0.96	0.94	0.0004
13.16	789.86	1.02	0.98	0.0012
13.25	795.01	1.02	1.00	0.0006
36.00	777.25	1.00	1.00	0.0000

Table A-24: Diffusion coefficients of various biomolecules in SNAP and calcium alginate gels, and in water.

Biomolecules	D_{water} cm^2/s	D_{gel}, cm^2/s		
		densely cxn SNAP	moderate cxn SNAP	Ca-algiante
B12	0.000002328	0.000002007	0.000002146	0.000001676
Insulin monomer	0.000001825	0.000001518	0.000001703	0.000001124
Lysozyme	0.000001066	0.000000776	0.000000954	0.000000587
Subtilisin	0.000000812	0.000000572	0.000000714	0.000000345
Hexameric insulin	0.000000750	0.000000541	0.000000646	0.000000180
BSA	0.000000562	0.000000359	0.000000463	0.000000050
Urease	0.000000289	0.000000154	0.000000205	0

Table A-25: Pore sizes determined from swelling model, DSC and protein diffusion. Data was used for plotting Figure 5-4.

Densely crosslinked SNAP				
Pore diameter determined from DSC	35	nm		
Pore diameter estimated by swelling model	40	nm		
	MW	Stoke radii (nm)	D_{gel}/D_{water}	Pore diameter (nm)
B12	1.3	0.87	0.8622	34.36
Insulin monomer	5.8	1.11	0.8323	31.54
Lysozyme	14.3	1.9	0.7282	25.38
Subtilisin	22.8	2.5	0.7055	28.33
Hexameric insulin	34.2	2.7	0.7223	32.43
BSA	66.4	3.6	0.6398	29.50
Urease	545.6	7	0.5358	37.76
Moderate crosslinked SNAP				
Pore diameter determined from DSC	72	nm		
Pore diameter estimated by swelling model	80	nm		
B12	1.3	0.87	0.9222	64.28
Insulin monomer	5.8	1.11	0.9334	86.77
Lysozyme	14.3	1.9	0.8952	75.81
Subtilisin	22.8	2.5	0.8802	80.34
Hexameric insulin	34.2	2.7	0.8622	73.14
BSA	66.4	3.8	0.8241	73.53
Urease	545.6	7	0.7100	70.16
Calcium alginate				
Pore diameter determined from DSC	18	nm		
B12	1.3	0.87	0.7200	14.60
Insulin monomer	5.8	1.11	0.6160	10.92
Lysozyme	14.3	1.9	0.5512	12.74
Subtilisin	22.8	2.5	0.4250	10.57
Hexameric insulin	34.2	2.7	0.2410	6.13
BSA	66.4	3.6	0.0900	4.12
Urease	545.6	7	0.0001	1.01